TECHNICAL REPORT ARBRL-TR-02486

MULTIZONE ARTILLERY PROPELLING CHARGE STUDIES

Carl R. Ruth
Thomas C. Minor

May 1983

US ARMY ARMAMENT RESEARCH AND DEVELOPMENT COMMAND
BALLISTIC RESEARCH LABORATORY
ABERDEEN PROVING GROUND, MARYLAND

UNCLASSIFIED

SECURITY CLASSIFICATION OF THIS PAGE *(When Data Entered)*

REPORT DOCUMENTATION PAGE		READ INSTRUCTIONS BEFORE COMPLETING FORM
1. REPORT NUMBER TECHNICAL REPORT ARBRL-TR-02486	2. GOVT ACCESSION NO.	3. RECIPIENT'S CATALOG NUMBER
4. TITLE *(and Subtitle)* MULTIZONE ARTILLERY PROPELLING CHARGE STUDIES		5. TYPE OF REPORT & PERIOD COVERED Oct 1981 - Sep 1982 6. PERFORMING ORG. REPORT NUMBER
7. AUTHOR(s) Carl R. Ruth and Thomas C. Minor		8. CONTRACT OR GRANT NUMBER(s)
9. PERFORMING ORGANIZATION NAME AND ADDRESS US Army Ballistic Research Laboratory ATTN: DRDAR-BLI Aberdeen Proving Ground, MD 21005		10. PROGRAM ELEMENT, PROJECT, TASK AREA & WORK UNIT NUMBERS 1L162618AH80
11. CONTROLLING OFFICE NAME AND ADDRESS US Army Armament Research & Development Command US Army Ballistic Research Laboratory (DRDAR-BLA-S) Aberdeen Proving Ground, MD 21005		12. REPORT DATE May 1983 13. NUMBER OF PAGES 153
14. MONITORING AGENCY NAME & ADDRESS*(if different from Controlling Office)*		15. SECURITY CLASS. *(of this report)* UNCLASSIFIED 15a. DECLASSIFICATION/DOWNGRADING SCHEDULE

16. DISTRIBUTION STATEMENT *(of this Report)*

Approved for public release; distribution unlimited.

17. DISTRIBUTION STATEMENT *(of the abstract entered in Block 20, if different from Report)*

18. SUPPLEMENTARY NOTES

Presented at 1981 JANNAF Propulsion Meeting

19. KEY WORDS *(Continue on reverse side if necessary and identify by block number)*

Interior Ballistics
Pressure Waves
Howitzers
Grain Geometry
Charge Geometry
Multizone Propelling Charges

20. ABSTRACT *(Continue on reverse side if necessary and identify by block number)* jaf

The requirements for the design of a multizone charge are demanding in that pressure waves must be minimized at all zone levels without compromising low-zone performance. The development program for the 155-mm, Zones 3-6, XM211, Propelling Charge, highlighted the need for careful selection of the interrelated components that comprise a large-caliber propelling charge. As a specific example, severe pressure waves in high-temperature firings (63°C) at Zone 5 resulted with one of the charge configurations investigated. This

DD FORM 1 JAN 73 1473 EDITION OF 1 NOV 65 IS OBSOLETE

UNCLASSIFIED

SECURITY CLASSIFICATION OF THIS PAGE *(When Data Entered)*

instability was thought to be due possibly to dynamics of charge movement and impact on the projectile base. Although breechblows are not likely at this loading density, projectile or fuze malfunctions and ballistic variability are a concern.

This study investigated, specifically, the influence of charge interzone permeability, distribution of ullage, charge increment movement, igniter brisance, placement of parasitic components, etc., on the formation of pressure waves and charge component dynamics. Test charges used to address these issues were fabricated to resemble the earlier XM211 configuration that produced pressure waves. Gun tests with these charges were conducted using M483A1 projectiles fired from an M199 cannon instrumented with six chamber pressure gages. Data for each series fired in the standard gun are presented in detail. To better understand the events occurring early in the ignition cycle and their relationship to the formation of pressure waves, multizone charges were fired in a 155-mm howitzer simulator which used a plastic tube for the M199 chamber. Charge/chamber configurations were selected to determine the effects of vigorous movement of masses of solid propellant, depending on loading conditions and other physical constraints placed on the charge, on pressure-wave formation. While some simulator results were inconclusive, other tests in it and the howitzer yielded results which indicated that substantial motion of packages of propellant is a potential cause of pressure waves arising with this type charge.

TABLE OF CONTENTS

LIST OF ILLUSTRATIONS

LIST OF TABLES

I. INTRODUCTION

A propelling charge configuration that is frequently employed in Army howitzers is the multizone charge. This type of charge, schematically illustrated in Figure 1, consists of several discrete packages of propellant bound together in some fashion, as with tie straps. The principal rationale for this charge is that a particular velocity can be achieved dependent on the number of packages loaded into the weapon chamber, and this selectable velocity, coupled with the permitted variation of weapon launch angle, allows a wide range coverage by indirect fire weapons.

The requirements on design of a multizone charge are demanding. The charge must exhibit reliable performance at the low-zone end without compromising performance at any other zone level.[1,2] A case in point is the recent development program, now terminated, for the 155-mm, XM211, Propelling Charge.[3,4] The need for a new charge such as the XM211 arose with the advent of long-range, large-chamber 155-mm howitzers and new projectiles with larger rotating bands. When the existing charges were fired with these new weapons and projectiles, the projectiles frequently stuck. The probable cause was the lack of a sufficiently high peak pressure and pressure-rise rate to propel the projectile through the critical engraving region. To overcome this, a very fast-burning propellant was incorporated in the base XM211 increment (Zone 3). Coupling a very rapidly burning localized ignition source (Zone 3) to forward packages of less rapidly burning propellant (Zones 4, 5 and 6) in the XM211 then led to the formation of axial pressure waves, particularly at the Zone 5 level with charges conditioned to 63°C. We see then that it is necessary to consider all the interrelated components that make up the charge in order to optimize performance at all zone levels.

As motivation for the experimental studies we will shortly discuss, let us consider the phenomenology of the multiple-increment charge of Figure 1. The charge is base-ignited, and the several increments of propellant are packaged individually in cloth bags, which are secured together with fabric tie straps. The charge is undersized with respect to both chamber length and diameter, creating ullage axially between the charge and projectile base and

---

[1] *I. W. May, "The Role of Ignition and Combustion in Gun Propulsion: A Survey of Developmental Efforts," Proceedings of 13th JANNAF Combustion Meeting, CPIA Publication 281, Vol. I, pp. 315-340, September 1976.*

[2] *I. W. May and A. W. Horst, "Charge Design Considerations and Their Effect on Pressure Waves in Guns," ARBRL-TR-02277, Ballistic Research Laboratory, USA ARRADCOM, December 1980 (AD A095342).*

[3] *T. C. Minor and J. DeLorenzo, "Charge Design Approaches to the Reduction of Low Zone Stickers," Proceedings of 1976 JANNAF Propulsion Meeting, CPIA Publication 280, Vol. III, pp. 403-434, December 1976.*

[4] *R. J. DeKleine, "155-mm XM211 Propelling Charge Zones 3-6 - Design Review Minutes," Office of Project Manager, Cannon Artillery Weapons Systems, Dover, NJ, April 9, 1980.*

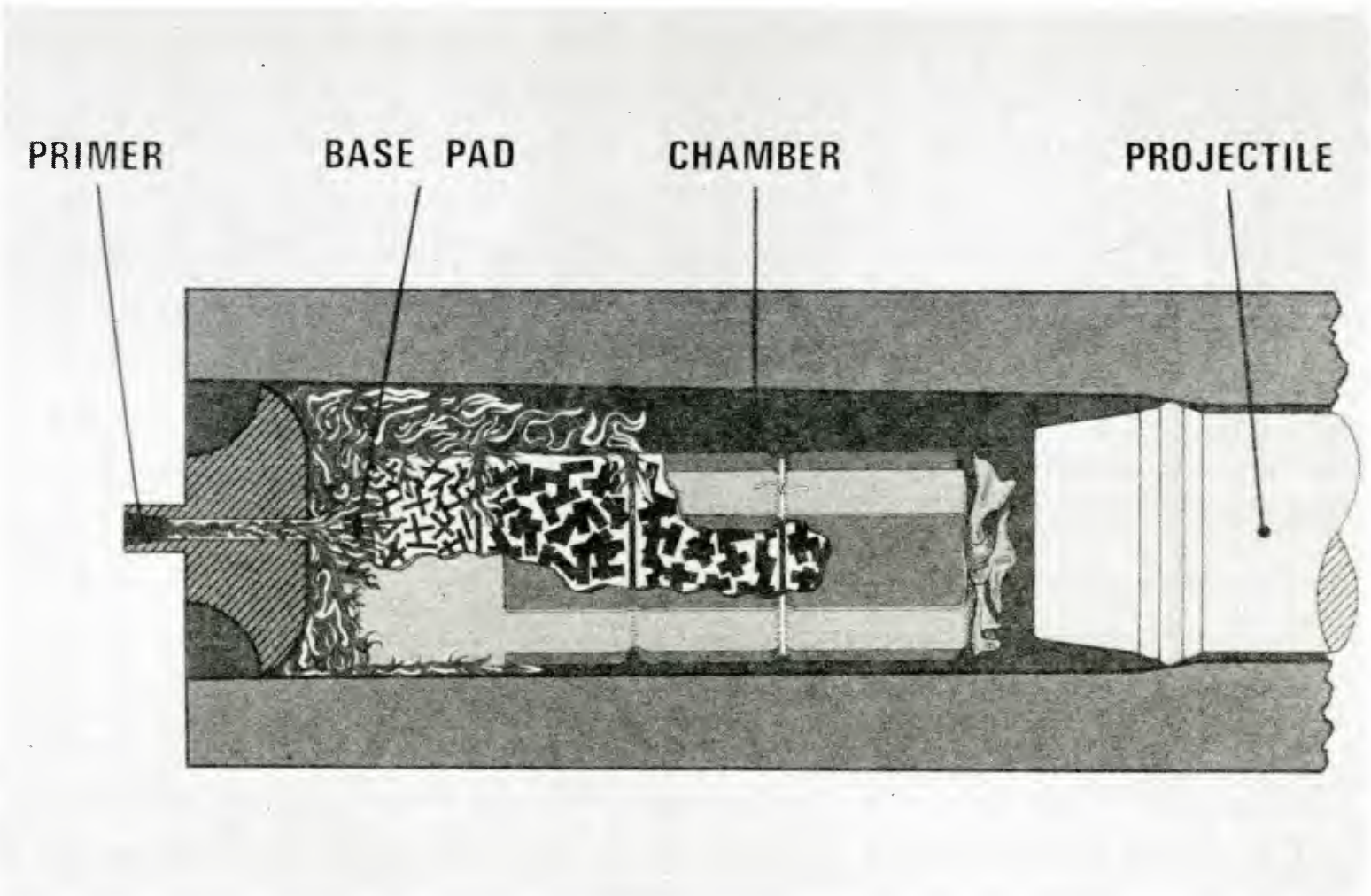

Figure 1. Typical Multizone Charge Configuration

between the charge and spindle (standoff), and radially between the charge and chamber wall. This allows for a variety of complex gas- and solid-phase flows depending on the initial loading configuration. After the initiation of the basepad, the igniter gases may pass through the fabric into the propellant bed of low permeability and locally ignite the base of the charge, or they may follow the path of less resistance through the radial ullage toward the forward end of the charge. In this fashion, the charge may be ignited at any point along its length, or indeed, at the forward end. The flow of igniter and propellant gases is further complicated by the casing material itself, generally fabric, and by parasitic components, such as flash-reducer pads, which may be located along the charge or imbedded between charge increments. Since this multiple-increment charge may consist of more than one granulation of propellant, the localized ignition of a very rapidly burning base-increment propellant can induce pressure waves and perhaps even considerable movement of relatively massive packages of propellant. Grain fracture may then create unprogrammed burning surfaces, which would further aggravate the production of pressure waves. In short, the external constraints on a bagged, multizone charge of grossly nonuniform strength and permeability give rise to a host of scenarios of gas flow, bag rupture, propellant movement and fracture, and the like. It is clear, then, that in addition to well-documented problems usually associated with pressure waves, such as in a high-loading-density M203 charge, the deleterious effect in low-loading-density charges of the impact of large quantities of propellant on the projectile base on the projectile's safety and performance is now of concern. And, as we will see later, pressure waves themselves in this low-loading-density charge may not present a breech safety problem, but they may adversely affect more delicate weapon mechanisms.

The experimental investigations reported herein attempted to assess the influence of loading conditions and variation of the interrelated components which comprise a medium-performance, large-caliber, multizone propelling charge on pressure-wave formation. These investigations were conducted via test firings of a multizone charge in a standard, well-instrumented 155-mm howitzer and in a 155-mm howitzer simulator.

II. TEST SETUP

A. Weapon

A 155-mm, M199 tube modified with pressure ports at thirteen axial locations was the test weapon for all the large-caliber firings. The standard muzzle brake was replaced with a special pressure-gage adapter used in support of a muzzle-pressure program that was conducted concurrently with the multizone firings. In order to measure system breech pressure, the standard M199 spindle was modified with two pressure ports without altering the two standoff bumps integral to the spindle system. For this weapon, the standard, lanyard-operated, spring-driven firing pin was replaced by a gas-activated firing pin.[5] The gas necessary to drive the modified firing pin into the M82

---

[5] *J. J. Rocchio, R. A. Hartman, and N. J. Gerri, "An Electric Primer-Operated Firing Pin Actuator for Large Caliber Guns," ARBRL-MR-02897, Ballistic Research Laboratory, USA ARRADCOM, January 1979 (AD A069109).*

percussion primer was obtained from an M52A3B1 electric detonating cap. The rapid and reproducible functioning of the M52A3B1 enabled instrumentation to be accurately timed by this firing system. After the M52A3B1 cap was detonated, there was, approximately, a 1-ms delay until the M82 primer functioned. An M158 recoil mechanism in conjunction with the upper carriage from a 155-mm, M59 gun was used to mount the APG sleigh which housed the 155-mm, M199 cannon. All tests with this system were done at the Sandy Point Firing Facility (Range 18) located at the Ballistic Research Laboratory (BRL).

B. Instrumentation

Instrumentation on all tests consisted of six Kistler 607C3 piezoelectric pressure transducers housed in the gun chamber: two each side-by-side in the spindle, two each 180 degrees apart at mid-chamber, and two each 30 degrees apart at the forward end of the chamber (Figure 2). These six gages (a redundant gage at each chamber position) were sufficient to yield an approximation to the pressure profile in the chamber. By differencing either of the spindle and forward-chamber gages (P1-P5, P1-P6, P2-P6, P2-P5), the first negative pressure gradient, $-\Delta P_i$, was determined. Projectile velocity was calculated using the distance between and the projectile arrival times at two solenoid coils located approximately 20 and 35 meters, respectively, forward of the gun muzzle. Ignition delay was defined as the time interval between the firing pulse and a spindle pressure of 7 MPa.

Generally, the data were recorded in real-time by the Ballistic Data Acquisition System (BALDAS) under the control of a PDP 11/45 minicomputer. If the data were not recorded by BALDAS because of some unusual ignition delay or computer malfunction, they were later digitized from an analog recording made of each test round.

C. Firing Components

The M483A1 projectile, Lot CG0-77J-008-001, inert-loaded with wax to 46.7 kg was used for all tests. For one series where in-bore interferometer data were taken, the M73 dummy fuze on the front of the projectile was modified with a flat surface to enhance the microwave return.

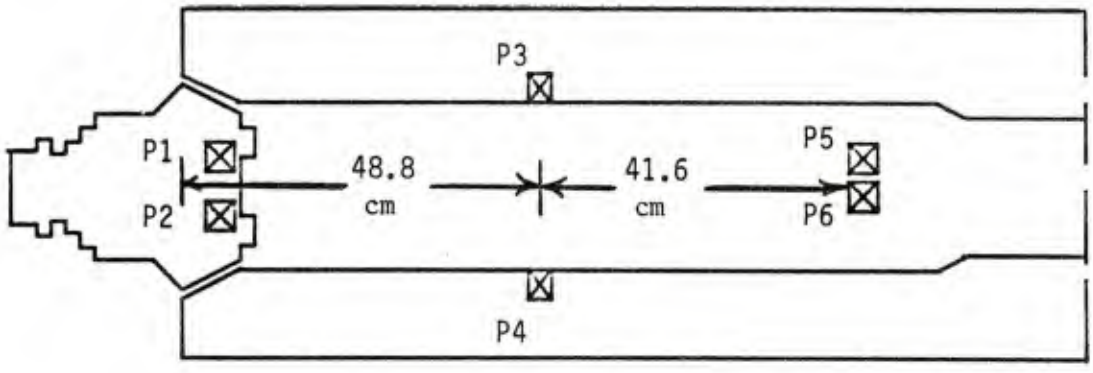

Figure 2. Locations of Pressure Transducers in M199 Chamber

The main propelling charge consisted, basically, of a Zone 3, Zone 4, and Zone 5 increment, each of which varied (Table 1) depending on test parameters. A photograph of a typical BRL multizone charge showing the two types of M1 propellant used in most of the tests is shown in Figure 3. Fabrication of bag increments and loading of charges were done at the Materiel Test Directorate (MTD), Aberdeen Proving Ground. All charges, except those used for Series 3, were conditioned at a temperature of 63°C for at least 24 hours prior to firing. The charges were loaded into the cannon chamber in varying configurations depending on the requirements of the test.

III. RESULTS

Nineteen series of 3 to 5 test rounds each were fired. To facilitate discussion, we have divided them into the following groups: Pressure-Wave Verification (Group A), Interzone Permeability (Group B), Energetic Components (Group C), Charge Position and Motion (Group D), and Initial Ignition Stimulus (Group E). Table 2 indicates the firing sequence with a rationale and general result for each series. Unless otherwise noted, the standoff from spindle face to basepad was 25 mm for each series.

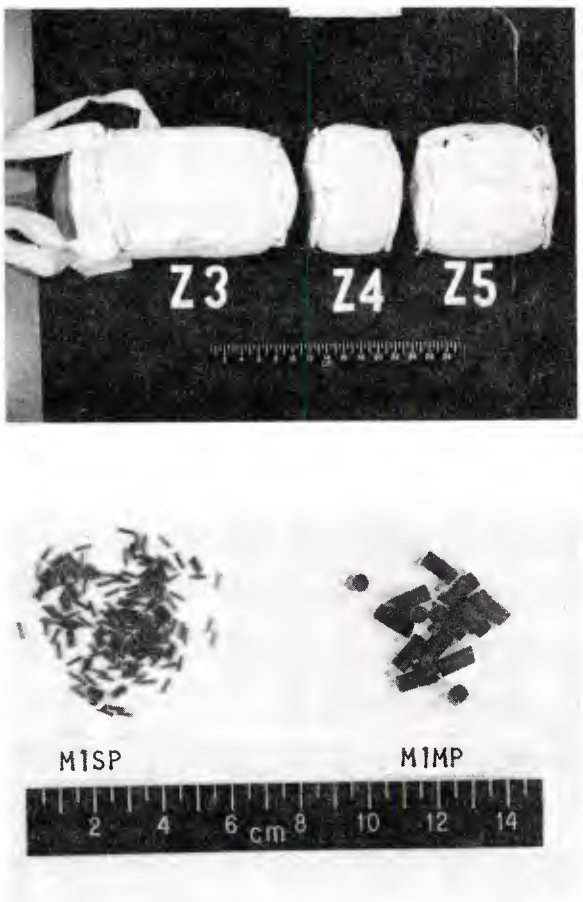

Figure 3. BRL Multizone Charge Fabricated from M1SP and M1MP Propellant

TABLE 1. CHARGE COMPOSITION

Series	Propellant at Each Increment Position*												Energetic Additive	Comment
	Basepad			Zone 3			Zone 4			Zone 5				
	Type	Wt (kg)	Web (mm)	Type	Wt (kg)	Web (mm)	Type	Wt (kg)	Web (mm)	Type	Wt (kg)	Web (mm)	(kg)	
1,2,3,4 5,6,7,8 9,10,11 12,18,19	CBI	0.085	N/A	M1SP	1.674	0.330	M1MP	0.794	0.853	M1MP	1.447	0.853	N/A	Basic charge used for most tests. Parasitic components added to individual series as noted in Table 2.
13	CBI	0.085	N/A	M1SP	1.674	0.419	M1MP	0.794	0.853	M1MP	1.447	0.853	N/A	Zone 3 propellant web change.
14	BP	0.085	Class 5	M1SP	1.674	0.330	M1MP	0.794	0.853	M1MP	1.447	0.853	N/A	Basepad composition change.
15	CBI	0.085	N/A	M1SP	1.674	0.330	M1MP	0.794	0.853	M1MP	1.447	0.853	0.284	Nitrocellulose tubes are part of the charge fabrication.
16	CBI	0.085	N/A	M1SP	1.674	0.330	M1MP	0.794	0.853	M1MP	1.447	0.853	0.636	
17	CBI	0.170	N/A	M1SP	1.674	0.330	M1MP	0.794	0.853	M1MP	1.447	0.853	N/A	Weight of CBI doubled (2 basepads).

*All charges except Series 3 were conditioned at 63°C for at least 24 hours prior to firing. Series 3 was conditioned at 21°C.

TABLE 2. TEST RATIONALE AND RESULTS*

Group	Series	Charge Description**	Test Rationale		Result****
			General	Specific	
A	1	Advanced Development XM211 bags (Class 1, Spec MIL-C-40070 and Class 2, Spec MIL-C-43157.) Charges loaded at Materiel Test Directorate (MTD). Flash reducer bag placed between Zone 4 & 5 increments	Verify pressure wave phenomena observed at other installations	Does changing loading facility significantly affect firing results?	Large pressure waves
	2	Ballistic Research Laboratory (BRL) fabricated bags (acrylic rayon), test-loaded at MTD		Does thinner bag material and/or conditioning temperature affect firing results?	Large pressure waves
	3*				Small pressure waves
B	4	Zones 4 & 5 increments consolidated into one long bag	Effect of interzone permeability in the charge	Does parasitic bag material and/or propellant interfaces between zones affect firing results?	Large pressure waves
	5	Zones 3, 4, & 5 increments consolidated into one long bag. The M1MP (Zones 4 & 5) stacked on top of the M1SP (Zone 3)			Large pressure waves
	18	Zones 3, 4, & 5 increments blended and consolidated into one long bag			Small pressure waves
	6	Flash reducer bag placed between Zones 3 & 4 increments		Does parasitic bag and/or chemical additives interspersed between zones affect firing results?	Large pressure waves
	7	Flash reducer bag placed between Zones 4 & 5 increments			Large pressure waves
C	15	Nitrocellulose slit tubes axially inclosing the Zone 3 increment.	Effect of energetic components on the charge	Does energetic*** nitrocellulose material axially inclosing the charge affect firing results?	Large pressure waves
	16	Nitrocellulose slit tubes axially inclosing the Zones 3, 4, & 5 increments			Extremely large pressure waves

* All series except Series 3 were conditioned at 63°C. Series 3 was conditioned at 21°C. All charges except those in Series 1 were fabricated with bag material available at MTD. All firings were with basepad at 2.5-cm standoff unless noted otherwise.

** Composition details are noted in Table 1.

*** Nitrocellulose sleeves were 54% NC, 46% resin and additives and were obtained from a commercial company.

**** Small Pressure Waves (0 to 10 MPa); Medium Pressure Waves (10 to 20 MPa); Large Pressure Waves (20 to 60 MPa); Extremely Large Pressure Waves (Larger than 60 MPa).

TABLE 2. (continued) TEST RATIONALE AND RESULTS*

Group	Series	Charge Description**	Test Rationale		Result***
			General	Specific	
D	8	Cardboard spacer placed between the charge and projectile	Effect of charge position and motion	Does absence of charge motion early in the ignition cycle affect firing results?	Large pressure waves
	9	Nylon tape used to tightly bind charge increments together		Does charge integrity affect firing results?	Large pressure waves
	10	Zone 3 & 4 increments at spindle, Zone 5 increment at projectile base		Does initial positioning of charge increments affect firing results?	Small pressure waves
	11	Zone 3 increment at spindle, Zone 4 & 5 increments at projectile base			Small pressure waves
	12	Charge (Zones 3, 4, & 5) at projectile base (40 cm from spindle face)			Small pressure waves
E					
	13	Propellant web for Zone 3 increment increased	Effect of ignition stimulus	Does a larger web MISP in the Zone 3 increment affect firing results?	Large pressure waves
	19	Propellant ignition order changed from CBI/Zone 3/Zone 4/Zone 5 to CBI/Zone 4/Zone 5/Zone 3		Does the order of ignition of a two-web charge affect firing results?	Medium pressure waves
	14	CBI in basepad replaced with fast-burning Class 5 black powder		Does a fast igniter affect firing results?	Large pressure waves
	17	Two (2) CBI basepads used on charge. Propellant order is CBI/Zone 3/Zone 4/ Zone 5/CBI		Does multiple ignition sources affect firing results?	Medium pressure waves

* All series except Series 3 were conditioned at 63°C. Series 3 was conditioned at 21°C. All charges except those in Series 1 were fabricated with bag material available at MTD. All firings were with basepad at 2.5-cm standoff unless noted otherwise.

** Composition details are noted in Table 1.

*** Small Pressure Waves (0 to 10 MPa); Medium Pressure Waves (10 to 20 MPa); Large Pressure Waves (20 to 60 MPa); Extremely Large Pressure Waves (Larger than 60 MPa).

A. Pressure-Wave Verification (Group A)

Rounds fired in Group A were to verify pressure-wave phenomena reported in previous XM211 firings at other facilities and establish a baseline charge for this study. Figure 4 depicts the spatial relationships of chamber/charge configuration for the pressure-wave verification series. Series 1 used standard Advanced Development XM211 bags loaded at MTD. Series 2 and 3, made using XM211 bags as the model, were fabricated from cloth available locally. The charges for Series 1 were slightly smaller in diameter and longer in length than the baseline charges. All three series consisted of the Zones 3, 4, and 5 increments base-ignited with 85 g of CBI.* Series 3 was conditioned at 21°C while Series 1 and 2 were conditioned at 63°C. Table 3 summarizes the firing results.

Table 3. Summary of Firing Data* for Group A

Series	P_{max} (MPa)	$-\Delta P_i$ (MPa)	Coil Velocity (m/s)	Ignition Delay (ms)
1	149.3 (2.2)	48.5 (6.0)	449.8 (0.9)	42 (9.0)
2	146.9 (1.2)	36.4 (7.2)	454.4 (0.9)	36 (3.0)
3**	123.7 (3.8)	5.2 (3.9)	442.8 (1.1)	83 (21.2)

* Values shown are averages for 4 or 5 firings. Series standard deviations are shown in parentheses.

** Series 3 conditioned at 21°C.

Pressure-wave levels were large for Series 1 and 2, and were similar to previous XM211 firings. The change in bag material and loading facility operation had, apparently, little or no influence on this aspect of the burning characteristics of the charges. These two series verified the pressure-wave phenomena reported at other facilities and established the Series 2 charge for use as a baseline. Figure 5 shows plots of spindle and forward-chamber pressure and pressure difference versus time which are typical of all series with large magnitude pressure waves ($-\Delta P_i$ between 20 and 60 MPa). Here we have used the conventional indicator of pressure-wave magnitude, namely, the initial negative difference between the pressure recorded at the spindle and that recorded near the projectile base, $-\Delta P_i$, to determine combustion instability. Series 3 was fired to determine if ambient conditioning (21°C), as opposed to the more involved high-temperature conditioning (63°C), was sufficient to generate substantial pressure waves. Although small pressure waves were observed, they were not of sufficient magnitude to assess the

* Clean burning igniter

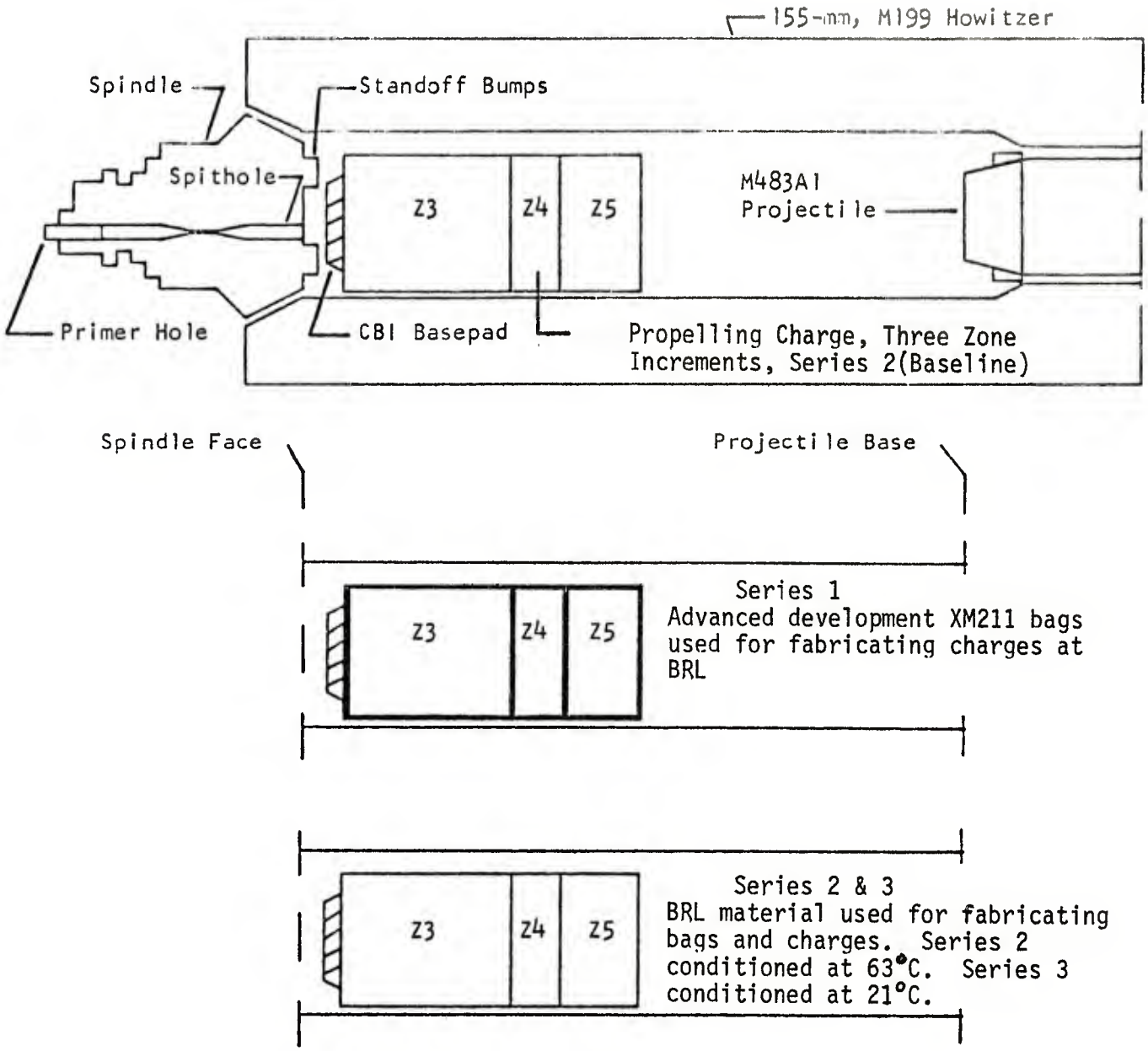

Figure 4. Charge/Chamber Configurations for Pressure-Wave Verification Tests, Group A

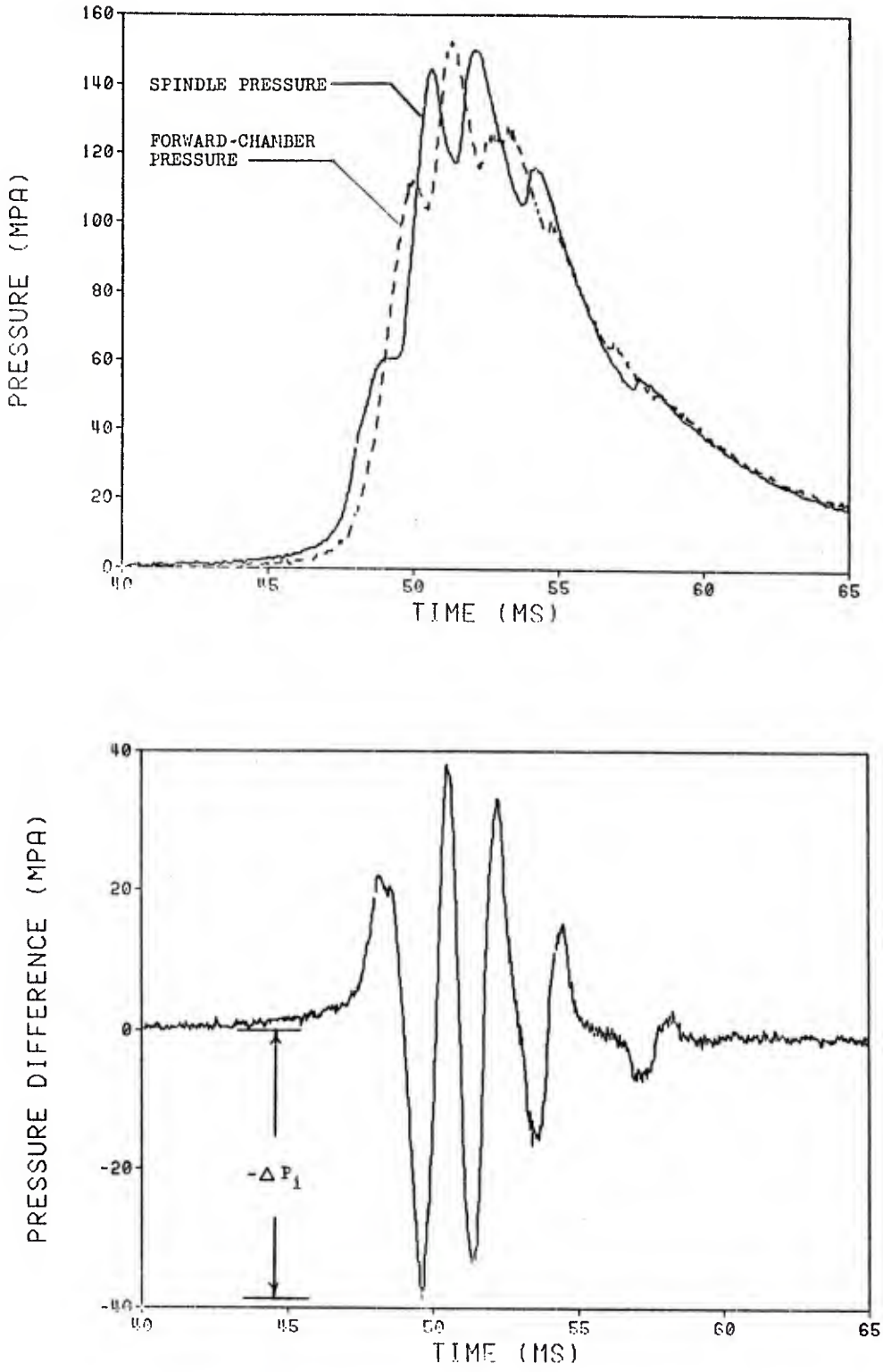

Figure 5. Pressure and Pressure Difference for Charges with Large Pressure Waves, Typical of Series 1,2,4,5,6,7,8,9,13,14 and 15

effects of compositional and/or spatial chamber/charge changes on pressure-wave formation. The data of Figure 6 are typical of all series with small pressure waves ($-\Delta P_i$ between 0 and 10 MPa). Since ambient conditions were not suitable for these tests, all subsequent charges were conditioned and fired at 63°C.

B. Interzone Permeability (Group B)

Five series of rounds were fired in Group B (Table 2) to determine the extent to which nonenergetic, interzone barriers (Series 4, 5, 6, and 7) or altered propellant interfaces between zones of a charge (Series 18) affect the formation of pressure waves. The alteration to each series from that of the baseline (Series 2) is depicted in Figure 7. The number of nonenergetic, interzone cloth end caps was reduced from four in the baseline series to two in Series 4 to none in Series 5 and 18. In addition, the propellant loading was varied from layered in Series 5 (M1SP/M1MP/M1MP) to a composite blend of the M1SP and M1MP in Series 18, a condition which rendered uniform overall charge permeability. Instead of two distinct propellant layers, each with its own porosity, permeability, and ignition characteristics, there was now only one. By eliminating these distinct propellant layers, the flow of igniter gases through the propellant bed was substantially altered. For Series 6 and 7, the standard geometry of three zone increments was used, except that small cloth discs containing 57 g of potassium nitrate flash reducer were inserted between Zones 3 and 4 for Series 6 and between Zones 4 and 5 for Series 7 prior to firing. The results are summarized in Table 4.

Table 4. Summary of Firing Data* for Group B

Series	P_{max} (MPa)	$-\Delta P_i$ (MPa)	Coil Velocity (m/s)	Ignition Delay (ms)
4	148.4 (1.5)	35.6 (3.9)	450.3 (1.0)	52 (5.9)
5	156.2 (7.1)	46.0 (9.9)	447.6 (1.3)	41 (2.9)
18	136.1 (1.2)	7.8 (1.0)	449.6 (0.8)	38 (1.9)
6	145.0 (3.6)	41.3 (8.7)	452.0 (1.2)	44 (4.6)
7	142.4 (2.3)	34.5 (3.1)	450.2 (0.9)	45 (1.9)

* Values shown are averages for 4 or 5 firings. Series standard deviations are shown in parentheses.

Large pressure waves were observed in all but Series 18, wherein small pressure waves and a slightly reduced maximum pressure occurred with no loss in average coil velocity. Blending of the M1SP and M1MP propellants altered the ignition, flamespreading, and charge dynamics from the baseline, a

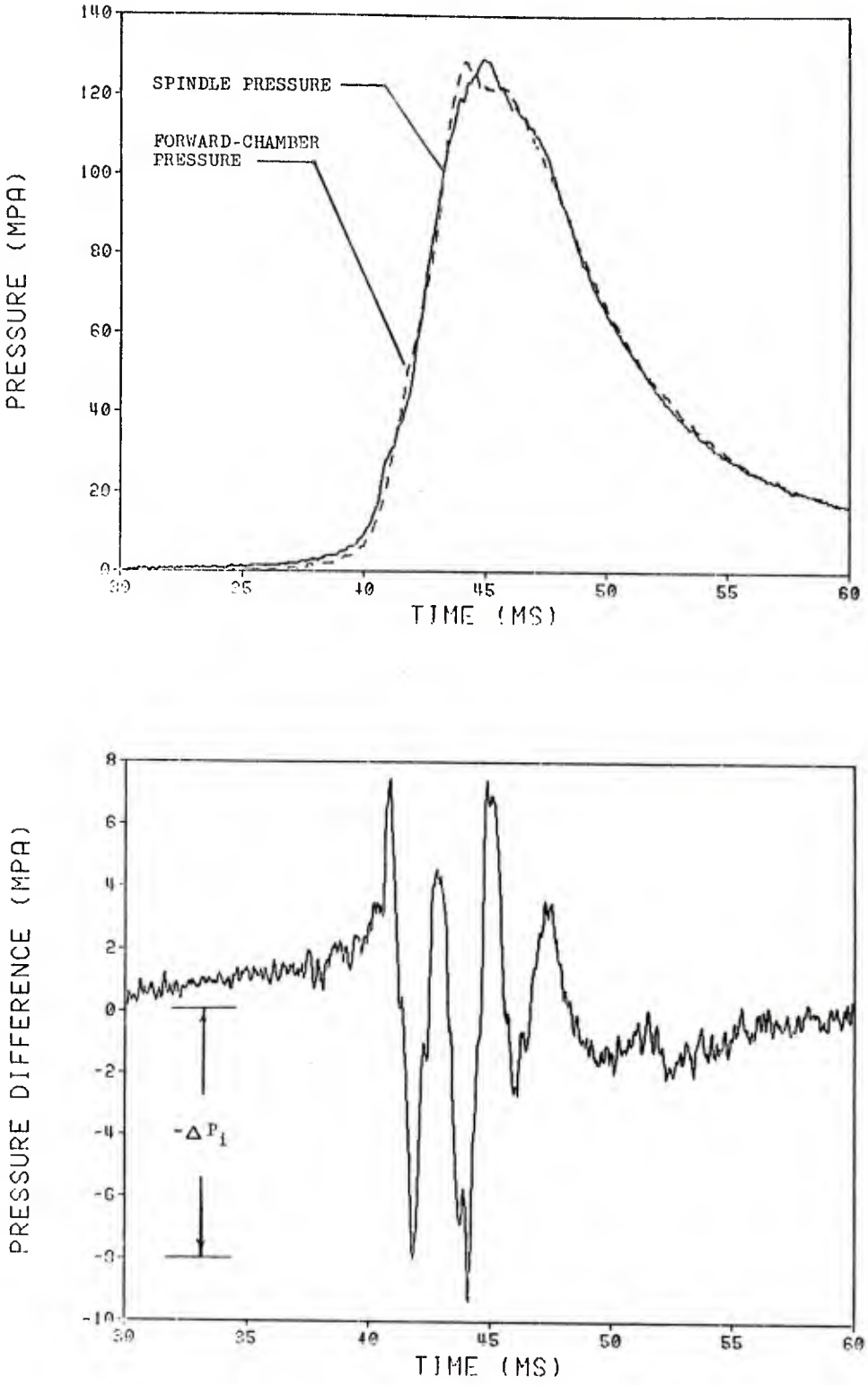

Figure 6. Pressure and Pressure Difference for Charges with Small Pressure Waves, Typical of Series 3, 10, 11, 12, and 18

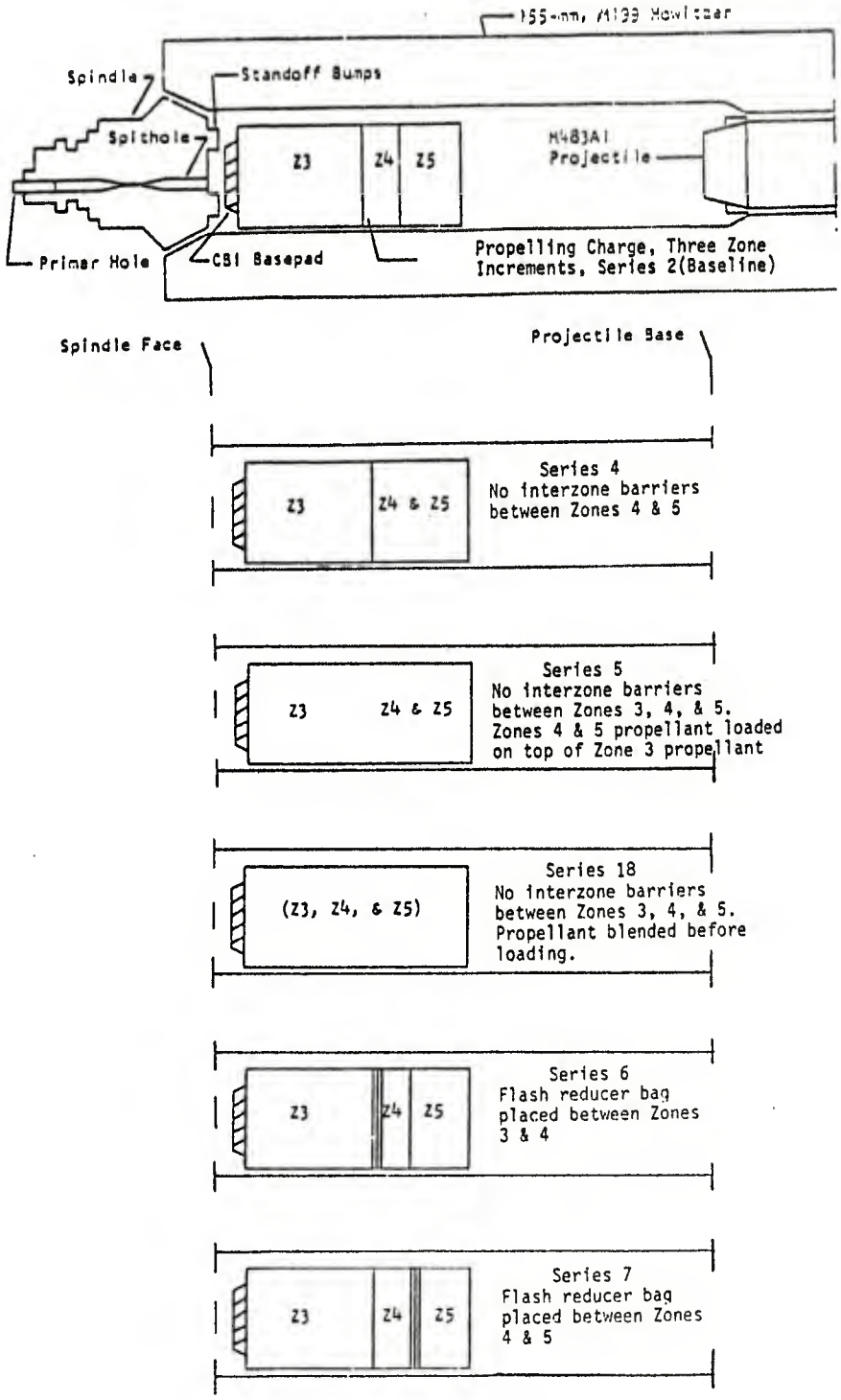

Figure 7. Charge/Chamber Configurations for Inter-Zone Permeability Tests, Group B

phenomenon not observed with the addition or deletion of bag endcaps and/or flash reducer bags.

C. Energetic Components (Group C)

Rigid, combustible sleeves were added to the charge to determine what effect the radial constraint coupled with the additional energy would have on charge performance. Series 15 and 16 were fabricated using energetic nitrocellulose (NC) tubes on the outside of the charge (Table 2 and Figure 8). Both Series 15 and 16 had NC tubes that were slit along their length and placed around the bag charge increments so that the NC tubes overlapped each other by 2 cm. The tubes were then circumferentially taped to increase charge rigidity and structural stability. For Series 15, two NC tubes were used covering just the Zone 3 increment; for Series 16, four NC tubes were used covering the entire charge. In both series, the base and front ends of the charge were unaltered with the CBI basepad and front cloth endcap both open to the chamber. The results are summarized in Table 5.

Table 5. Summary of Firing Data* for Group C

Series	P_{max} (MPa)	$-\Delta P_i$ (MPa)	Coil Velocity (m/s)	Ignition Delay (ms)
15	160.2 (4.6)	46.9 (4.9)	456.8 (0.8)	43 (4.1)
16	220.6 (11.3)	109.4 (16.2)	491.2 (--)	37 (3.2)

* Values shown are averages for 3 or 5 firings. Series standard deviations are shown in parentheses for all paremeters except Coil Velocity, Series 16, wherein data for only 2 of the 3 firings were obtained.

Combustion anomalies for Series 15, as measured by $-\Delta P_i$, were similar to those observed in earlier series even though P_{max} and velocity were somewhat higher. The slightly higher P_{max} and velocity may be attributable to the energy available from the addition of NC tubes into the charge burning cycle. When the NC tubes were approximately doubled and the charge further confined for Series 16, all measured parameters except ignition delay increased dramatically. The substantial increase in P_{max} from 160.2 MPa to 220.6 MPa (Figure 9) cannot be attributed, according to lumped-parameter interior ballistic calculations, to just the additional energy available in the NC sleeves. The pressure waves were so intense that damage was done to the spring in the firing housing assembly on each successive round. After the third of five rounds was fired, part of the housing assembly broke. Due to the increased charge diameter (four NC tubes around the charge) and the reduced charge-surface permeability (NC-tube wall rather than cloth-bag wall), the flow of igniter and early combustion gases was significantly altered in comparison to the baseline series, and it is likely that highly vigorous base ignition of the charge occurred. This localized ignition resulted in the high-level pressure waves noted, with a dramatic coupling of these waves into the overall chamber pressurization to produce the large increase in P_{max}. As would be expected, velocity increased with the increase in chamber pressure.

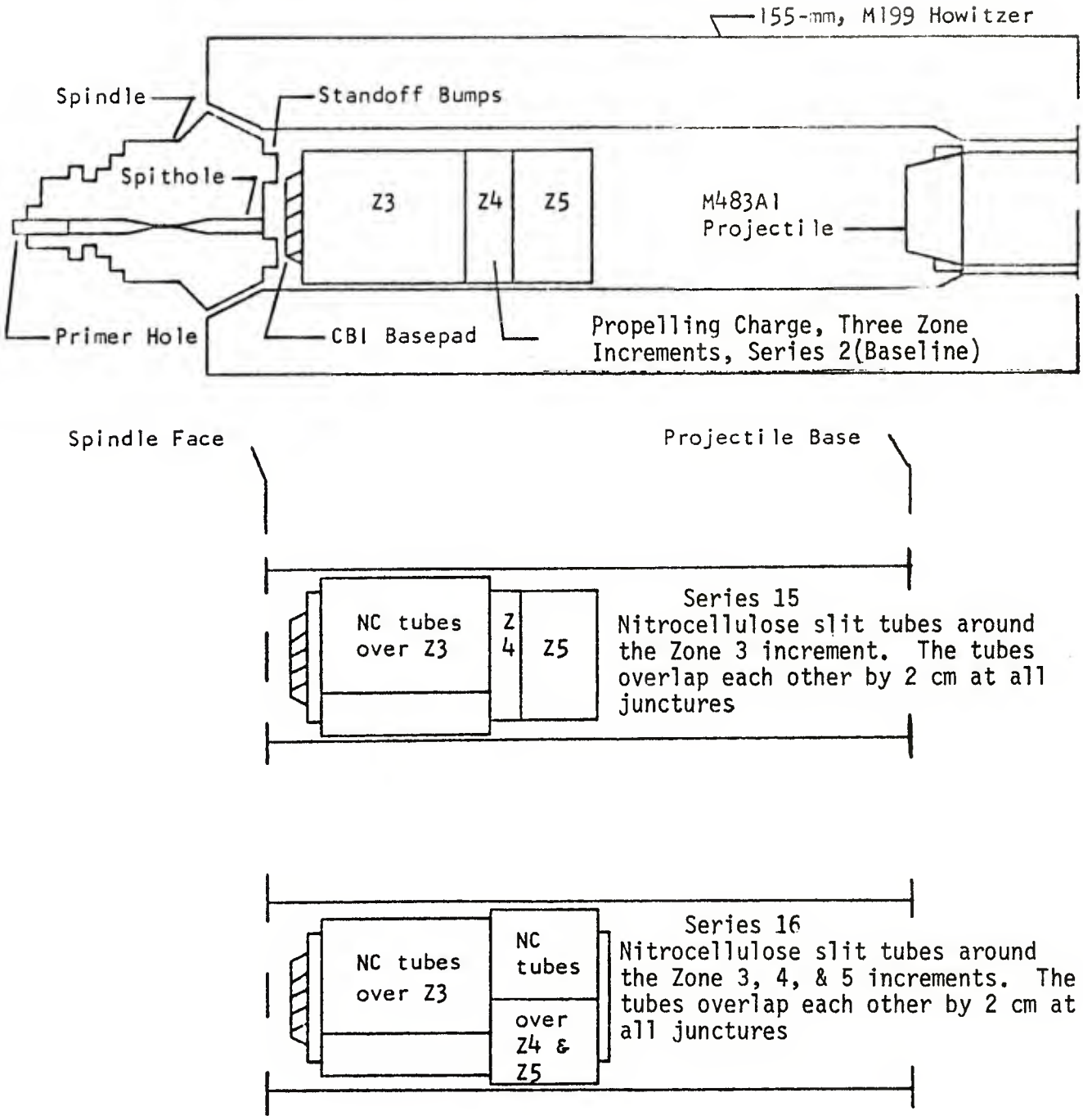

Figure 8. Charge/Chamber Configurations for Energetic Component Tests, Group C

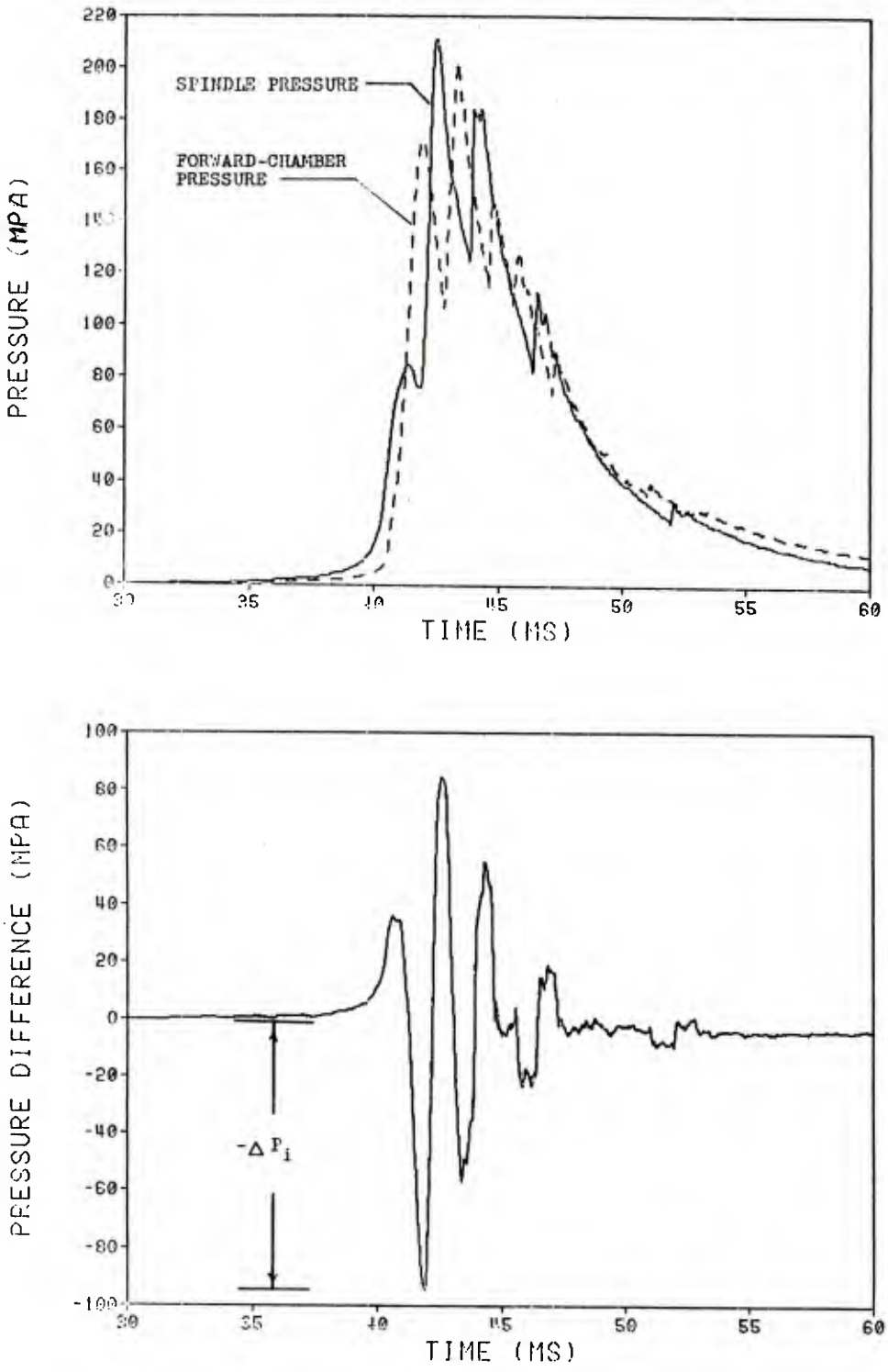

Figure 9. Pressure and Pressure Difference for Charges with Extremely Large Pressure Waves, Series 16

D. Charge Position and Motion (Group D)

Initial charge position (standoff) and charge motion during the early ignition cycle, especially with low-loading-density charges, can affect the charge performance. In Group D, several aspects of charge motion were explored. Details for each series are noted in Table 2 and Figure 10. In Series 8, a cardboard spacer was placed between the base of the projectile and the front of the baseline charge in an attempt to prevent charge motion during the early phase of the ignition process. In Series 9, the baseline charge was tightly bound with nylon tape. Four circumferential wraps (two each on Zone 3, one each on Zones 4 and 5) were made to radially constrain the charge. Two axial wraps, each starting at the base of the charge and ninety degrees apart, ran the length of the charge, across the top of the charge, and back down again to the base of the charge. These wraps were made in an attempt to prevent the zones from separating and expanding axially into the base of the projectile as separate increments during the early ignition cycle. Series 10, 11, and 12 were variations on initial zone increment positioning. For Series 10, the Zones 3 and 4 increments were at 2.5-cm standoff, the Zone 5 increment was forward against the base of the projectile; for Series 11, the Zone 3 increment was at 2.5-cm standoff, the Zones 4 and 5 increments were forward against the base of the projectile; and for Series 12, all three increments were at maximum standoff. (Basepad was 40 cm from spindle face.) Firing results for each of these series are shown on Table 6.

Table 6. Summary of Firing Data* for Group D

Series	P_{max} (MPa)	$-\Delta P_i$ (MPa)	Coil Velocity (m/s)	Ignition Delay (ms)
8	150.4 (1.4)	51.6 (2.7)	450.0 (0.8)	44 (4.0)
9	147.1 (3.1)	42.7 (4.5)	450.7 (1.3)	46 (5.6)
10	131.3 (1.2)	6.7 (2.7)	448.2 (1.4)	47 (5.7)
11	128.0 (2.7)	2.6 (0.9)	448.3 (0.8)	42 (14.5)
12	128.4 (1.1)	10.7 (0.7)	447.4 (1.1)	117 (13.3)

* Values shown are averages for 5 firings. Series standard deviations are shown in parentheses. Series 10 and 11 have initial increment separation.

Both the restriction on initial charge motion (Series 8) and initial increment separation (Series 9) during the early ignition cycle had no effect on the level of pressure waves of these rounds, as indicated by the large $-\Delta P_i$. For Series 10, 11, and 12, initial increment placement for a three-increment charge had a dramatic effect on the combustion process as shown by the low $-\Delta P_i$ and P_{max}. Moving the charge to the front of the chamber

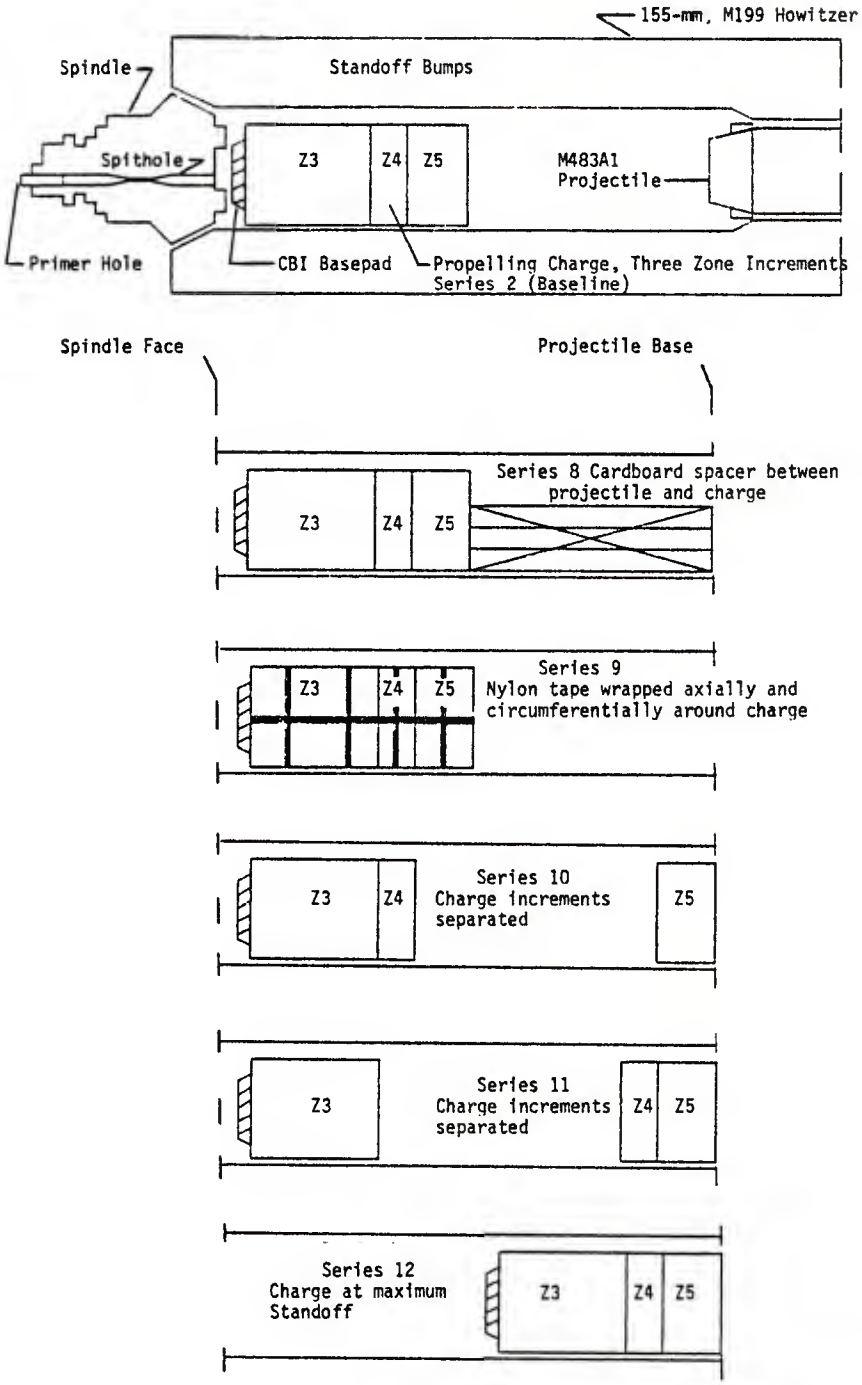

Figure 10. Charge/Chamber Configurations for Charge Position and Motion Tests, Group D

(Series 12) reduced $-\Delta P_i$ from previously seen values of 30 to 110 MPa to 10.7 MPa. Separating the charge into its zone increments further reduced $-\Delta P_i$. With only the Zone 5 increment initially placed at the projectile base (Series 10), $-\Delta P_i$ was reduced to 6.7 MPa, and when both the Zones 4 and 5 increments were loaded at the projectile base, the $-\Delta P_i$ was lowered to 2.6 MPa, a value smaller even than the Series 3 firing with ambient propellant.

E. Initial Ignition Stimulus (Group E)

Many times a slight change in the ignition process can alter the flame-spread and initial combustion process significantly so that a marginally stable round becomes stable. The effects of both faster and slower ignition on the combustion stability of the charge were examined. Details on each of the series are noted in Tables 1 and 2 and Figure 11. For Series 13, initial brisance was reduced by using a larger web propellant in the Zone 3 increment (0.42-mm web versus the standard 0.33-mm web). Another technique for reducing the initial flamespread and combustion rate was to alter the ignition sequence from the standard round (Basepad/Zone 3/Zone 4/Zone 5) to that noted in Series 19 (Basepad/Zone 4/Zone 5/Zone 3). Here the CBI basepad impacted directly on the Zone 4 propellant (M1MP) rather than on the faster burning Zone 3 propellant (M1SP). To increase the initial combustion rate, both faster burning basepad propellant and multiple basepads were used. In Series 14, the much faster burning Class 5 Black Powder replaced the standard CBI. In Series 17, two CBI basepads, one at its standard position on the base of the Zone 3 increment and the other on the forward face of the Zone 5 increment, replaced the standard system. Firing results for the four series are indicated in Table 7.

Table 7. Summary of Firing Data* for Group E

Series	P_{max} (MPa)	$-\Delta P_i$ (MPa)	Coil Velocity (m/s)	Ignition Delay (ms)
13	154.3 (2.6)	44.9 (5.8)	448.4 (0.9)	42 (6.2)
19	151.3 (11.6)	16.8 (6.9)	450.4 (2.1)	44 (2.4)
14	153.2 (9.6)	51.3 (9.4)	448.2 (3.1)	15 (4.1)
17	146.0 (2.1)	19.0 (5.7)	457.0 (0.6)	44 (3.9)

* Values shown are averages for 5 firings. Series standard deviations are shown in parentheses.

Results were mixed with one partial improvement in each category of faster and slower ignition. Increasing the web of the Zone 3 propellant or employing the faster black powder igniter did not reduce combustion instability. The $-\Delta P_i$ was large for each group (Series 13 and 14). Ignition delay for Series 14 was, as expected, significantly reduced. Altering the

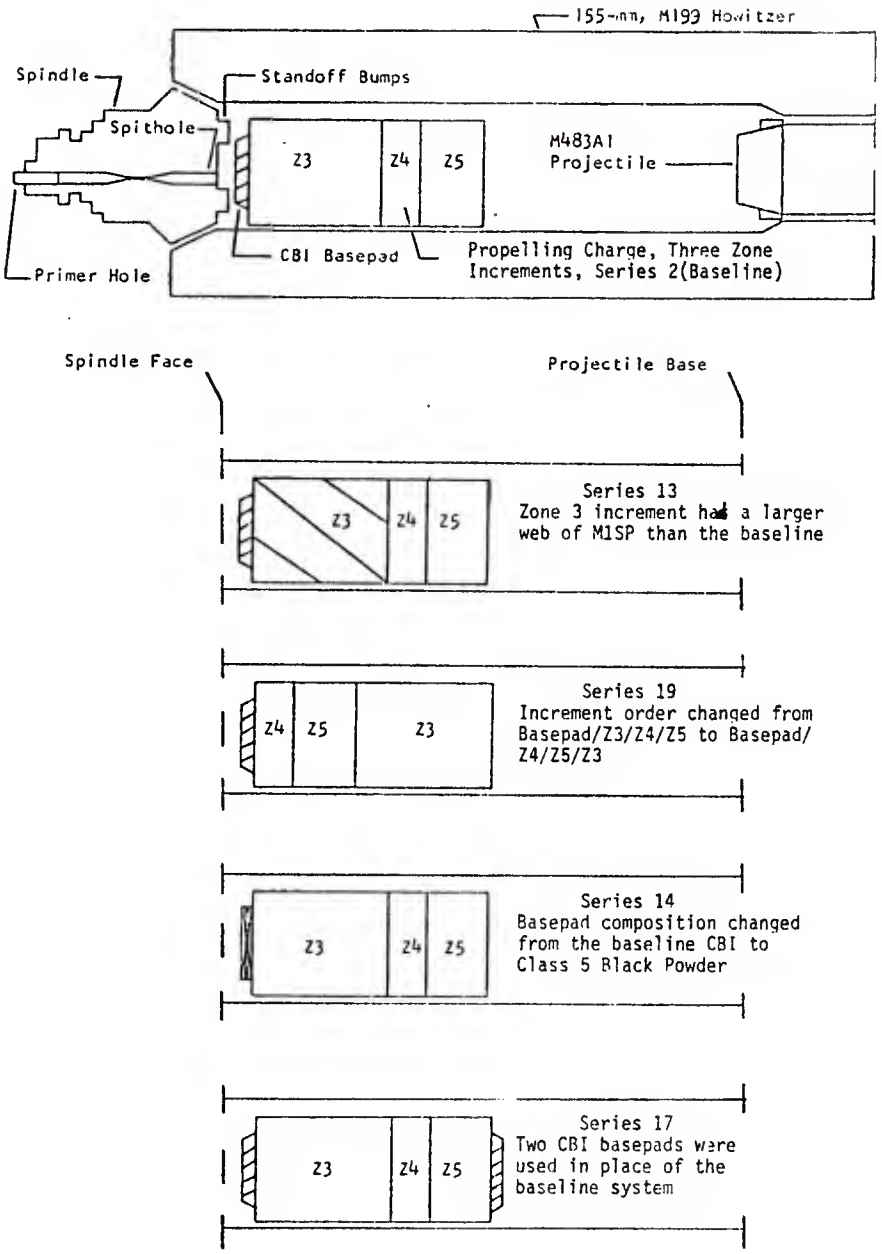

Figure 11. Charge/Chamber Configurations for Initial Ignition Stimulus Tests, Group E

sequence of propellant ignition (Series 19) or using two basepads (Series 17) for multiple ignition did significantly reduce pressure waves (Figure 12).

F. 155-mm Howitzer Simulator Firings

The 155-mm howitzer simulator used to conduct a variety of studies at the Ballistic Research Laboratory into the detailed phenomenology of propelling charges is shown in Figure 13. The massive mount, constructed of armor plate, accepts either plastic chambers or axially reinforced, filament-wound fiberglass chambers. The chambers used for this study were available cast acrylic tubing with nominal inner and outer diameters of 165 mm and 191 mm, respectively. The clear plastic offers much better visibility of the events transpiring within than does the fiberglass, but it fractures at significantly lower pressures. The pressure limit for these tubes has been found to be variable from sample to sample, and is pressure-rise-rate dependent. The fiberglass chambers were manufactured by NSWC/DL, and are wound on a mandrel to the interior dimensions of the 155-mm, M199 cannon chamber. The muzzle end of the chamber is closed by a projectile seated in a section of gun tube machined to the dimensions of the M199. The projectile may include onboard instrumentation. The breech end of the apparatus can be closed by one of four spindles: the mushroom configuration of the M199 or M185, or flattened-face versions of each. The M185 mushroom which was used for this study can be instrumented to take three Kistler 607C piezoelectric pressure transducers. Strain patches may be affixed to the chambers to monitor stresses induced by solid-phase dynamics.

Photographic data were recorded with a Hycam 40, high-speed, 16-mm camera. For the tests reported here, the data were recorded on Kodak Ektachrome 7241 film at a framing rate of approximately 5200 pictures per second. A 1-kHz timing signal was placed on the film by electronics internal to the camera, and the firing fiducial (time at which the firing voltage is applied to the gun) was also placed on the film to aid in correlation of the film data with other data. A mirror was positioned behind the mount to allow simultaneous recording on each single frame of the events occurring on both sides of the chamber.

Prior to and serving as a motivation of the standard gun test firings, a Zone 5 charge similar to those fired in the gun was test fired in the simulator. The charge was conditioned to 63°C prior to firing. A portion of the photographic data for this shot is shown in Figure 14. The top photograph shows the charge prior to firing, with the spindle at the right and the projectile at the left of the figure. Shown next in the figure is the early igniter functioning. After this, a mild luminous front oscillated between the spindle and projectile (not shown). As the charge began to burn, it became cocked so that the rear end was lifted off and the forward end remained on the bottom of the chamber. Further into the cycle, a slug of propellant (Zone 5 increment) separated from the charge and was propelled toward the projectile. Each of the seven final photographs of Figure 14 are separated by about 0.4 ms. The plastic tube failed in the frame succeeding the final photograph, and the velocity of the slug of propellant at this time was approximately 150 meters per second.

Given the behavior seen in this single test firing, one round each of the same charge composition and loading of Series 2, 8, 9, 10, and 11 was fired in

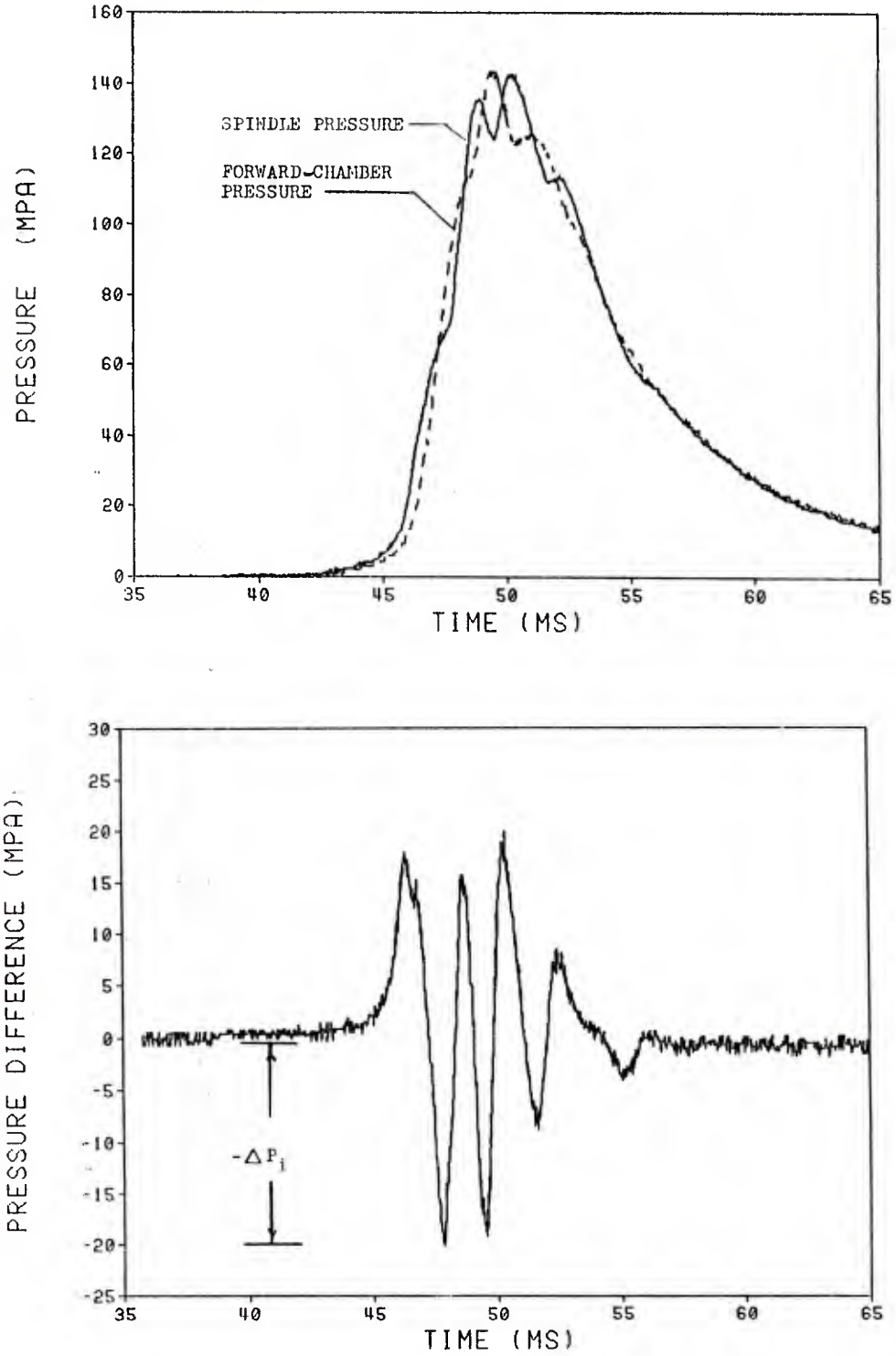

Figure 12. Pressure and Pressure Difference for Charges with Medium Pressure Waves, Typical of Series 17 and 19

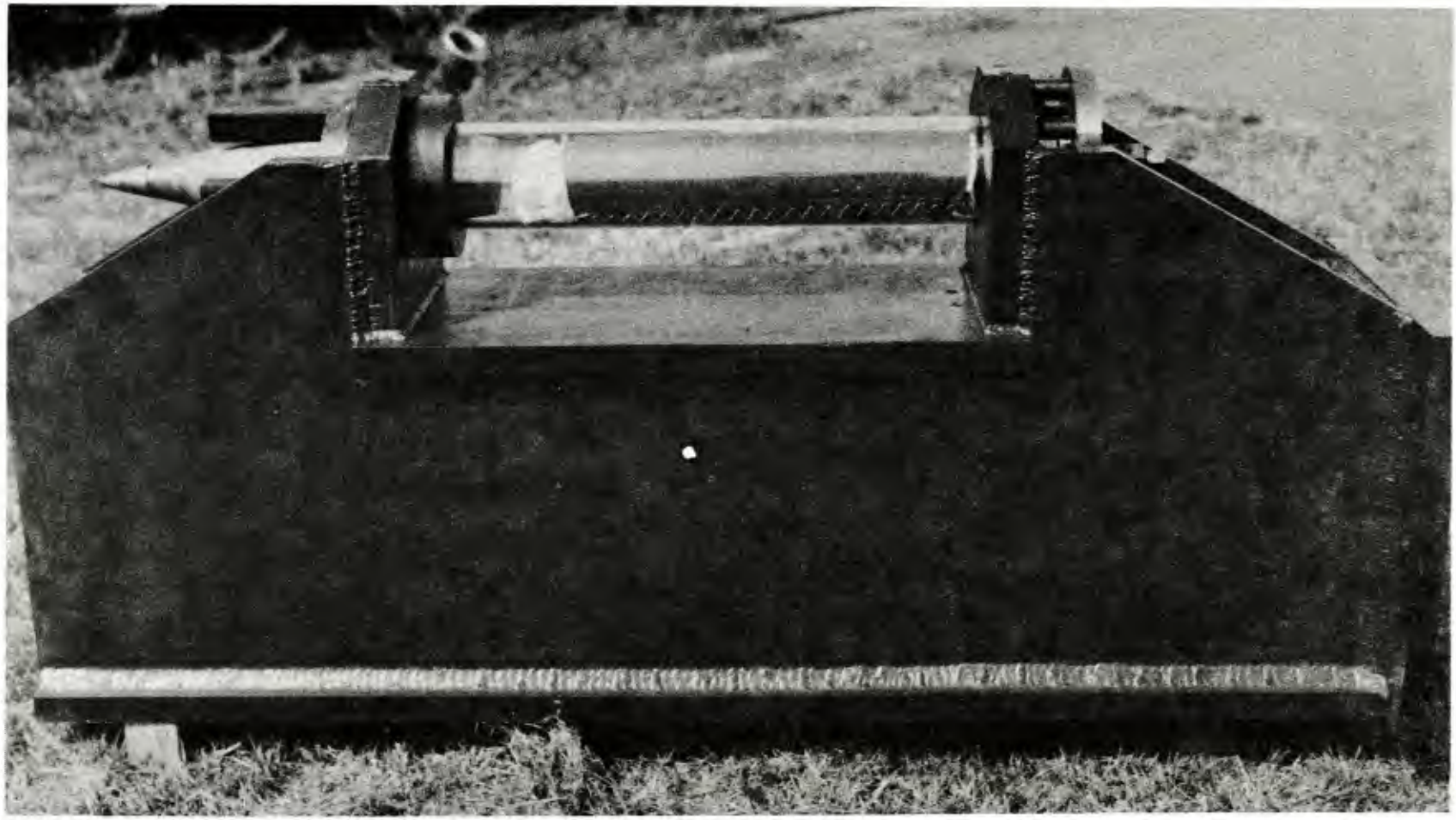

Figure 13. Photograph of Experimental Apparatus, 155-mm Howitzer Simulator

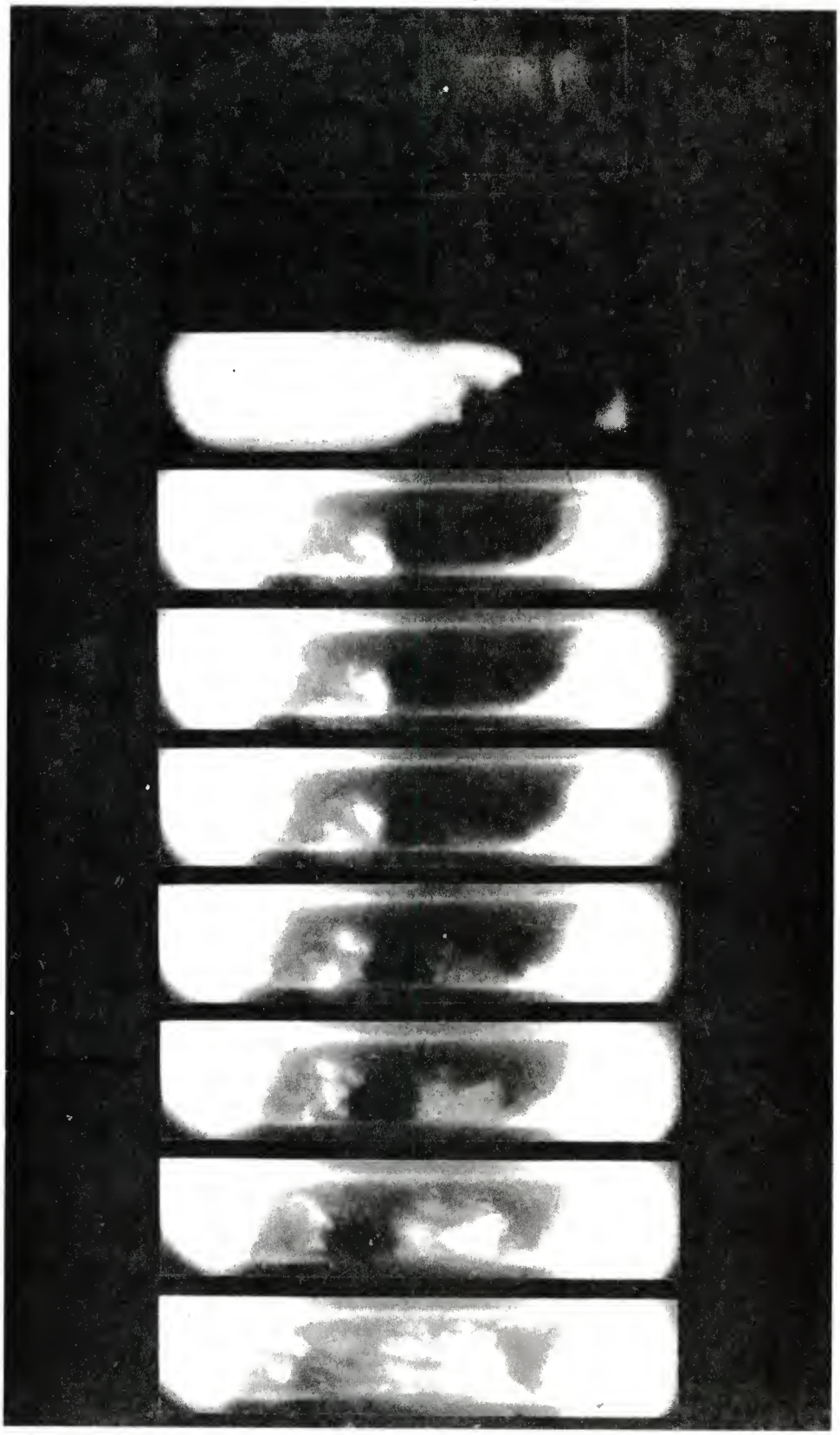

Figure 14. Film Flame Data, Zone 5 Charge

the simulator. The Series 2 firing was essentially a repeat of the shot just described. The plastic tube failed before any motion of packages of propellant was noticeable. Likewise, the tubes failed before charge movement in shots for Series 8 and 9, where the movement was constrained by reinforced tie straps or a cardboard spacer. Since these configurations yielded large pressure waves in the gun environment, it was hypothesized that the constraints probably failed at higher pressures, allowing movement of the propellant. The shots for Series 10 and 11, with increments separated in the chamber, showed no movement of any of the packages, a result consistent with the lower-level pressure waves produced in the gun.

IV. DISCUSSION AND CONCLUSIONS

In this study, the influences of charge interzone permeability, distribution of ullage, charge increment movement, igniter brisance and placement of parasitic components on the formation of pressure waves in temperature-conditioned, multizone charges were investigated. These are the parameters we earlier identified as those most likely to affect the detailed gas flow, bag rupture, and propellant motion characteristics of multizone charges. Figure 15 graphically illustrates the large range of peak chamber pressure and $-\Delta P_t$ obtained by changes in charge/chamber configuration and/or charge interzone parasitics.

Within the range of parameters studied, the results of this investigation are consistent with, but not a direct demonstration of, propellant motion and possible grain fracture as mechanisms for production of pressure waves in this type of charge. We note, in all instances for the 63°C-conditioned charge, where the forward increment could move during the flamespread cycle, albeit after initial confinement, that we obtained large-magnitude pressure waves. This motion is probably testimony to the strongly localized base ignition of a very rapidly burning package of propellant (Zone 3), whose product gases cannot percolate through the forward propellant bed and interzone barriers without inducing considerable motion of the forward package(s). This is particularly true of instances where the gases find no avenue of relief, as with the charge loaded completely in radially confining tubes (Series 16). In situations in which the forward element truly cannot move, such as at maximum standoff or with initial increment separation, the pressure waves are small. Further indication of this amelioration is presented by the low-level waves with the uniformly blended charge, where there are no interzone physical or porosity barriers, and with the double-basepad charge, which may have generated enough reverse thrust at the forward end of the charge to preclude substantial motion.

The overwhelming conclusion reached from this study is that the performance of the multizone charge is truly a function of many interacting processes, which are affected by the many interrelated components comprising the charge. We have identified areas of concern for bagged multizone charges; studies currently underway will indicate whether the concerns are valid for more rigidly confined charges of the future which will employ combustible cases.

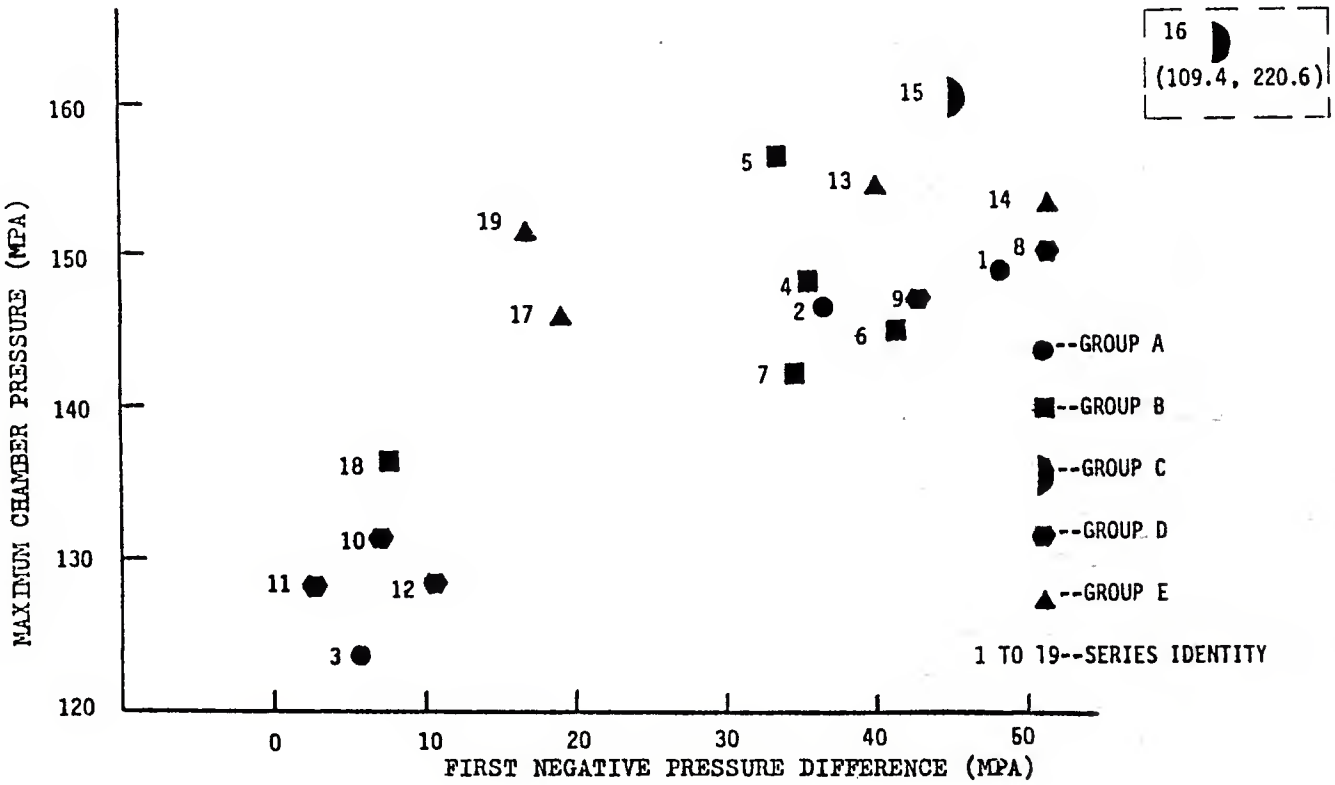

Figure 15. Sensitivity of Maximum Chamber Pressure to Pressure-Wave Level

REFERENCES

1. I. W. May, "The Role of Ignition and Combustion in Gun Propulsion: A Survey of Developmental Efforts," Proceedings of 13th JANNAF Combustion Meeting, CPIA Publication 281, Vol. I, pp. 315-340, September 1976.

2. I. W. May and A. W. Horst, "Charge Design Considerations and Their Effect on Pressure Waves in Guns," ARBRL-TR-02277, Ballistic Research Laboratory, USA ARRADCOM, December 1980 (AD A095342).

3. T. C. Minor and J. DeLorenzo, "Charge Design Approaches to the Reduction of Low Zone Stickers," Proceedings of 1976 JANNAF Propulsion Meeting, CPIA Publication 280, Vol. III, pp. 403-434, December 1976.

4. R. J. DeKleine, "155-mm XM211 Propelling Charge Zones 3-6 - Design Review Minutes," Office of Project Manager, Cannon Artillery Weapons Systems, Dover, NJ, April 9, 1980.

5. J. J. Rocchio, R. A. Hartman, and N. J. Gerri, "An Electric Primer-Operated Firing Pin Actuator for Large Caliber Guns," ARBRL-MR-02897, Ballistic Research Laboratory, USA ARRADCOM, January 1979 (AD A069109).

APPENDIX A

PLOTS OF SPINDLE PRESSURE (SOLID LINE), FORWARD-CHAMBER PRESSURE (DASHED LINE) AND PRESSURE DIFFERENCE VERSUS TIME

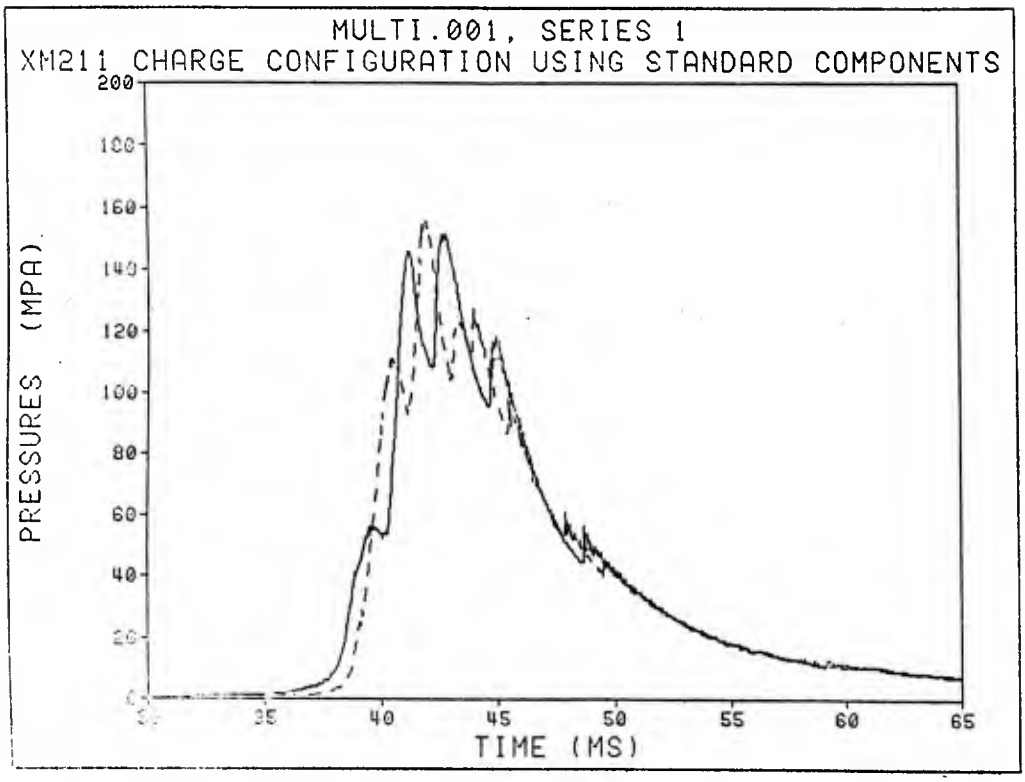
MULTI.001, SERIES 1
XM211 CHARGE CONFIGURATION USING STANDARD COMPONENTS
PRESSURES (MPA)
200
180
160
140
120
100
80
60
40
20
0
30
35
40
45
50
55
60
65
TIME (MS)

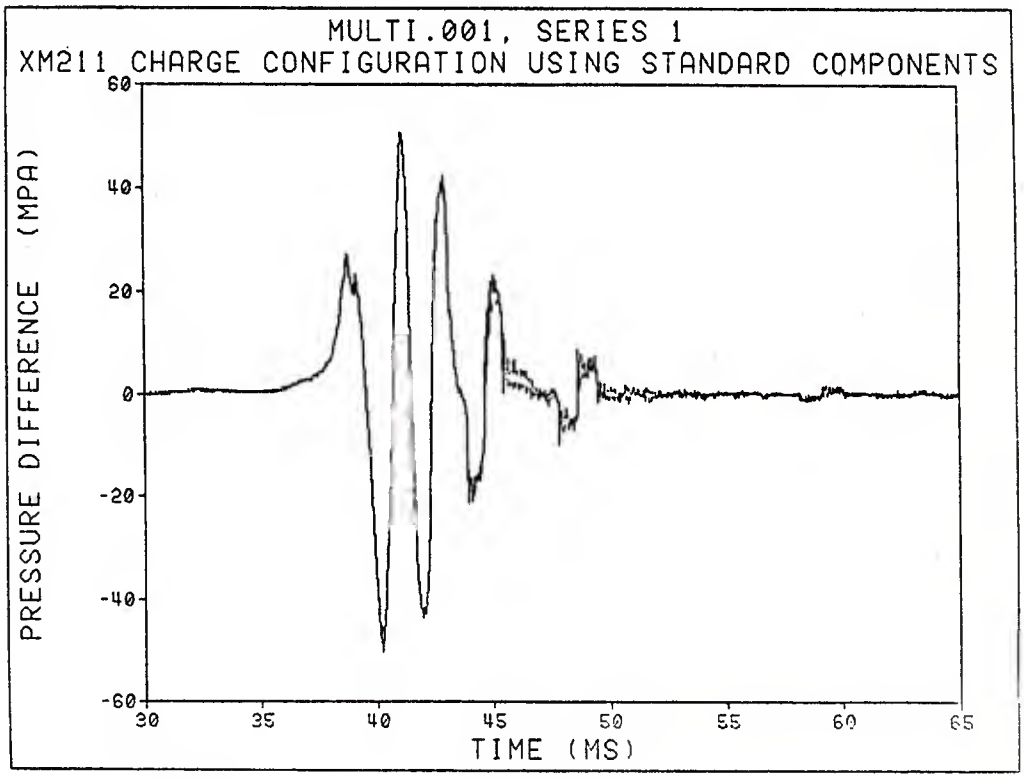
MULTI.001, SERIES 1
XM211 CHARGE CONFIGURATION USING STANDARD COMPONENTS
PRESSURE DIFFERENCE (MPA)
60
40
20
0
-20
-40
-60
30
35
40
45
50
55
60
65
TIME (MS)

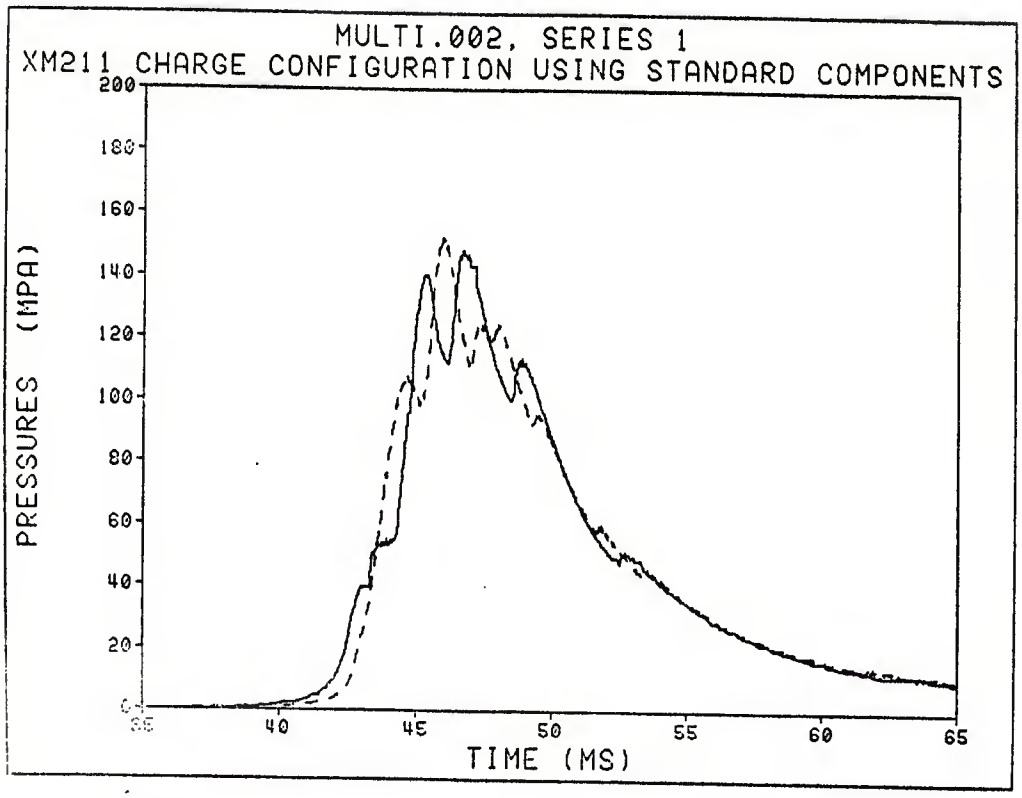
MULTI.002, SERIES 1
XM211 CHARGE CONFIGURATION USING STANDARD COMPONENTS
PRESSURES (MPA)
200
180
160
140
120
100
80
60
40
20
0
35
40
45
50
55
60
65
TIME (MS)

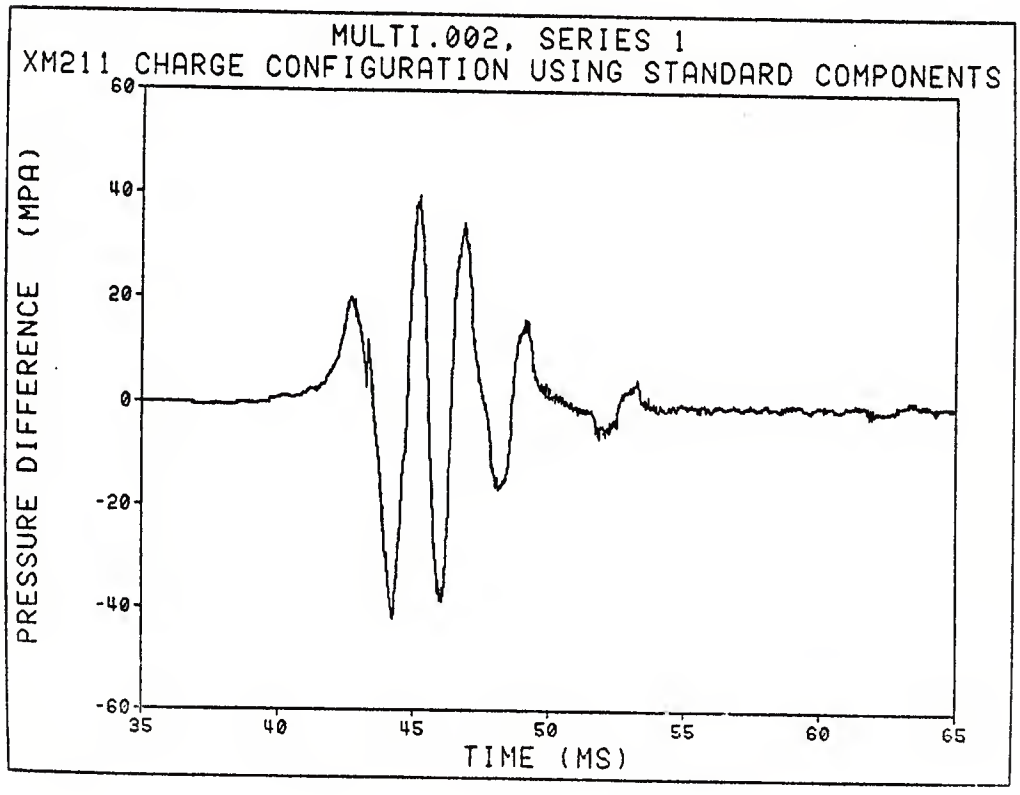
MULTI.002, SERIES 1
XM211 CHARGE CONFIGURATION USING STANDARD COMPONENTS
PRESSURE DIFFERENCE (MPA)
60
40
20
0
-20
-40
-60
35
40
45
50
55
60
65
TIME (MS)

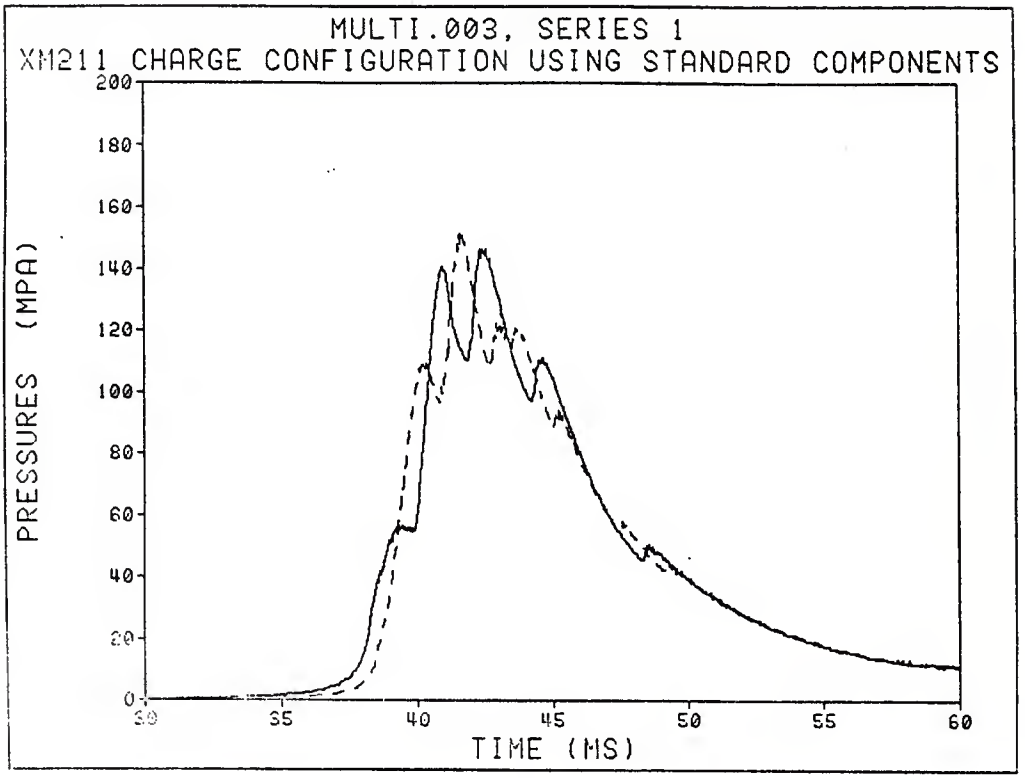
MULTI.003, SERIES 1
XM211 CHARGE CONFIGURATION USING STANDARD COMPONENTS
PRESSURES (MPA)
200
180
160
140
120
100
80
60
40
20
0
30
35
40
45
50
55
60
TIME (MS)

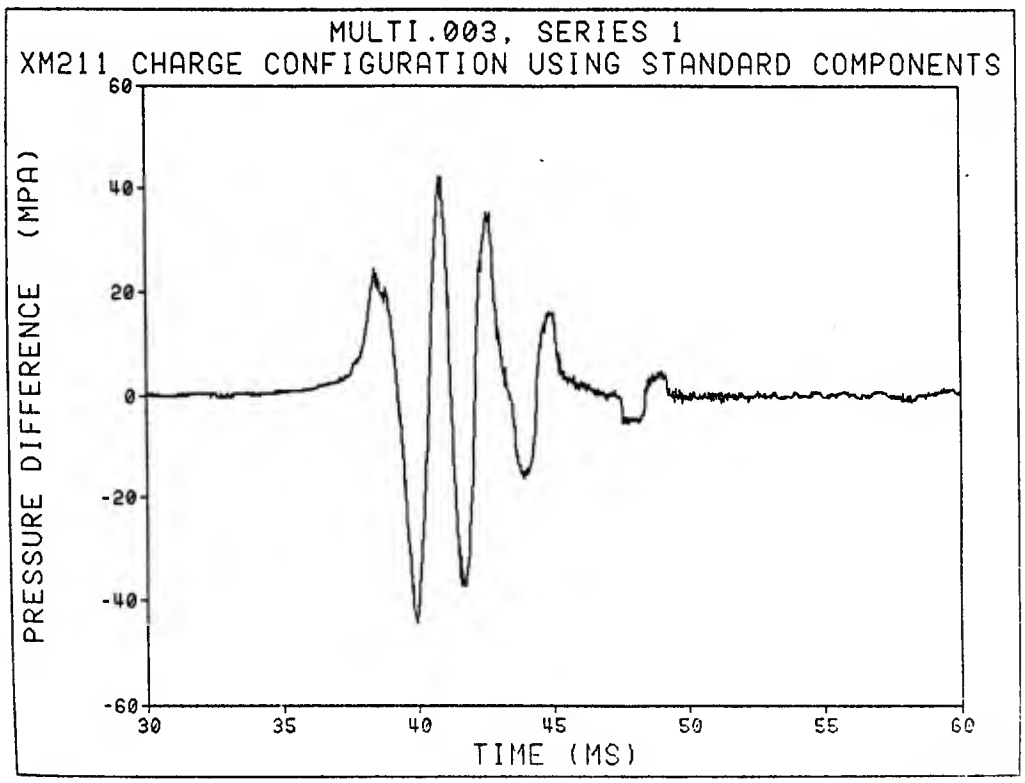
MULTI.003, SERIES 1
XM211 CHARGE CONFIGURATION USING STANDARD COMPONENTS
PRESSURE DIFFERENCE (MPA)
60
40
20
0
-20
-40
-60
30
35
40
45
50
55
60
TIME (MS)

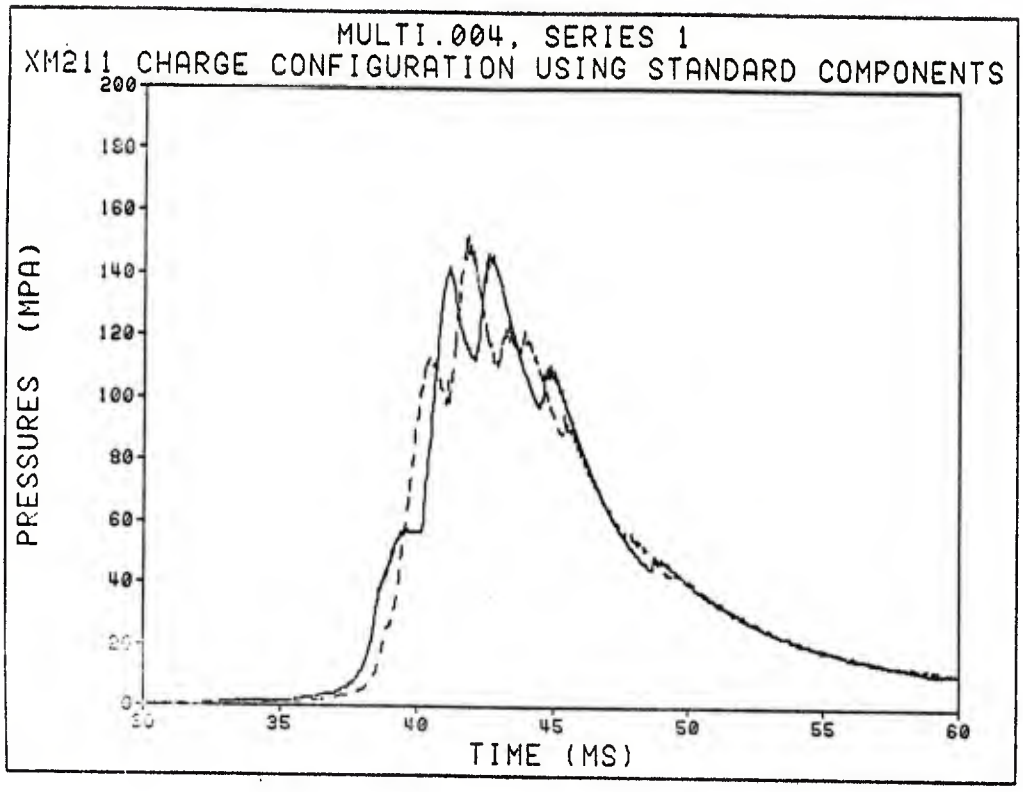
MULTI.004, SERIES 1
XM211 CHARGE CONFIGURATION USING STANDARD COMPONENTS
PRESSURES (MPA)
200
180
160
140
120
100
80
60
40
20
0
30
35
40
45
50
55
60
TIME (MS)

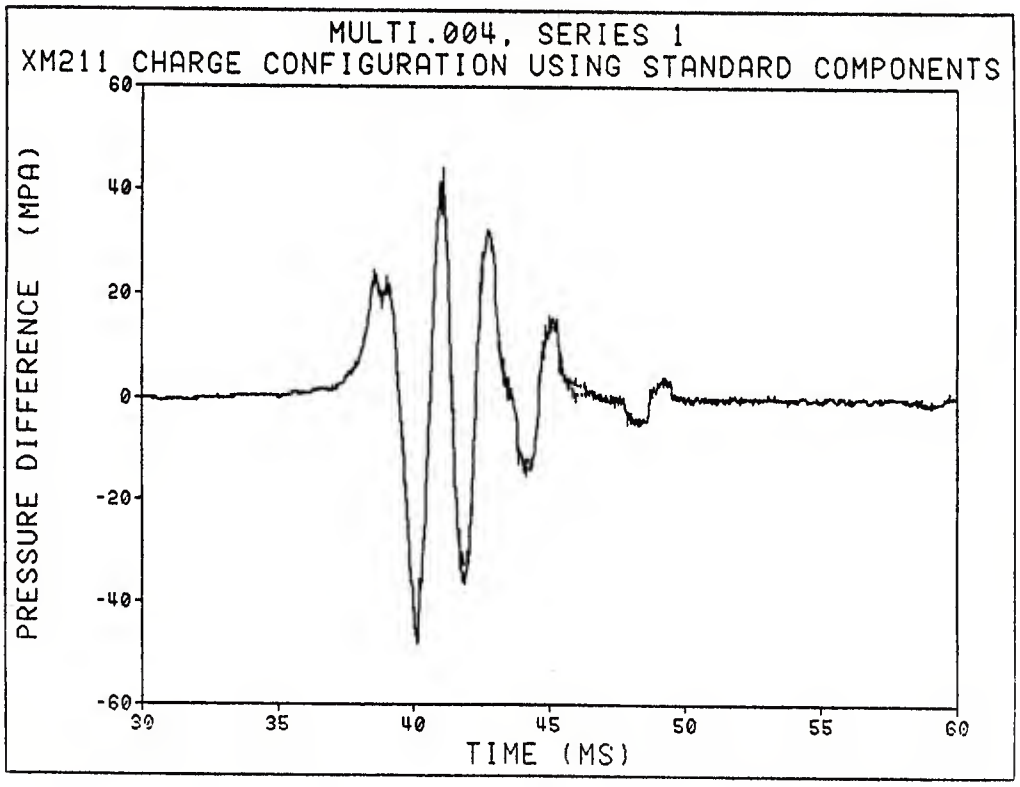
MULTI.004, SERIES 1
XM211 CHARGE CONFIGURATION USING STANDARD COMPONENTS
PRESSURE DIFFERENCE (MPA)
60
40
20
0
-20
-40
-60
30
35
40
45
50
55
60
TIME (MS)

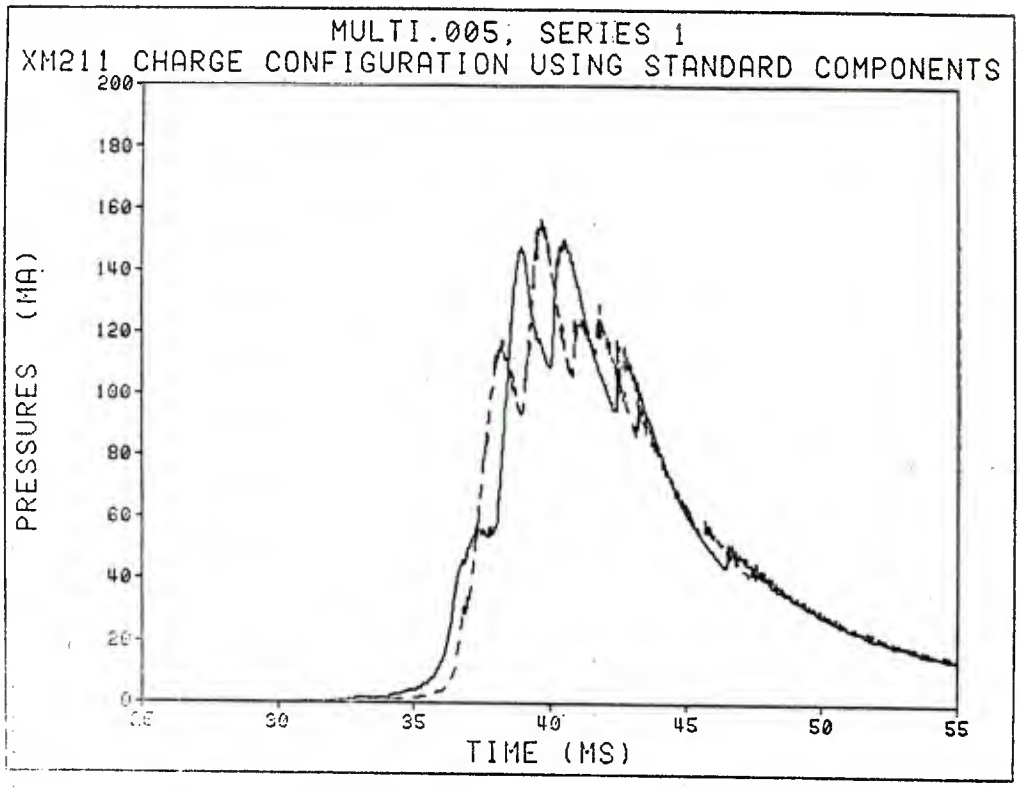
MULTI.005, SERIES 1
XM211 CHARGE CONFIGURATION USING STANDARD COMPONENTS
PRESSURES (MA)
200
180
160
140
120
100
80
60
40
20
0
30
35
40
45
50
55
TIME (MS)

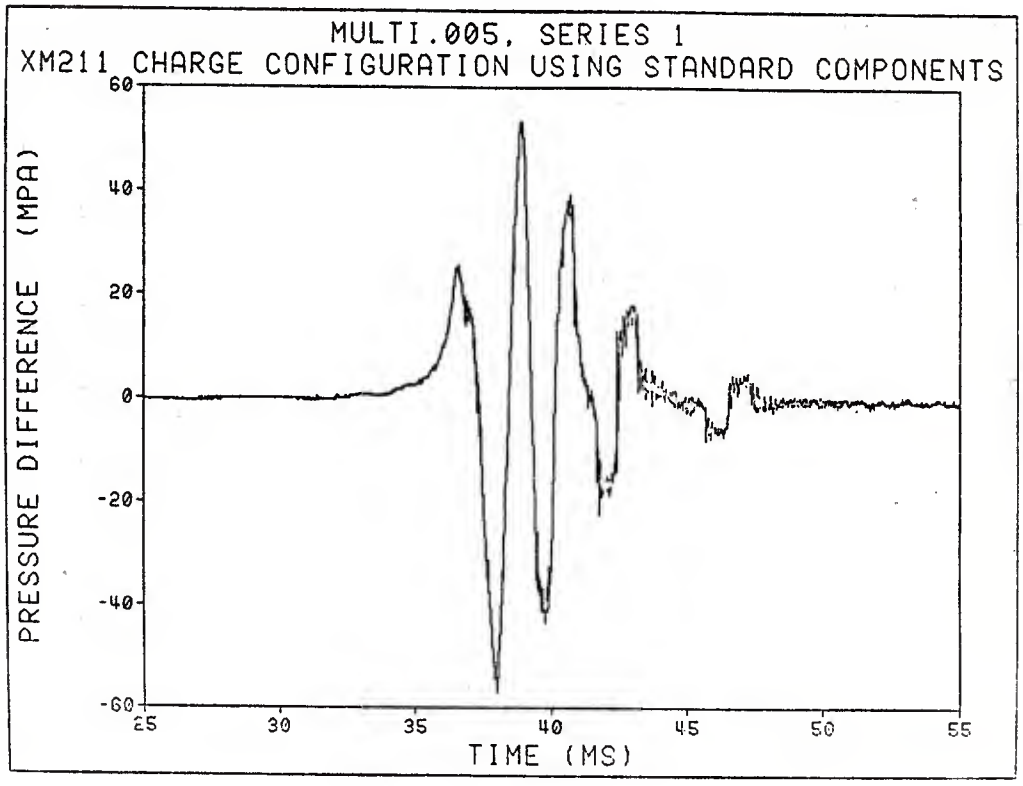
MULTI.005, SERIES 1
XM211 CHARGE CONFIGURATION USING STANDARD COMPONENTS
PRESSURE DIFFERENCE (MPA)
60
40
20
0
-20
-40
-60
25
30
35
40
45
50
55
TIME (MS)

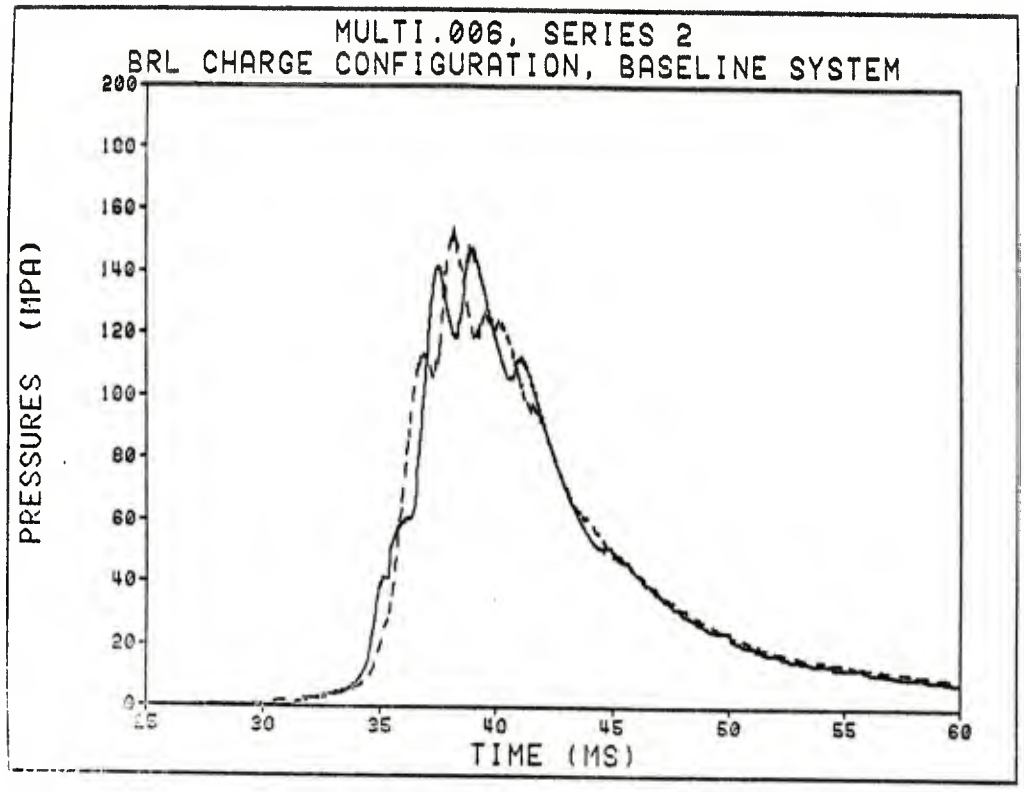
MULTI.006, SERIES 2
BRL CHARGE CONFIGURATION, BASELINE SYSTEM
PRESSURES (MPA)
200
180
160
140
120
100
80
60
40
20
0
25
30
35
40
45
50
55
60
TIME (MS)

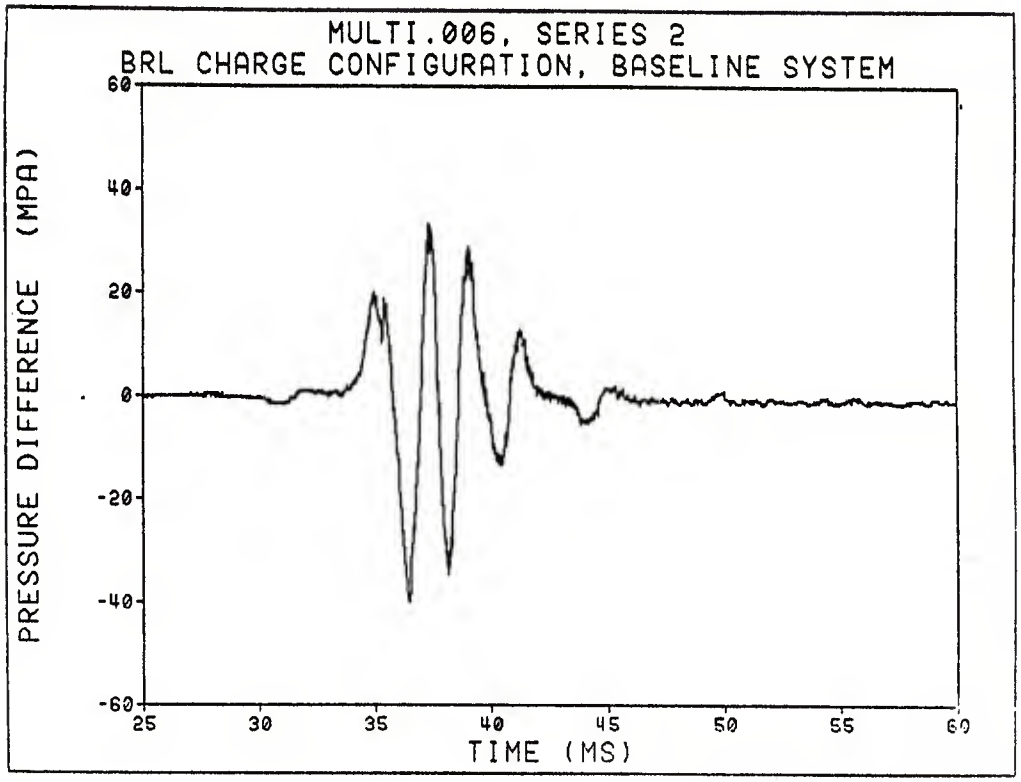
MULTI.006, SERIES 2
BRL CHARGE CONFIGURATION, BASELINE SYSTEM
PRESSURE DIFFERENCE (MPA)
60
40
20
0
-20
-40
-60
25
30
35
40
45
50
55
60
TIME (MS)

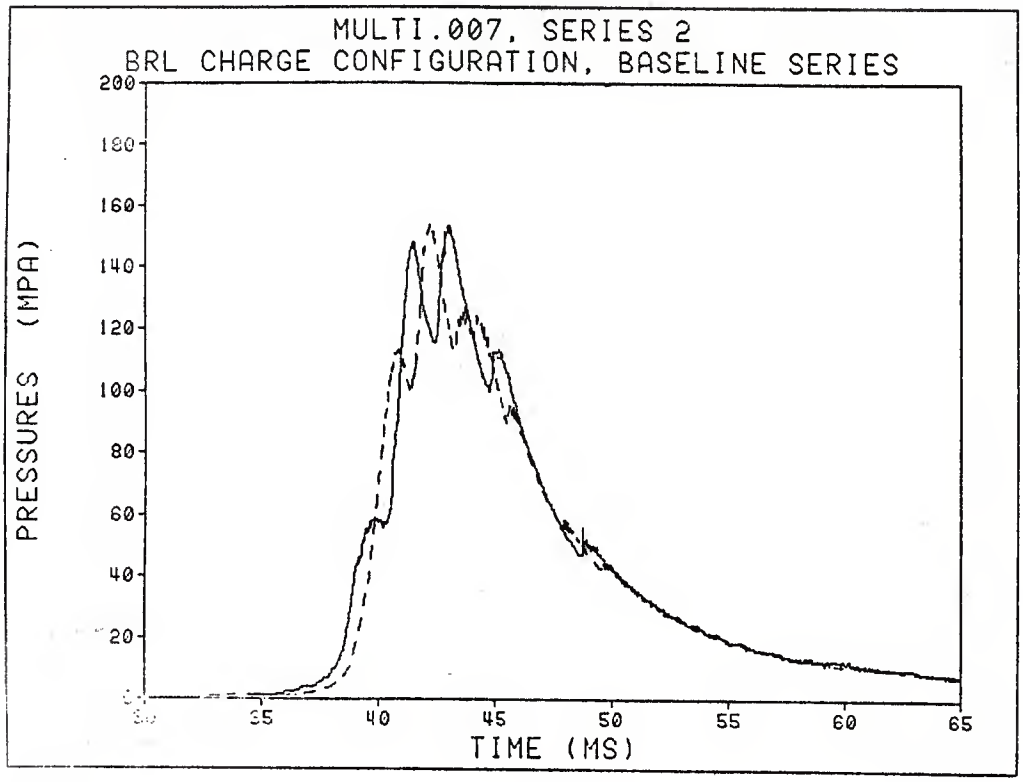
MULTI.007, SERIES 2
BRL CHARGE CONFIGURATION, BASELINE SERIES
PRESSURES (MPA)
200
180
160
140
120
100
80
60
40
20
0
35
40
45
50
55
60
65
TIME (MS)

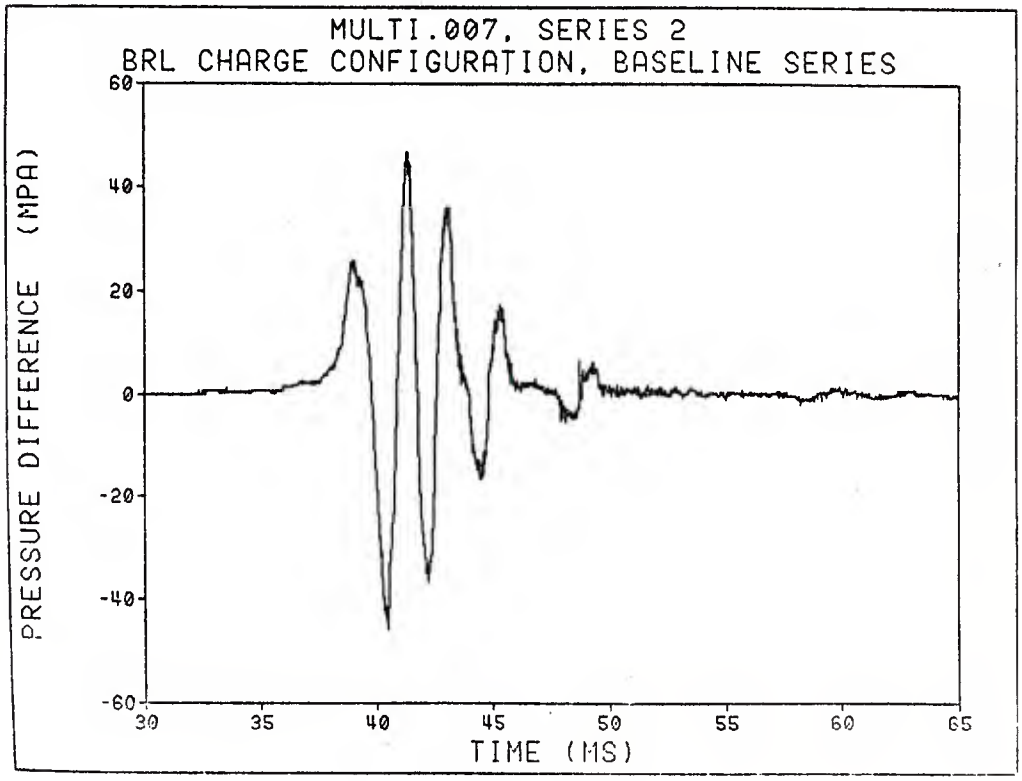
MULTI.007, SERIES 2
BRL CHARGE CONFIGURATION, BASELINE SERIES
PRESSURE DIFFERENCE (MPA)
60
40
20
0
-20
-40
-60
30
35
40
45
50
55
60
65
TIME (MS)

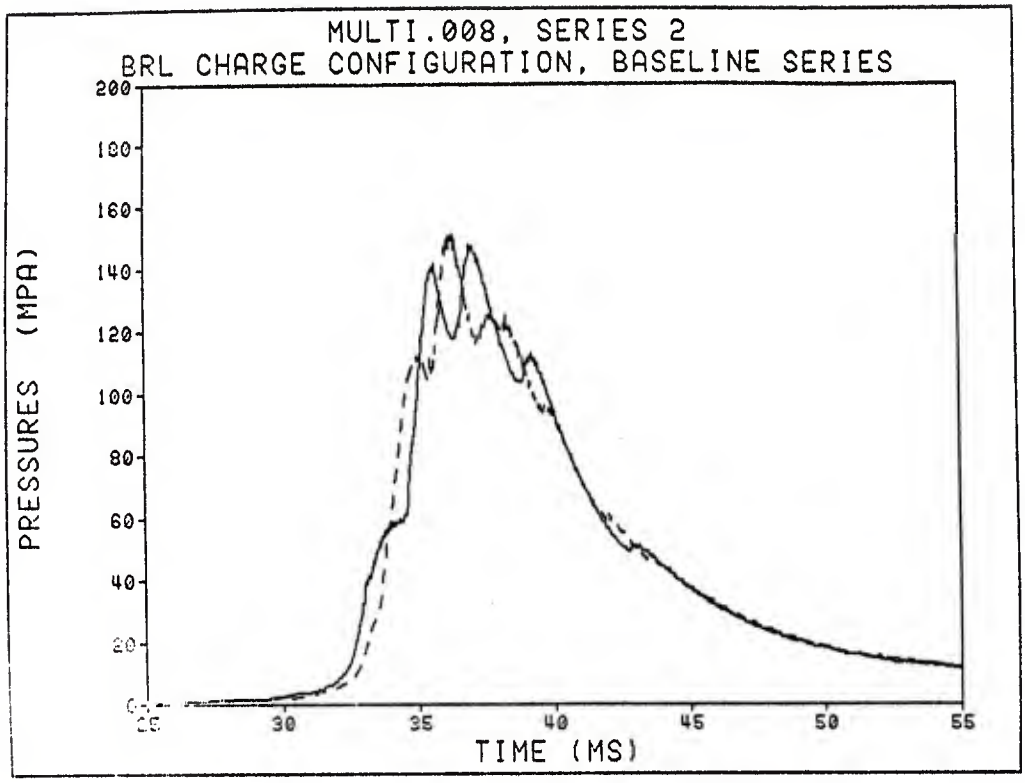
MULTI.008, SERIES 2
BRL CHARGE CONFIGURATION, BASELINE SERIES
PRESSURES (MPA)
200
180
160
140
120
100
80
60
40
20
0
25
30
35
40
45
50
55
TIME (MS)

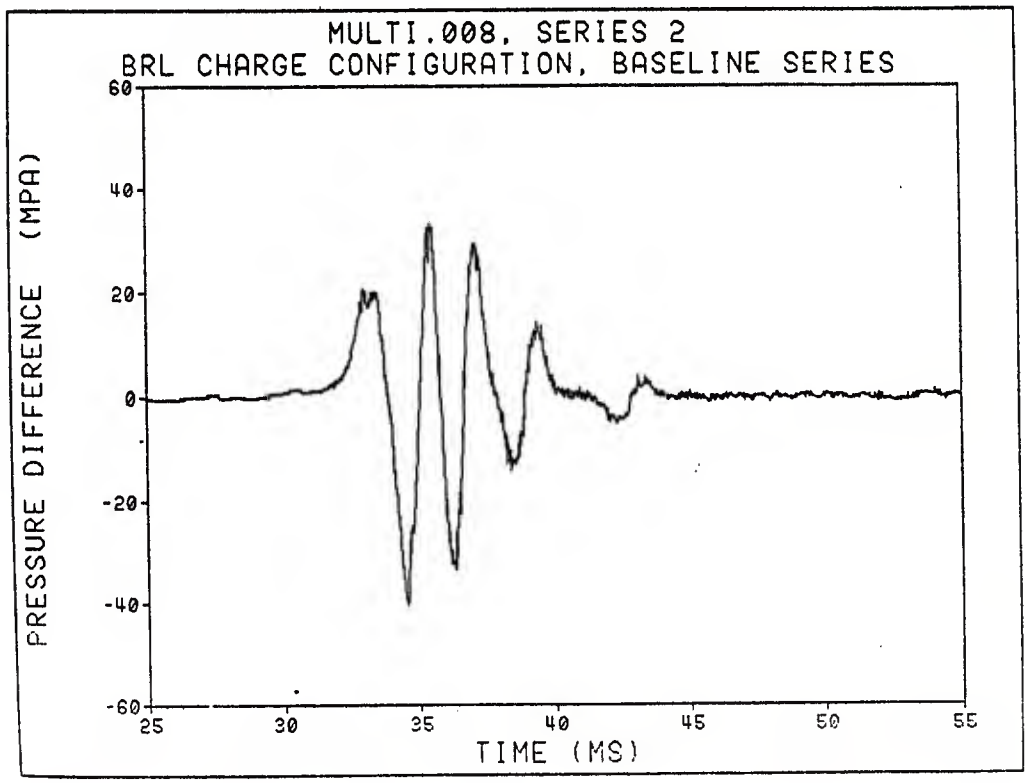
MULTI.008, SERIES 2
BRL CHARGE CONFIGURATION, BASELINE SERIES
PRESSURE DIFFERENCE (MPA)
60
40
20
0
-20
-40
-60
25
30
35
40
45
50
55
TIME (MS)

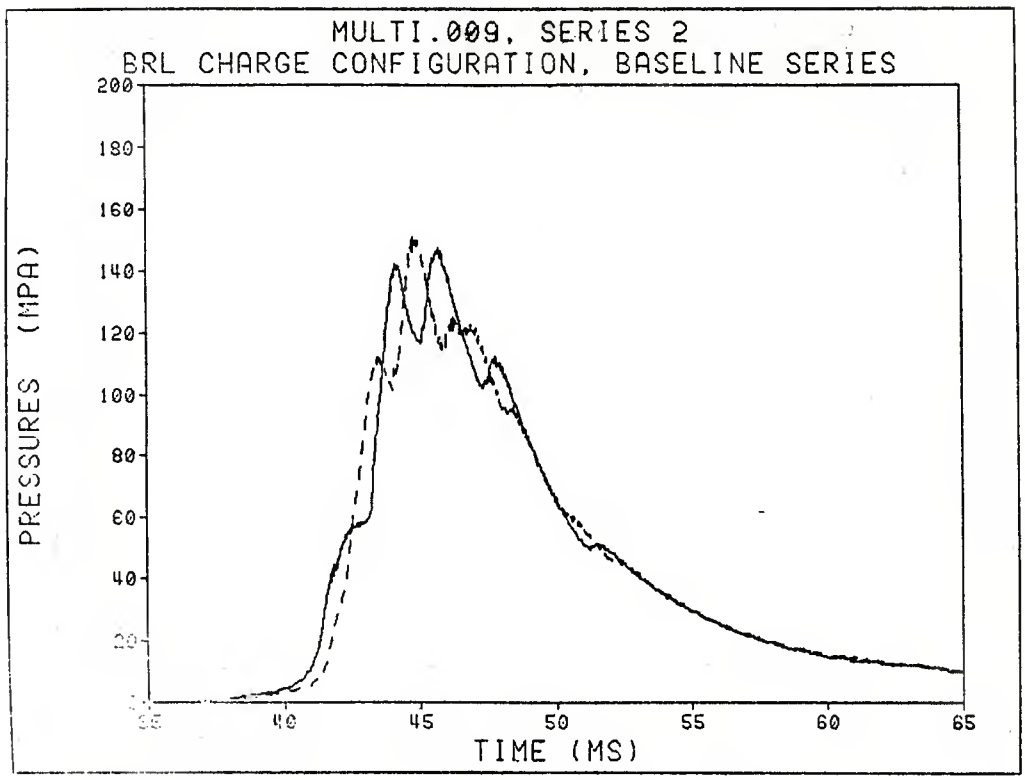
MULTI.009, SERIES 2
BRL CHARGE CONFIGURATION, BASELINE SERIES
PRESSURES (MPA)
200
180
160
140
120
100
80
60
40
20
35
40
45
50
55
60
65
TIME (MS)

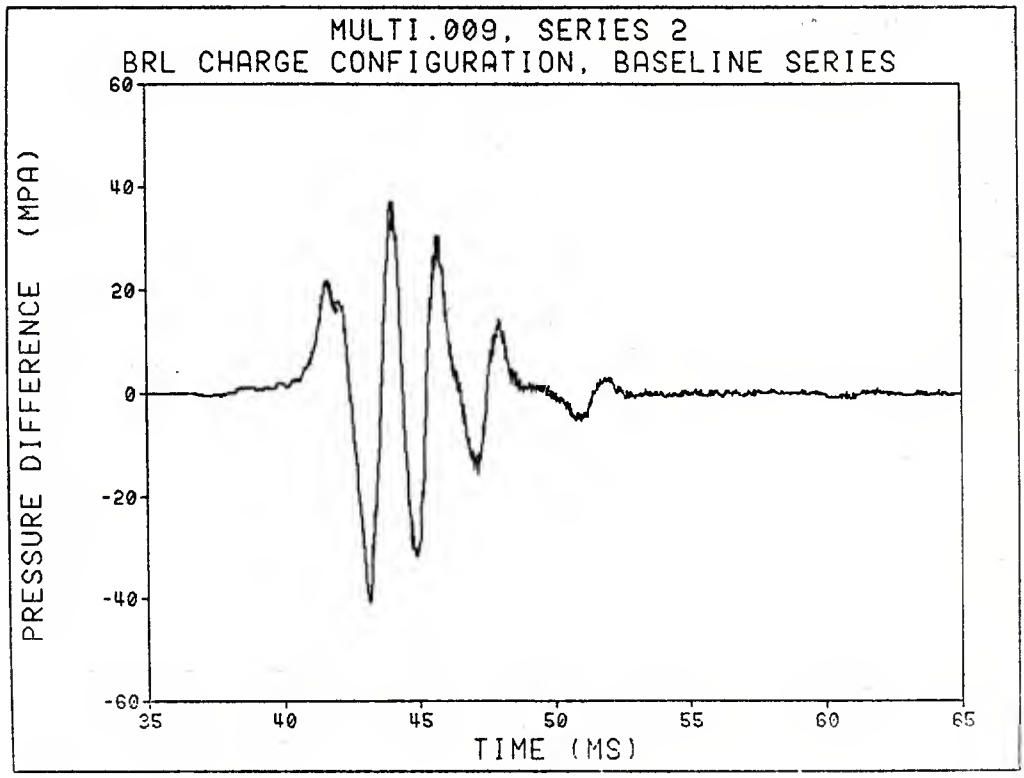
MULTI.009, SERIES 2
BRL CHARGE CONFIGURATION, BASELINE SERIES
PRESSURE DIFFERENCE (MPA)
60
40
20
0
-20
-40
-60
35
40
45
50
55
60
65
TIME (MS)

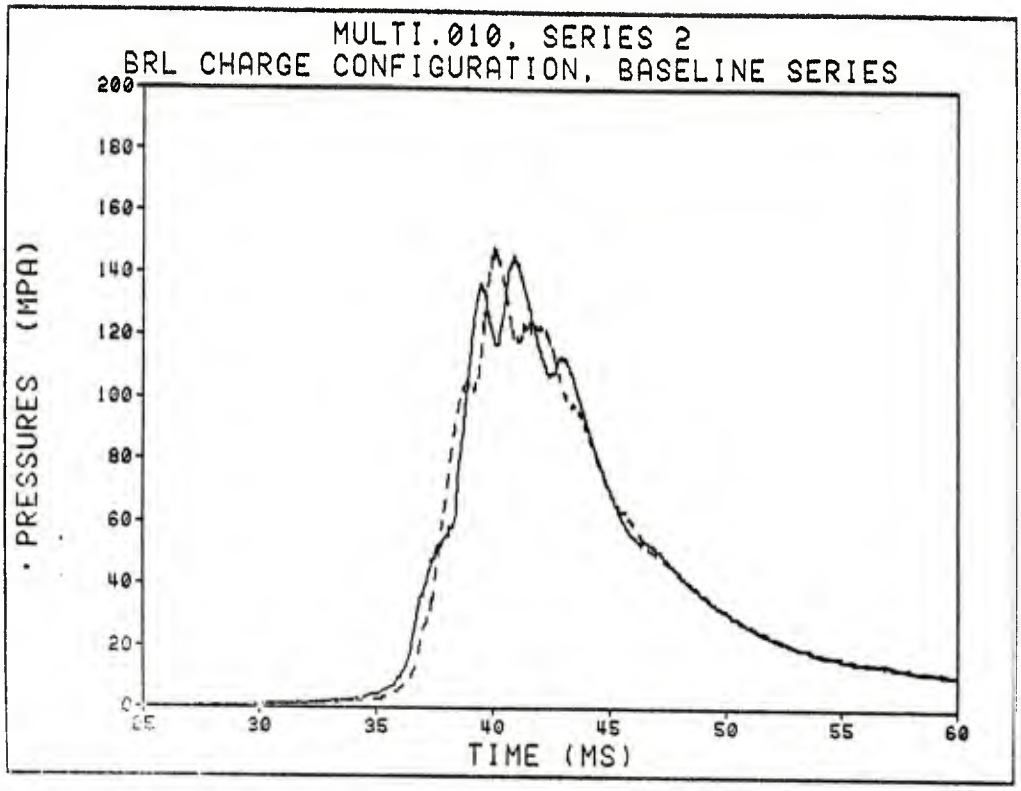
MULTI.010, SERIES 2
BRL CHARGE CONFIGURATION, BASELINE SERIES
PRESSURES (MPA)
200
180
160
140
120
100
80
60
40
20
0
25
30
35
40
45
50
55
60
TIME (MS)

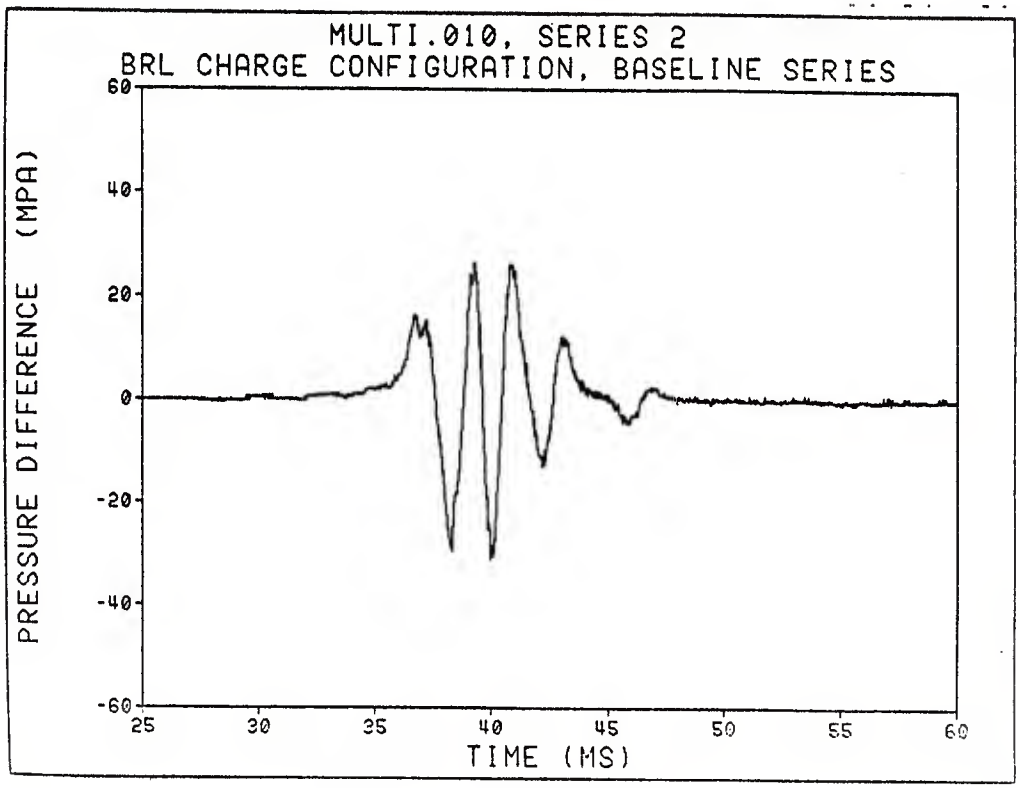
MULTI.010, SERIES 2
BRL CHARGE CONFIGURATION, BASELINE SERIES
PRESSURE DIFFERENCE (MPA)
60
40
20
0
-20
-40
-60
25
30
35
40
45
50
55
60
TIME (MS)

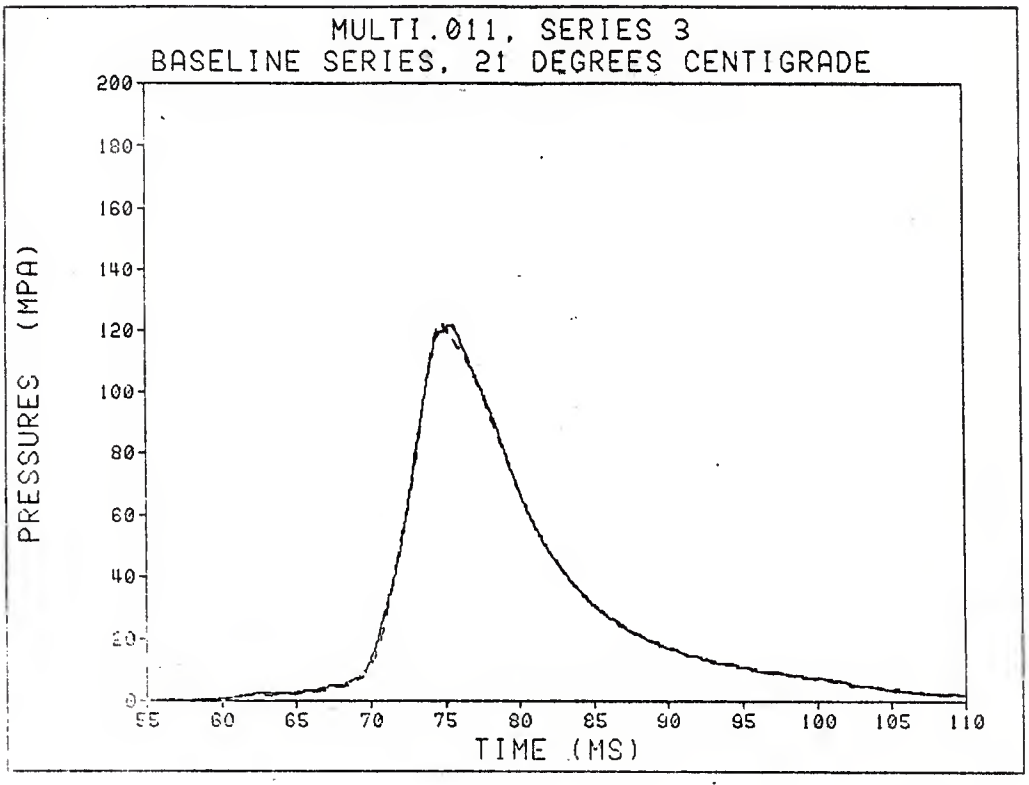
MULTI.011, SERIES 3
BASELINE SERIES, 21 DEGREES CENTIGRADE
PRESSURES (MPA)
200
180
160
140
120
100
80
60
40
20
0
55
60
65
70
75
80
85
90
95
100
105
110
TIME (MS)

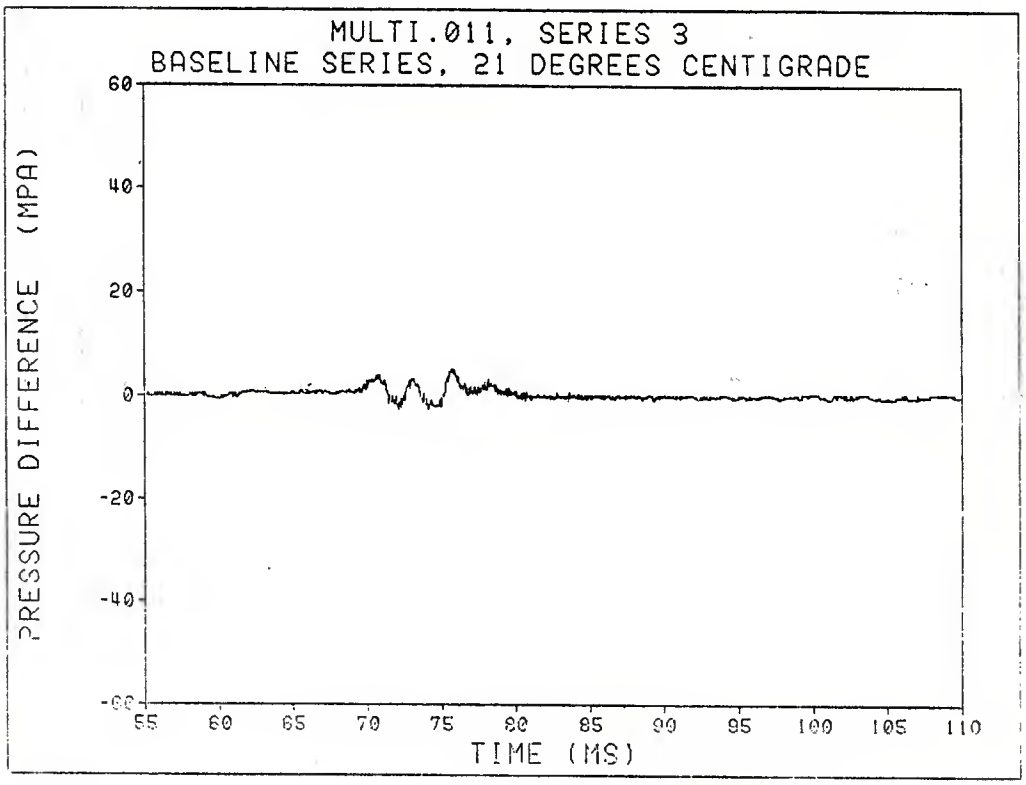
MULTI.011, SERIES 3
BASELINE SERIES, 21 DEGREES CENTIGRADE
PRESSURE DIFFERENCE (MPA)
60
40
20
0
-20
-40
55
60
65
70
75
80
85
90
95
100
105
110
TIME (MS)

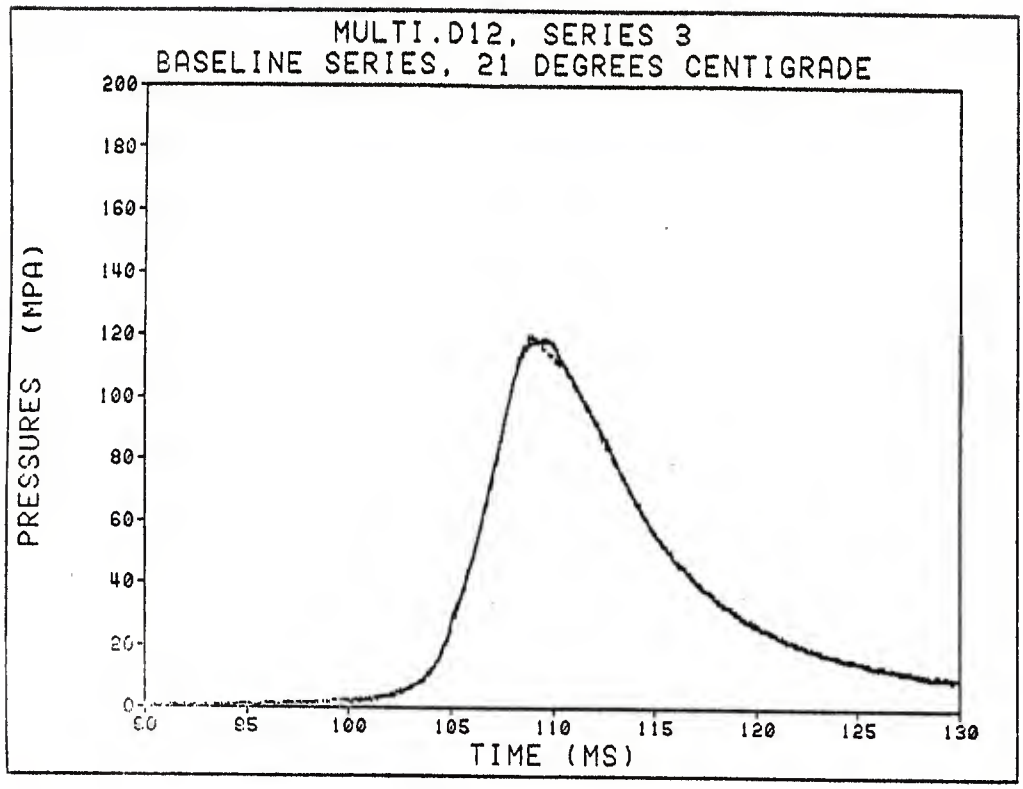
MULTI.D12, SERIES 3
BASELINE SERIES, 21 DEGREES CENTIGRADE
PRESSURES (MPA)
200
180
160
140
120
100
80
60
40
20
0
90
95
100
105
110
115
120
125
130
TIME (MS)

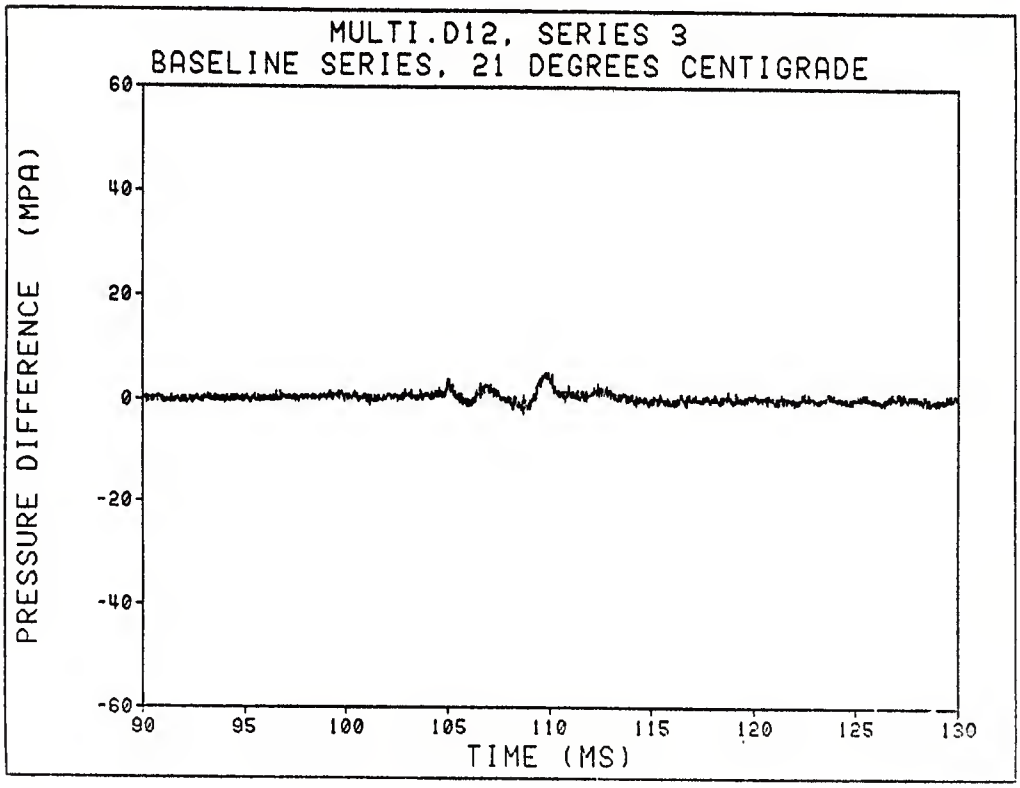
MULTI.D12, SERIES 3
BASELINE SERIES, 21 DEGREES CENTIGRADE
PRESSURE DIFFERENCE (MPA)
60
40
20
0
-20
-40
-60
90
95
100
105
110
115
120
125
130
TIME (MS)

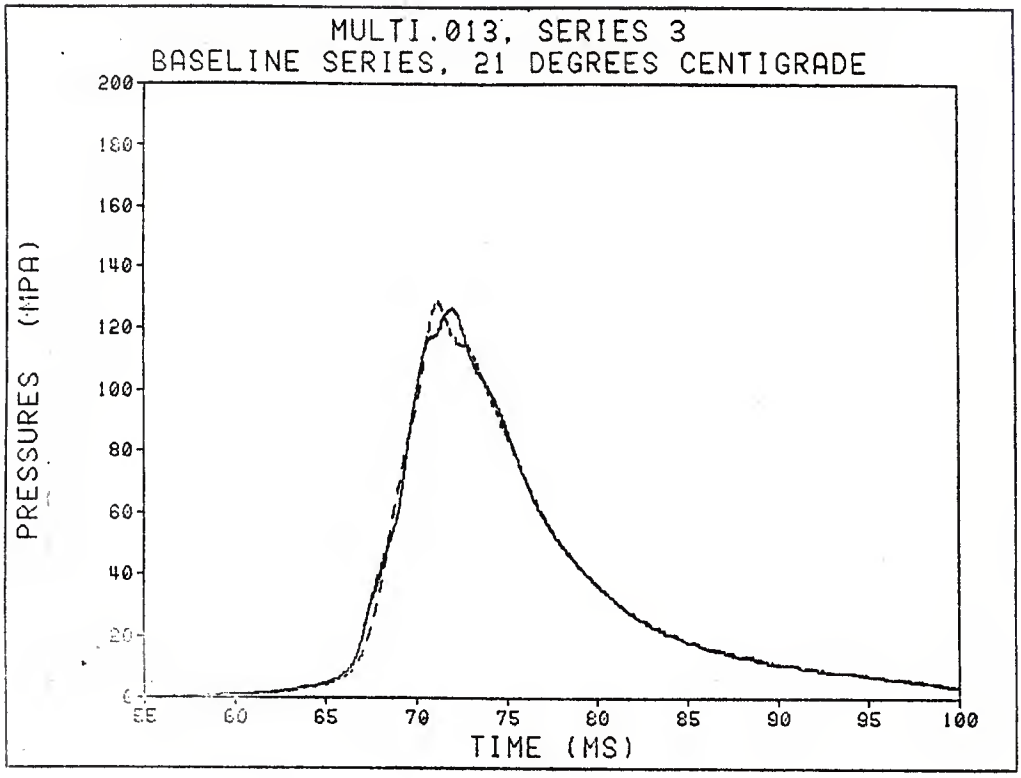
MULTI.013, SERIES 3
BASELINE SERIES, 21 DEGREES CENTIGRADE
PRESSURES (MPA)
200
180
160
140
120
100
80
60
40
20
0
55
60
65
70
75
80
85
90
95
100
TIME (MS)

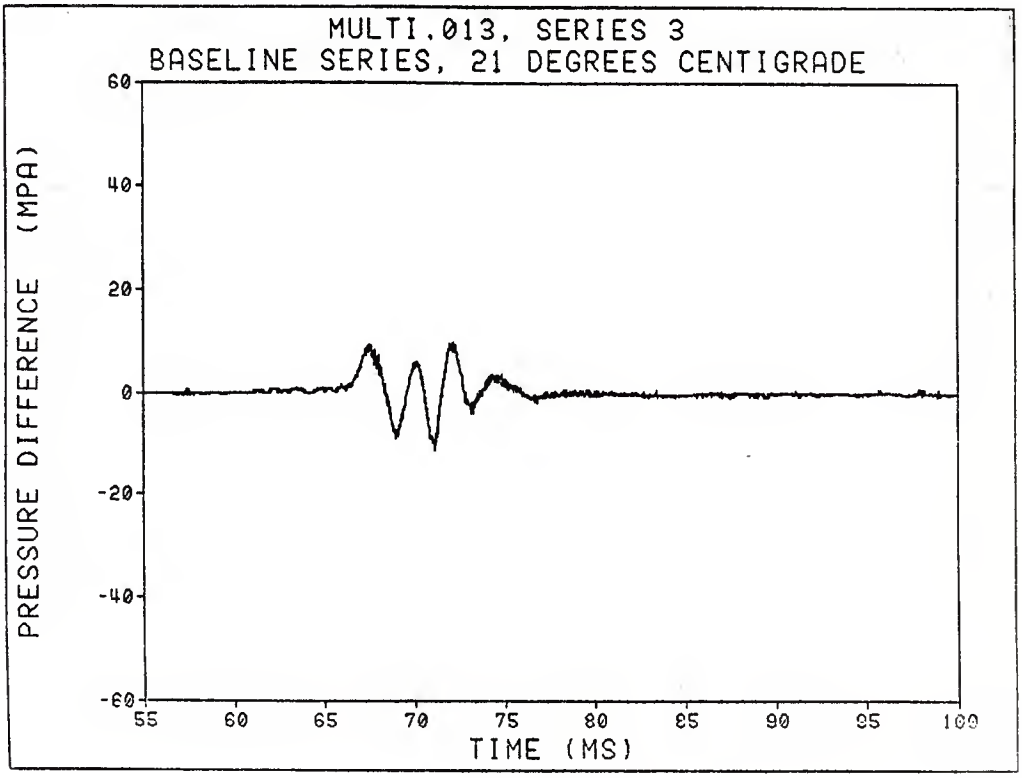
MULTI.013, SERIES 3
BASELINE SERIES, 21 DEGREES CENTIGRADE
PRESSURE DIFFERENCE (MPA)
60
40
20
0
-20
-40
-60
55
60
65
70
75
80
85
90
95
100
TIME (MS)

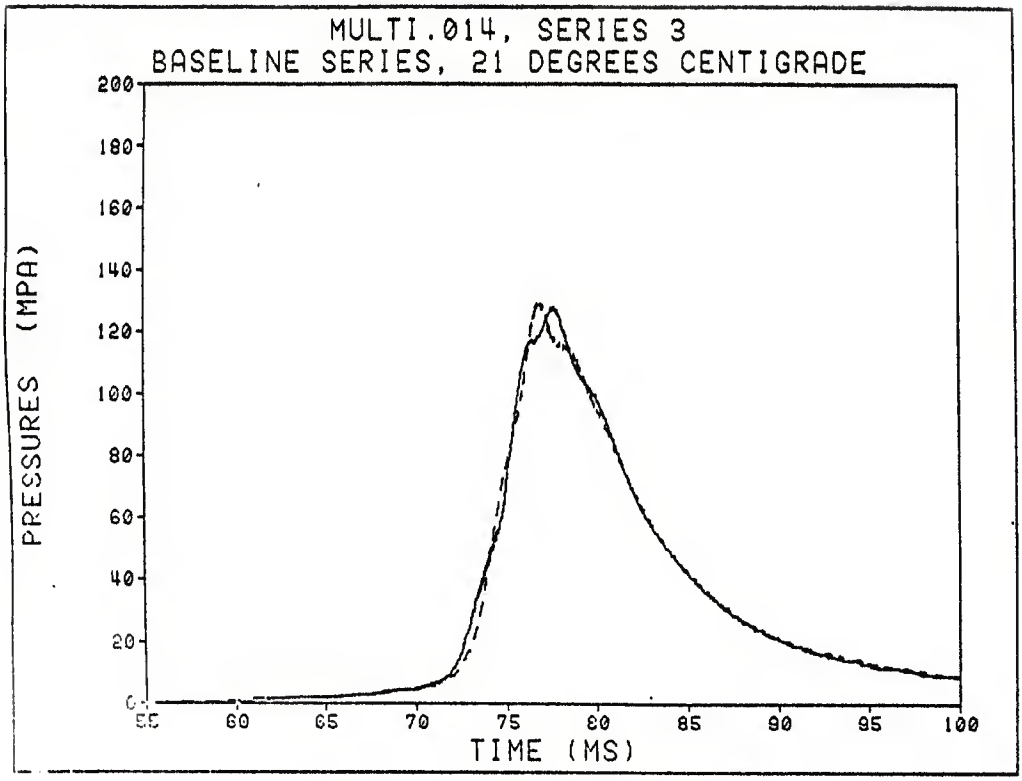
MULTI.014, SERIES 3
BASELINE SERIES, 21 DEGREES CENTIGRADE
PRESSURES (MPA)
200
180
160
140
120
100
80
60
40
20
0
55
60
65
70
75
80
85
90
95
100
TIME (MS)

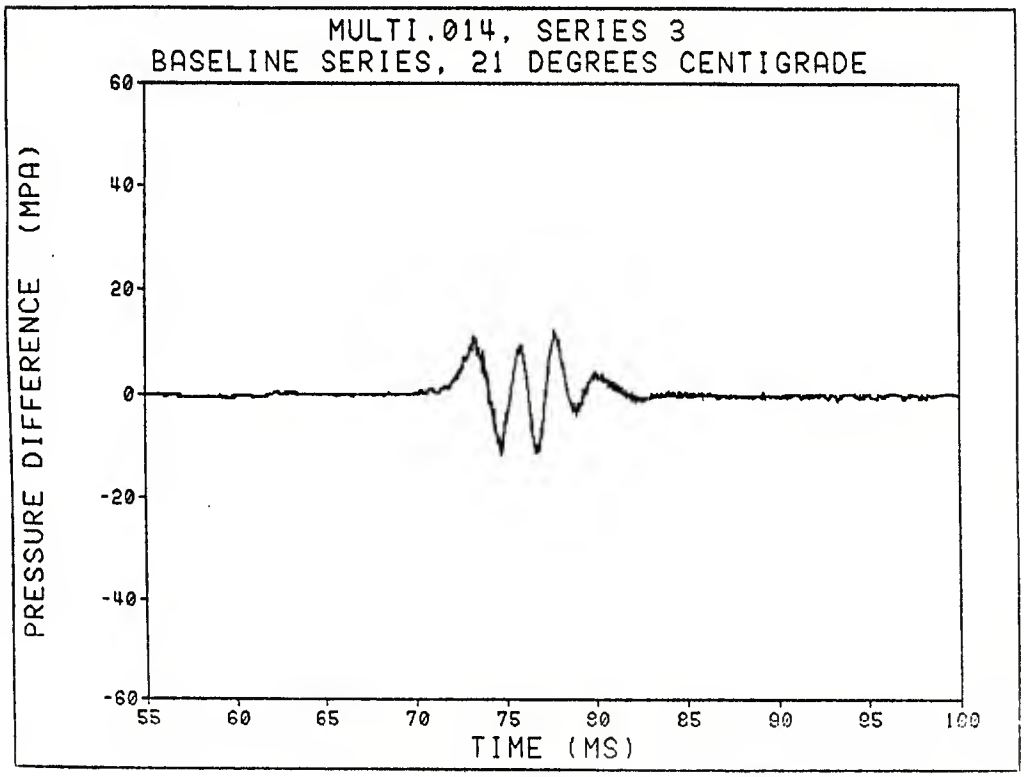
MULTI.014, SERIES 3
BASELINE SERIES, 21 DEGREES CENTIGRADE
PRESSURE DIFFERENCE (MPA)
60
40
20
0
-20
-40
-60
55
60
65
70
75
80
85
90
95
100
TIME (MS)

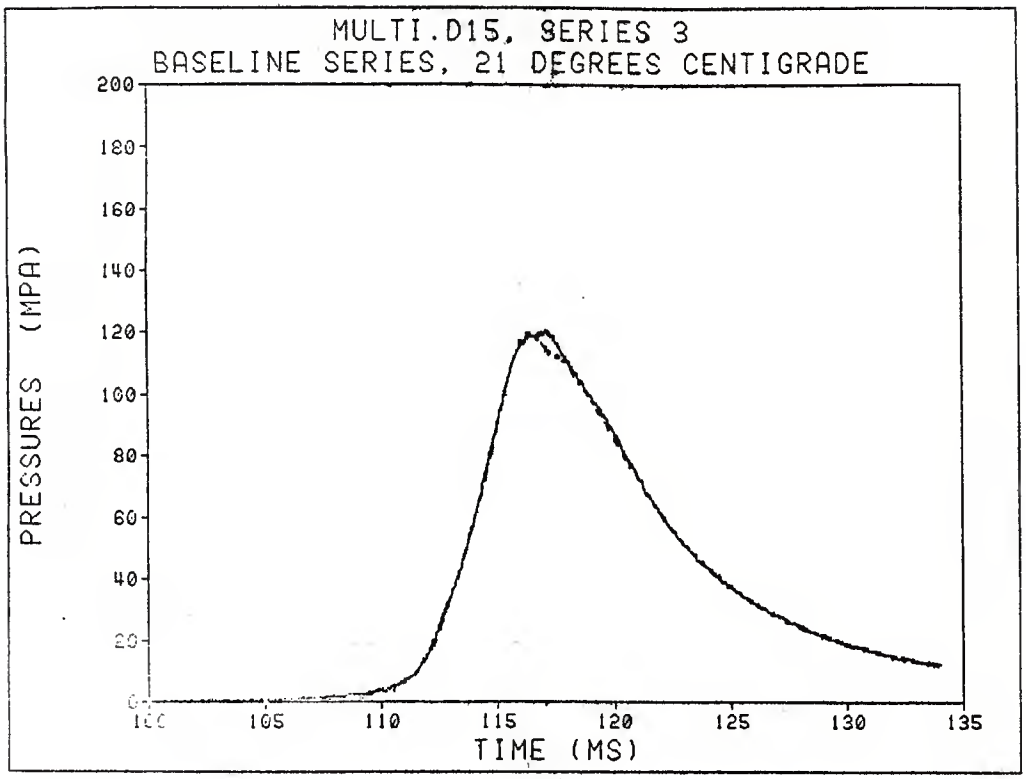
MULTI.D15, SERIES 3
BASELINE SERIES, 21 DEGREES CENTIGRADE
PRESSURES (MPA)
200
180
160
140
120
100
80
60
40
20
0
100
105
110
115
120
125
130
135
TIME (MS)

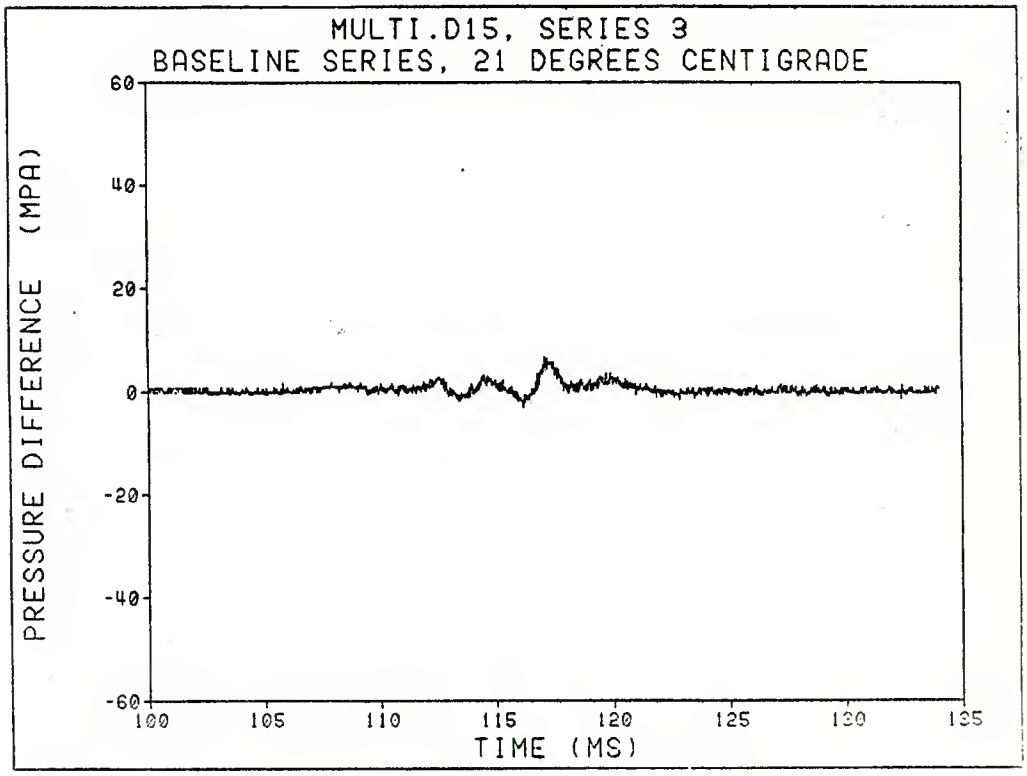
MULTI.D15, SERIES 3
BASELINE SERIES, 21 DEGREES CENTIGRADE
PRESSURE DIFFERENCE (MPA)
60
40
20
0
-20
-40
-60
100
105
110
115
120
125
130
135
TIME (MS)

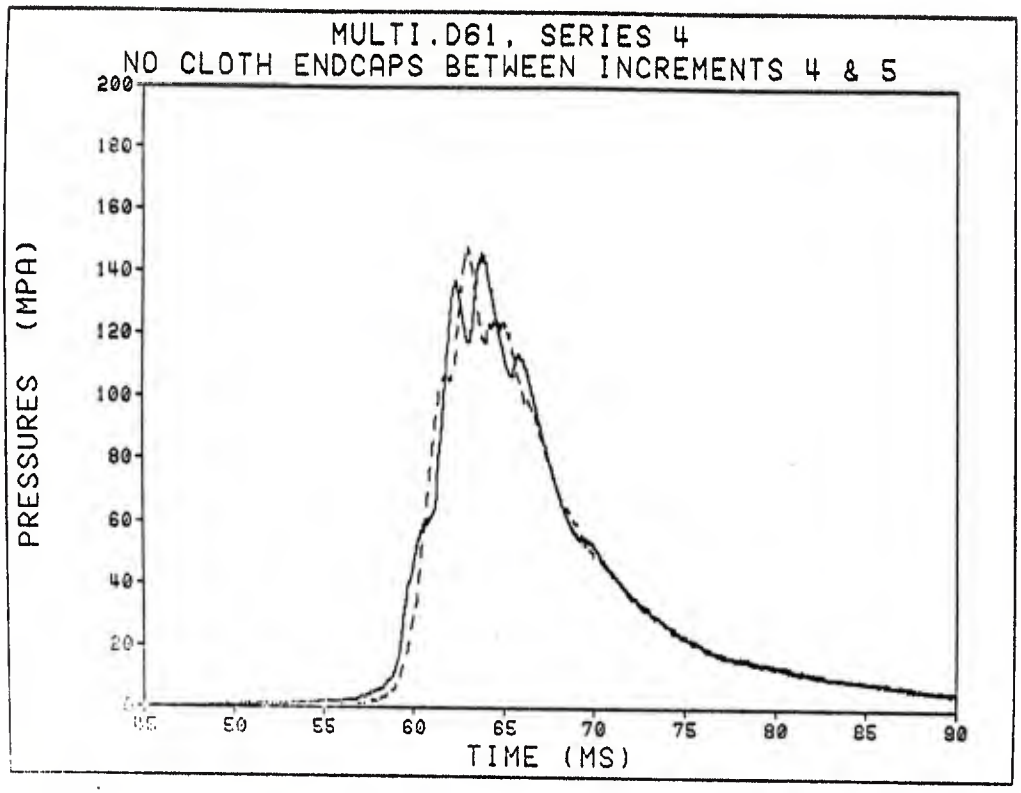
MULTI.D61, SERIES 4
NO CLOTH ENDCAPS BETWEEN INCREMENTS 4 & 5
PRESSURES (MPA)
200
180
160
140
120
100
80
60
40
20
45
50
55
60
65
70
75
80
85
90
TIME (MS)

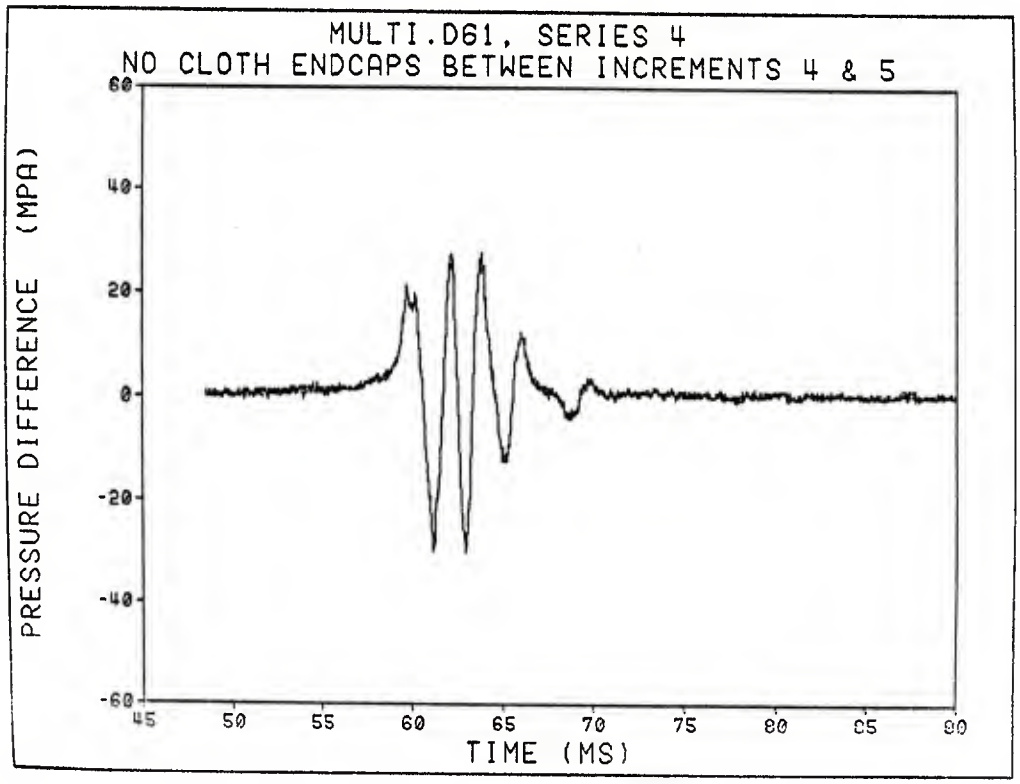
MULTI.D61, SERIES 4
NO CLOTH ENDCAPS BETWEEN INCREMENTS 4 & 5
PRESSURE DIFFERENCE (MPA)
60
40
20
0
-20
-40
-60
45
50
55
60
65
70
75
80
85
90
TIME (MS)

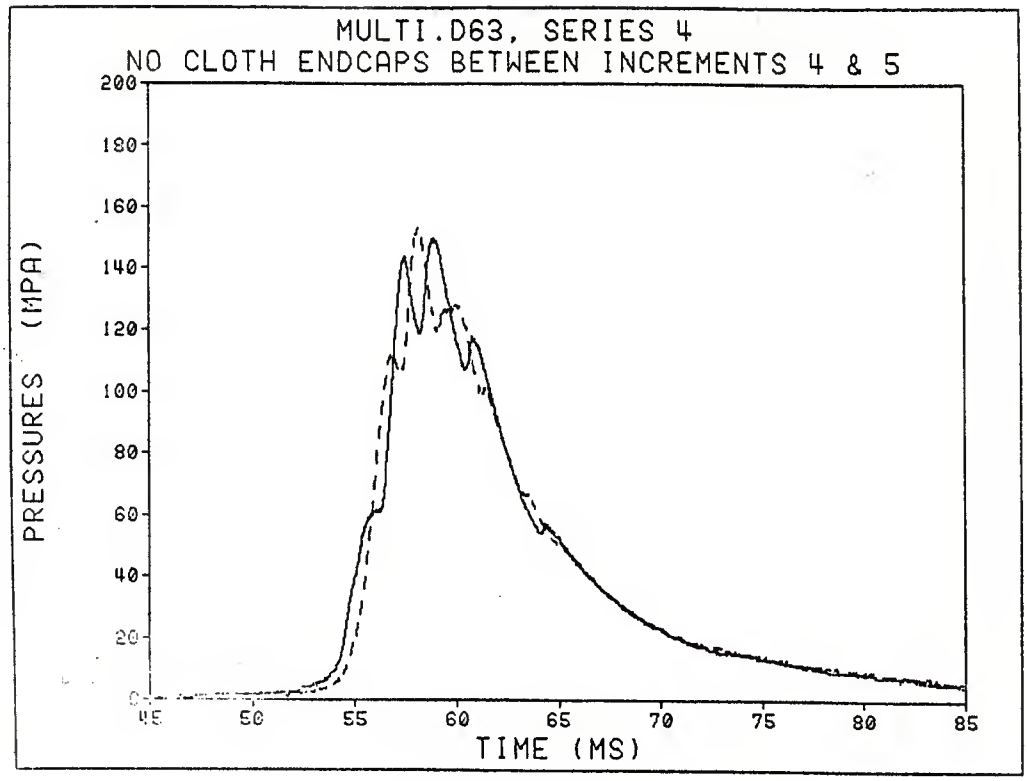
MULTI.D63, SERIES 4
NO CLOTH ENDCAPS BETWEEN INCREMENTS 4 & 5
PRESSURES (MPA)
200
180
160
140
120
100
80
60
40
20
0
45
50
55
60
65
70
75
80
85
TIME (MS)

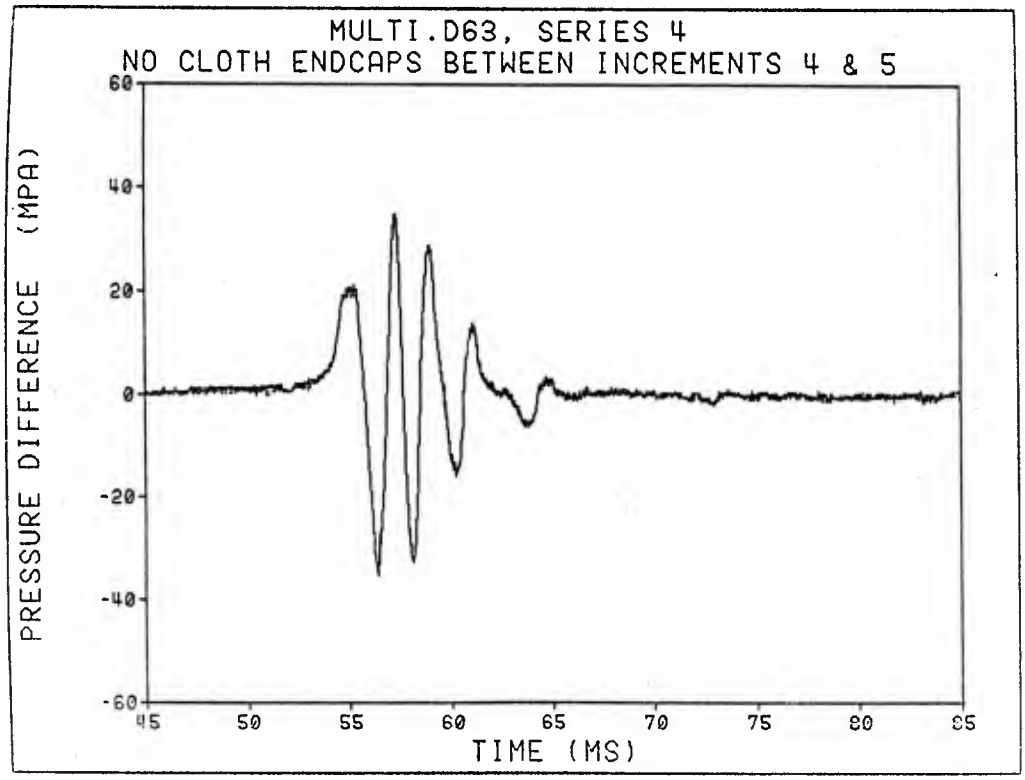
MULTI.D63, SERIES 4
NO CLOTH ENDCAPS BETWEEN INCREMENTS 4 & 5
PRESSURE DIFFERENCE (MPA)
60
40
20
0
-20
-40
-60
45
50
55
60
65
70
75
80
85
TIME (MS)

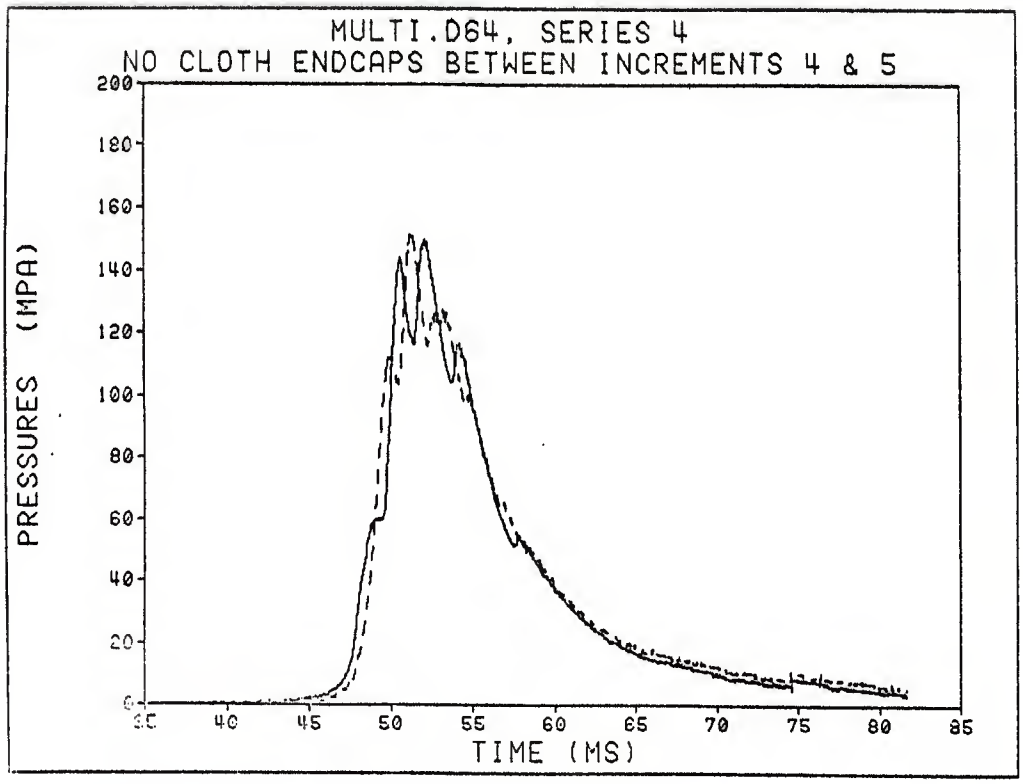
MULTI.D64, SERIES 4
NO CLOTH ENDCAPS BETWEEN INCREMENTS 4 & 5
PRESSURES (MPA)
200
180
160
140
120
100
80
60
40
20
0
35
40
45
50
55
60
65
70
75
80
85
TIME (MS)

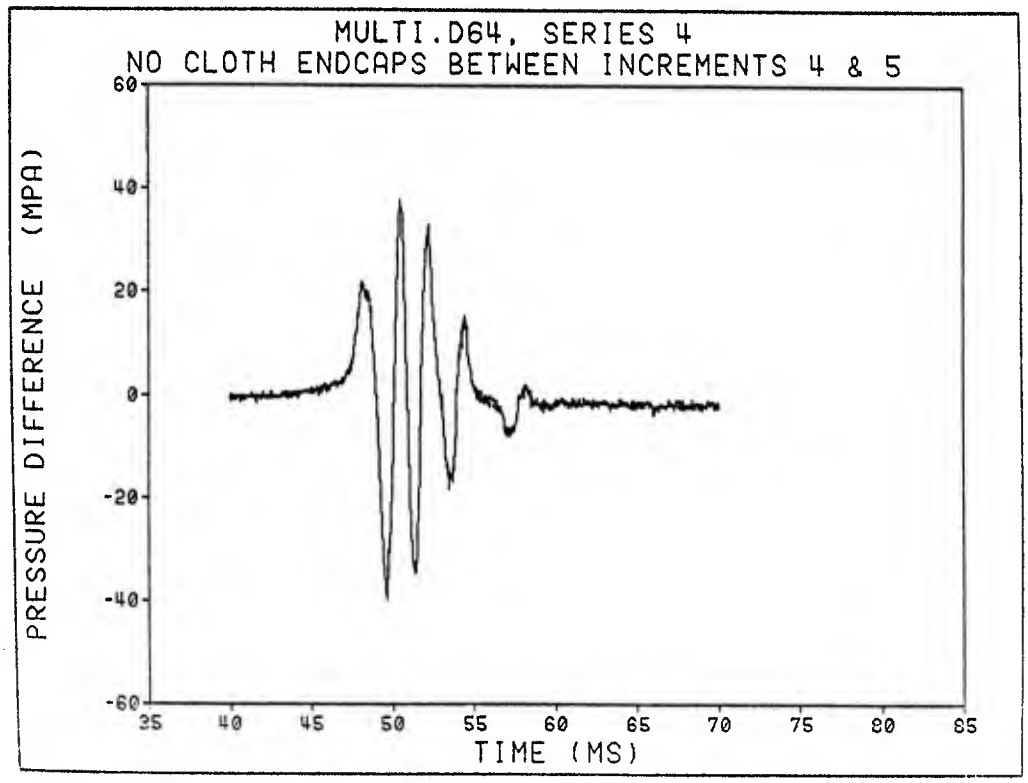
MULTI.D64, SERIES 4
NO CLOTH ENDCAPS BETWEEN INCREMENTS 4 & 5
PRESSURE DIFFERENCE (MPA)
60
40
20
0
-20
-40
-60
35
40
45
50
55
60
65
70
75
80
85
TIME (MS)

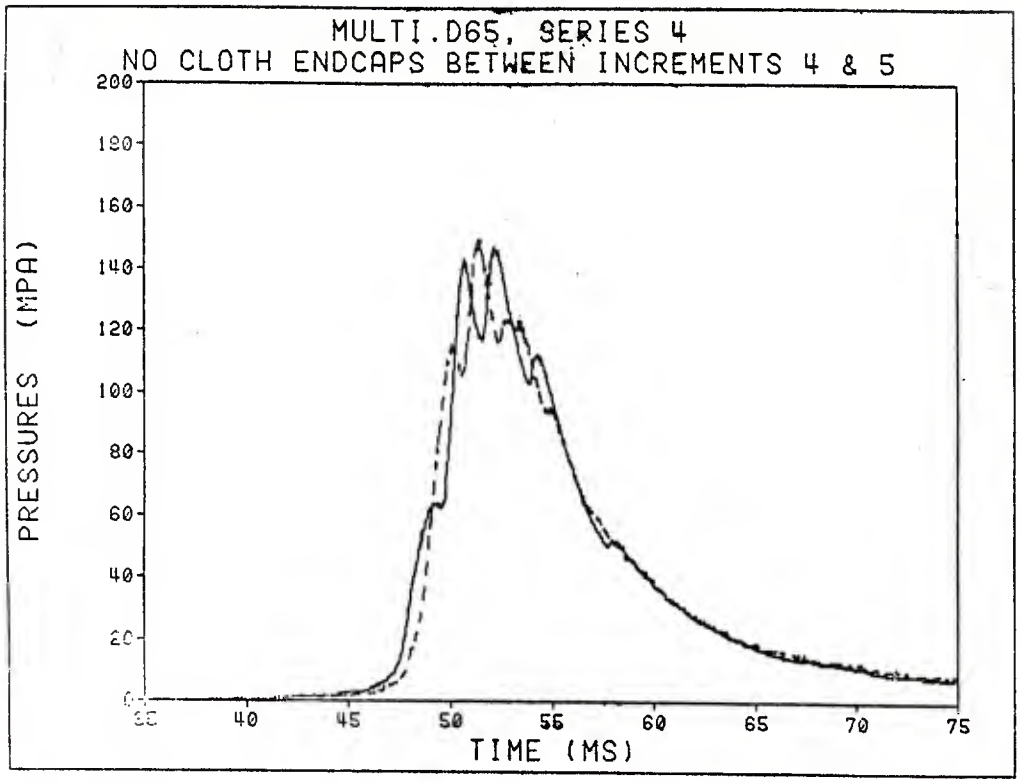
MULTI.D65, SERIES 4
NO CLOTH ENDCAPS BETWEEN INCREMENTS 4 & 5
PRESSURES (MPA)
200
180
160
140
120
100
80
60
40
20
0
35
40
45
50
55
60
65
70
75
TIME (MS)

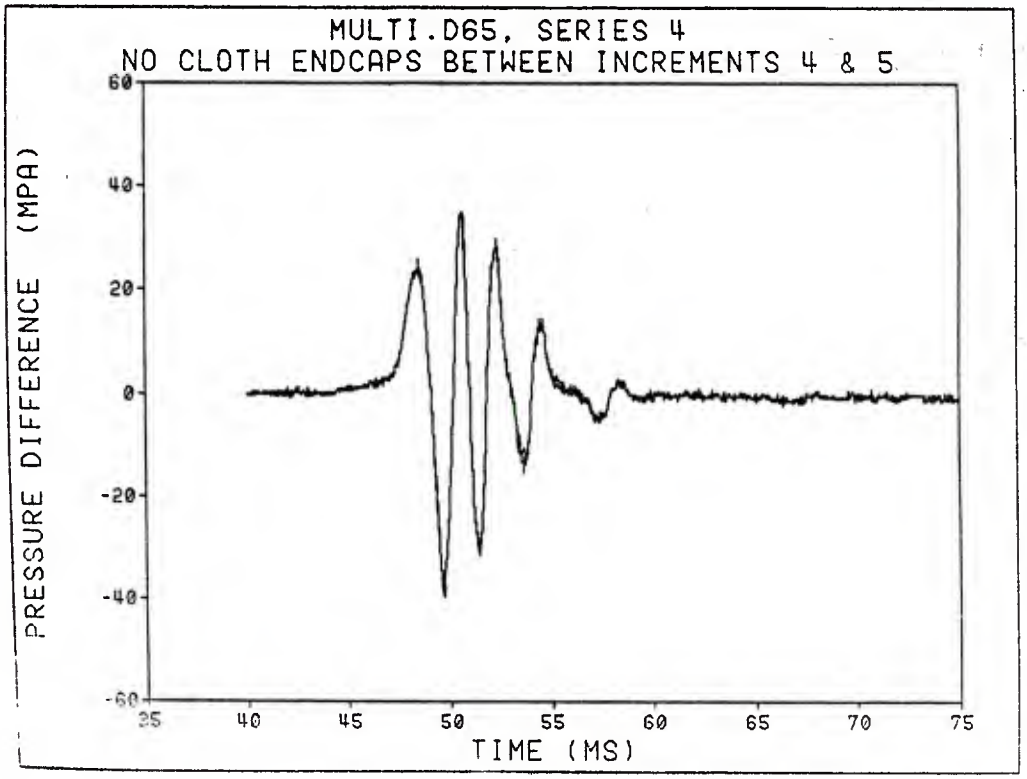
MULTI.D65, SERIES 4
NO CLOTH ENDCAPS BETWEEN INCREMENTS 4 & 5
PRESSURE DIFFERENCE (MPA)
60
40
20
0
-20
-40
-60
25
40
45
50
55
60
65
70
75
TIME (MS)

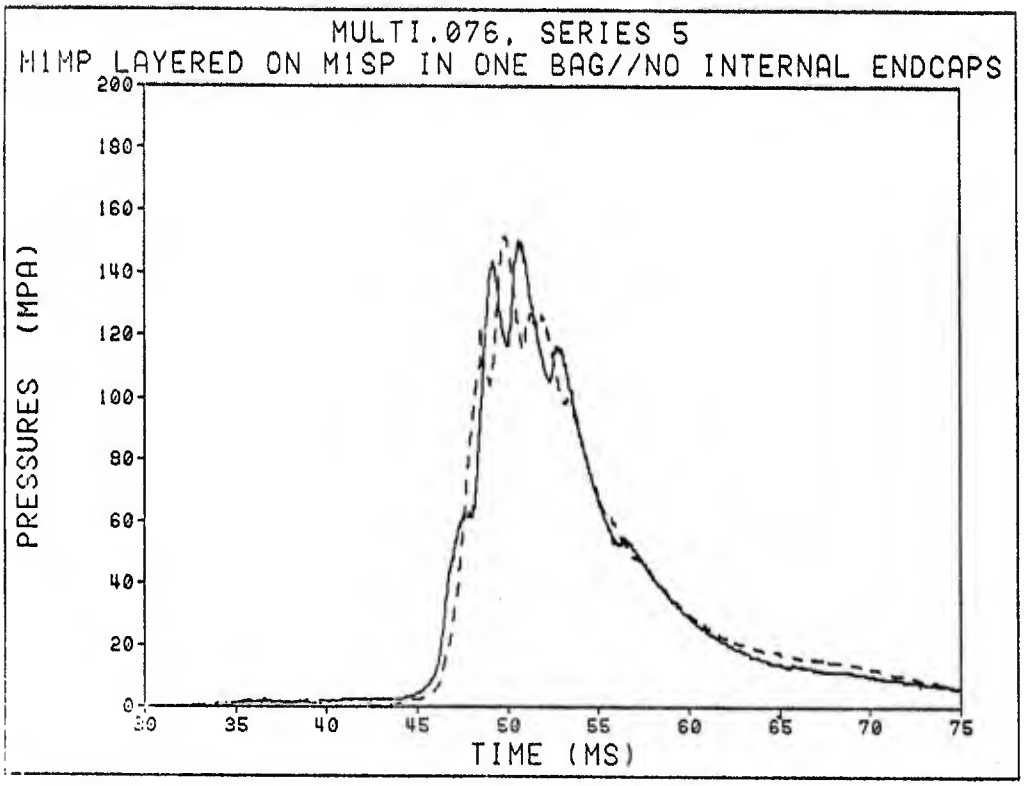
MULTI.076, SERIES 5
M1MP LAYERED ON M1SP IN ONE BAG//NO INTERNAL ENDCAPS
PRESSURES (MPA)
200
180
160
140
120
100
80
60
40
20
0
30
35
40
45
50
55
60
65
70
75
TIME (MS)

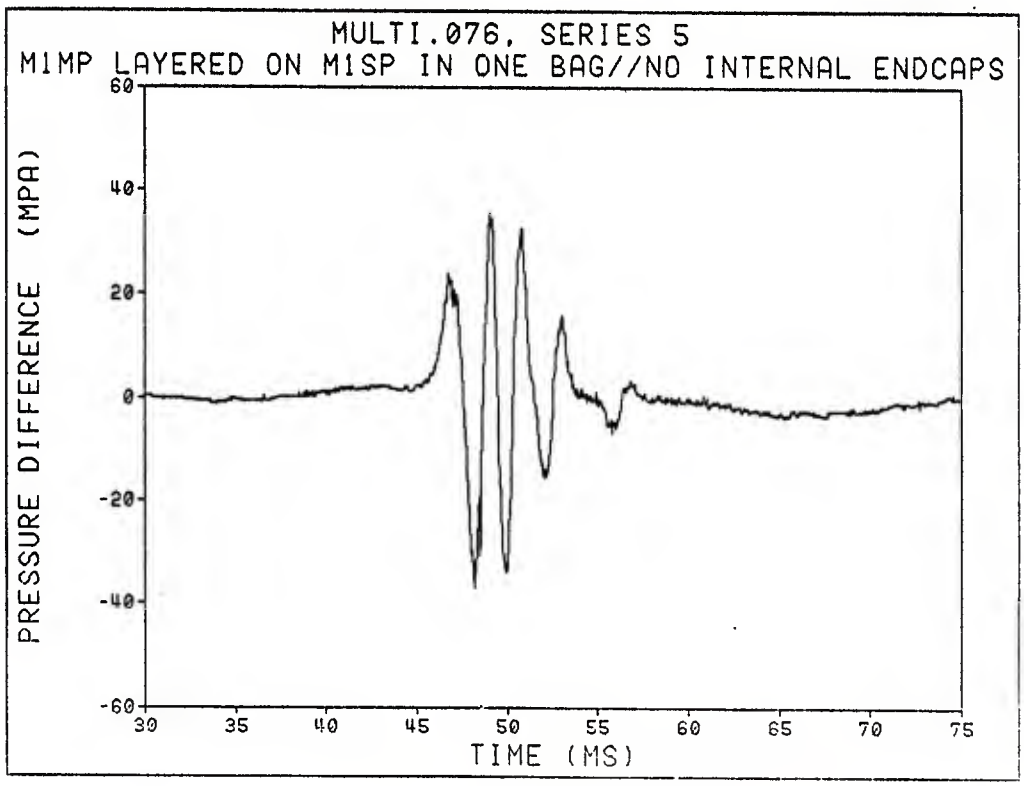
MULTI.076, SERIES 5
M1MP LAYERED ON M1SP IN ONE BAG//NO INTERNAL ENDCAPS
PRESSURE DIFFERENCE (MPA)
60
40
20
0
-20
-40
-60
30
35
40
45
50
55
60
65
70
75
TIME (MS)

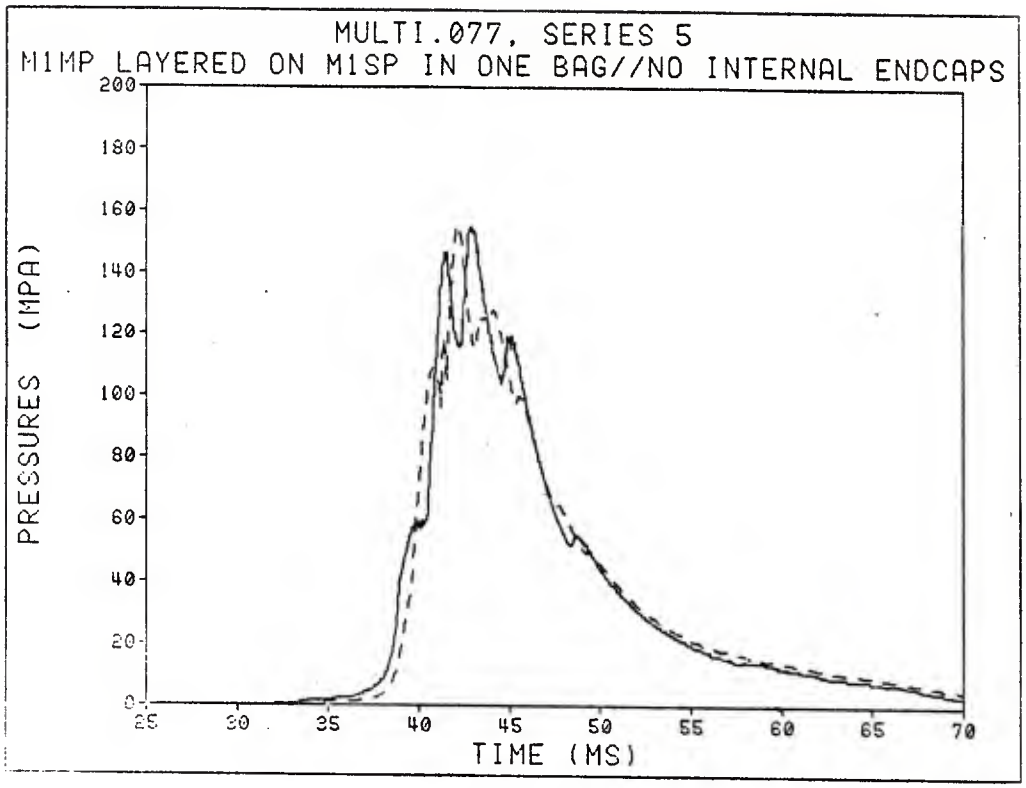
MULTI.077, SERIES 5
M1MP LAYERED ON M1SP IN ONE BAG//NO INTERNAL ENDCAPS
PRESSURES (MPA)
200
180
160
140
120
100
80
60
40
20
0
25
30
35
40
45
50
55
60
65
70
TIME (MS)

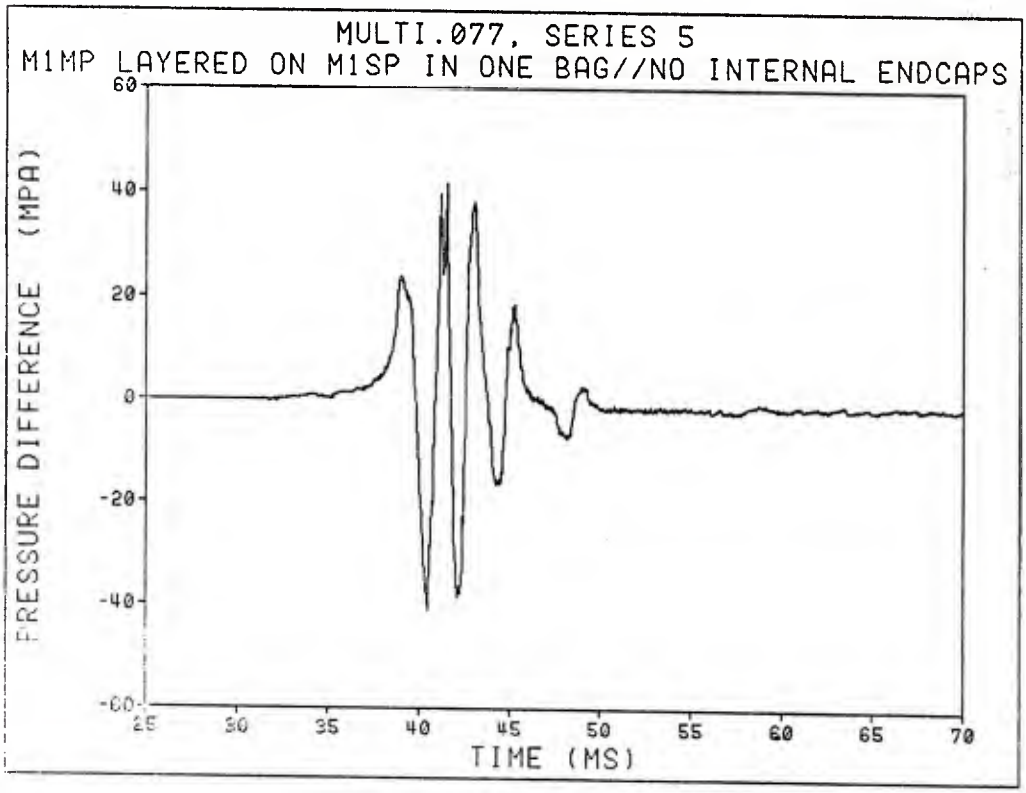
MULTI.077, SERIES 5
M1MP LAYERED ON M1SP IN ONE BAG//NO INTERNAL ENDCAPS
PRESSURE DIFFERENCE (MPA)
60
40
20
0
-20
-40
-60
25
30
35
40
45
50
55
60
65
70
TIME (MS)

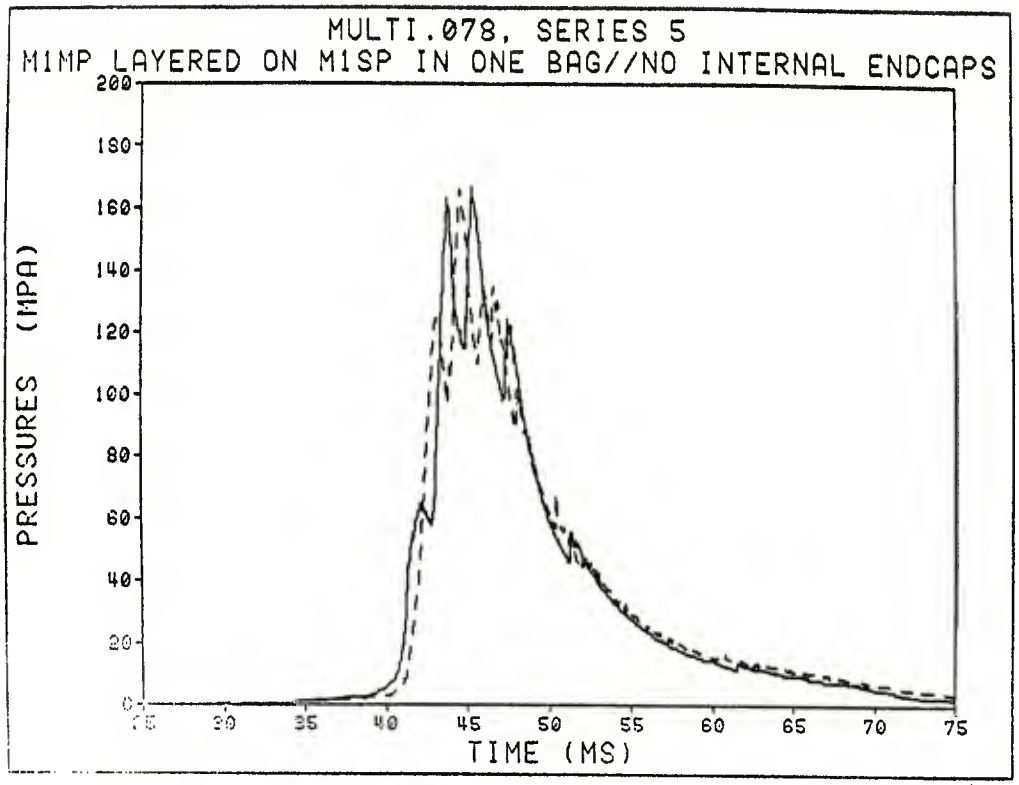
MULTI.078, SERIES 5
M1MP LAYERED ON M1SP IN ONE BAG//NO INTERNAL ENDCAPS
PRESSURES (MPA)
200
180
160
140
120
100
80
60
40
20
0
25
30
35
40
45
50
55
60
65
70
75
TIME (MS)

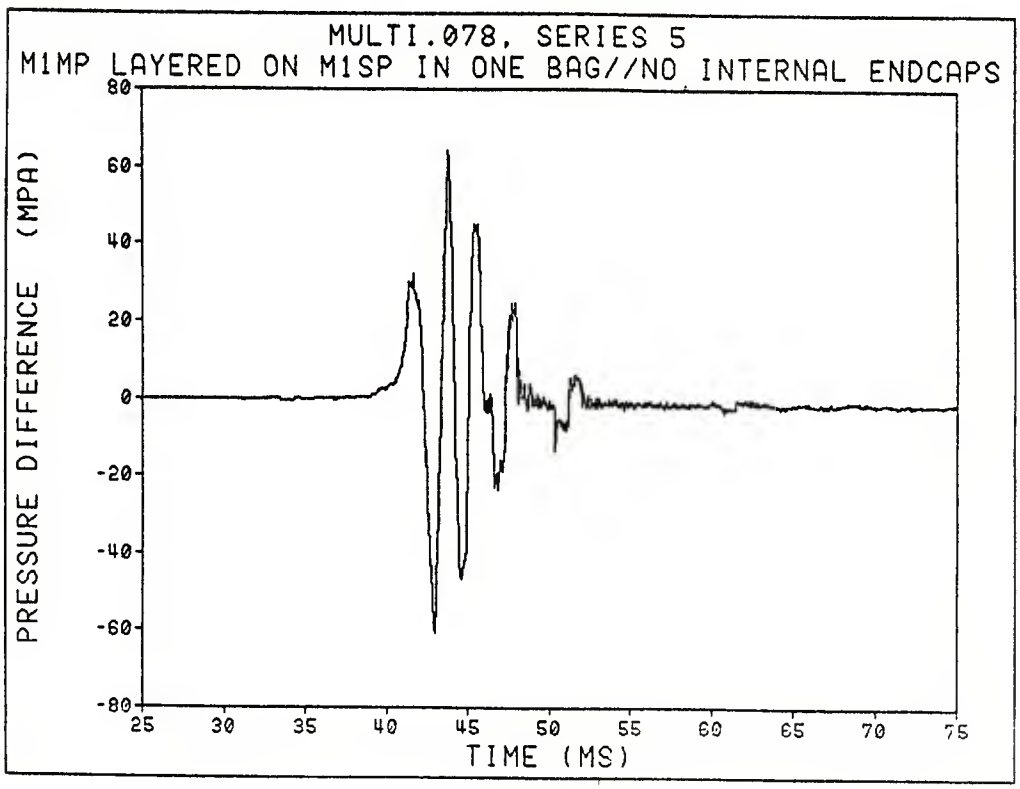
MULTI.078, SERIES 5
M1MP LAYERED ON M1SP IN ONE BAG//NO INTERNAL ENDCAPS
PRESSURE DIFFERENCE (MPA)
80
60
40
20
0
-20
-40
-60
-80
25
30
35
40
45
50
55
60
65
70
75
TIME (MS)

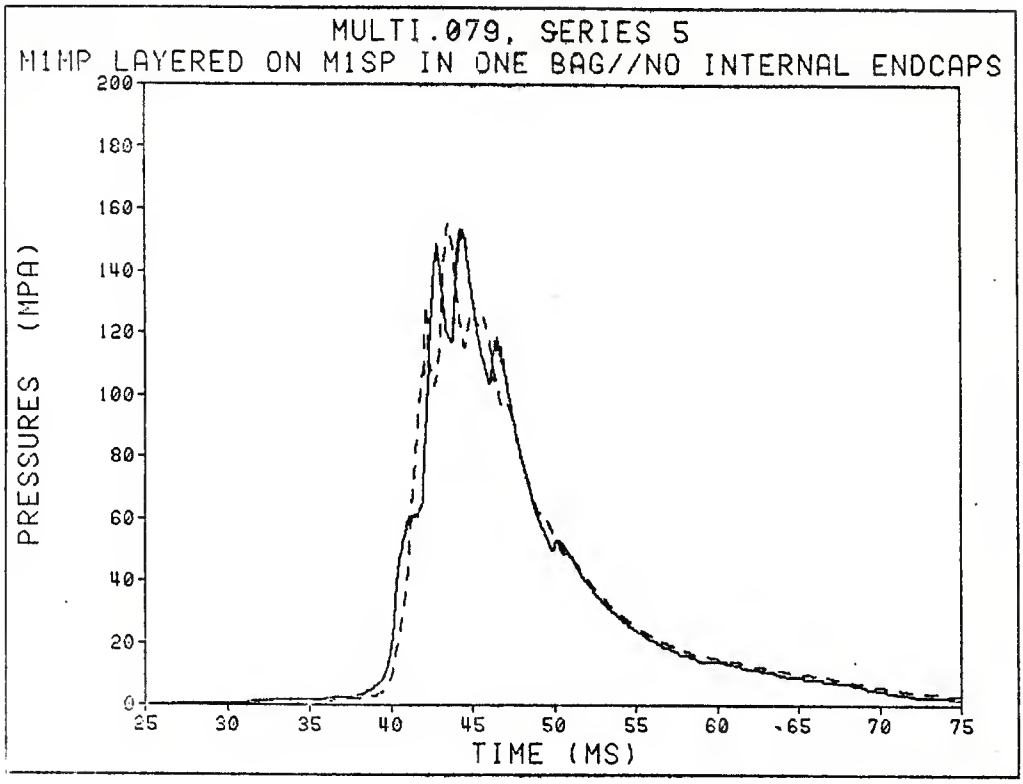
MULTI.079, SERIES 5
M1MP LAYERED ON M1SP IN ONE BAG//NO INTERNAL ENDCAPS
PRESSURES (MPA)
200
180
160
140
120
100
80
60
40
20
0
25
30
35
40
45
50
55
60
65
70
75
TIME (MS)

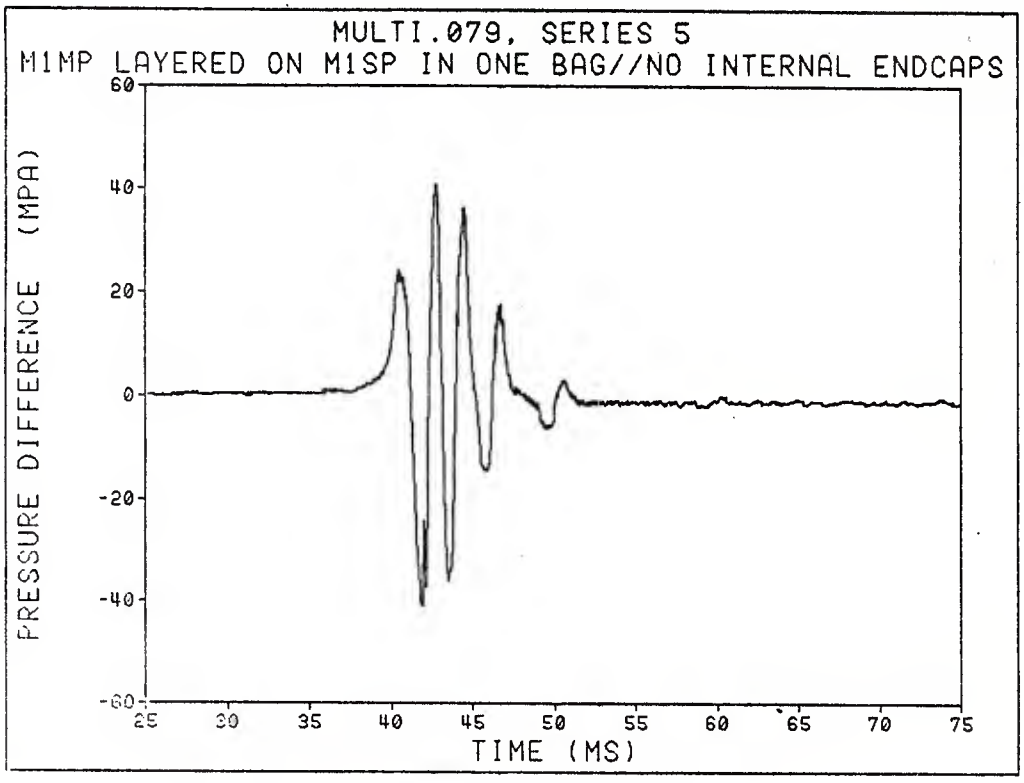
MULTI.079, SERIES 5
M1MP LAYERED ON M1SP IN ONE BAG//NO INTERNAL ENDCAPS
PRESSURE DIFFERENCE (MPA)
60
40
20
0
-20
-40
-60
25
30
35
40
45
50
55
60
65
70
75
TIME (MS)

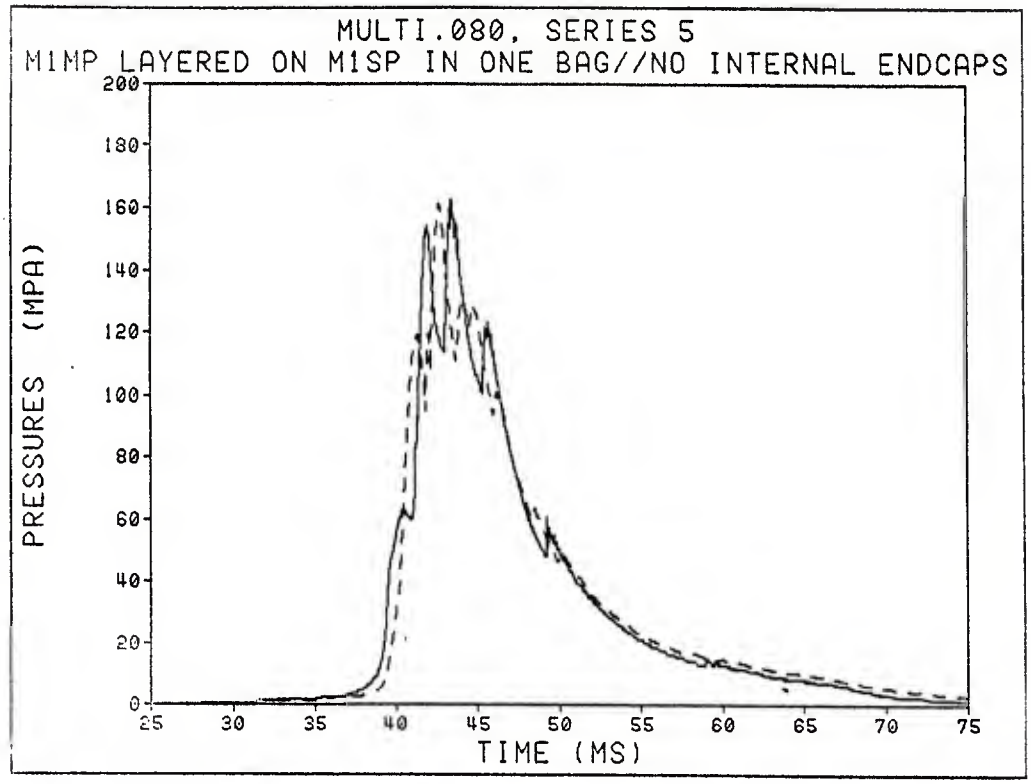
MULTI.080, SERIES 5
M1MP LAYERED ON M1SP IN ONE BAG//NO INTERNAL ENDCAPS
PRESSURES (MPA)
200
180
160
140
120
100
80
60
40
20
0
25
30
35
40
45
50
55
60
65
70
75
TIME (MS)

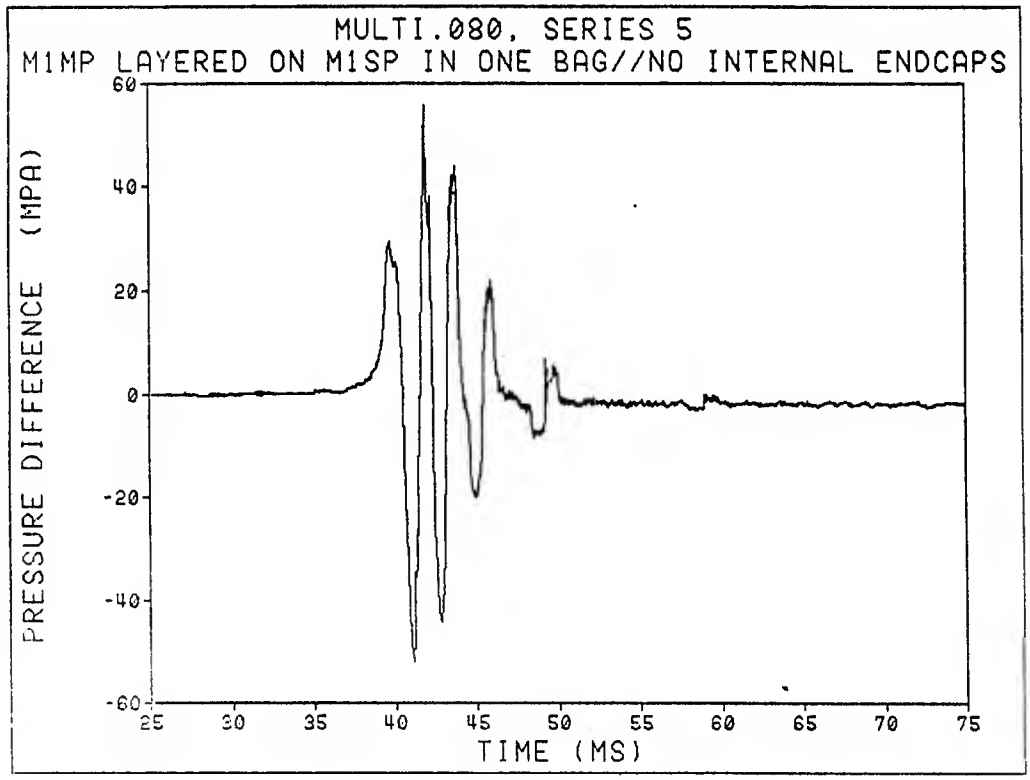
MULTI.080, SERIES 5
M1MP LAYERED ON M1SP IN ONE BAG//NO INTERNAL ENDCAPS
PRESSURE DIFFERENCE (MPA)
60
40
20
0
-20
-40
-60
25
30
35
40
45
50
55
60
65
70
75
TIME (MS)

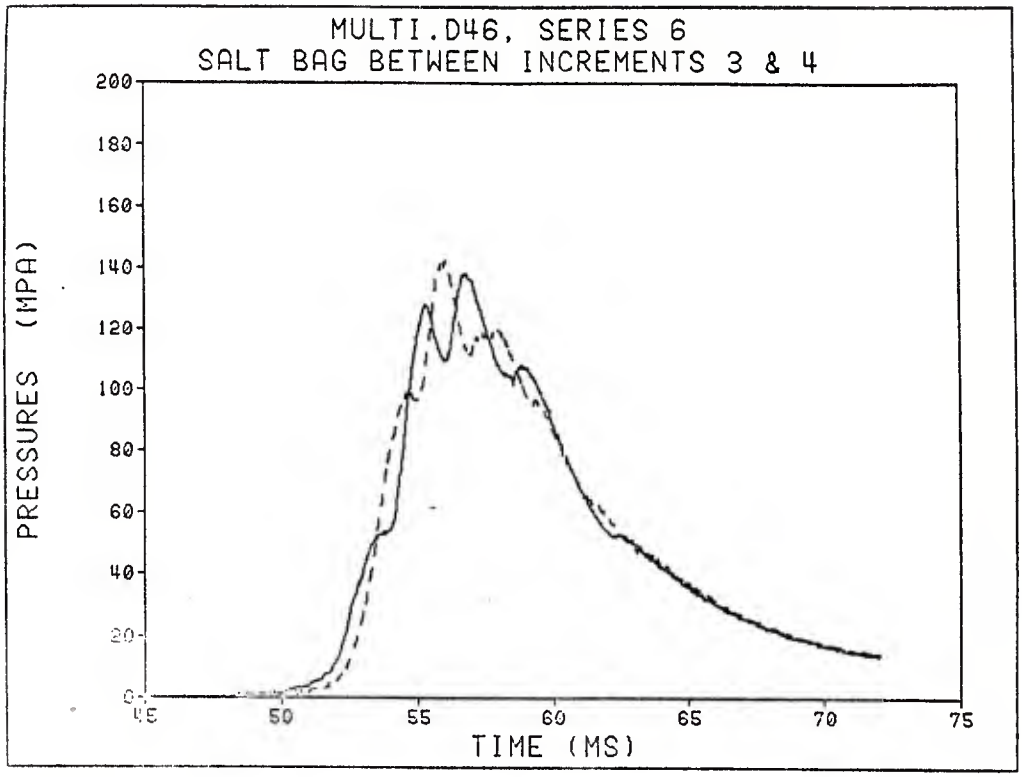
MULTI.D46, SERIES 6
SALT BAG BETWEEN INCREMENTS 3 & 4
PRESSURES (MPA)
200
180
160
140
120
100
80
60
40
20
0
45
50
55
60
65
70
75
TIME (MS)

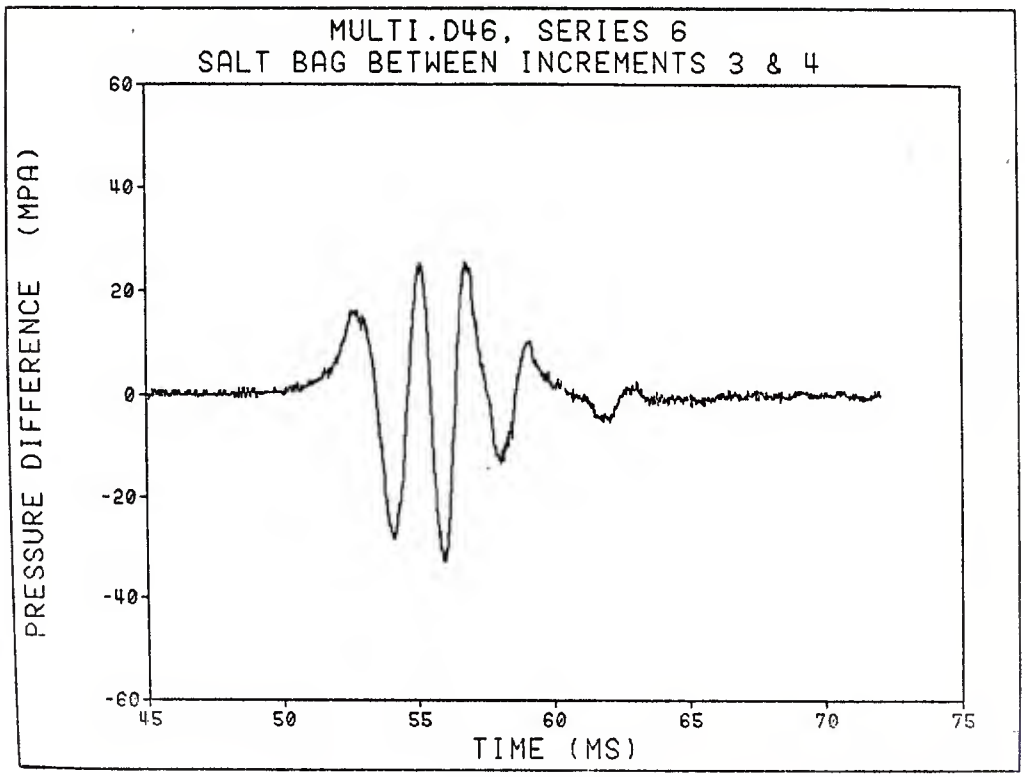
MULTI.D46, SERIES 6
SALT BAG BETWEEN INCREMENTS 3 & 4
PRESSURE DIFFERENCE (MPA)
60
40
20
0
-20
-40
-60
45
50
55
60
65
70
75
TIME (MS)

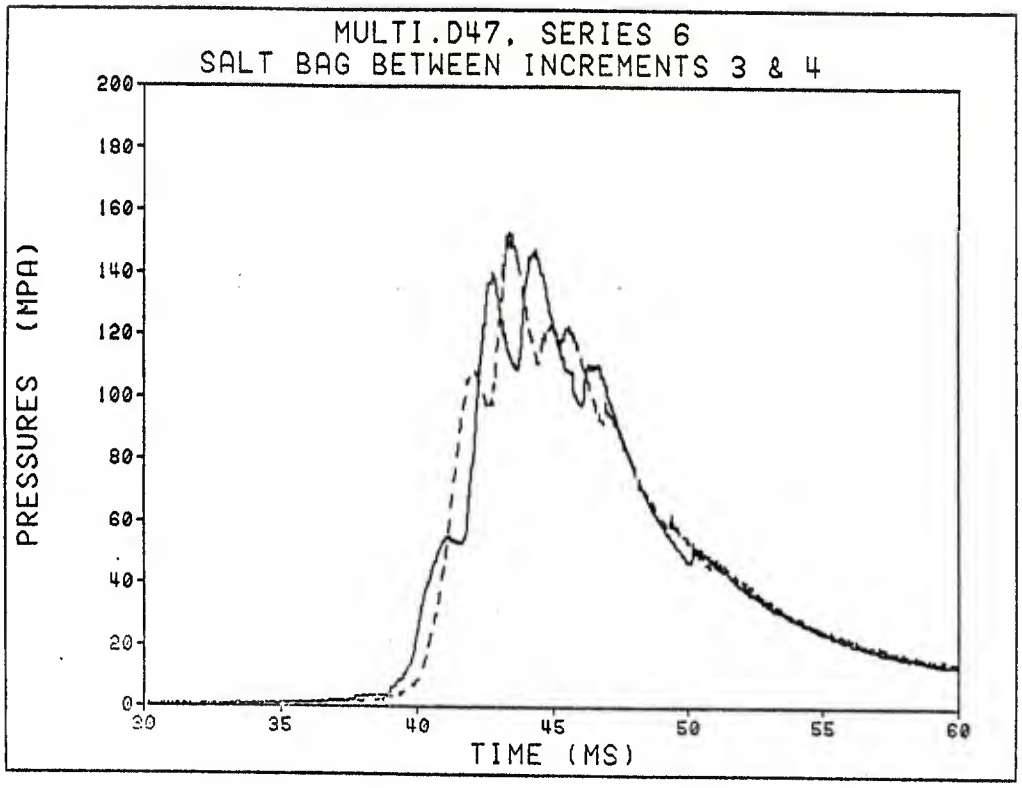
MULTI.D47, SERIES 6
SALT BAG BETWEEN INCREMENTS 3 & 4
PRESSURES (MPA)
200
180
160
140
120
100
80
60
40
20
0
30
35
40
45
50
55
60
TIME (MS)

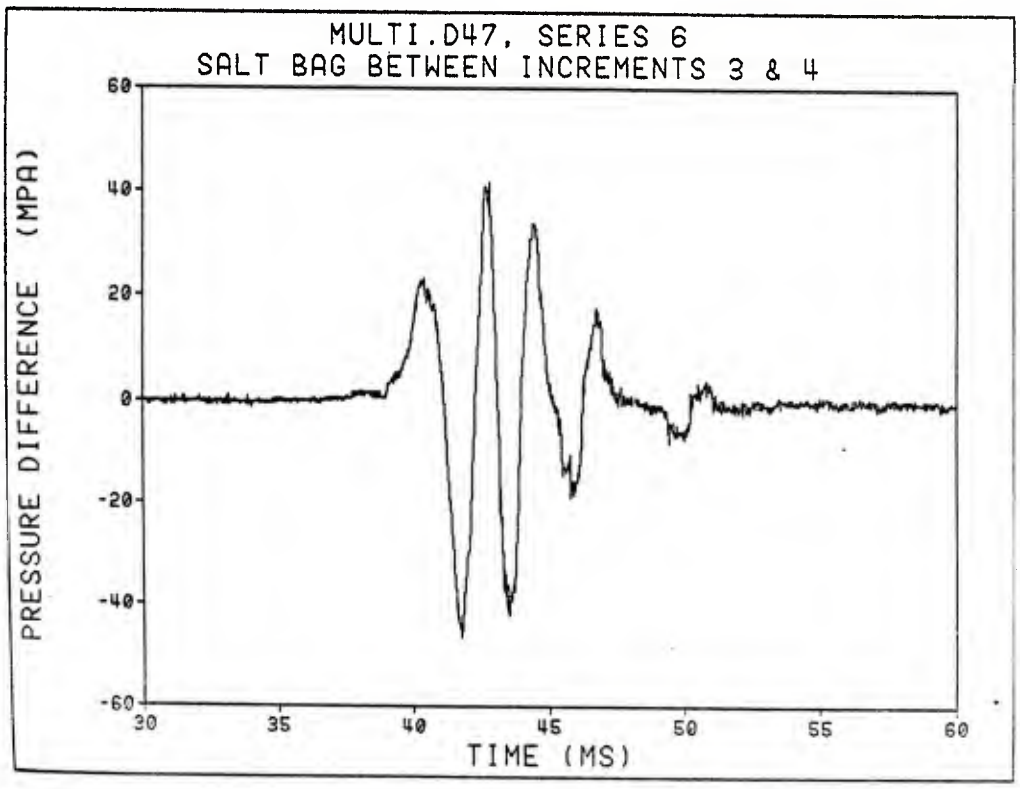
MULTI.D47, SERIES 6
SALT BAG BETWEEN INCREMENTS 3 & 4
PRESSURE DIFFERENCE (MPA)
60
40
20
0
-20
-40
-60
30
35
40
45
50
55
60
TIME (MS)

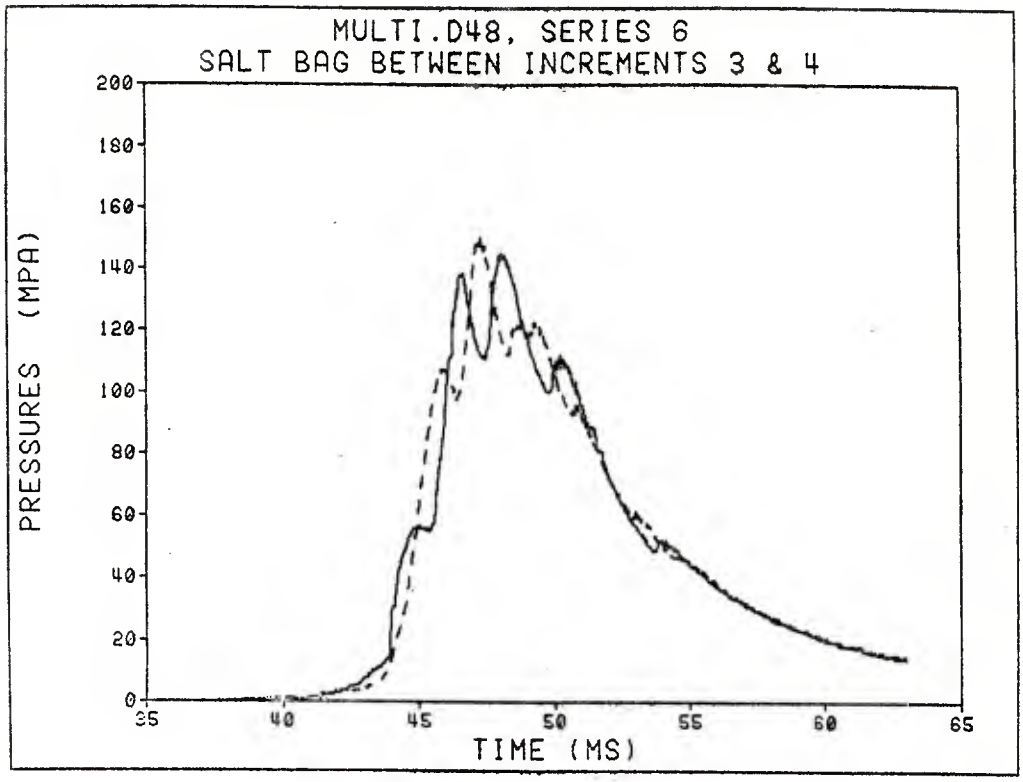
MULTI.D48, SERIES 6
SALT BAG BETWEEN INCREMENTS 3 & 4
PRESSURES (MPA)
200
180
160
140
120
100
80
60
40
20
0
35
40
45
50
55
60
65
TIME (MS)

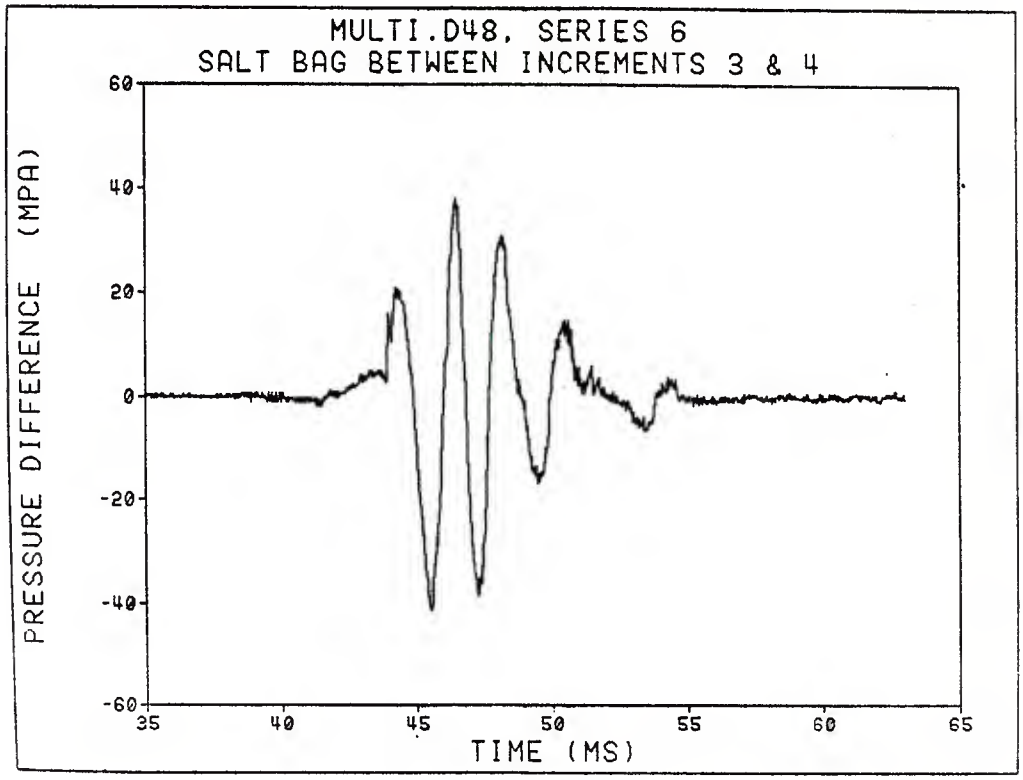
MULTI.D48, SERIES 6
SALT BAG BETWEEN INCREMENTS 3 & 4
PRESSURE DIFFERENCE (MPA)
60
40
20
0
-20
-40
-60
35
40
45
50
55
60
65
TIME (MS)

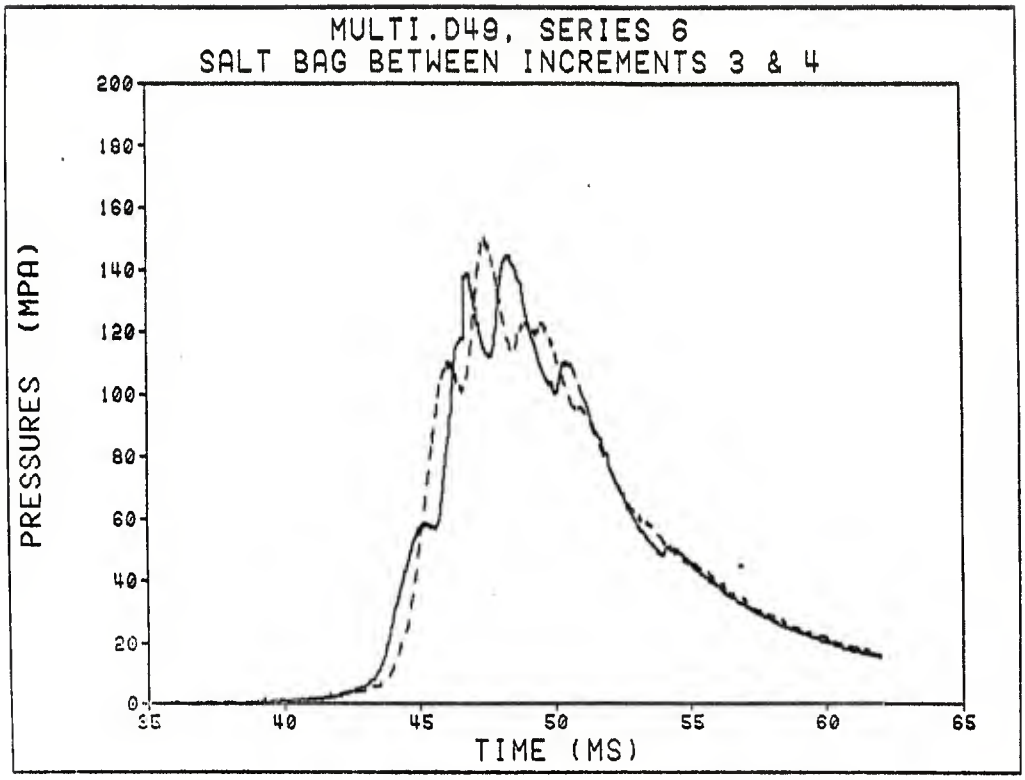
MULTI.D49, SERIES 6
SALT BAG BETWEEN INCREMENTS 3 & 4
PRESSURES (MPA)
200
180
160
140
120
100
80
60
40
20
0
35
40
45
50
55
60
65
TIME (MS)

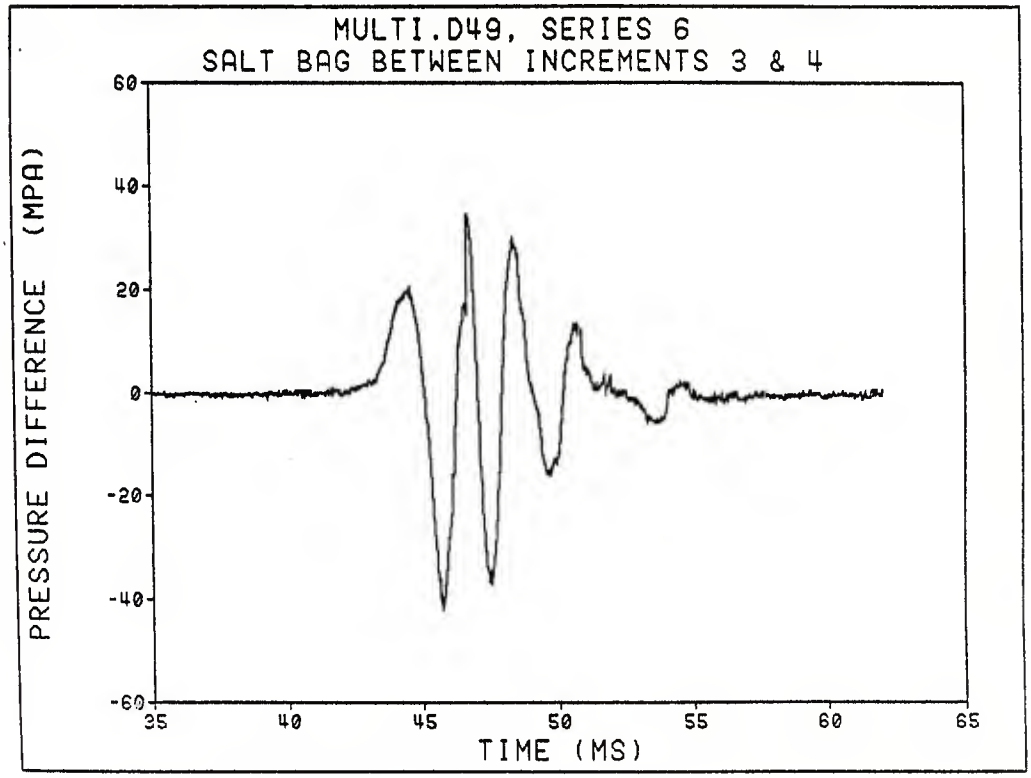
MULTI.D49, SERIES 6
SALT BAG BETWEEN INCREMENTS 3 & 4
PRESSURE DIFFERENCE (MPA)
60
40
20
0
-20
-40
-60
35
40
45
50
55
60
65
TIME (MS)

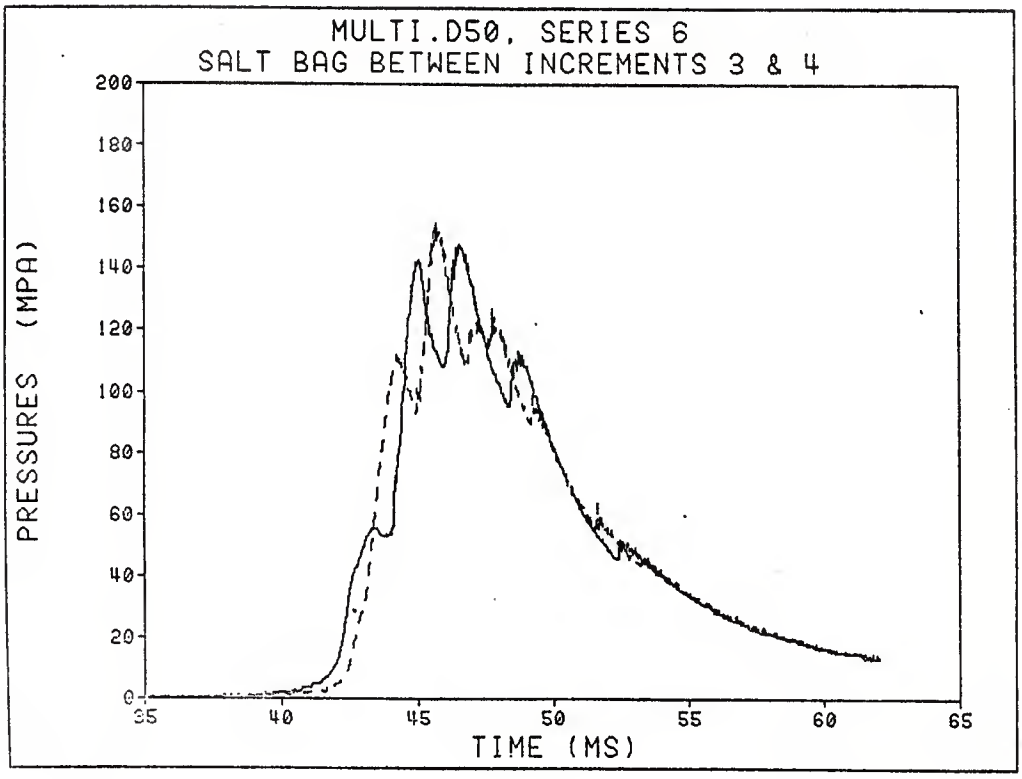
MULTI.D50, SERIES 6
SALT BAG BETWEEN INCREMENTS 3 & 4
PRESSURES (MPA)
200
180
160
140
120
100
80
60
40
20
0
35
40
45
50
55
60
65
TIME (MS)

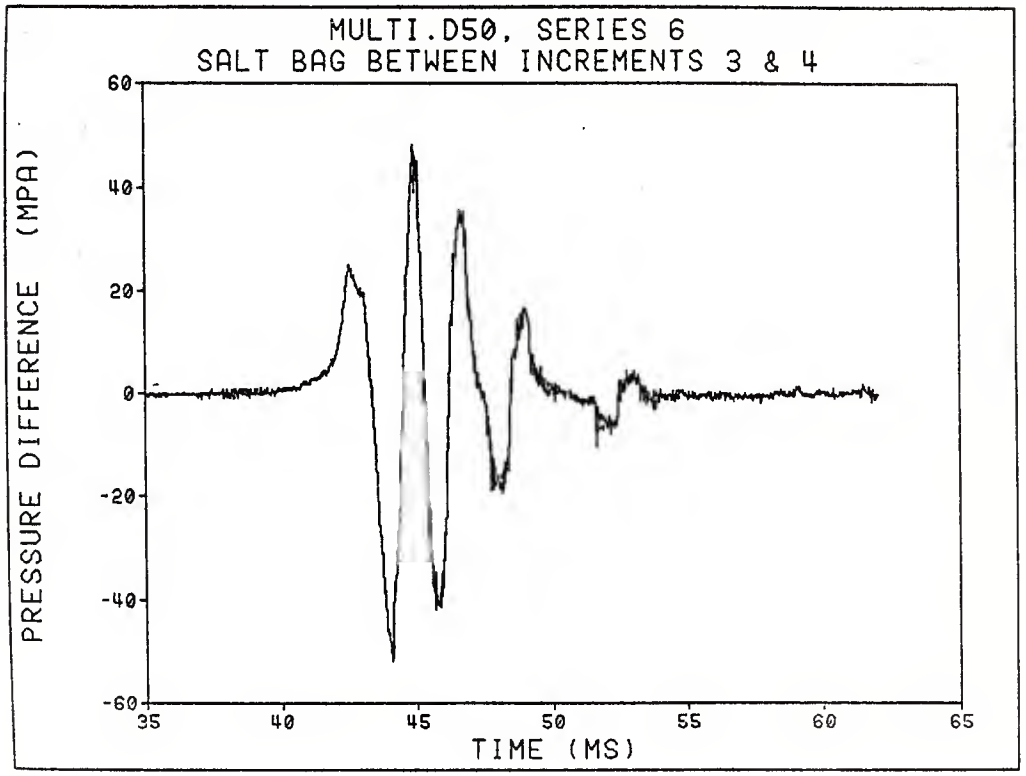
MULTI.D50, SERIES 6
SALT BAG BETWEEN INCREMENTS 3 & 4
PRESSURE DIFFERENCE (MPA)
60
40
20
0
-20
-40
-60
35
40
45
50
55
60
65
TIME (MS)

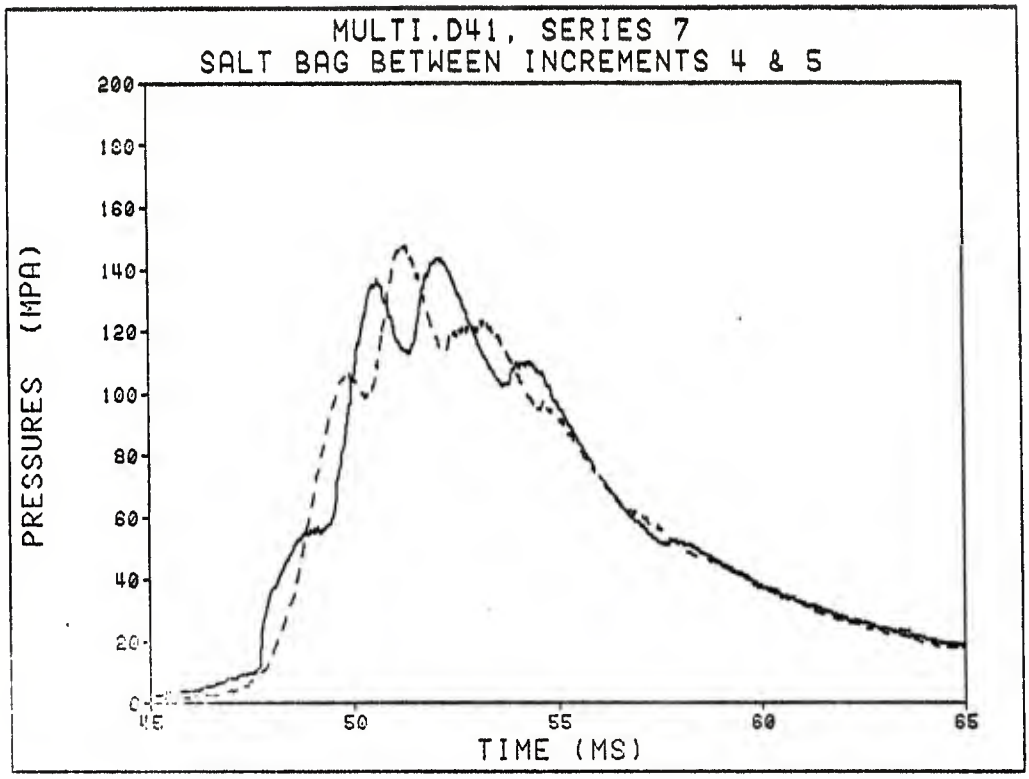
MULTI.D41, SERIES 7
SALT BAG BETWEEN INCREMENTS 4 & 5
PRESSURES (MPA)
200
180
160
140
120
100
80
60
40
20
0
45
50
55
60
65
TIME (MS)

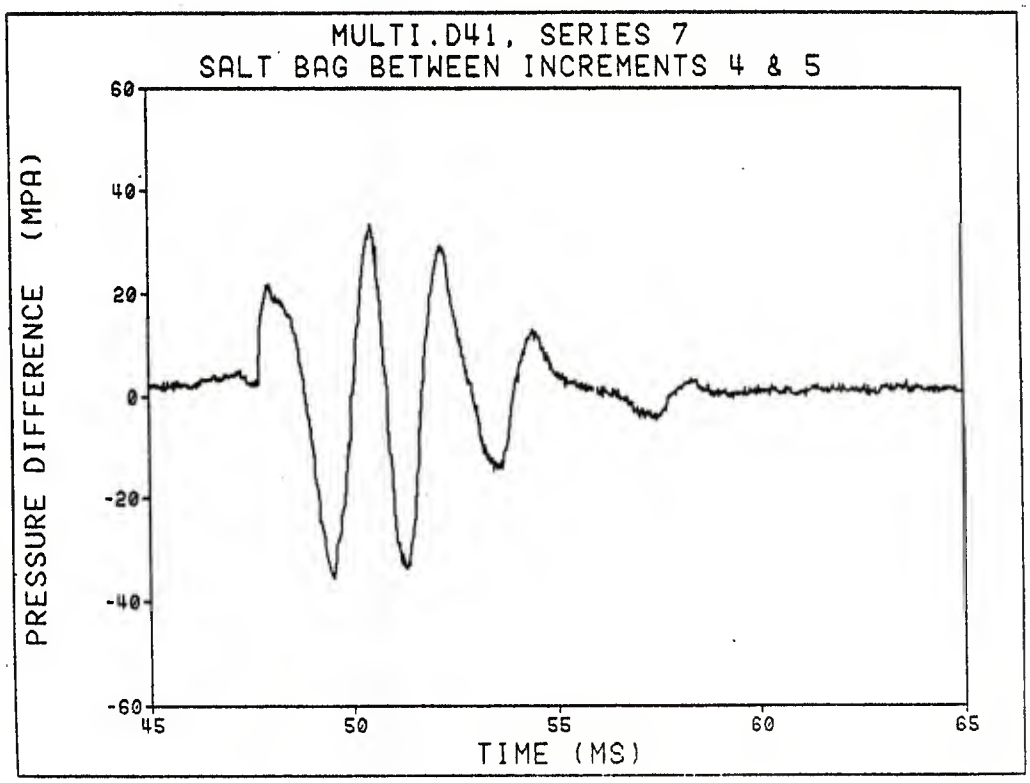
MULTI.D41, SERIES 7
SALT BAG BETWEEN INCREMENTS 4 & 5
PRESSURE DIFFERENCE (MPA)
60
40
20
0
-20
-40
-60
45
50
55
60
65
TIME (MS)

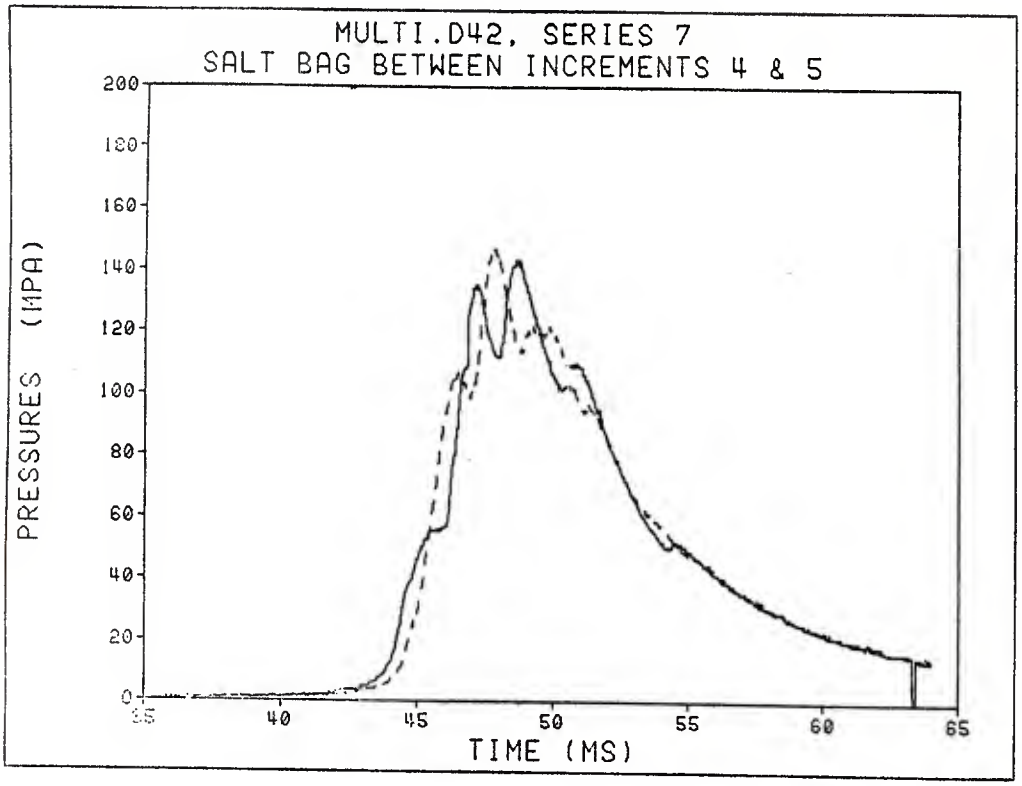
MULTI.D42, SERIES 7
SALT BAG BETWEEN INCREMENTS 4 & 5
PRESSURES (MPA)
200
180
160
140
120
100
80
60
40
20
0
35
40
45
50
55
60
65
TIME (MS)

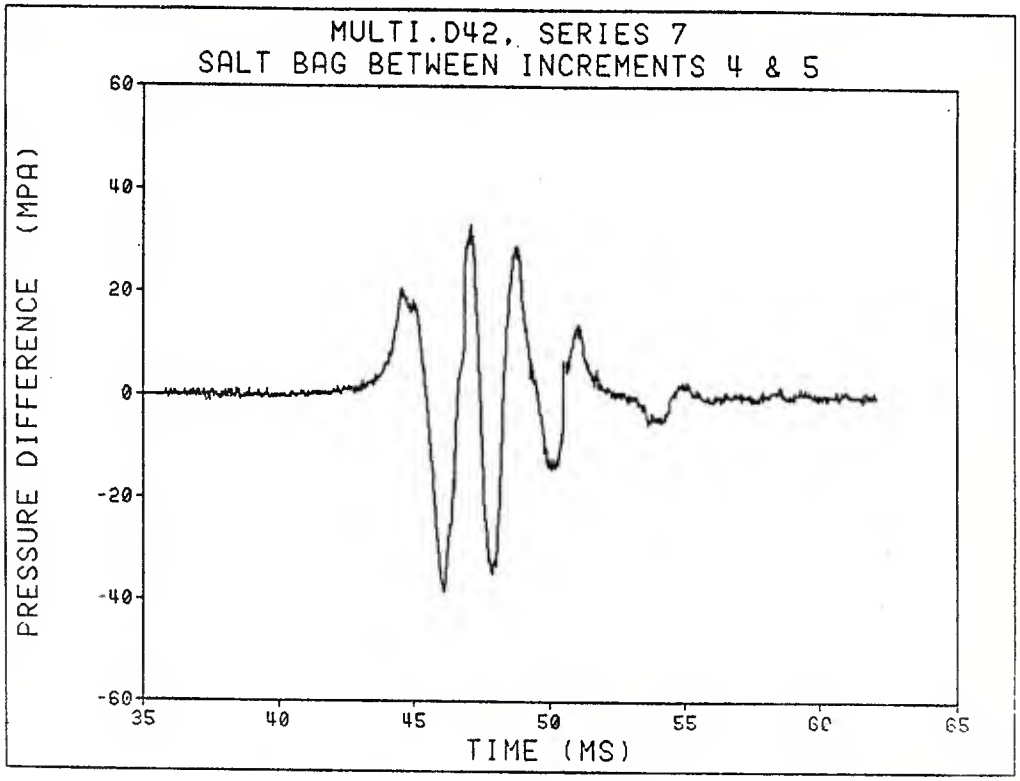
MULTI.D42, SERIES 7
SALT BAG BETWEEN INCREMENTS 4 & 5
PRESSURE DIFFERENCE (MPA)
60
40
20
0
-20
-40
-60
35
40
45
50
55
60
65
TIME (MS)

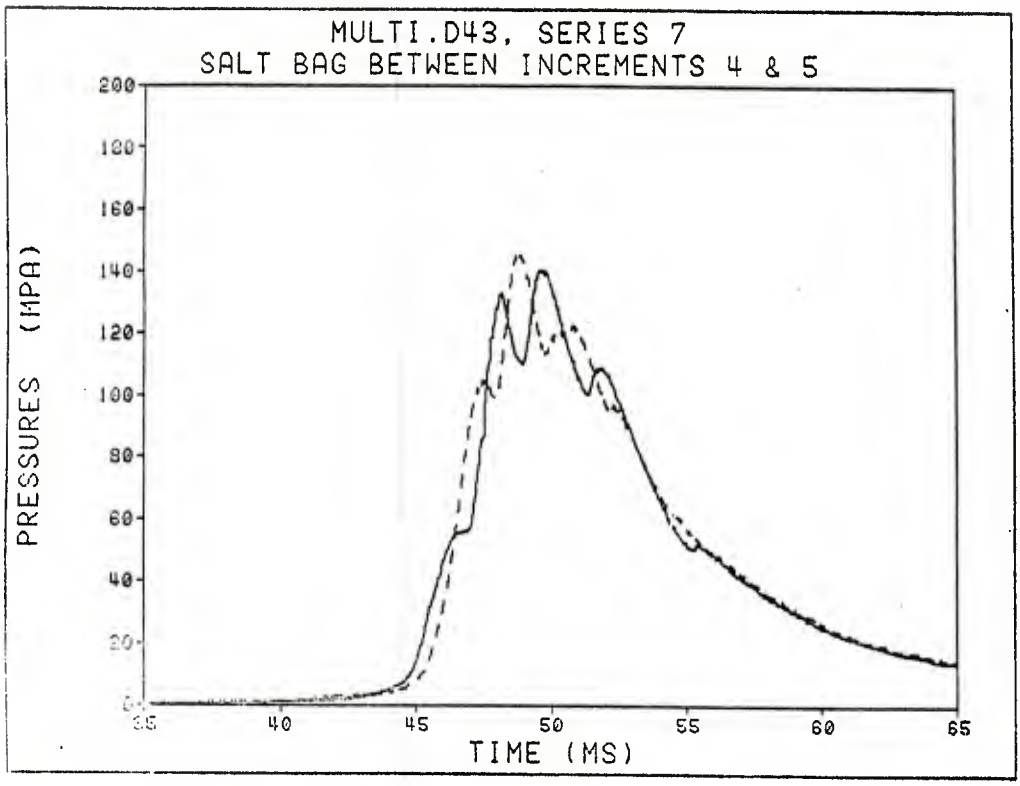
MULTI.D43, SERIES 7
SALT BAG BETWEEN INCREMENTS 4 & 5
PRESSURES (MPA)
200
180
160
140
120
100
80
60
40
20
0
35
40
45
50
55
60
65
TIME (MS)

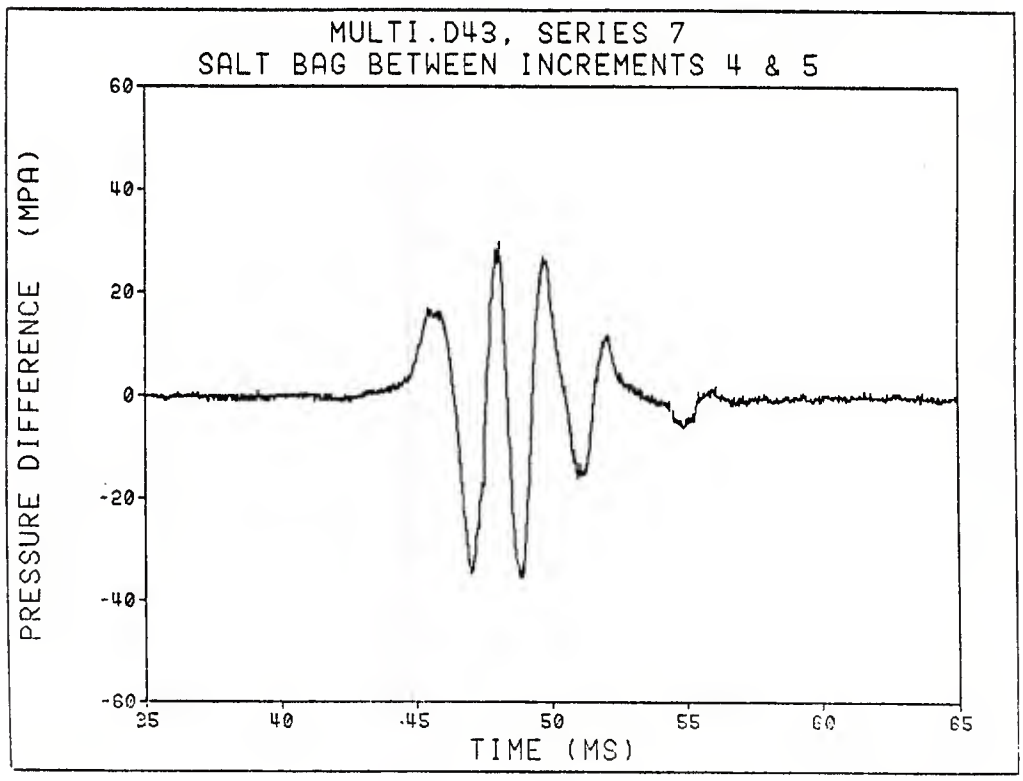
MULTI.D43, SERIES 7
SALT BAG BETWEEN INCREMENTS 4 & 5
PRESSURE DIFFERENCE (MPA)
60
40
20
0
-20
-40
-60
35
40
45
50
55
60
65
TIME (MS)

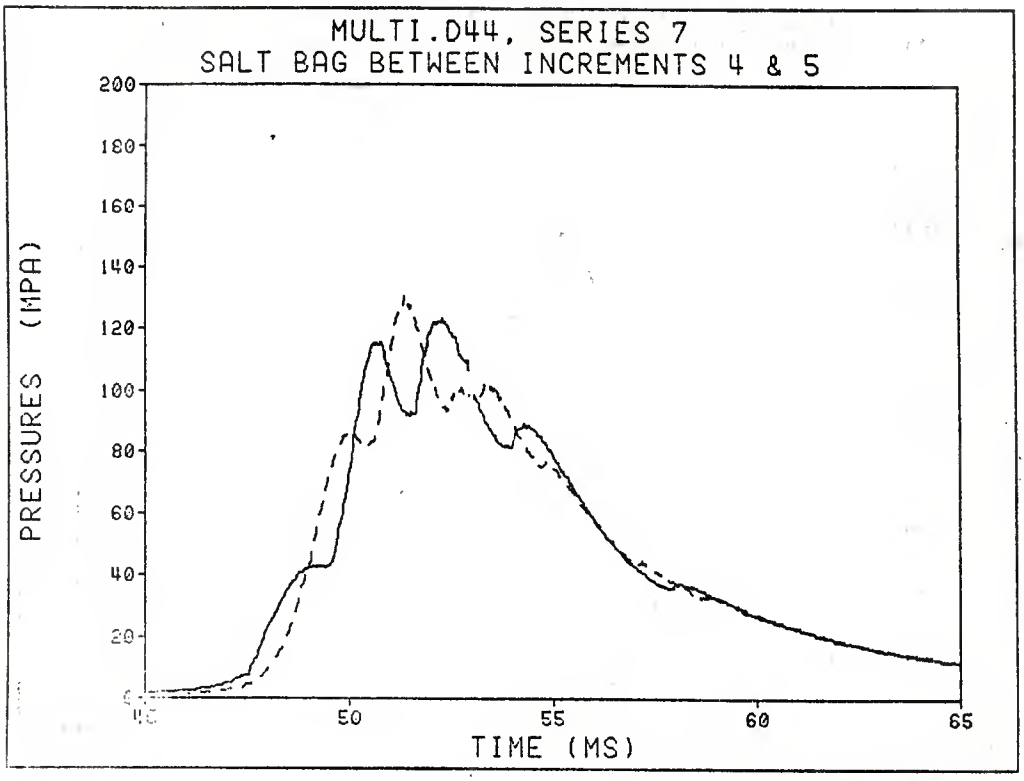
MULTI.D44, SERIES 7
SALT BAG BETWEEN INCREMENTS 4 & 5
PRESSURES (MPA)
200
180
160
140
120
100
80
60
40
20
0
45
50
55
60
65
TIME (MS)

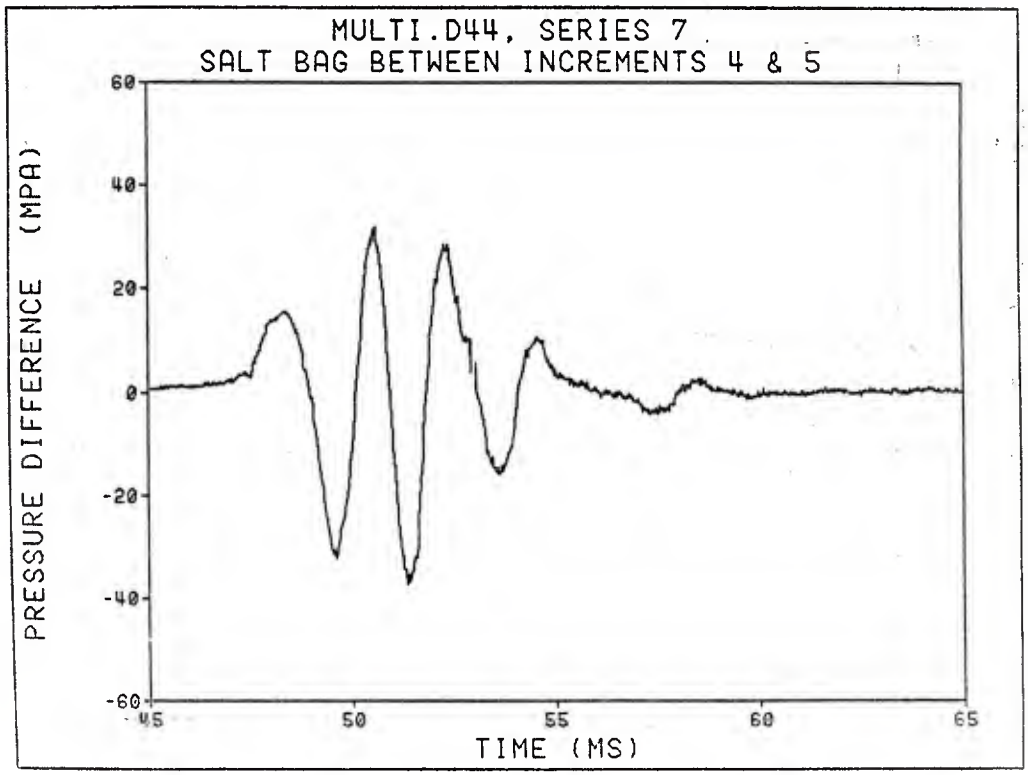
MULTI.D44, SERIES 7
SALT BAG BETWEEN INCREMENTS 4 & 5
PRESSURE DIFFERENCE (MPA)
60
40
20
0
-20
-40
-60
45
50
55
60
65
TIME (MS)

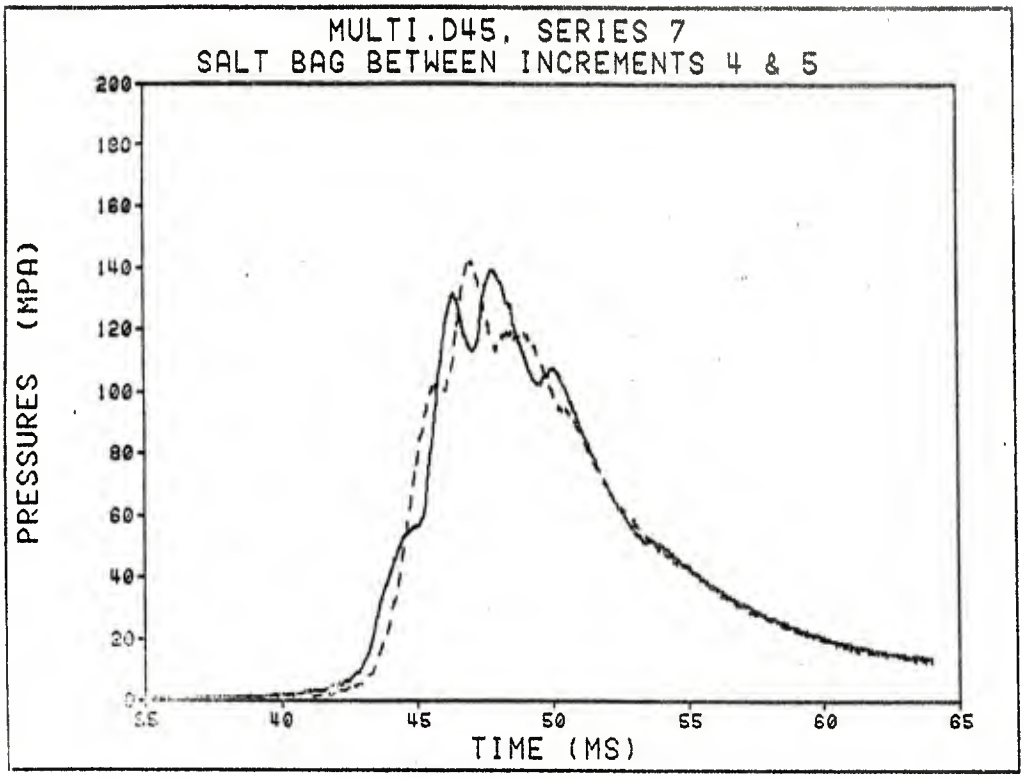
MULTI.D45, SERIES 7
SALT BAG BETWEEN INCREMENTS 4 & 5
PRESSURES (MPA)
200
180
160
140
120
100
80
60
40
20
0
35
40
45
50
55
60
65
TIME (MS)

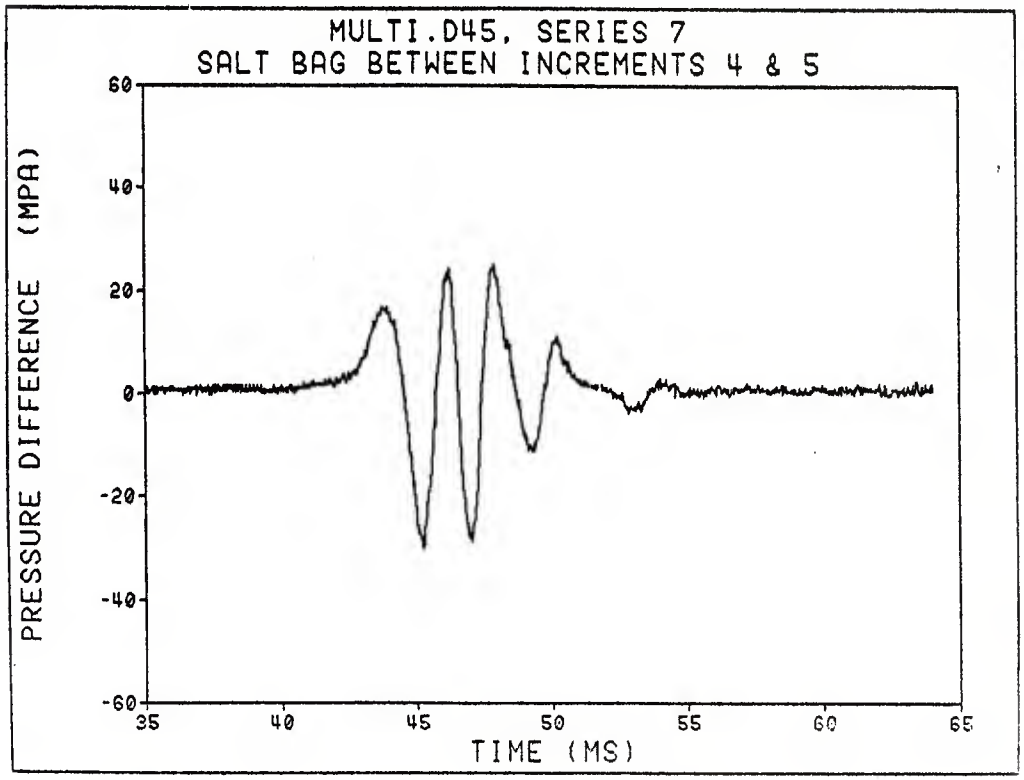
MULTI.D45, SERIES 7
SALT BAG BETWEEN INCREMENTS 4 & 5
PRESSURE DIFFERENCE (MPA)
60
40
20
0
-20
-40
-60
35
40
45
50
55
60
65
TIME (MS)

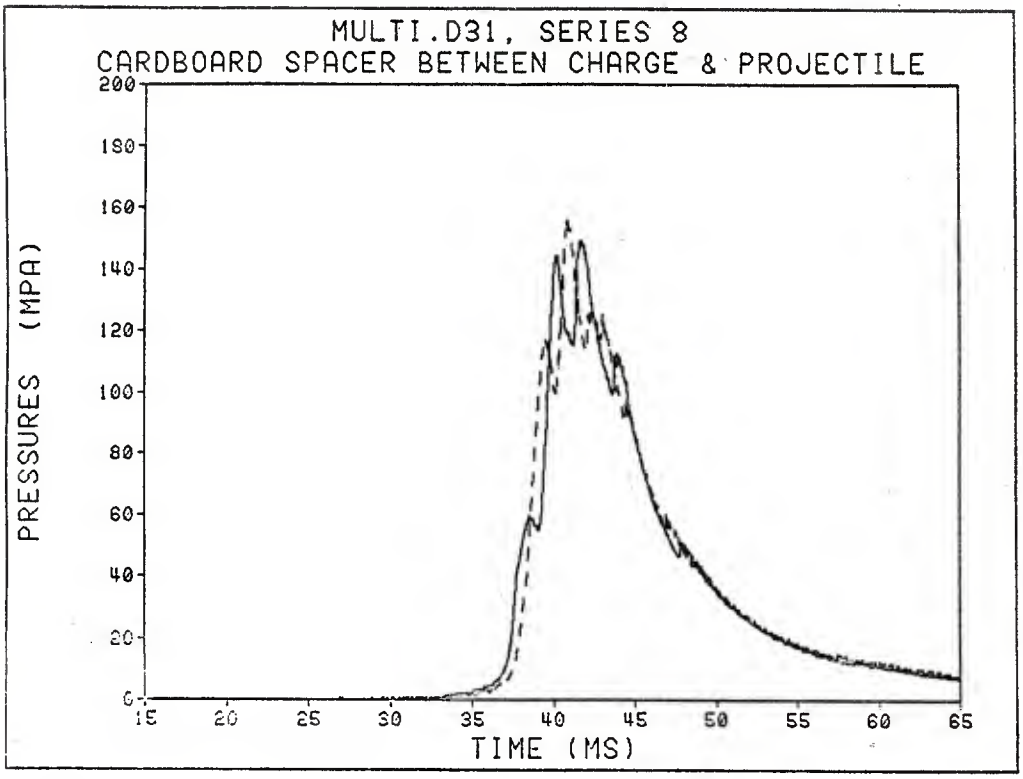
MULTI.D31, SERIES 8
CARDBOARD SPACER BETWEEN CHARGE & PROJECTILE
PRESSURES (MPA)
200
180
160
140
120
100
80
60
40
20
0
15
20
25
30
35
40
45
50
55
60
65
TIME (MS)

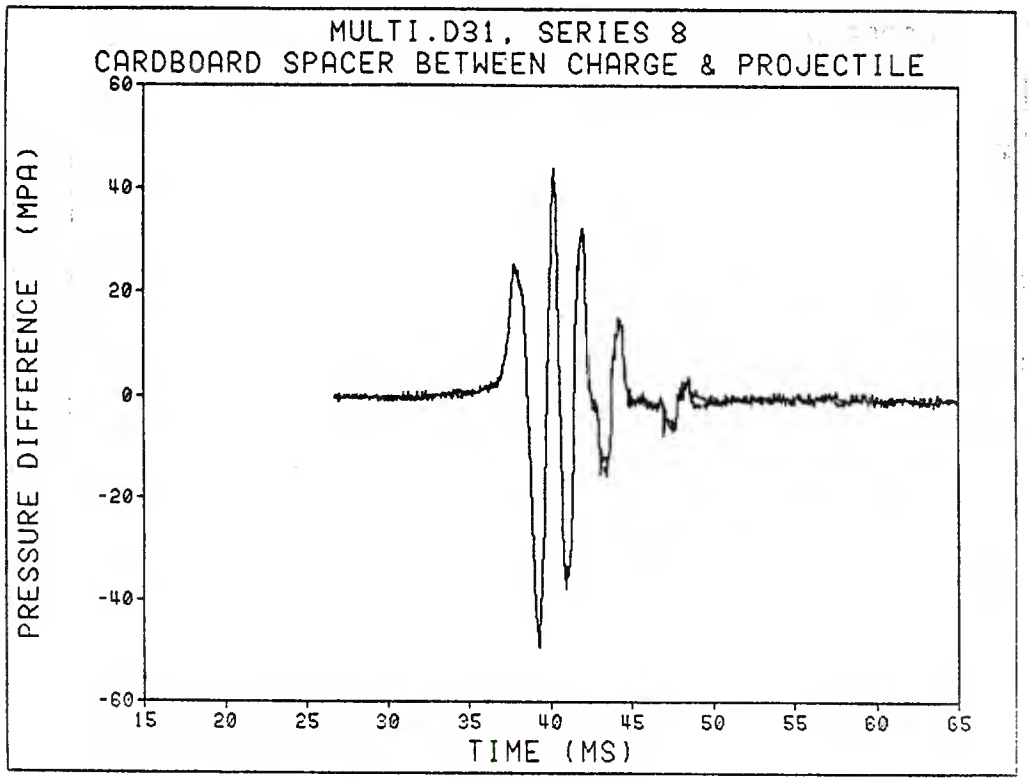
MULTI.D31, SERIES 8
CARDBOARD SPACER BETWEEN CHARGE & PROJECTILE
PRESSURE DIFFERENCE (MPA)
60
40
20
0
-20
-40
-60
15
20
25
30
35
40
45
50
55
60
65
TIME (MS)

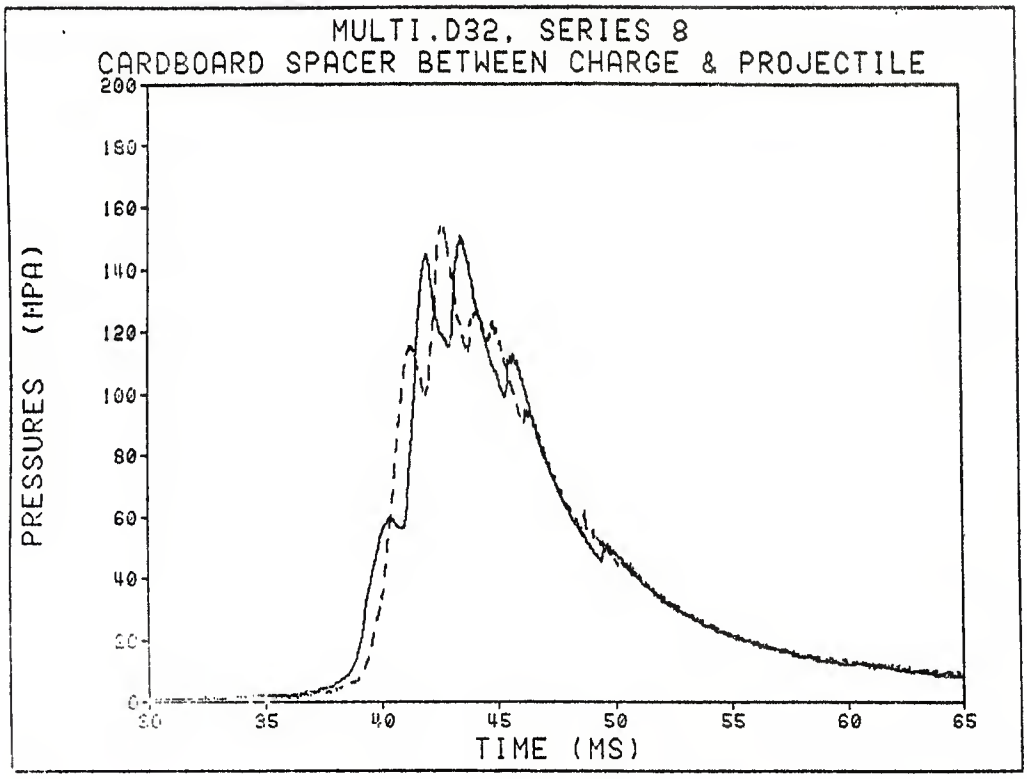
MULTI.D32, SERIES 8
CARDBOARD SPACER BETWEEN CHARGE & PROJECTILE
PRESSURES (MPA)
200
180
160
140
120
100
80
60
40
20
0
30
35
40
45
50
55
60
65
TIME (MS)

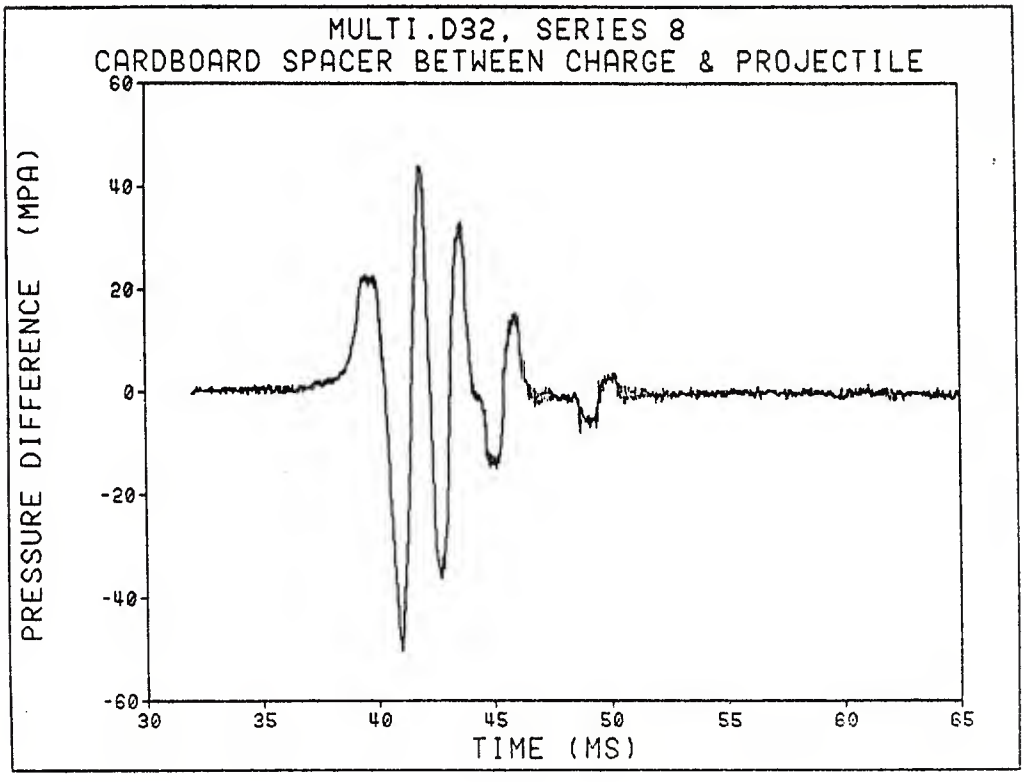
MULTI.D32, SERIES 8
CARDBOARD SPACER BETWEEN CHARGE & PROJECTILE
PRESSURE DIFFERENCE (MPA)
60
40
20
0
-20
-40
-60
30
35
40
45
50
55
60
65
TIME (MS)

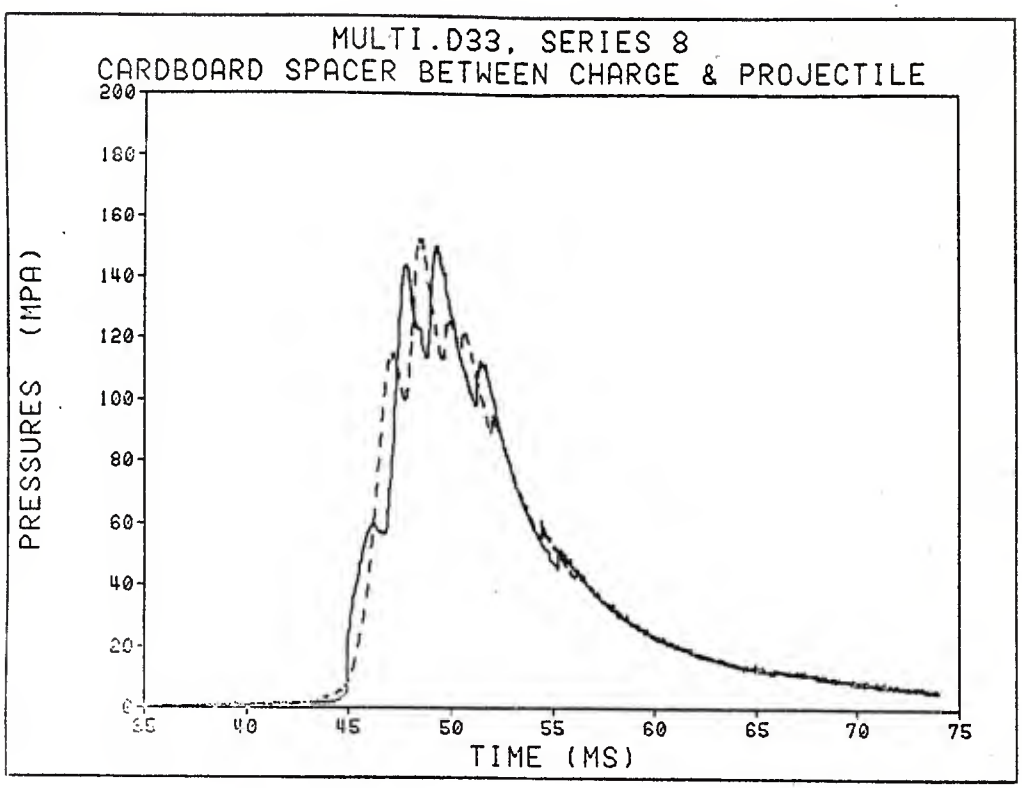
MULTI.D33, SERIES 8
CARDBOARD SPACER BETWEEN CHARGE & PROJECTILE
PRESSURES (MPA)
200
180
160
140
120
100
80
60
40
20
0
35
40
45
50
55
60
65
70
75
TIME (MS)

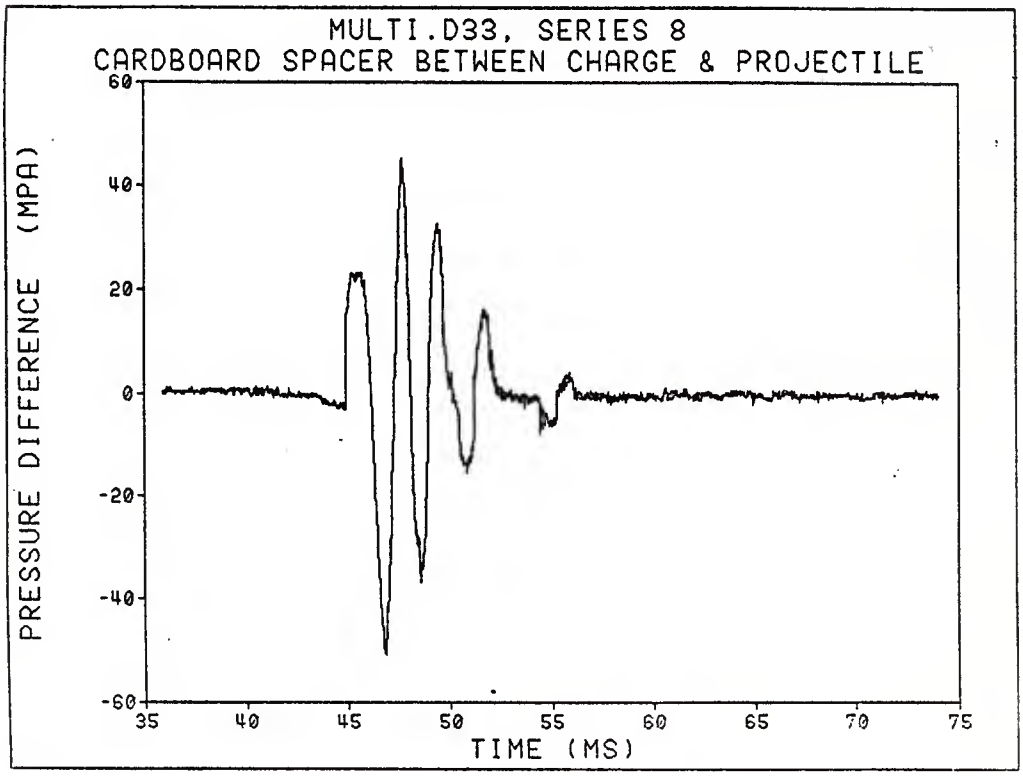
MULTI.D33, SERIES 8
CARDBOARD SPACER BETWEEN CHARGE & PROJECTILE
PRESSURE DIFFERENCE (MPA)
60
40
20
0
-20
-40
-60
35
40
45
50
55
60
65
70
75
TIME (MS)

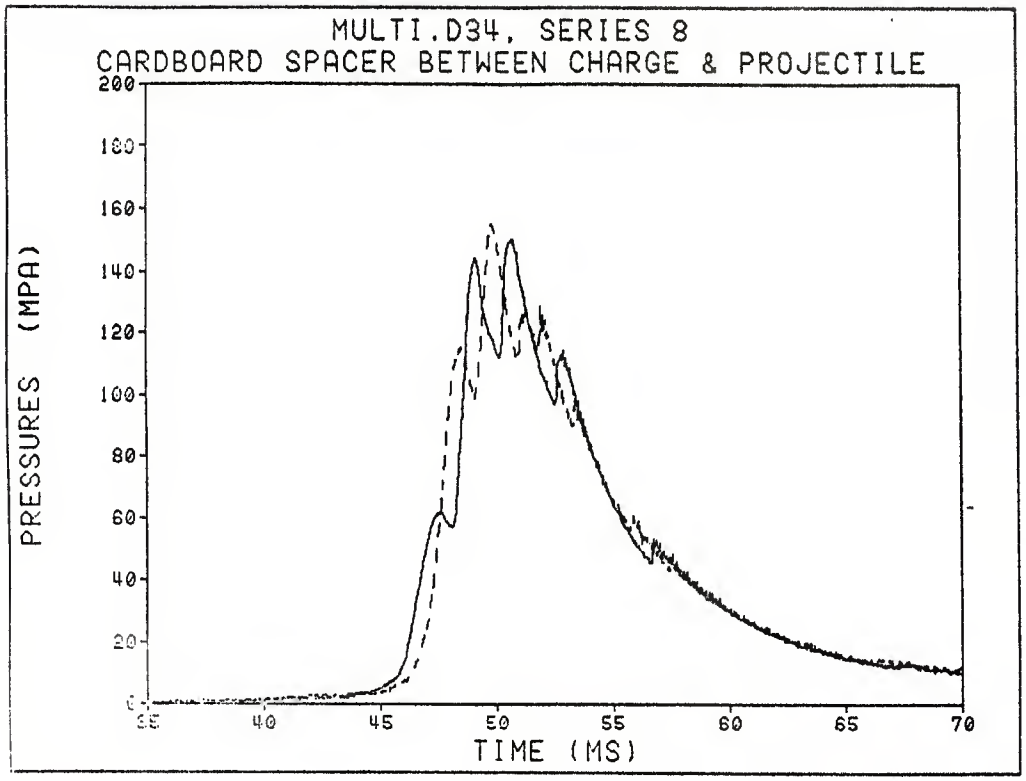
MULTI.D34, SERIES 8
CARDBOARD SPACER BETWEEN CHARGE & PROJECTILE
PRESSURES (MPA)
200
180
160
140
120
100
80
60
40
20
0
35
40
45
50
55
60
65
70
TIME (MS)

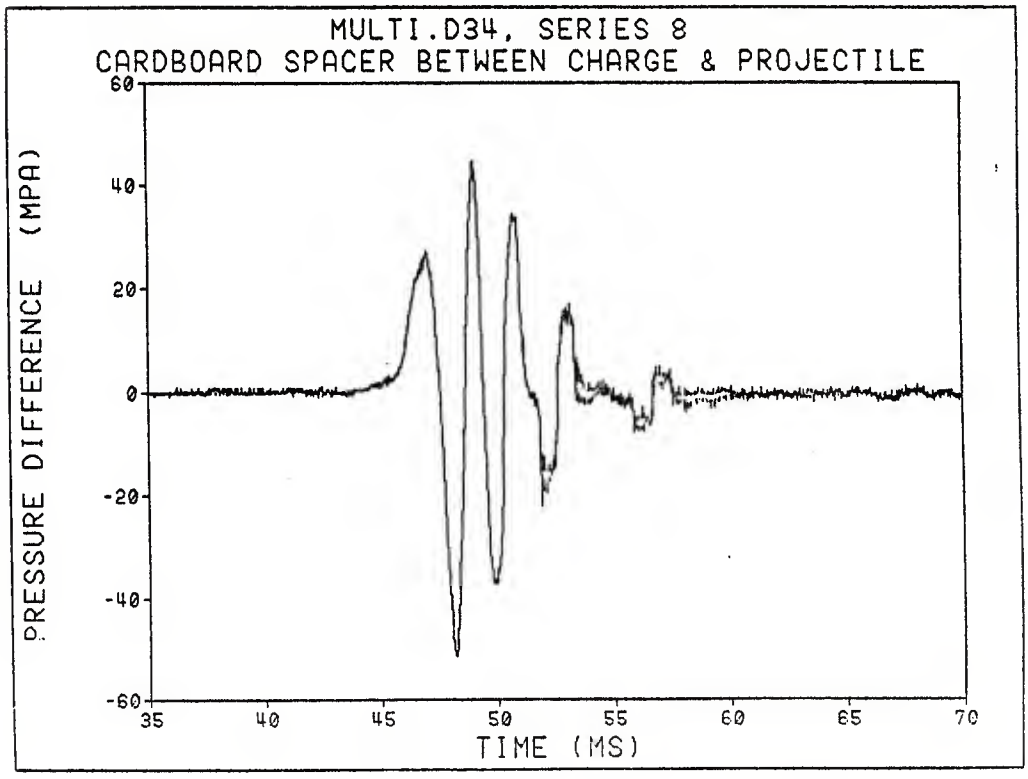
MULTI.D34, SERIES 8
CARDBOARD SPACER BETWEEN CHARGE & PROJECTILE
PRESSURE DIFFERENCE (MPA)
60
40
20
0
-20
-40
-60
35
40
45
50
55
60
65
70
TIME (MS)

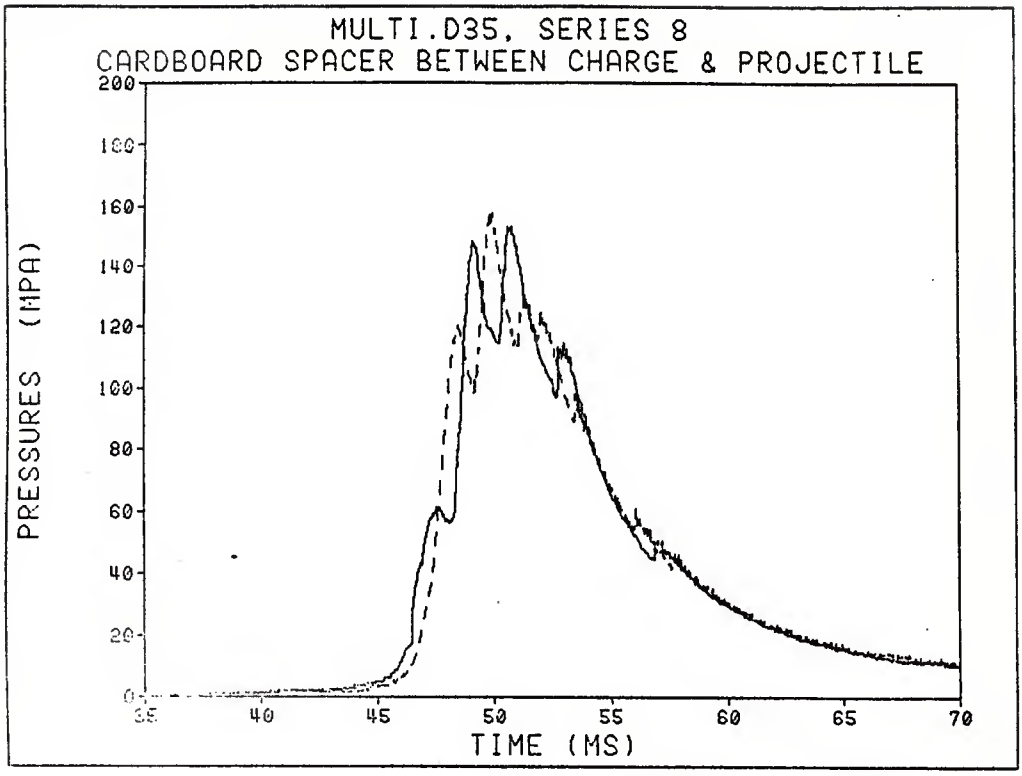
MULTI.D35, SERIES 8
CARDBOARD SPACER BETWEEN CHARGE & PROJECTILE
PRESSURES (MPA)
200
180
160
140
120
100
80
60
40
20
0
35
40
45
50
55
60
65
70
TIME (MS)

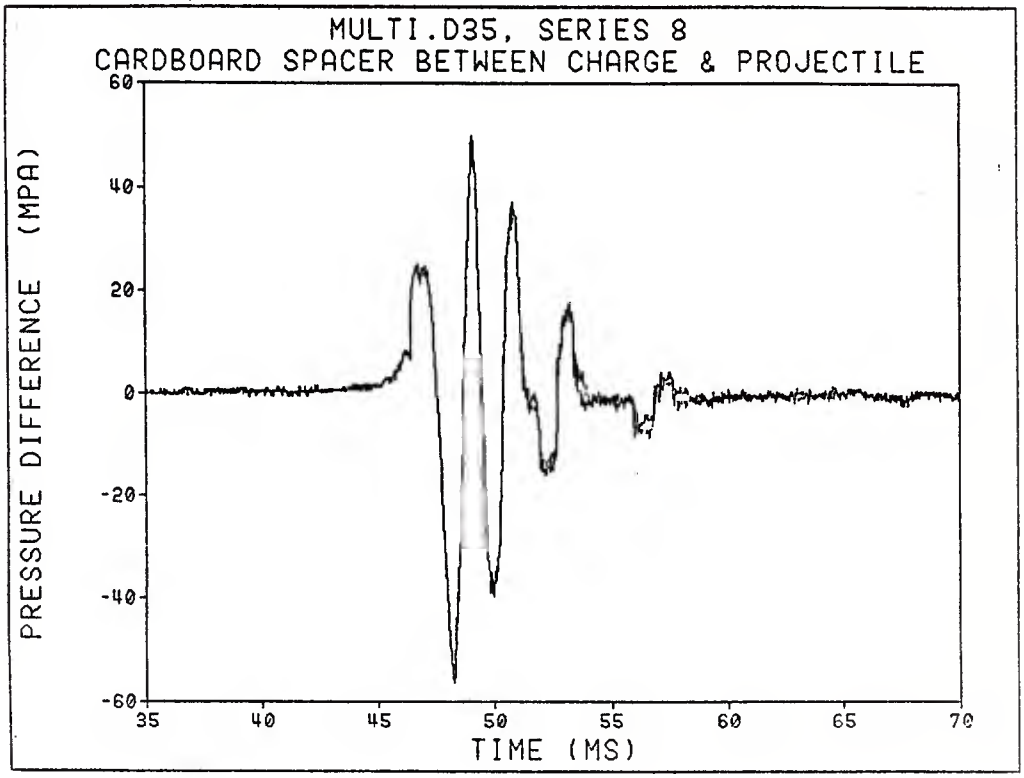
MULTI.D35, SERIES 8
CARDBOARD SPACER BETWEEN CHARGE & PROJECTILE
PRESSURE DIFFERENCE (MPA)
60
40
20
0
-20
-40
-60
35
40
45
50
55
60
65
70
TIME (MS)

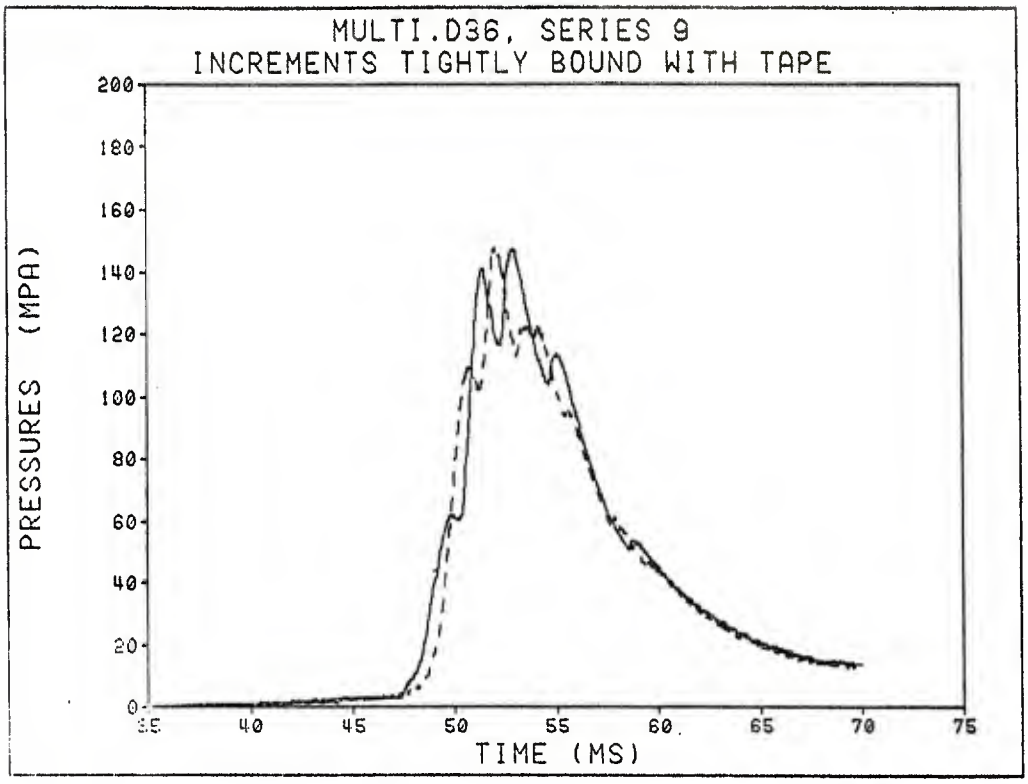
MULTI.D36, SERIES 9
INCREMENTS TIGHTLY BOUND WITH TAPE
PRESSURES (MPA)
200
180
160
140
120
100
80
60
40
20
0
35
40
45
50
55
60
65
70
75
TIME (MS)

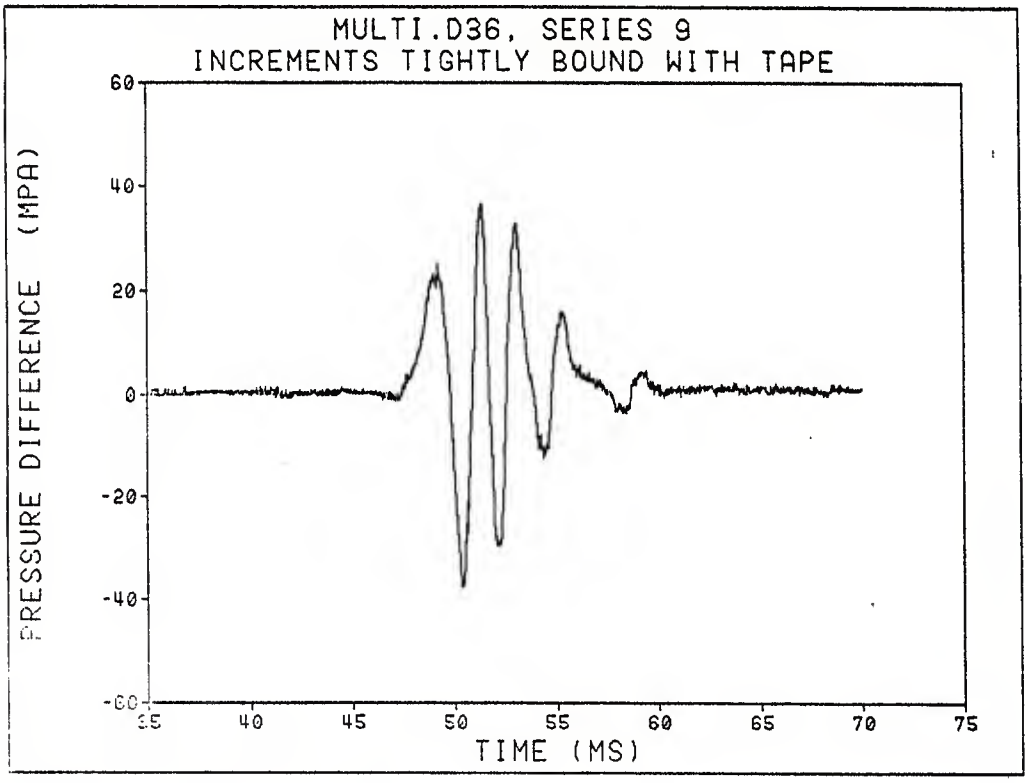
MULTI.D36, SERIES 9
INCREMENTS TIGHTLY BOUND WITH TAPE
PRESSURE DIFFERENCE (MPA)
60
40
20
0
-20
-40
35
40
45
50
55
60
65
70
75
TIME (MS)

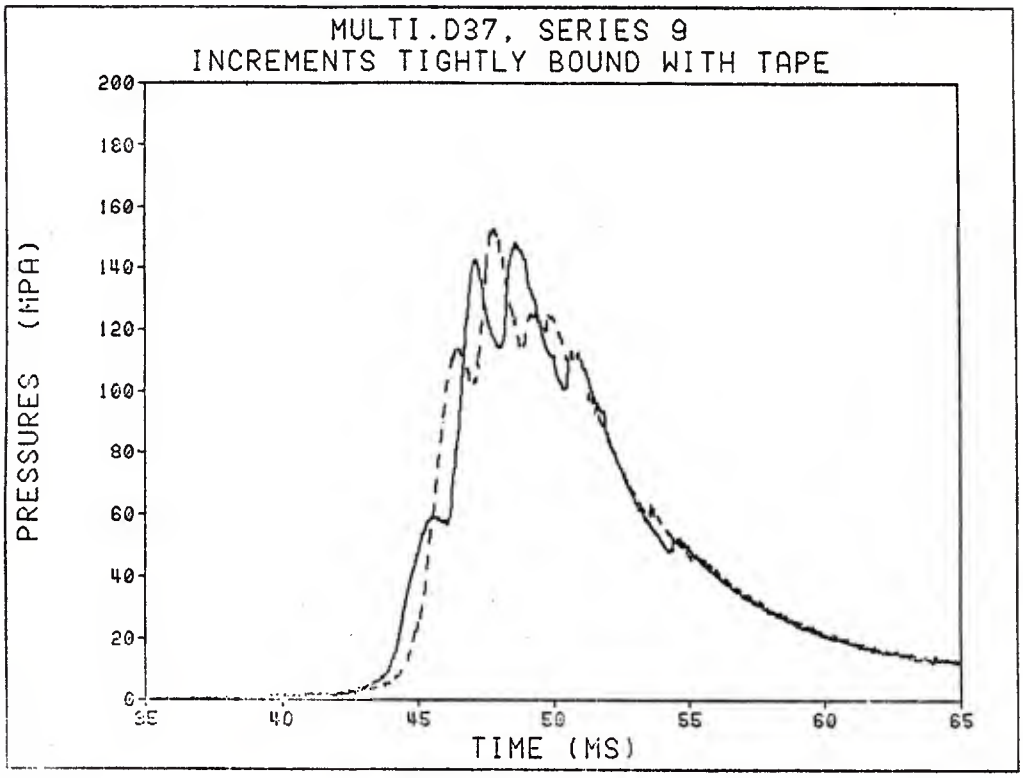
MULTI.D37, SERIES 9
INCREMENTS TIGHTLY BOUND WITH TAPE
PRESSURES (MPA)
200
180
160
140
120
100
80
60
40
20
0
35
40
45
50
55
60
65
TIME (MS)

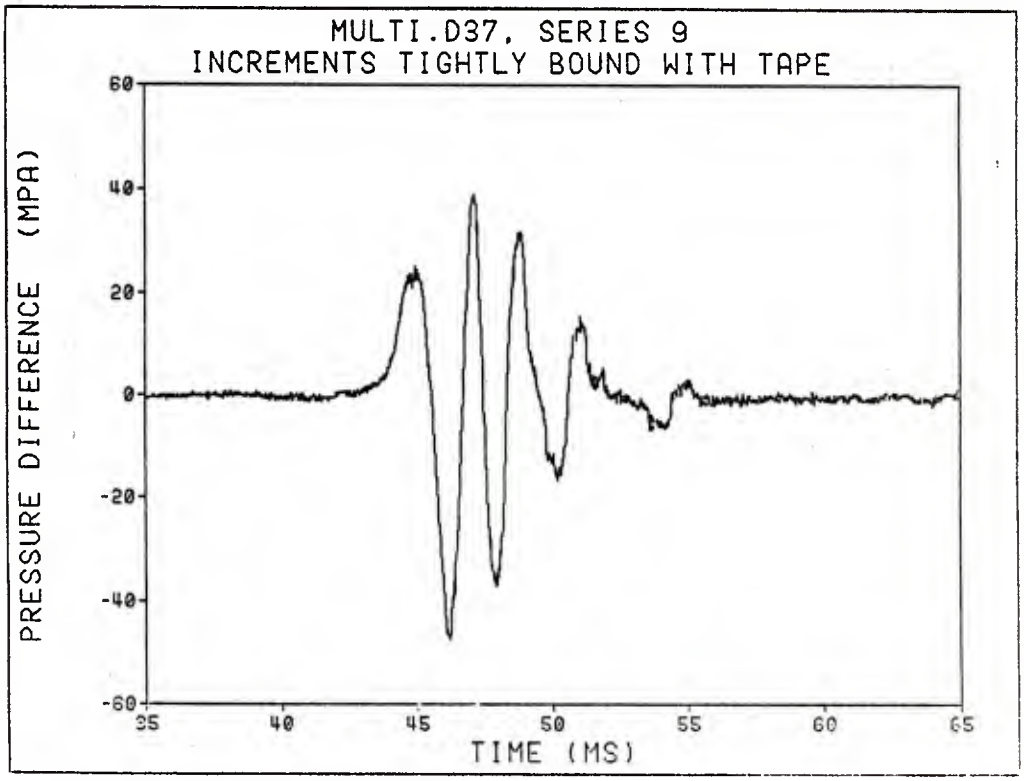
MULTI.D37, SERIES 9
INCREMENTS TIGHTLY BOUND WITH TAPE
PRESSURE DIFFERENCE (MPA)
60
40
20
0
-20
-40
-60
35
40
45
50
55
60
65
TIME (MS)

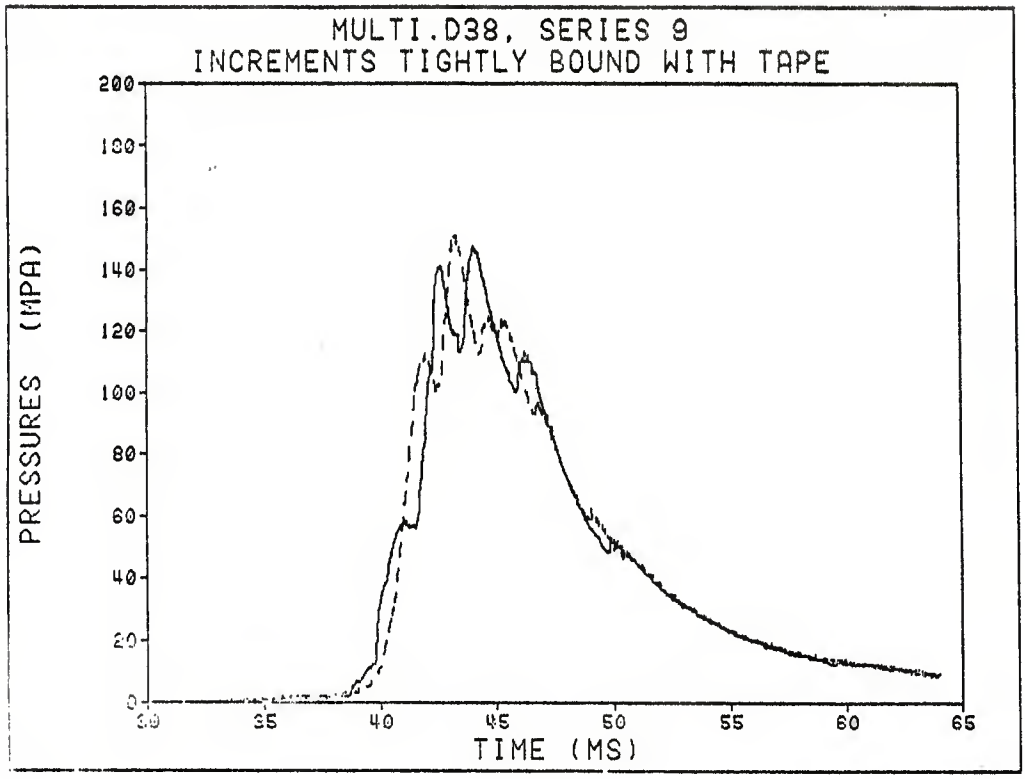
MULTI.D38, SERIES 9
INCREMENTS TIGHTLY BOUND WITH TAPE
PRESSURES (MPA)
200
180
160
140
120
100
80
60
40
20
0
30
35
40
45
50
55
60
65
TIME (MS)

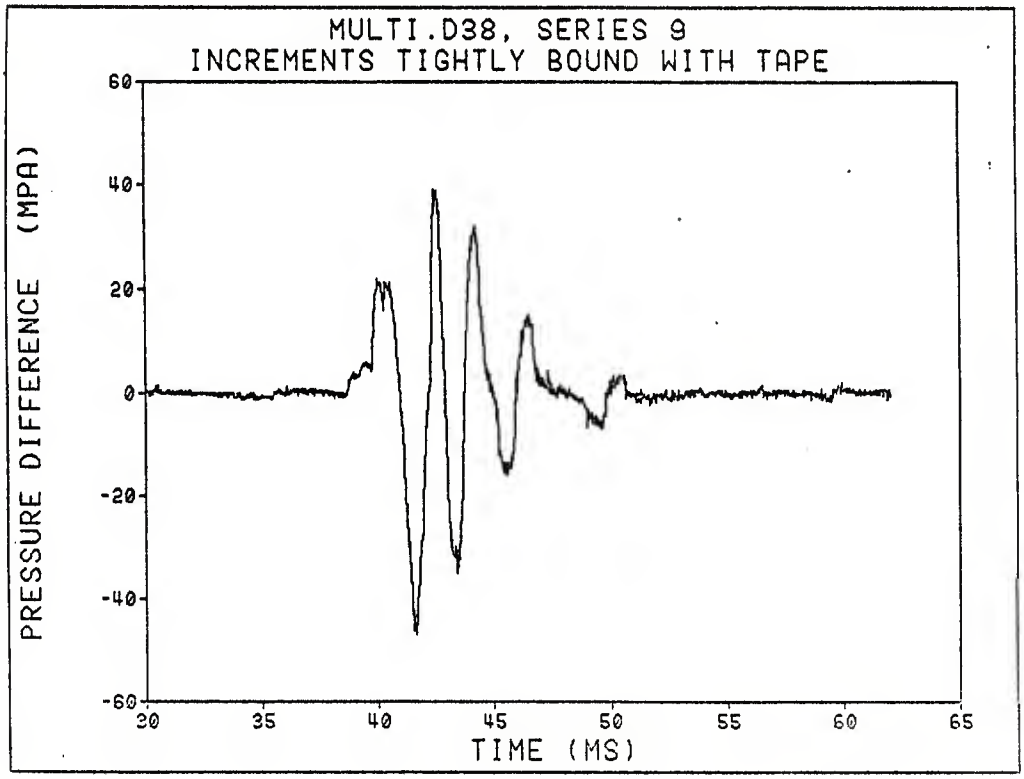
MULTI.D38, SERIES 9
INCREMENTS TIGHTLY BOUND WITH TAPE
PRESSURE DIFFERENCE (MPA)
60
40
20
0
-20
-40
-60
30
35
40
45
50
55
60
65
TIME (MS)

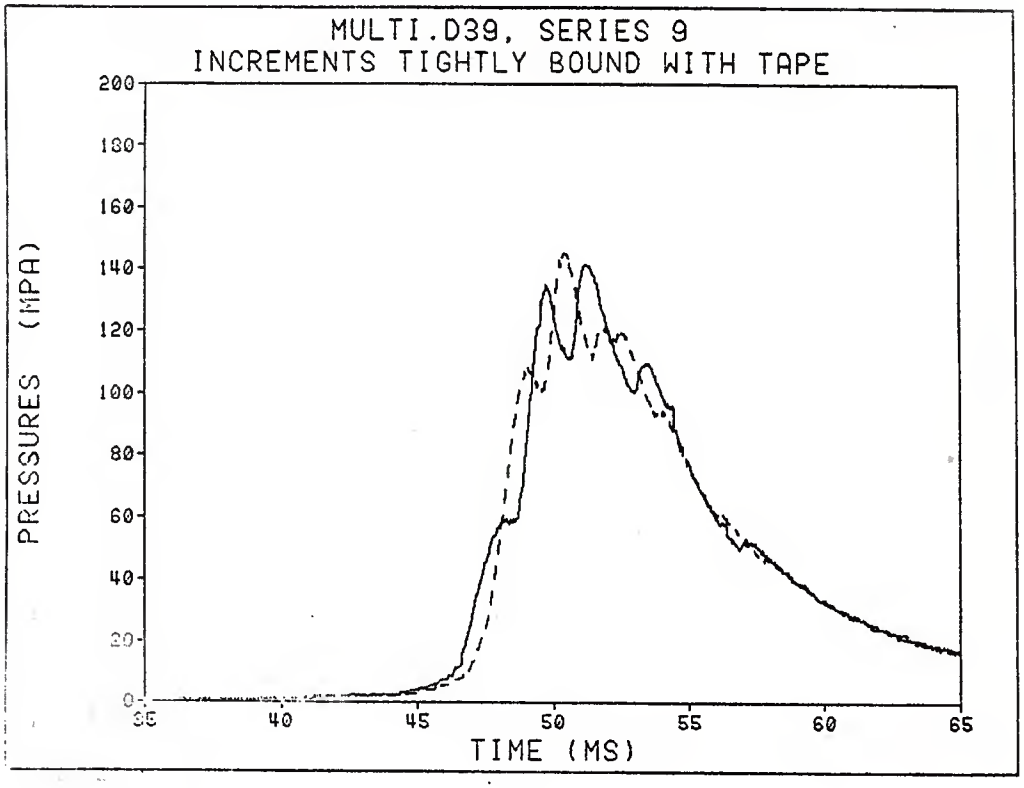
MULTI.D39, SERIES 9
INCREMENTS TIGHTLY BOUND WITH TAPE
PRESSURES (MPA)
200
180
160
140
120
100
80
60
40
20
0
35
40
45
50
55
60
65
TIME (MS)

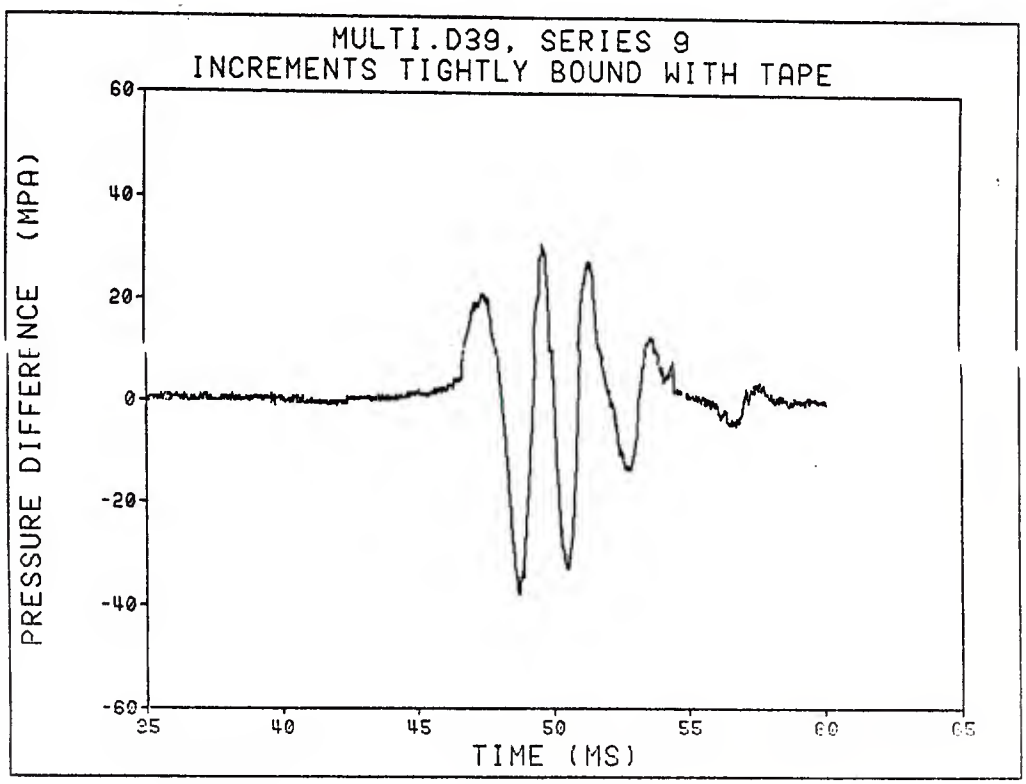
MULTI.D39, SERIES 9
INCREMENTS TIGHTLY BOUND WITH TAPE
PRESSURE DIFFERENCE (MPA)
60
40
20
0
-20
-40
-60
35
40
45
50
55
60
65
TIME (MS)

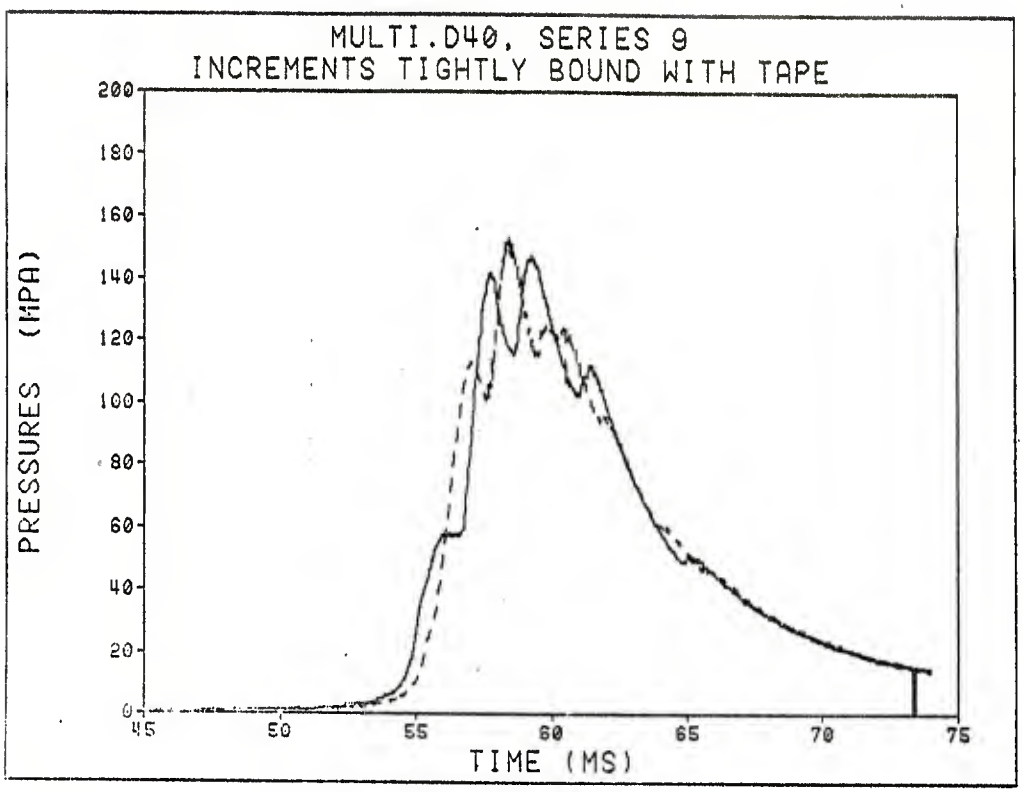
MULTI.D40, SERIES 9
INCREMENTS TIGHTLY BOUND WITH TAPE
PRESSURES (MPA)
200
180
160
140
120
100
80
60
40
20
0
45
50
55
60
65
70
75
TIME (MS)

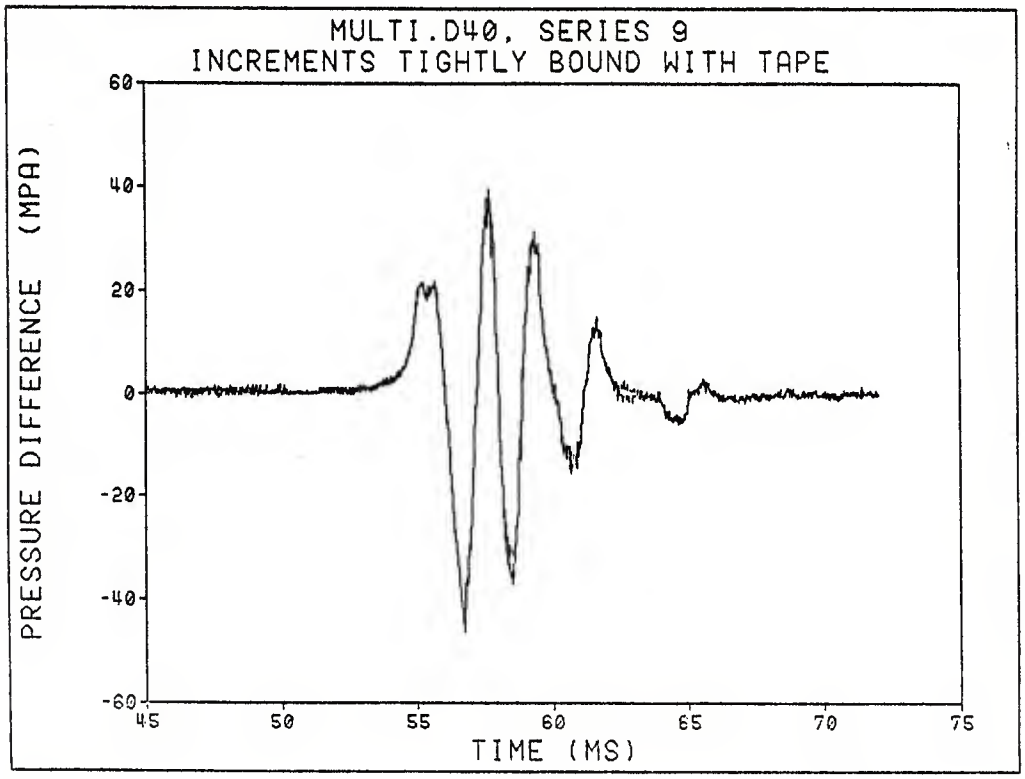
MULTI.D40, SERIES 9
INCREMENTS TIGHTLY BOUND WITH TAPE
PRESSURE DIFFERENCE (MPA)
60
40
20
0
-20
-40
-60
45
50
55
60
65
70
75
TIME (MS)

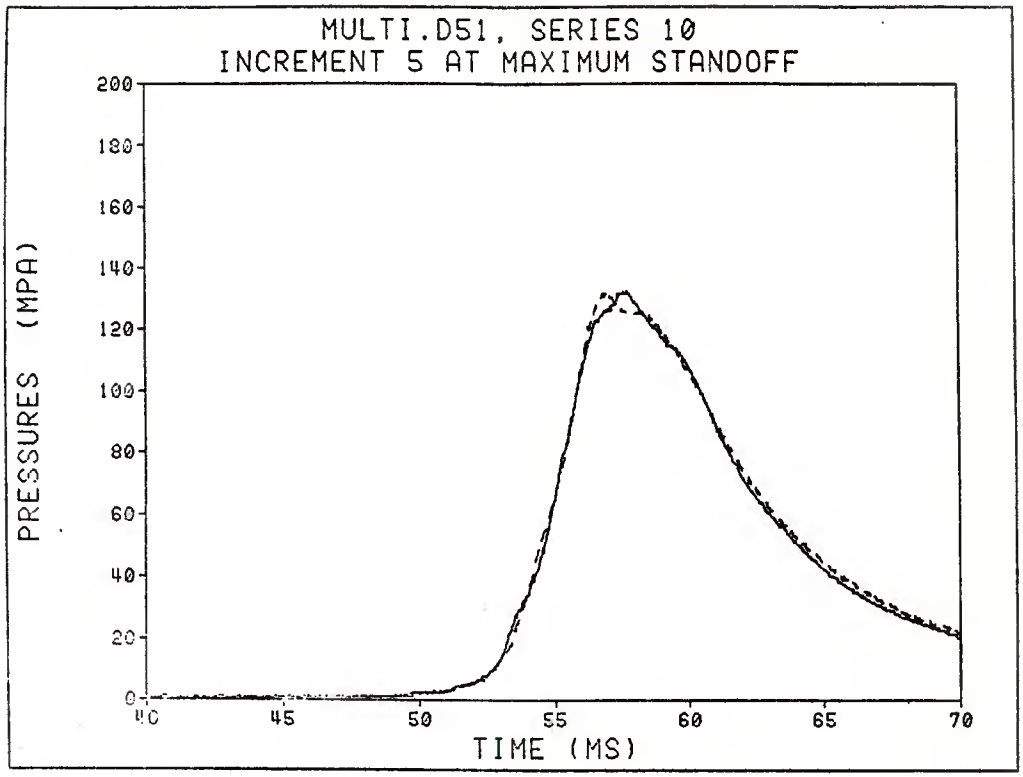
MULTI.D51, SERIES 10
INCREMENT 5 AT MAXIMUM STANDOFF
PRESSURES (MPA)
200
180
160
140
120
100
80
60
40
20
0
40
45
50
55
60
65
70
TIME (MS)

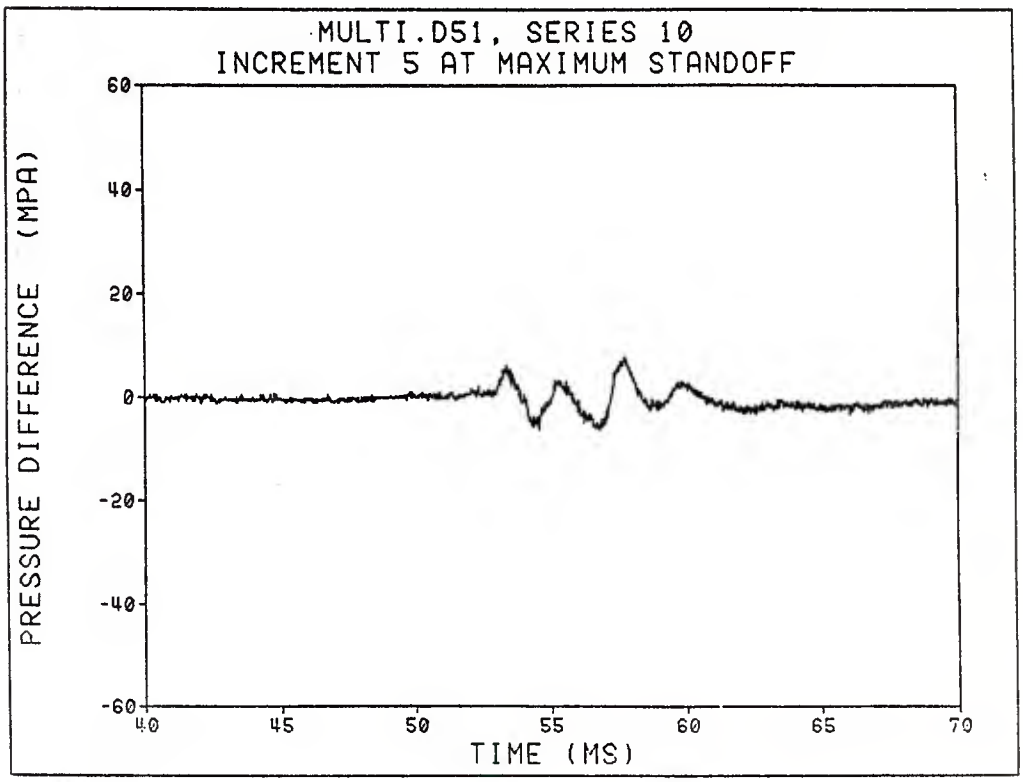
MULTI.D51, SERIES 10
INCREMENT 5 AT MAXIMUM STANDOFF
PRESSURE DIFFERENCE (MPA)
60
40
20
0
-20
-40
-60
40
45
50
55
60
65
70
TIME (MS)

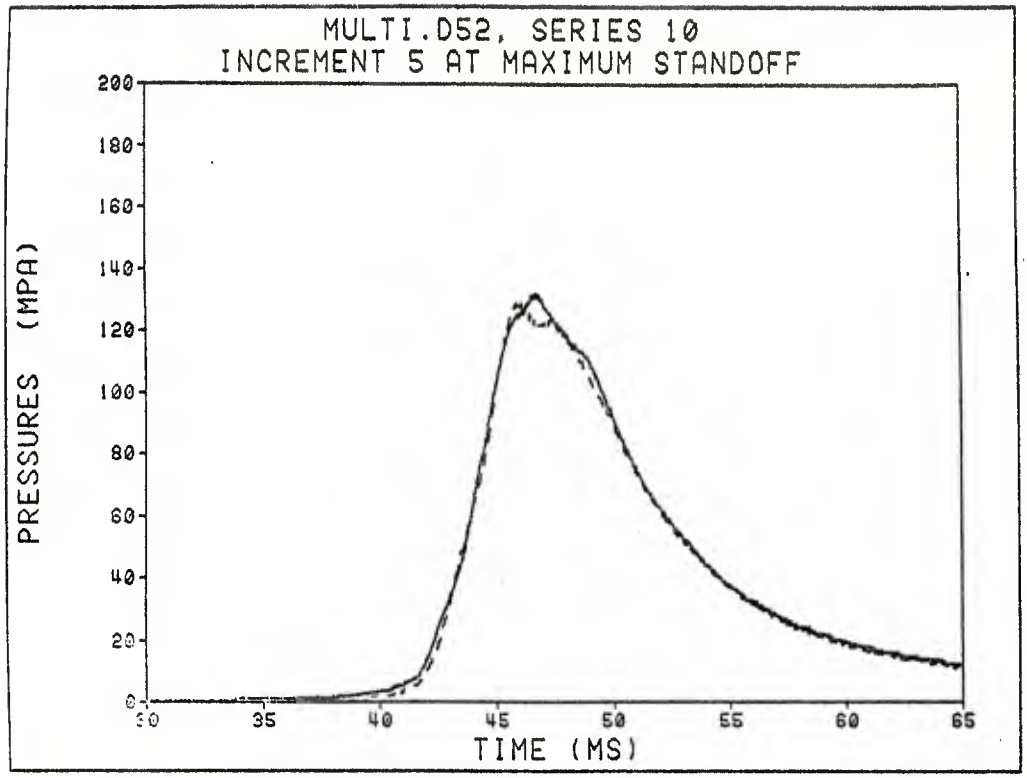
MULTI.D52, SERIES 10
INCREMENT 5 AT MAXIMUM STANDOFF
PRESSURES (MPA)
200
180
160
140
120
100
80
60
40
20
0
30
35
40
45
50
55
60
65
TIME (MS)

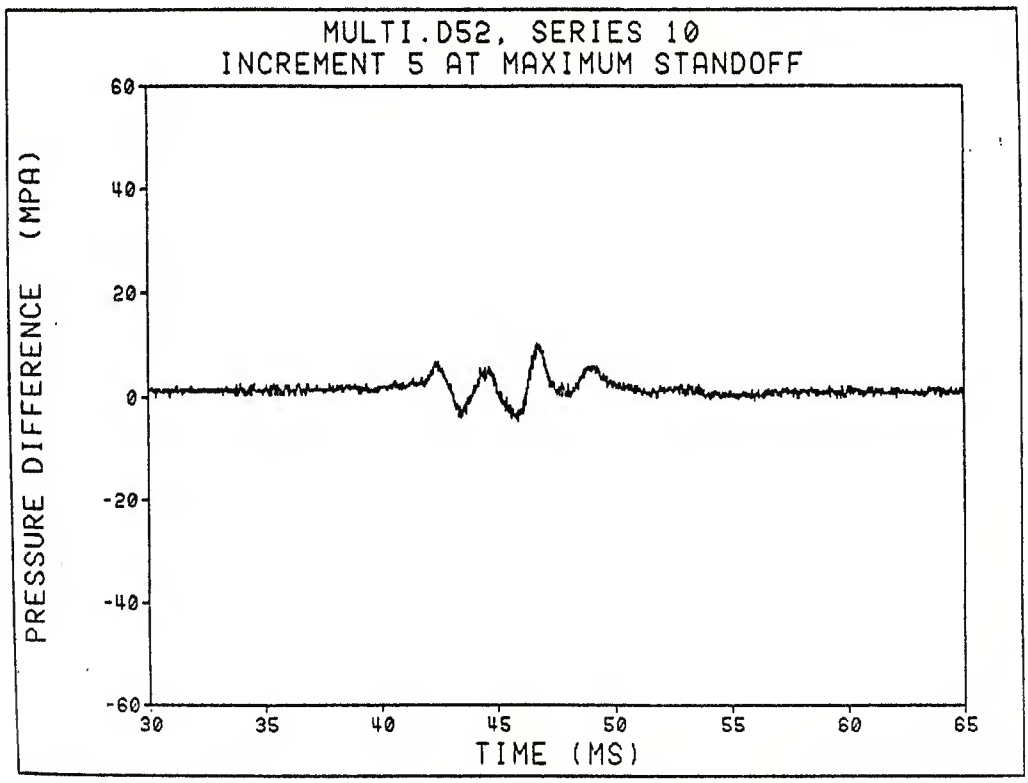
MULTI.D52, SERIES 10
INCREMENT 5 AT MAXIMUM STANDOFF
PRESSURE DIFFERENCE (MPA)
60
40
20
0
-20
-40
-60
30
35
40
45
50
55
60
65
TIME (MS)

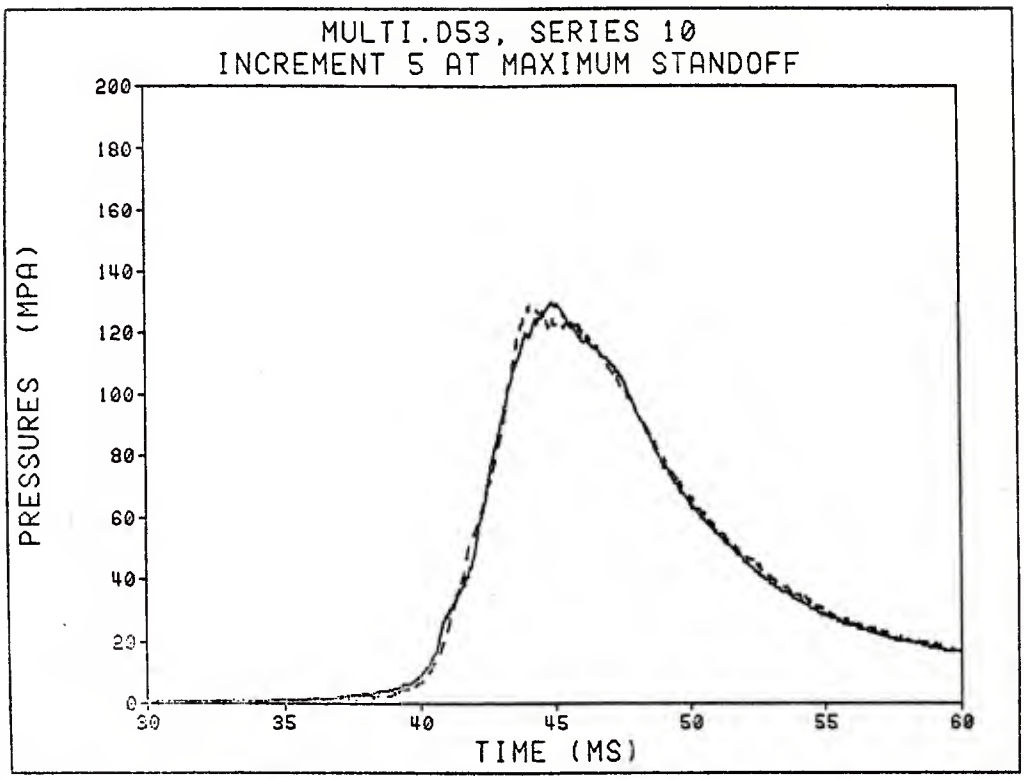
MULTI.D53, SERIES 10
INCREMENT 5 AT MAXIMUM STANDOFF
PRESSURES (MPA)
200
180
160
140
120
100
80
60
40
20
0
30
35
40
45
50
55
60
TIME (MS)

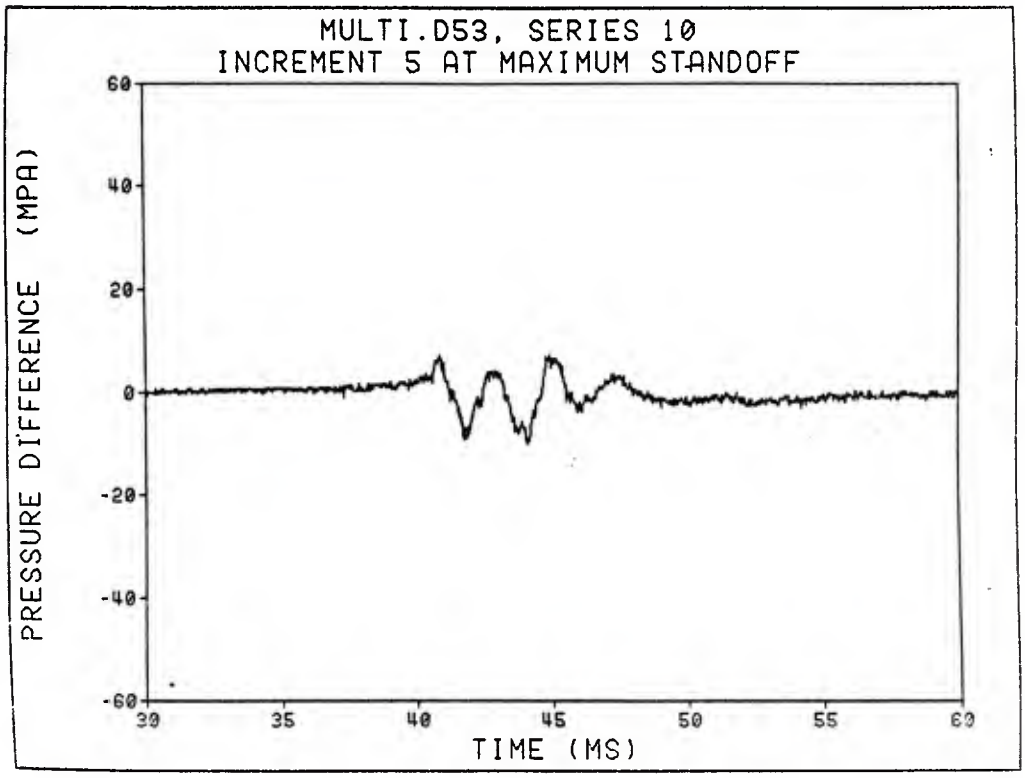
MULTI.D53, SERIES 10
INCREMENT 5 AT MAXIMUM STANDOFF
PRESSURE DIFFERENCE (MPA)
60
40
20
0
-20
-40
-60
30
35
40
45
50
55
60
TIME (MS)

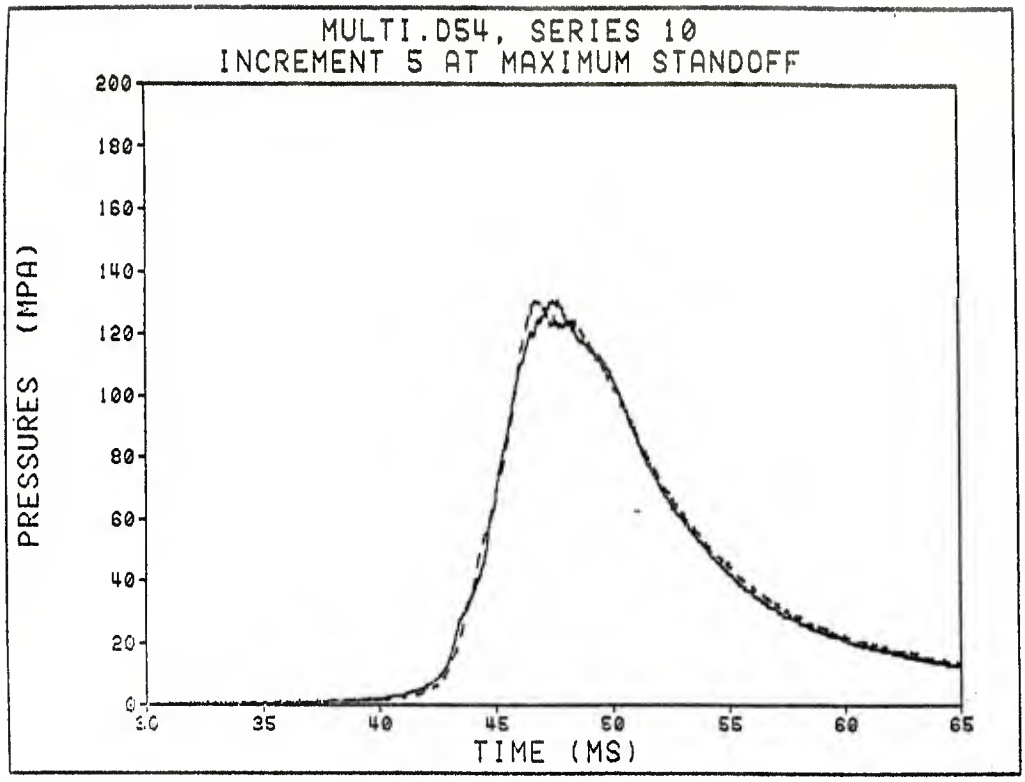
MULTI.D54, SERIES 10
INCREMENT 5 AT MAXIMUM STANDOFF
PRESSURES (MPA)
200
180
160
140
120
100
80
60
40
20
0
30
35
40
45
50
55
60
65
TIME (MS)

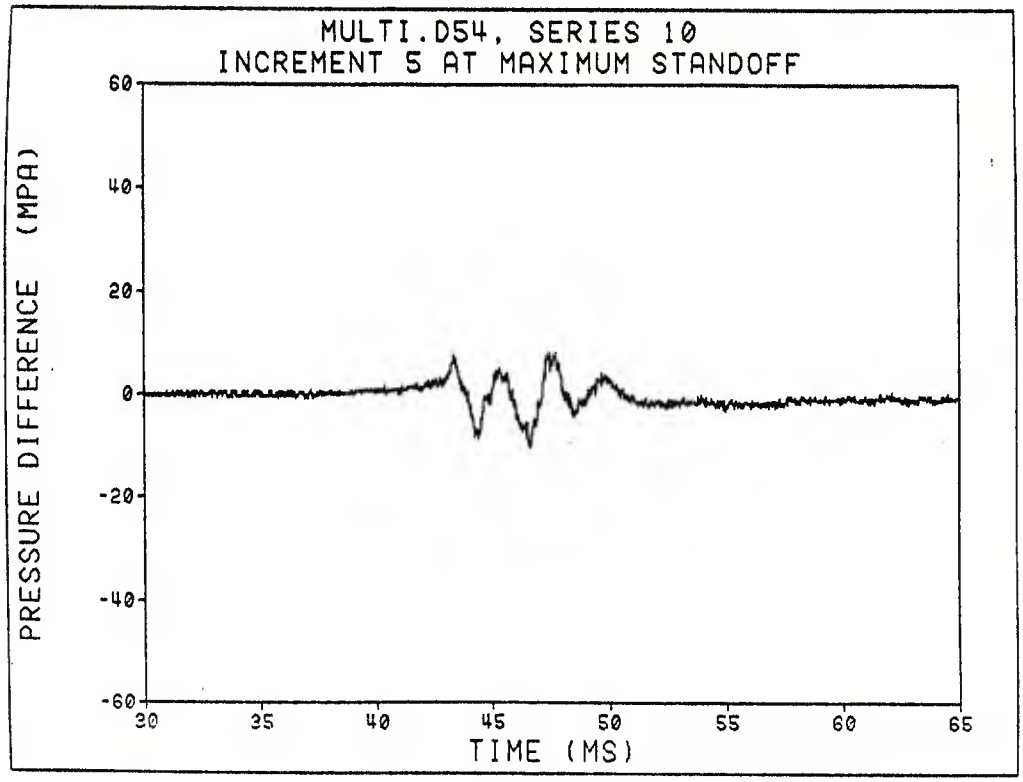
MULTI.D54, SERIES 10
INCREMENT 5 AT MAXIMUM STANDOFF
PRESSURE DIFFERENCE (MPA)
60
40
20
0
-20
-40
-60
30
35
40
45
50
55
60
65
TIME (MS)

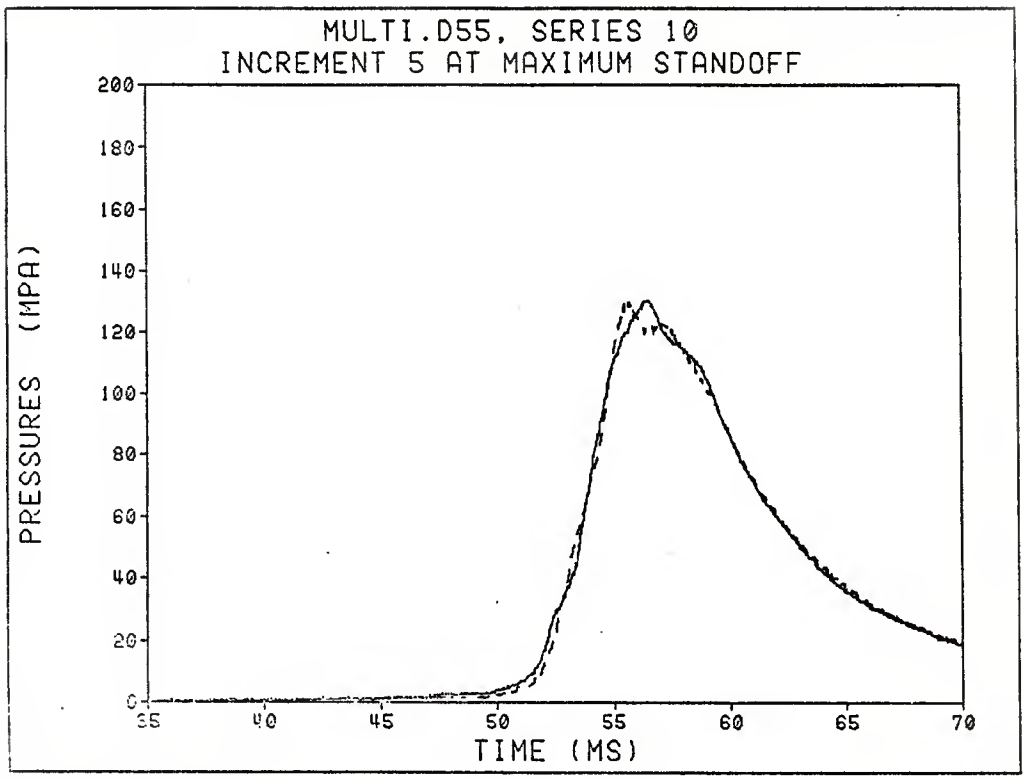
MULTI.D55, SERIES 10
INCREMENT 5 AT MAXIMUM STANDOFF
PRESSURES (MPA)
200
180
160
140
120
100
80
60
40
20
0
35
40
45
50
55
60
65
70
TIME (MS)

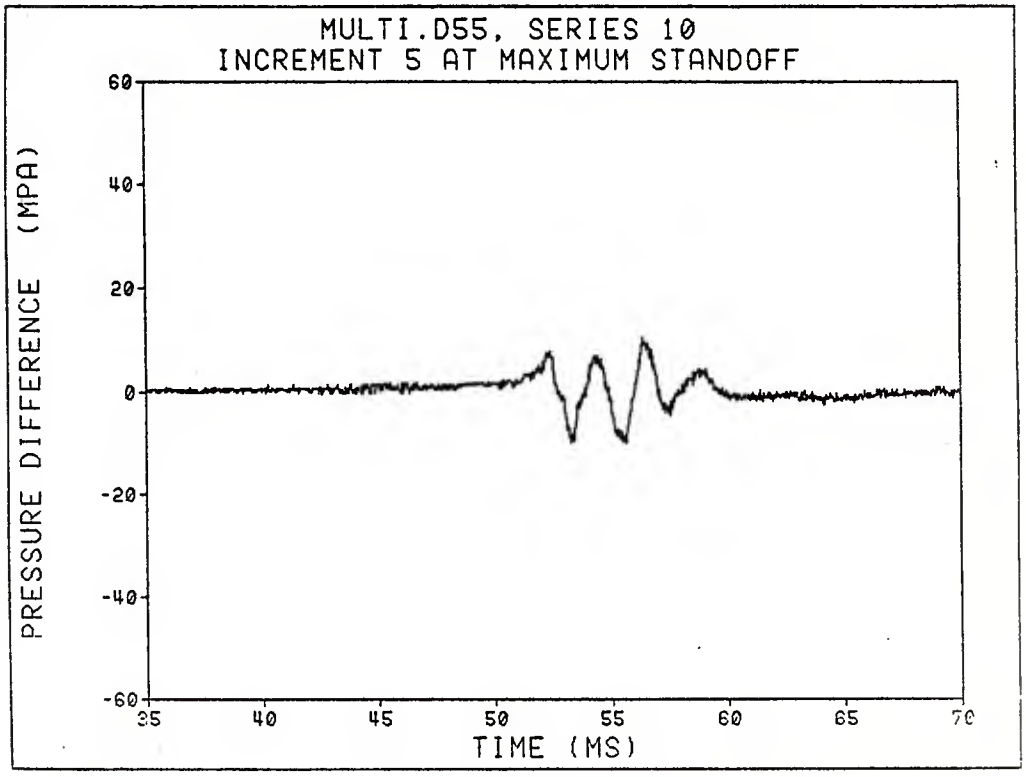
MULTI.D55, SERIES 10
INCREMENT 5 AT MAXIMUM STANDOFF
PRESSURE DIFFERENCE (MPA)
60
40
20
0
-20
-40
-60
35
40
45
50
55
60
65
70
TIME (MS)

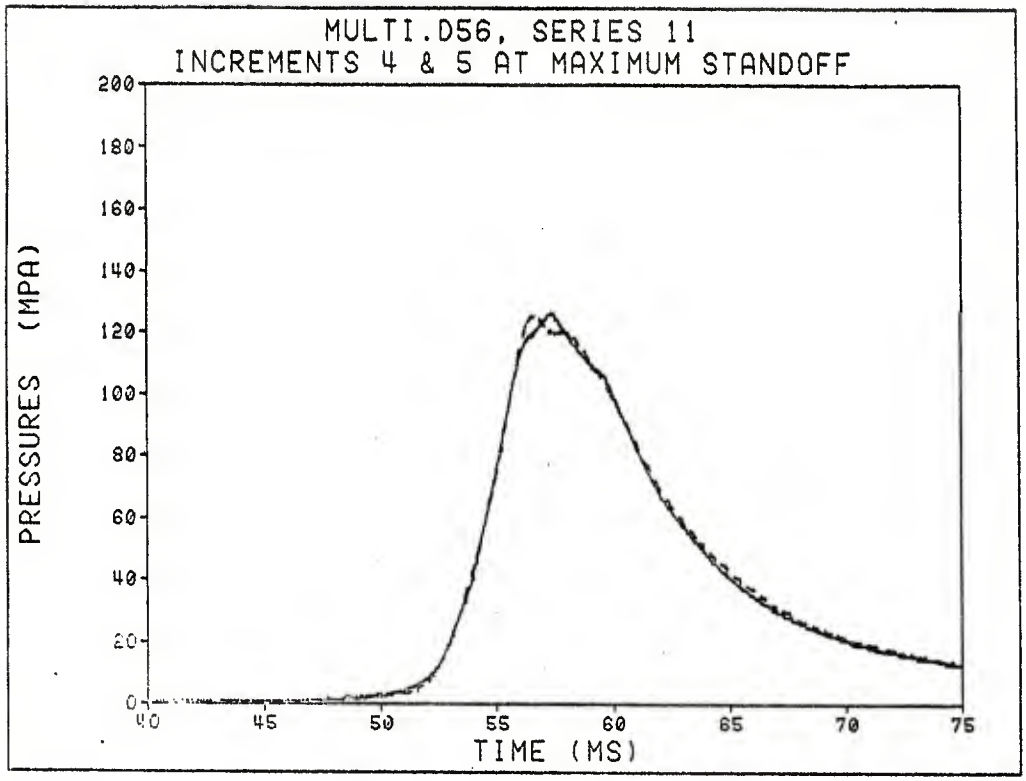
MULTI.D56, SERIES 11
INCREMENTS 4 & 5 AT MAXIMUM STANDOFF
PRESSURES (MPA)
200
180
160
140
120
100
80
60
40
20
0
40
45
50
55
60
65
70
75
TIME (MS)

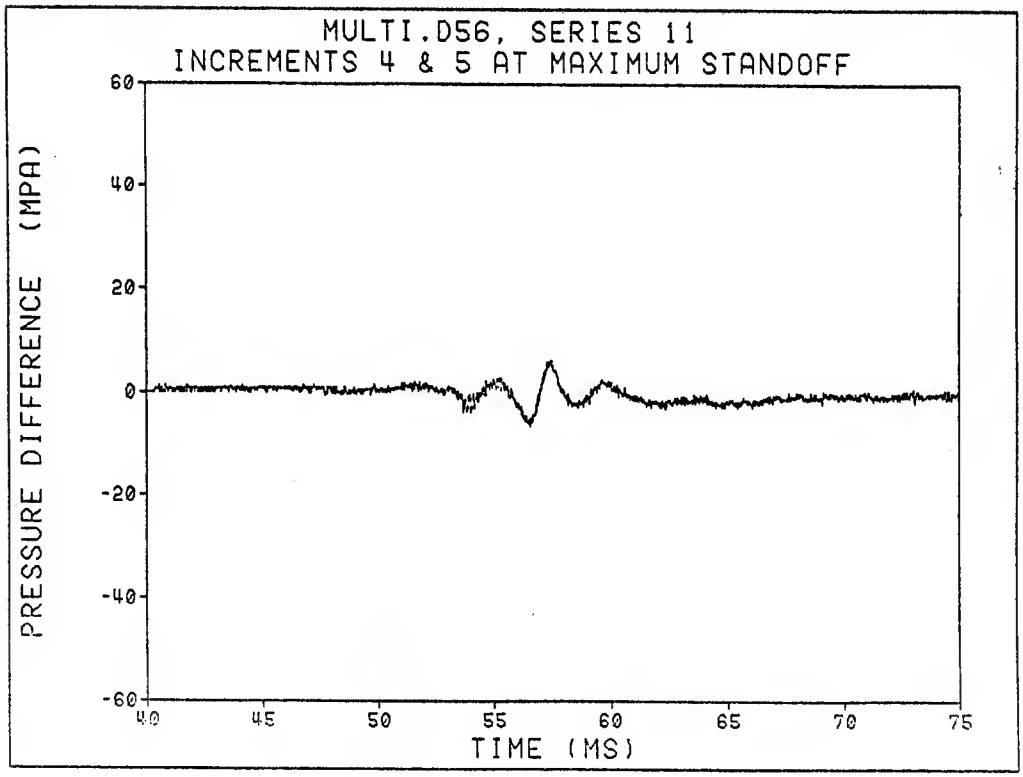
MULTI.D56, SERIES 11
INCREMENTS 4 & 5 AT MAXIMUM STANDOFF
PRESSURE DIFFERENCE (MPA)
60
40
20
0
-20
-40
-60
40
45
50
55
60
65
70
75
TIME (MS)

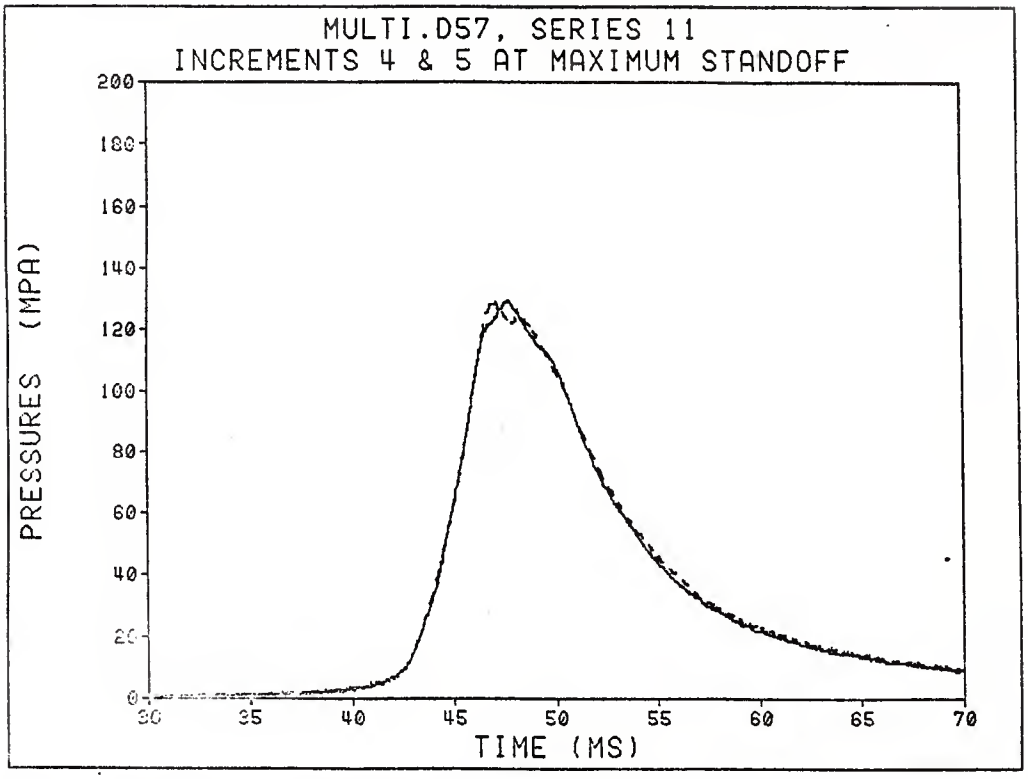
MULTI.D57, SERIES 11
INCREMENTS 4 & 5 AT MAXIMUM STANDOFF
PRESSURES (MPA)
200
180
160
140
120
100
80
60
40
20
0
30
35
40
45
50
55
60
65
70
TIME (MS)

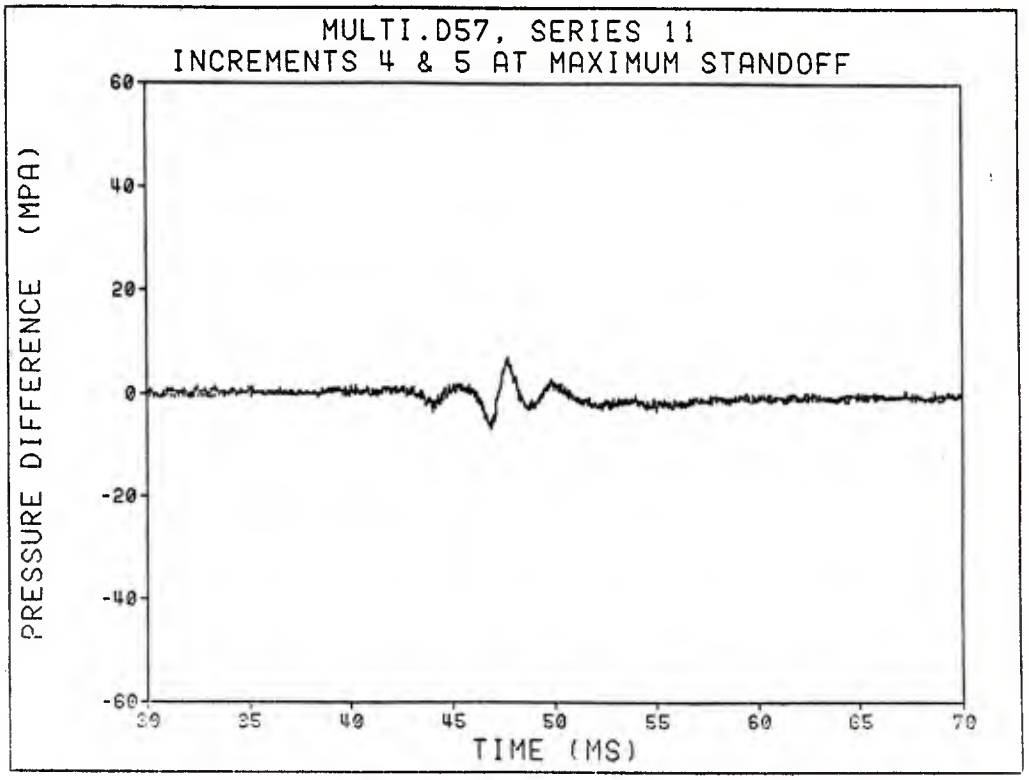
MULTI.D57, SERIES 11
INCREMENTS 4 & 5 AT MAXIMUM STANDOFF
PRESSURE DIFFERENCE (MPA)
60
40
20
0
-20
-40
-60
30
35
40
45
50
55
60
65
70
TIME (MS)

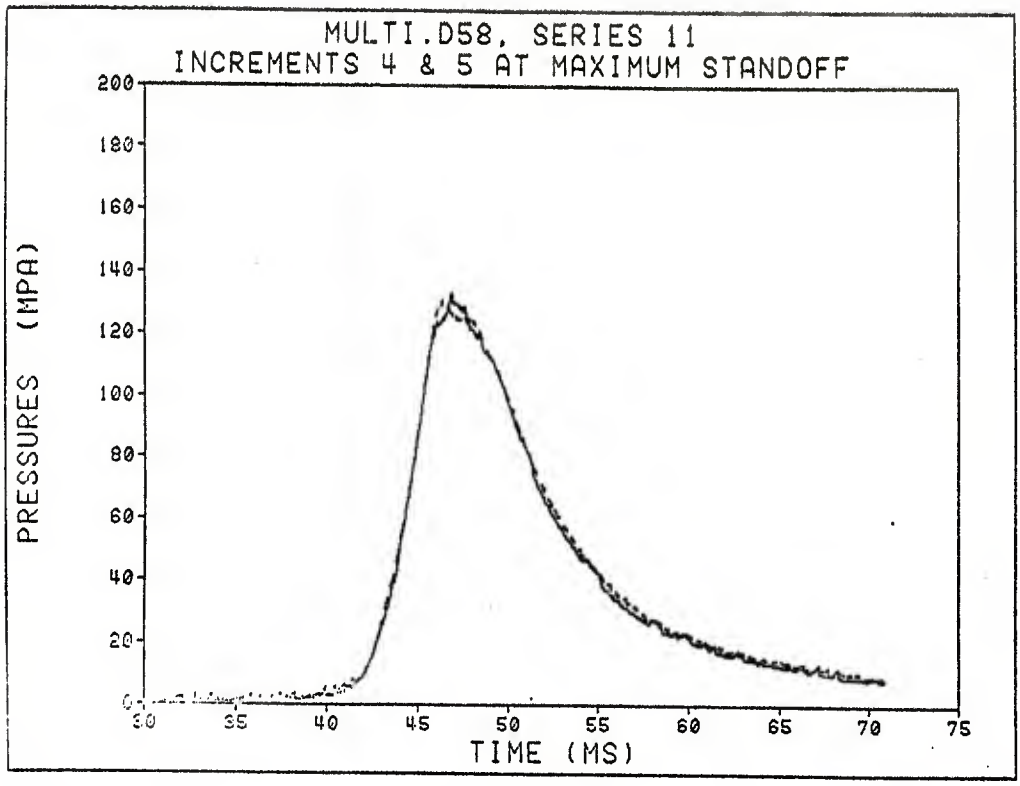
MULTI.D58, SERIES 11
INCREMENTS 4 & 5 AT MAXIMUM STANDOFF
PRESSURES (MPA)
200
180
160
140
120
100
80
60
40
20
0
30
35
40
45
50
55
60
65
70
75
TIME (MS)

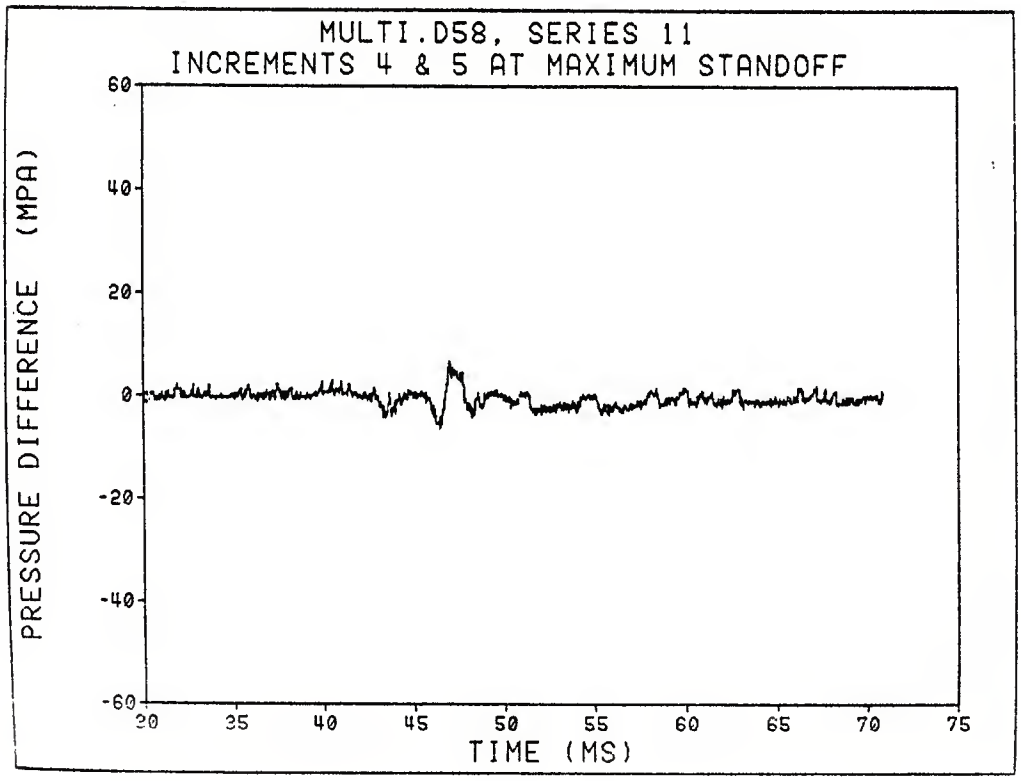
MULTI.D58, SERIES 11
INCREMENTS 4 & 5 AT MAXIMUM STANDOFF
PRESSURE DIFFERENCE (MPA)
60
40
20
0
-20
-40
-60
30
35
40
45
50
55
60
65
70
75
TIME (MS)

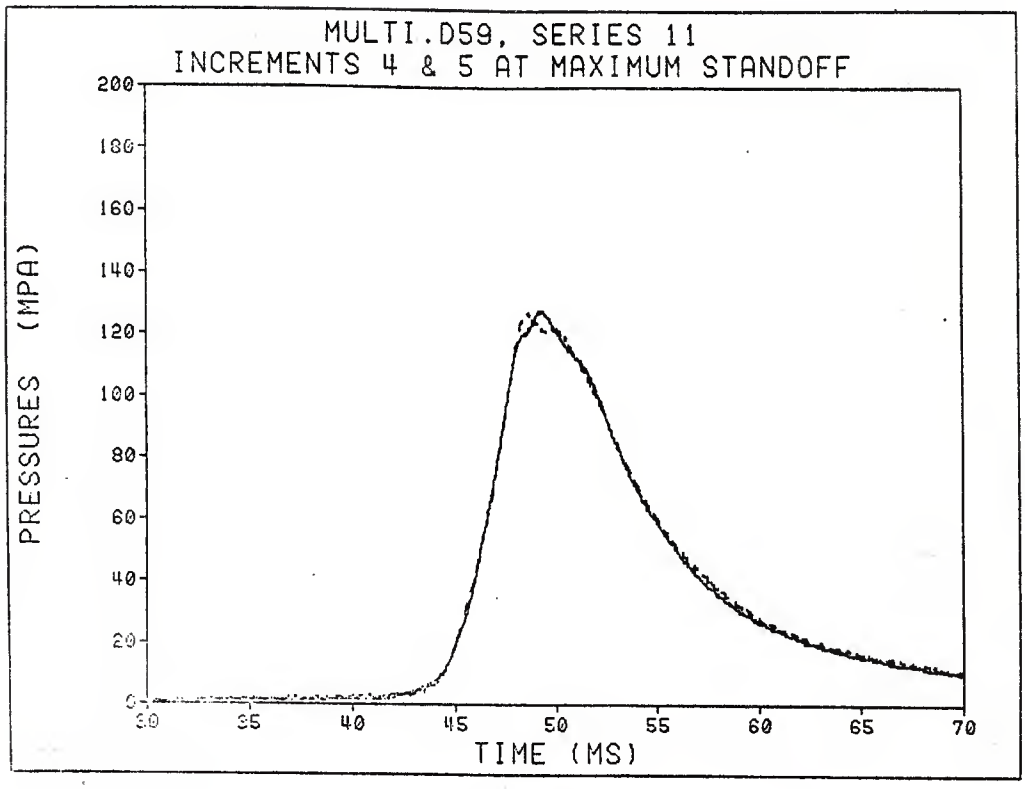
MULTI.D59, SERIES 11
INCREMENTS 4 & 5 AT MAXIMUM STANDOFF
PRESSURES (MPA)
200
180
160
140
120
100
80
60
40
20
0
30
35
40
45
50
55
60
65
70
TIME (MS)

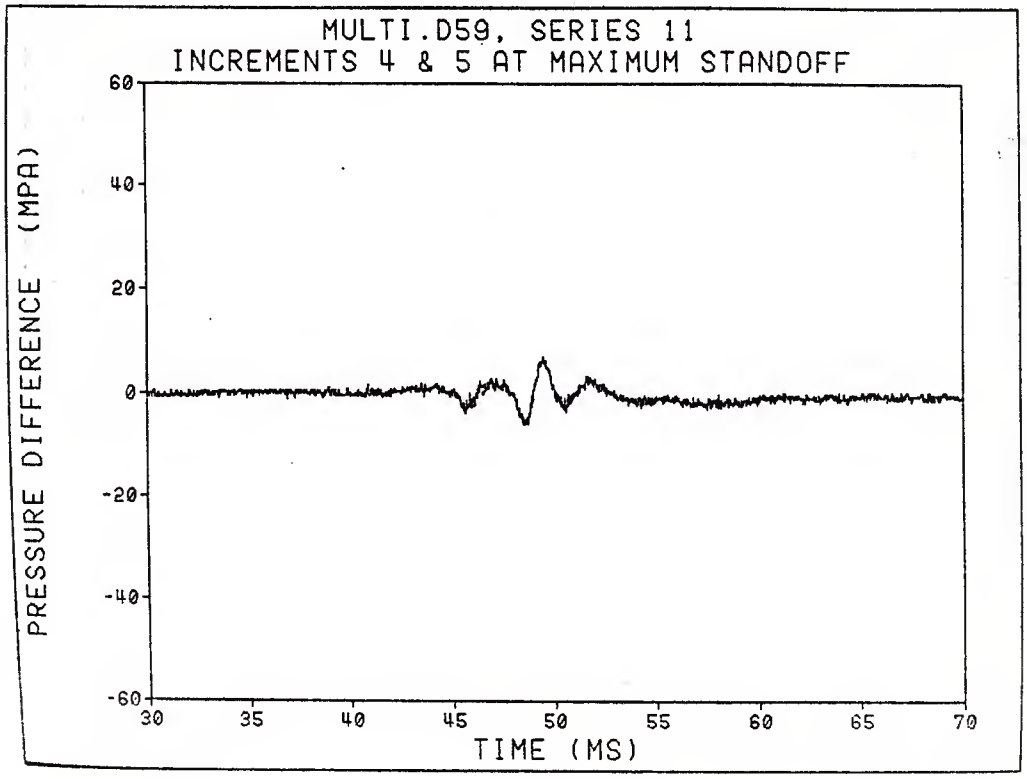
MULTI.D59, SERIES 11
INCREMENTS 4 & 5 AT MAXIMUM STANDOFF
PRESSURE DIFFERENCE (MPA)
60
40
20
0
-20
-40
-60
30
35
40
45
50
55
60
65
70
TIME (MS)

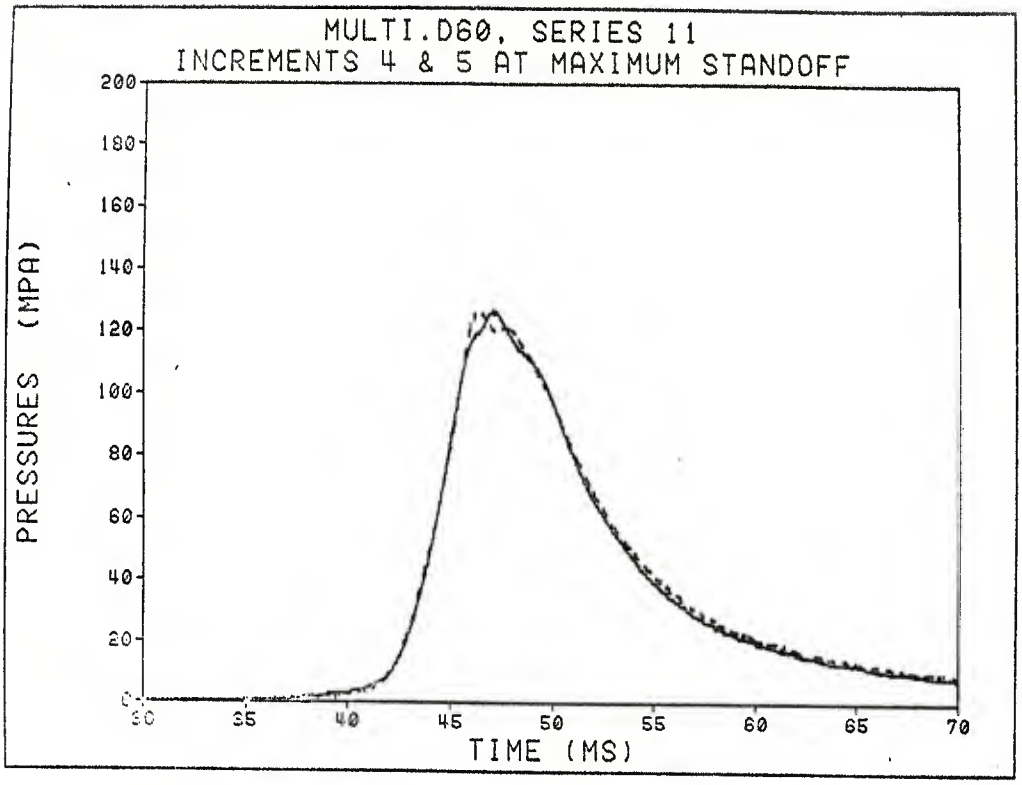
MULTI.D60, SERIES 11
INCREMENTS 4 & 5 AT MAXIMUM STANDOFF
PRESSURES (MPA)
200
180
160
140
120
100
80
60
40
20
0
30
35
40
45
50
55
60
65
70
TIME (MS)

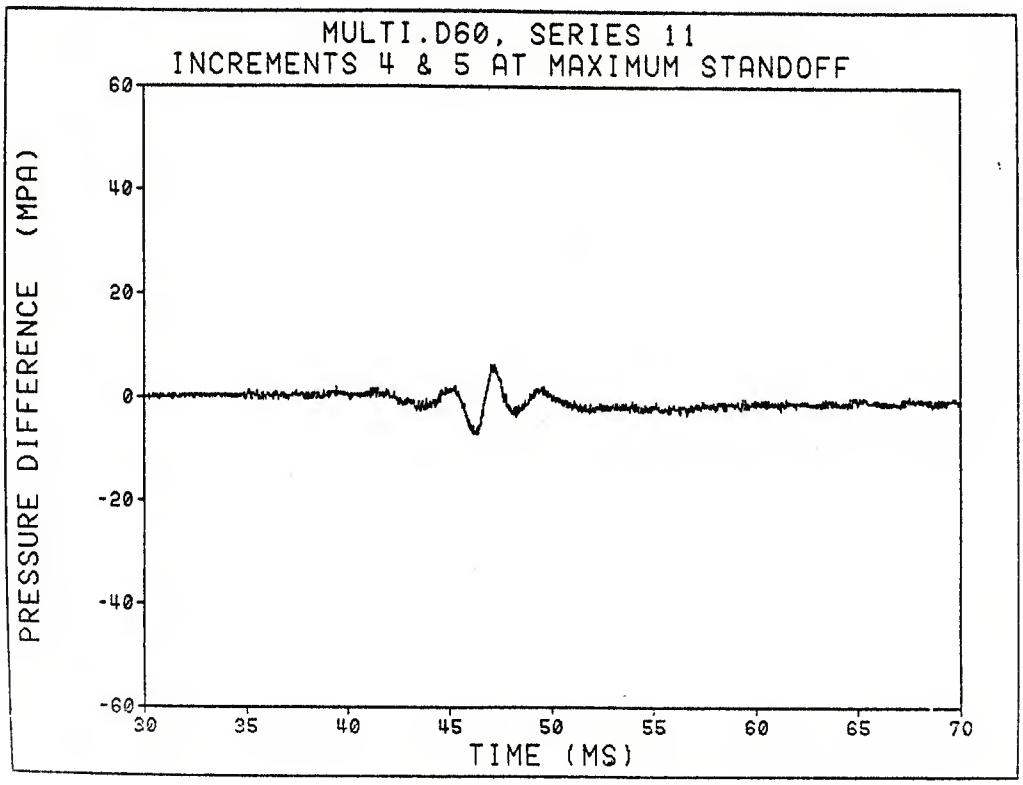
MULTI.D60, SERIES 11
INCREMENTS 4 & 5 AT MAXIMUM STANDOFF
PRESSURE DIFFERENCE (MPA)
60
40
20
0
-20
-40
-60
30
35
40
45
50
55
60
65
70
TIME (MS)

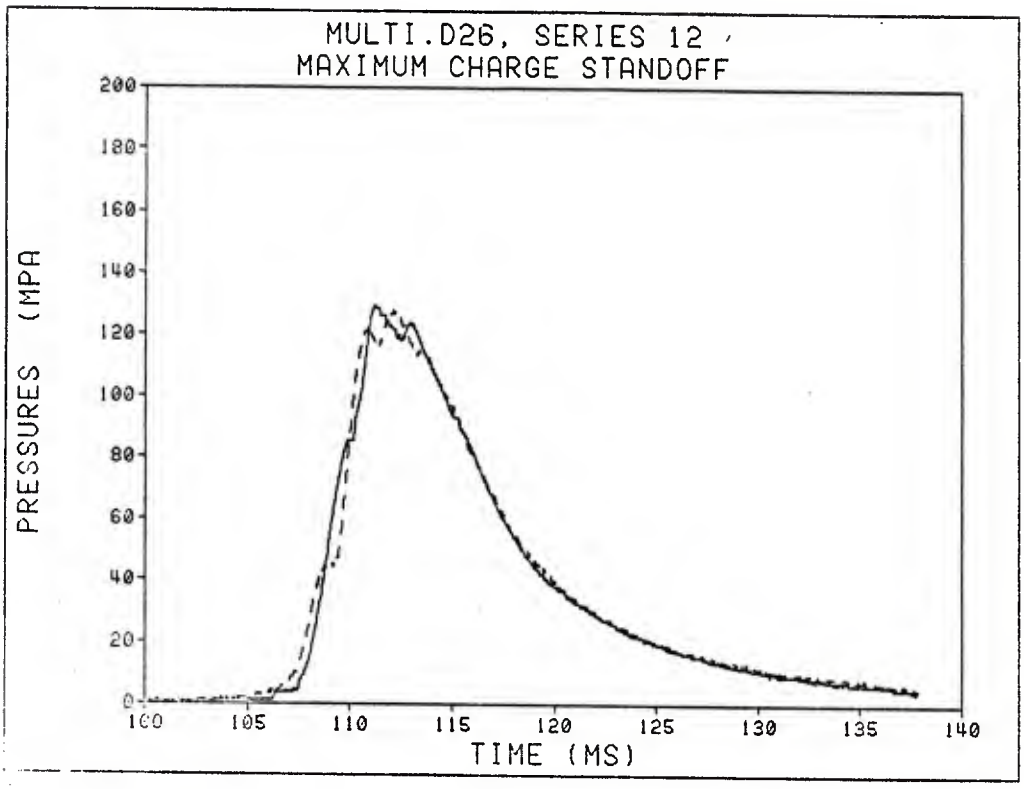
MULTI.D26, SERIES 12
MAXIMUM CHARGE STANDOFF
PRESSURES (MPA
200
180
160
140
120
100
80
60
40
20
0
100
105
110
115
120
125
130
135
140
TIME (MS)

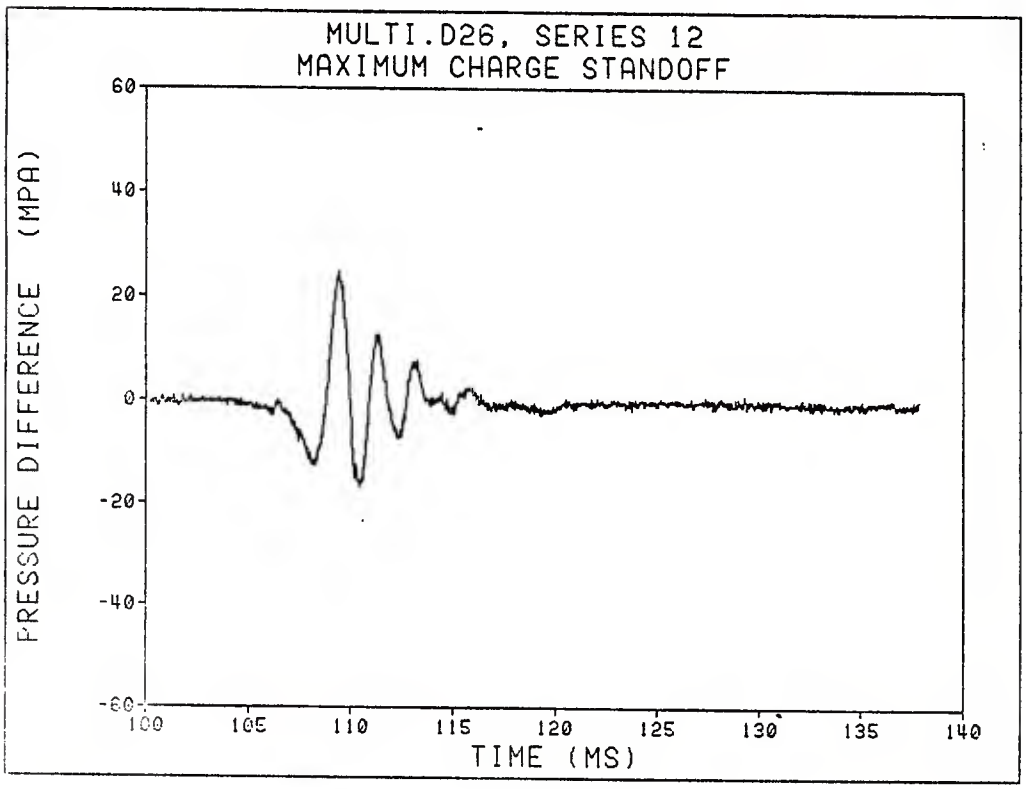
MULTI.D26, SERIES 12
MAXIMUM CHARGE STANDOFF
PRESSURE DIFFERENCE (MPA)
60
40
20
0
-20
-40
-60
100
105
110
115
120
125
130
135
140
TIME (MS)

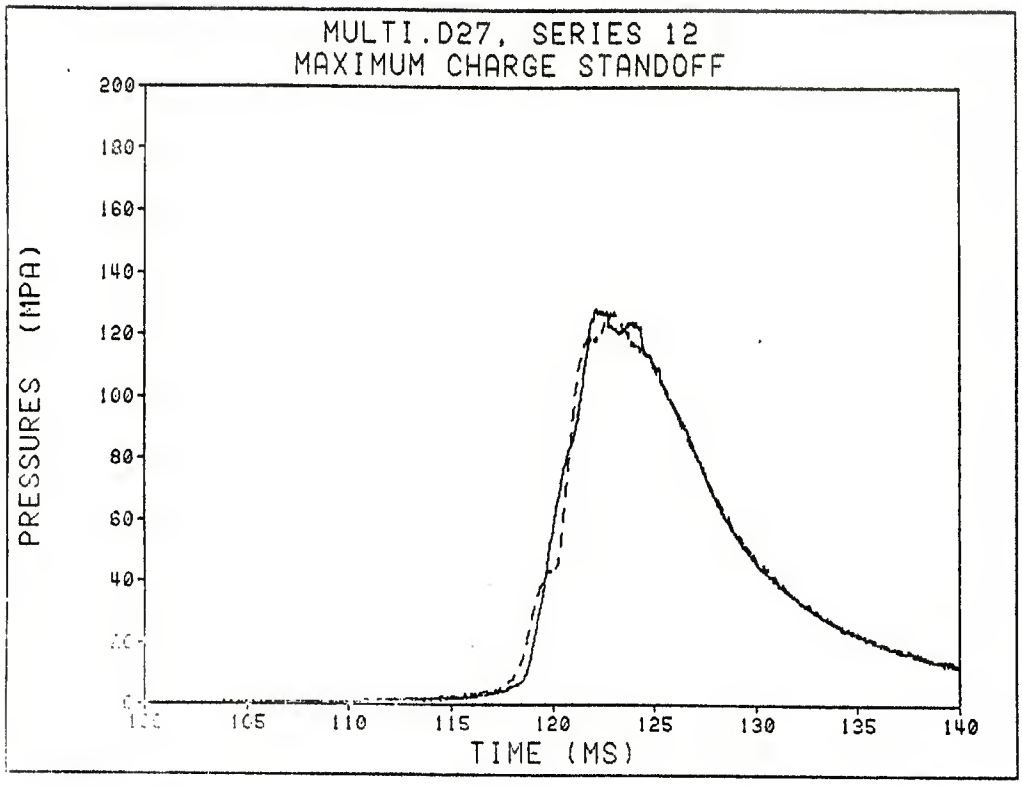
MULTI.D27, SERIES 12
MAXIMUM CHARGE STANDOFF
PRESSURES (MPA)
200
180
160
140
120
100
80
60
40
105
110
115
120
125
130
135
140
TIME (MS)

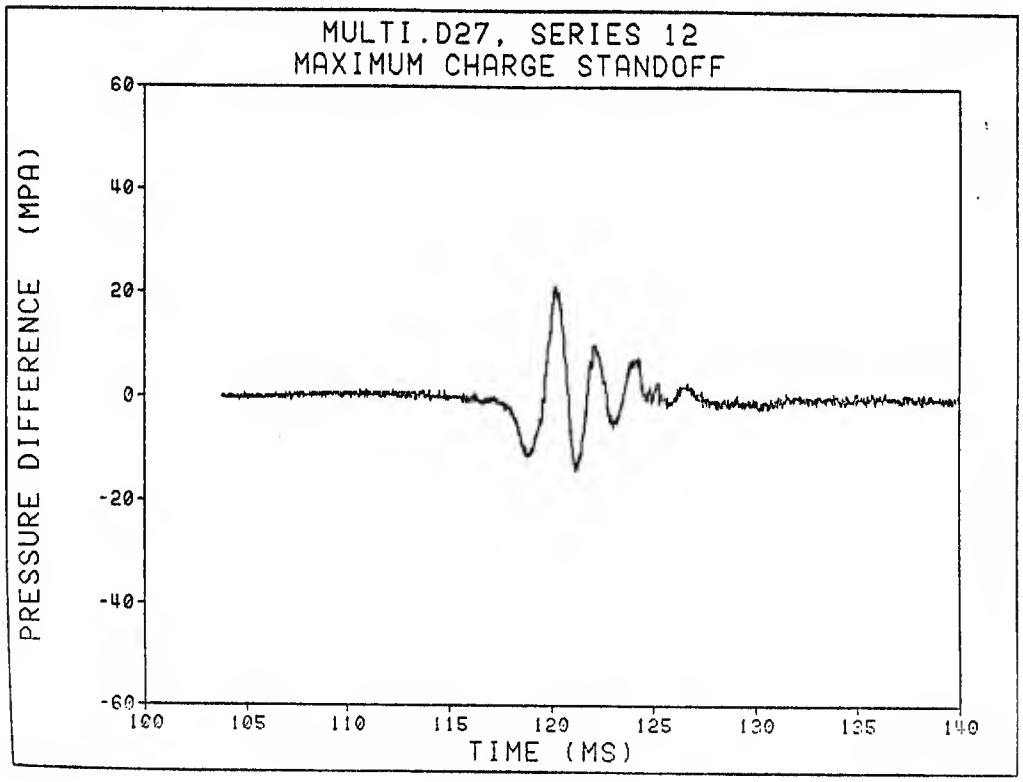
MULTI.D27, SERIES 12
MAXIMUM CHARGE STANDOFF
PRESSURE DIFFERENCE (MPA)
60
40
20
0
-20
-40
-60
100
105
110
115
120
125
130
135
140
TIME (MS)

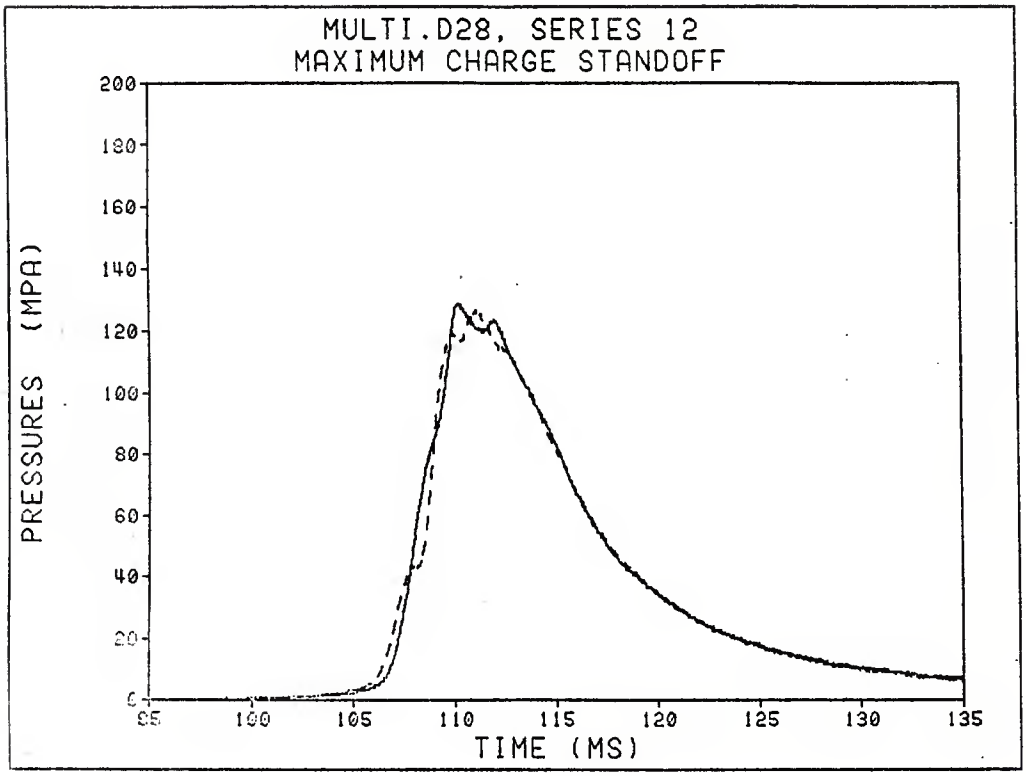
MULTI.D28, SERIES 12
MAXIMUM CHARGE STANDOFF
PRESSURES (MPA)
200
180
160
140
120
100
80
60
40
20
0
95
100
105
110
115
120
125
130
135
TIME (MS)

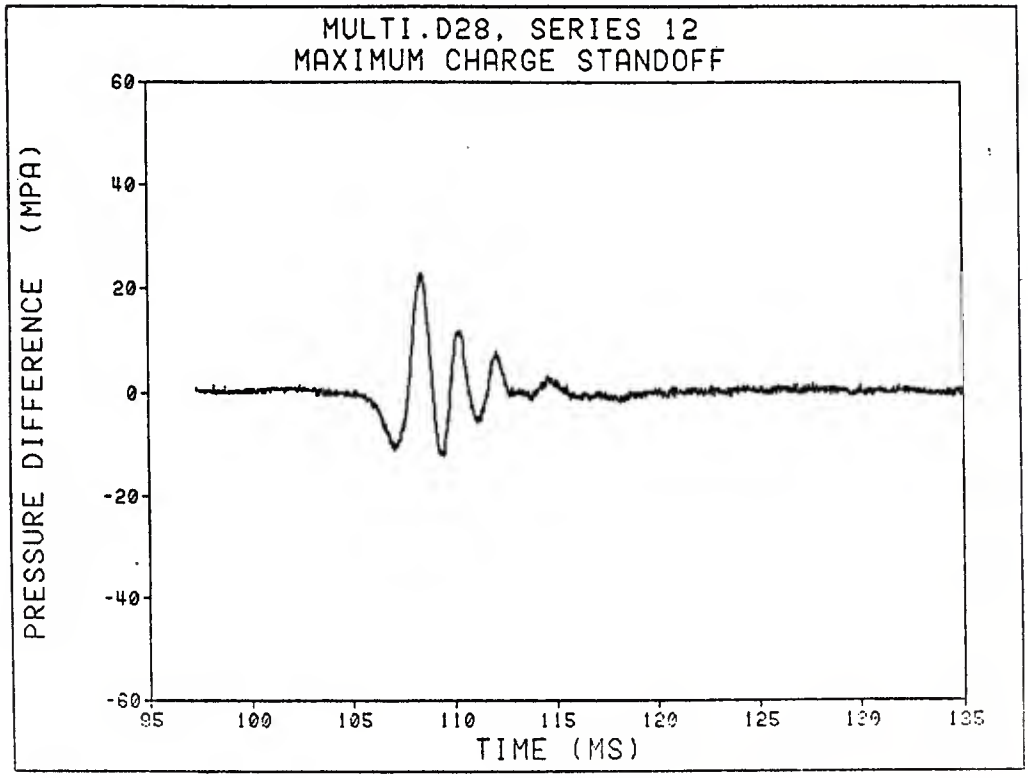
MULTI.D28, SERIES 12
MAXIMUM CHARGE STANDOFF
PRESSURE DIFFERENCE (MPA)
60
40
20
0
-20
-40
-60
95
100
105
110
115
120
125
130
135
TIME (MS)

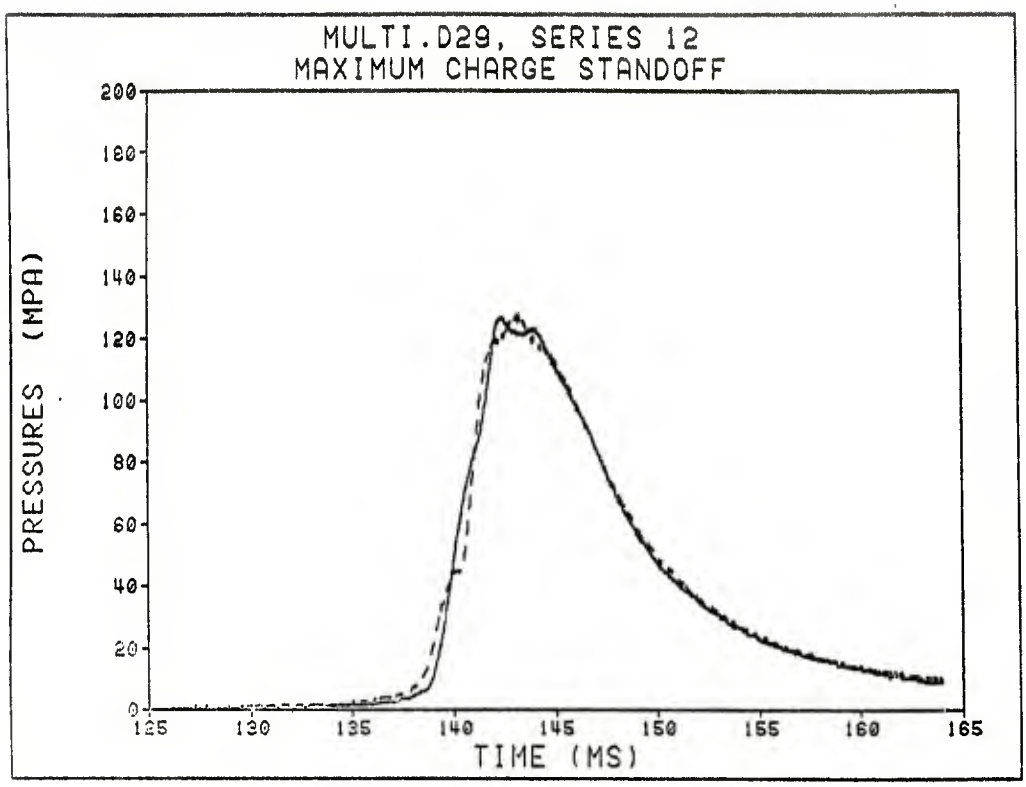
MULTI.D29, SERIES 12
MAXIMUM CHARGE STANDOFF
PRESSURES (MPA)
200
180
160
140
120
100
80
60
40
20
0
125
130
135
140
145
150
155
160
165
TIME (MS)

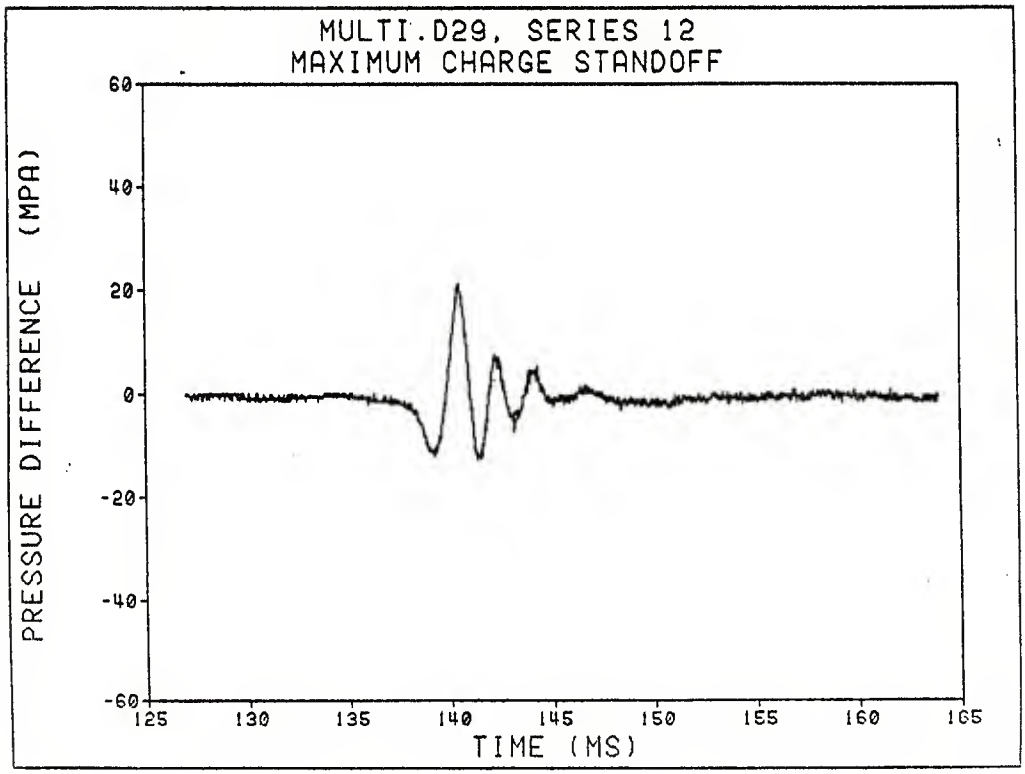
MULTI.D29, SERIES 12
MAXIMUM CHARGE STANDOFF
PRESSURE DIFFERENCE (MPA)
60
40
20
0
-20
-40
-60
125
130
135
140
145
150
155
160
165
TIME (MS)

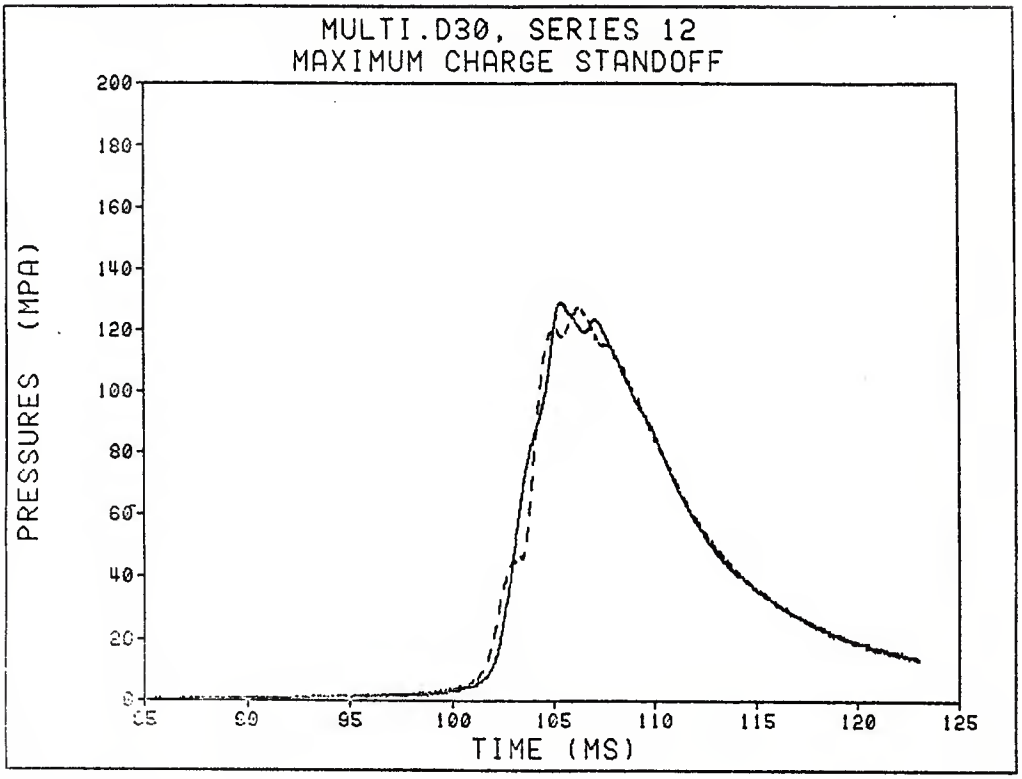
MULTI.D30, SERIES 12
MAXIMUM CHARGE STANDOFF
PRESSURES (MPA)
200
180
160
140
120
100
80
60
40
20
0
85
90
95
100
105
110
115
120
125
TIME (MS)

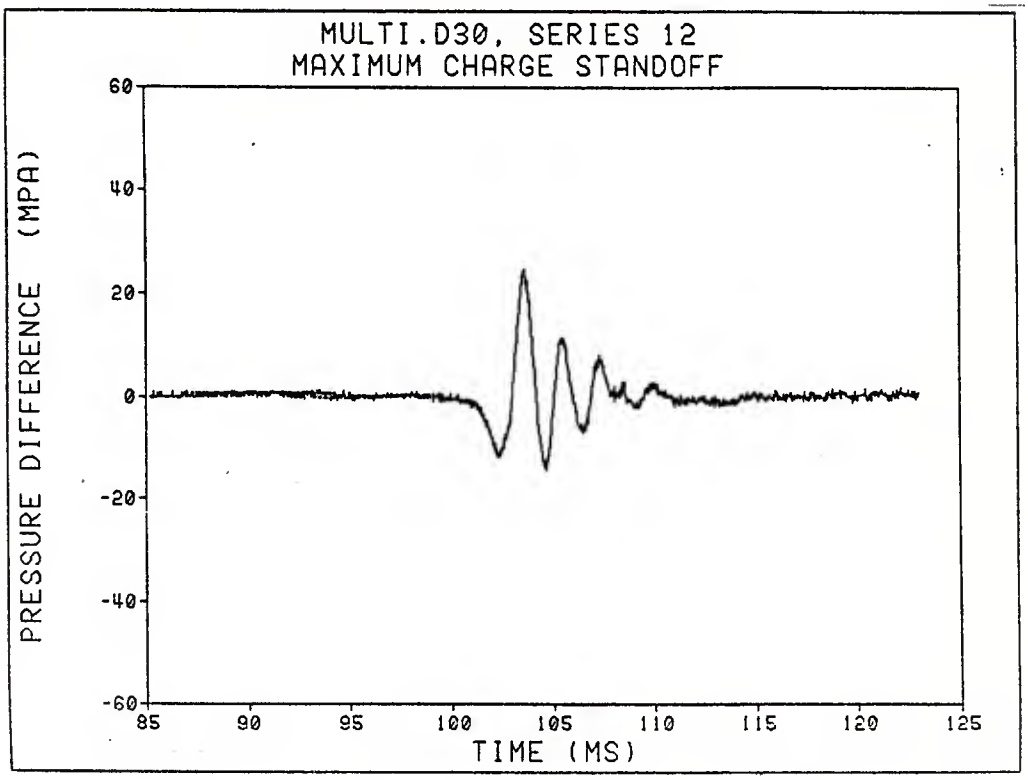
MULTI.D30, SERIES 12
MAXIMUM CHARGE STANDOFF
PRESSURE DIFFERENCE (MPA)
60
40
20
0
-20
-40
-60
85
90
95
100
105
110
115
120
125
TIME (MS)

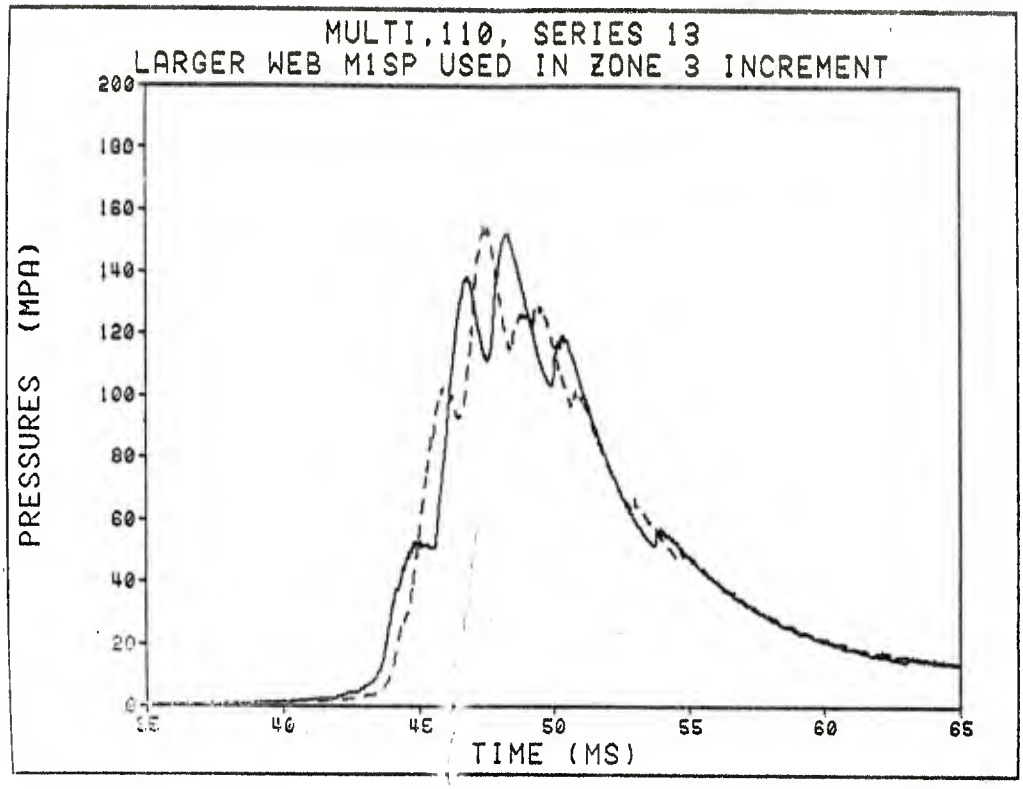
MULTI,110, SERIES 13
LARGER WEB MISP USED IN ZONE 3 INCREMENT
PRESSURES (MPA)
200
180
160
140
120
100
80
60
40
20
0
35
40
45
50
55
60
65
TIME (MS)

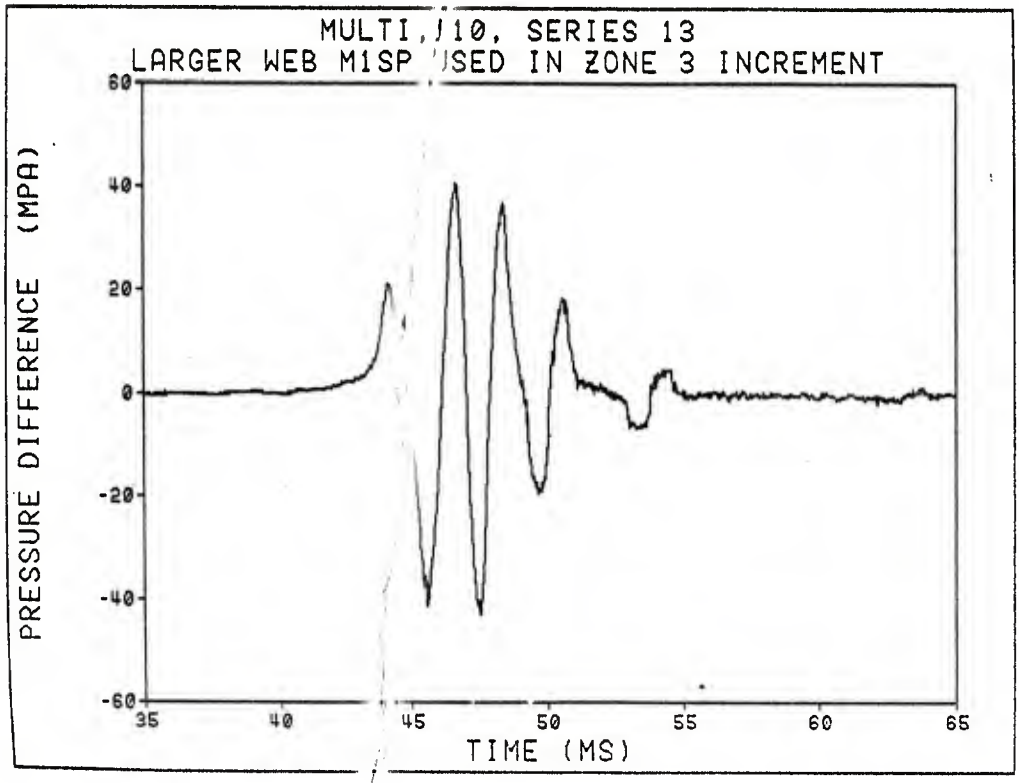
MULTI,110, SERIES 13
LARGER WEB MISP USED IN ZONE 3 INCREMENT
PRESSURE DIFFERENCE (MPA)
60
40
20
0
-20
-40
-60
35
40
45
50
55
60
65
TIME (MS)

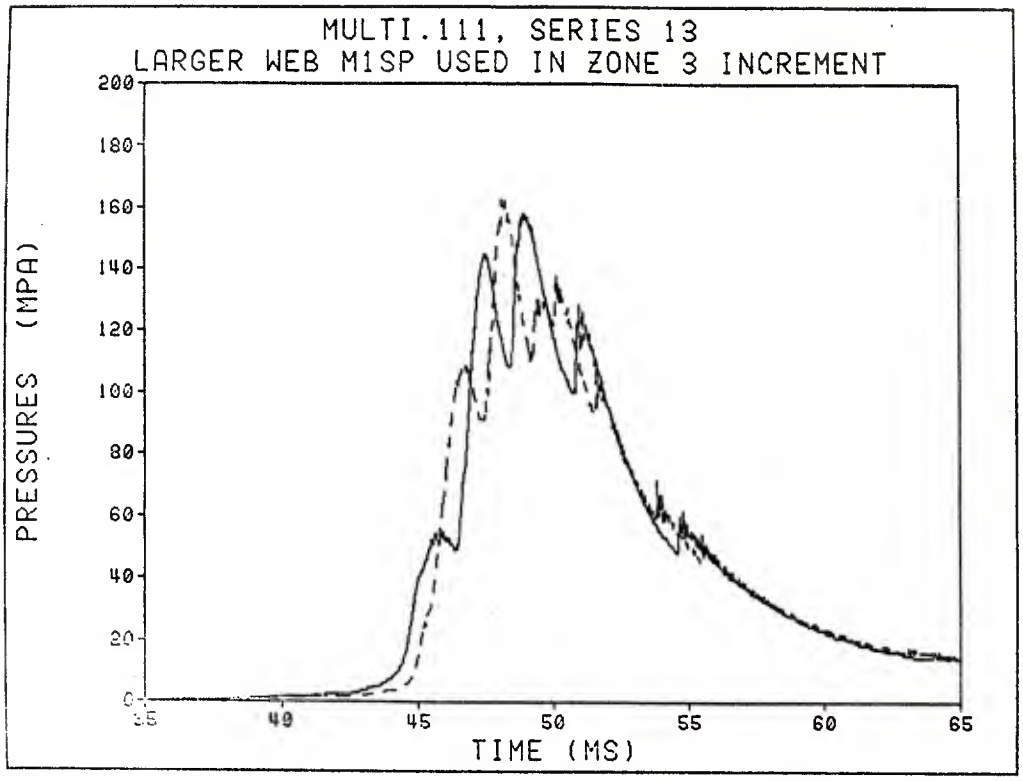
MULTI.111, SERIES 13
LARGER WEB M1SP USED IN ZONE 3 INCREMENT
PRESSURES (MPA)
200
180
160
140
120
100
80
60
40
20
0
35
40
45
50
55
60
65
TIME (MS)

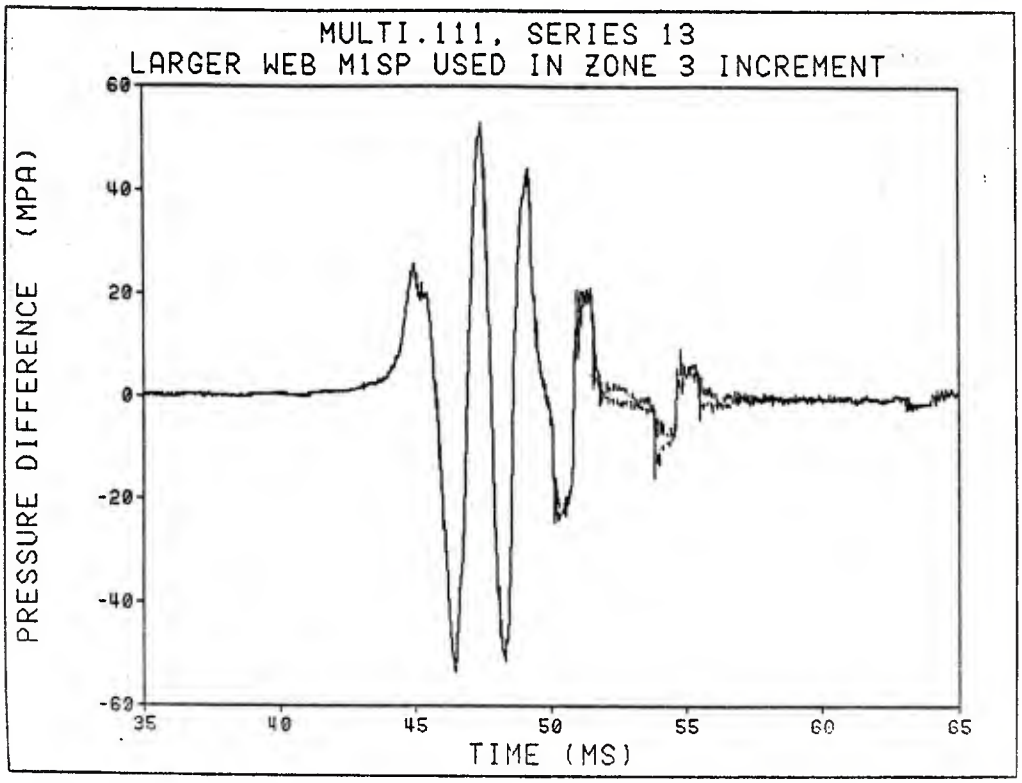
MULTI.111, SERIES 13
LARGER WEB M1SP USED IN ZONE 3 INCREMENT
PRESSURE DIFFERENCE (MPA)
60
40
20
0
-20
-40
-60
35
40
45
50
55
60
65
TIME (MS)

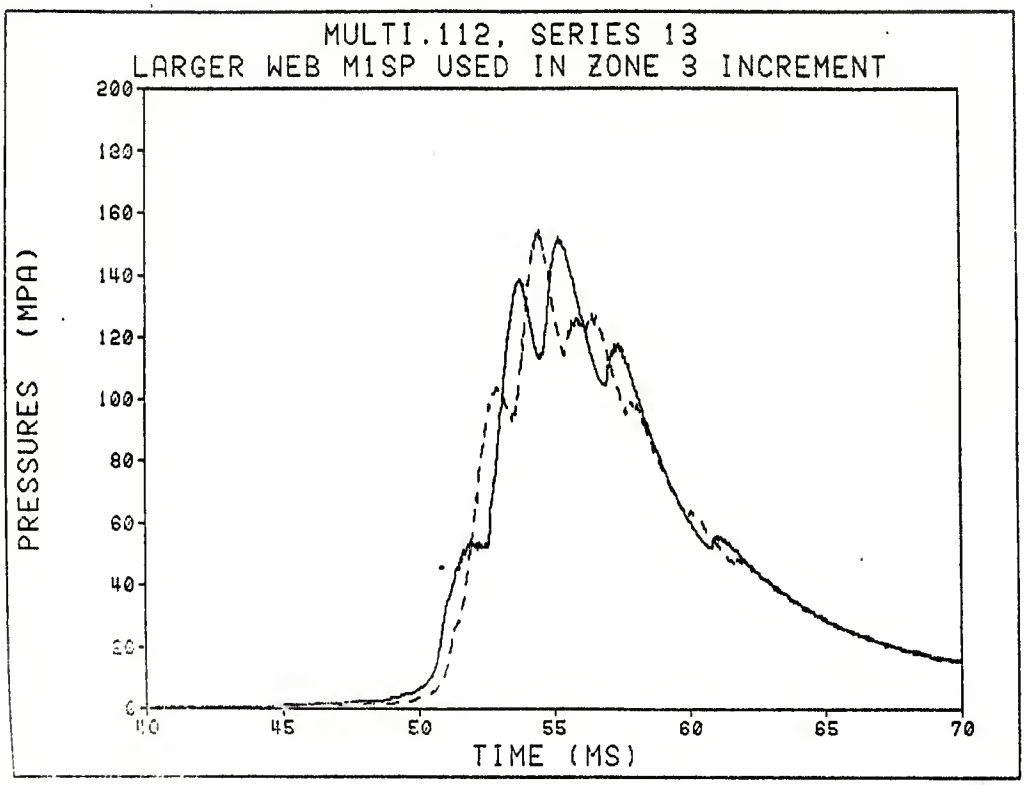
MULTI.112, SERIES 13
LARGER WEB M1SP USED IN ZONE 3 INCREMENT
PRESSURES (MPA)
200
180
160
140
120
100
80
60
40
20
0
40
45
50
55
60
65
70
TIME (MS)

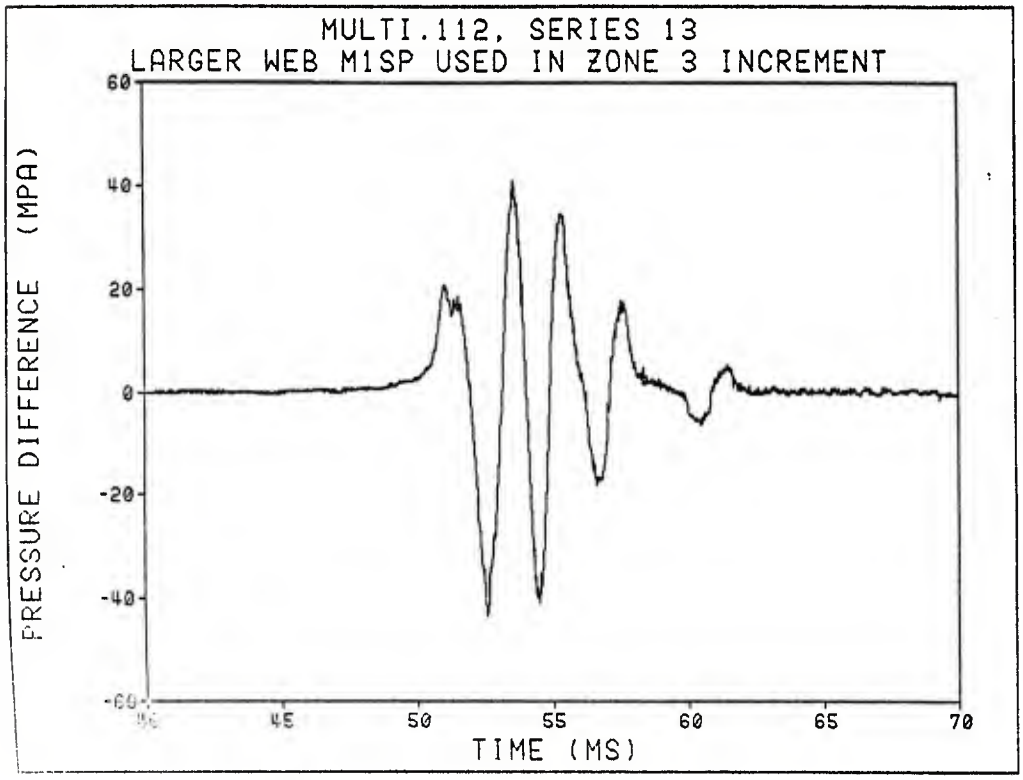
MULTI.112, SERIES 13
LARGER WEB M1SP USED IN ZONE 3 INCREMENT
PRESSURE DIFFERENCE (MPA)
60
40
20
0
-20
-40
-60
45
50
55
60
65
70
TIME (MS)

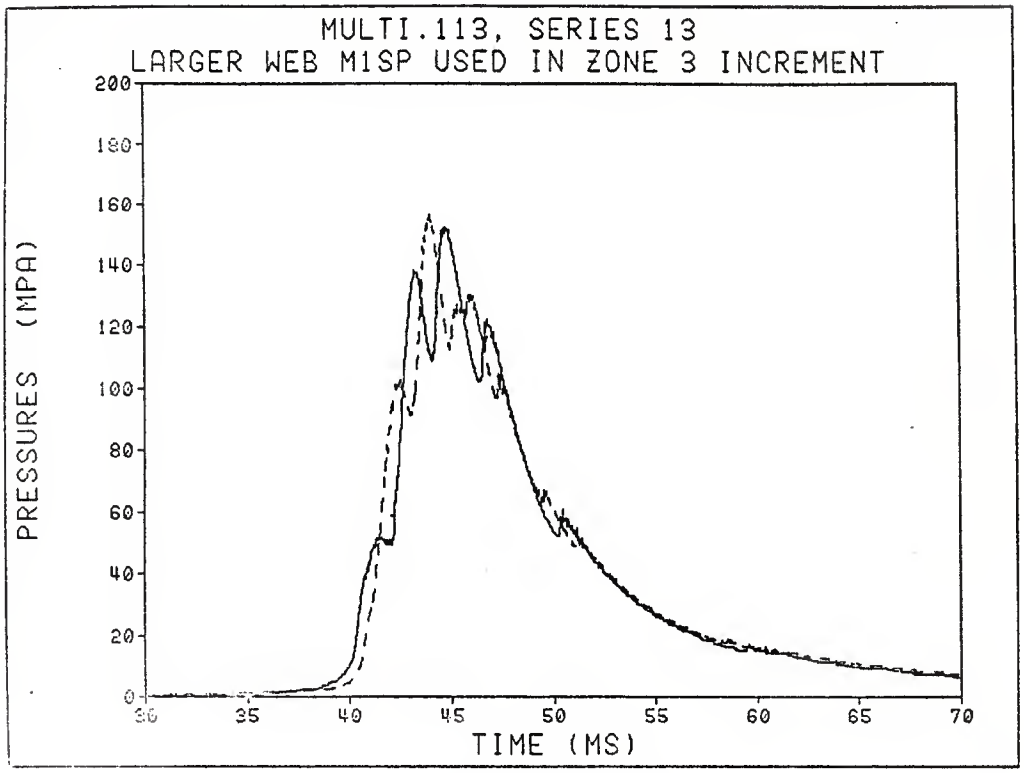
MULTI.113, SERIES 13
LARGER WEB M1SP USED IN ZONE 3 INCREMENT
PRESSURES (MPA)
200
180
160
140
120
100
80
60
40
20
0
30
35
40
45
50
55
60
65
70
TIME (MS)

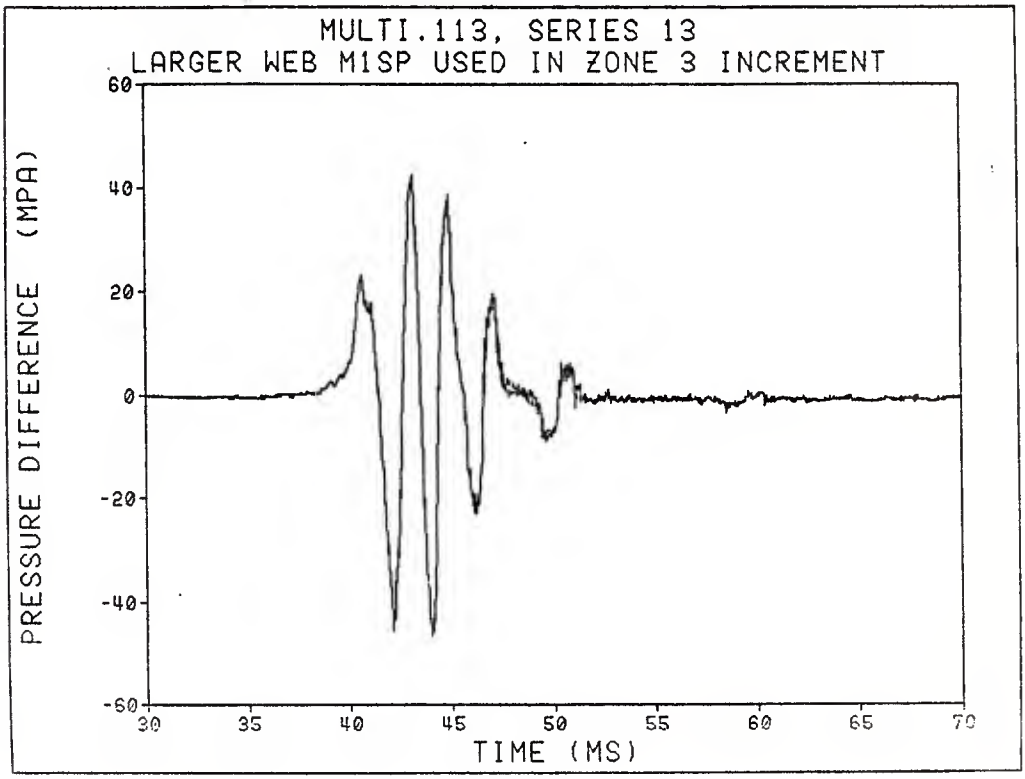
MULTI.113, SERIES 13
LARGER WEB M1SP USED IN ZONE 3 INCREMENT
PRESSURE DIFFERENCE (MPA)
60
40
20
0
-20
-40
-60
30
35
40
45
50
55
60
65
70
TIME (MS)

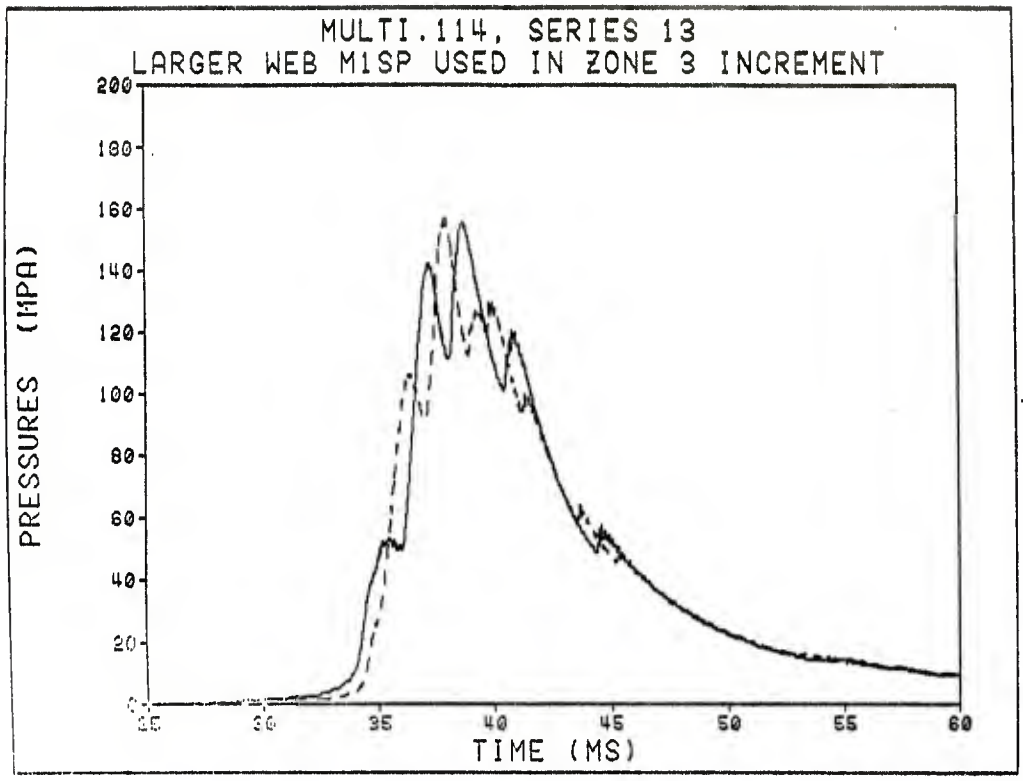
MULTI.114, SERIES 13
LARGER WEB M1SP USED IN ZONE 3 INCREMENT
PRESSURES (MPA)
200
180
160
140
120
100
80
60
40
20
0
25
30
35
40
45
50
55
60
TIME (MS)

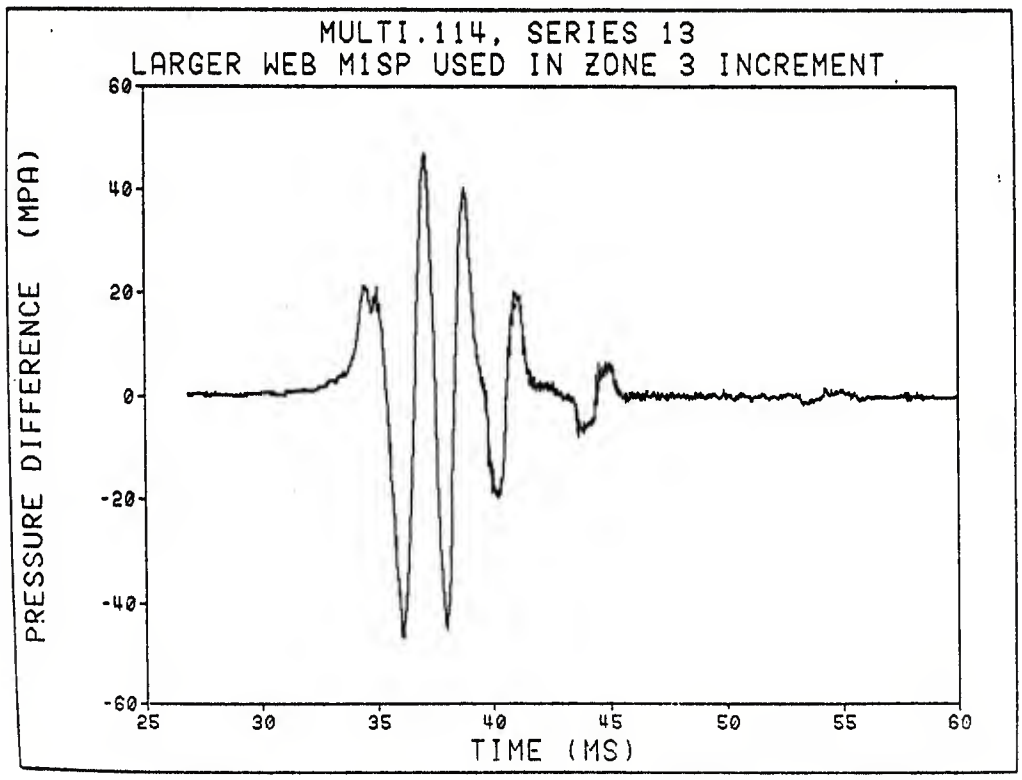
MULTI.114, SERIES 13
LARGER WEB M1SP USED IN ZONE 3 INCREMENT
PRESSURE DIFFERENCE (MPA)
60
40
20
0
-20
-40
-60
25
30
35
40
45
50
55
60
TIME (MS)

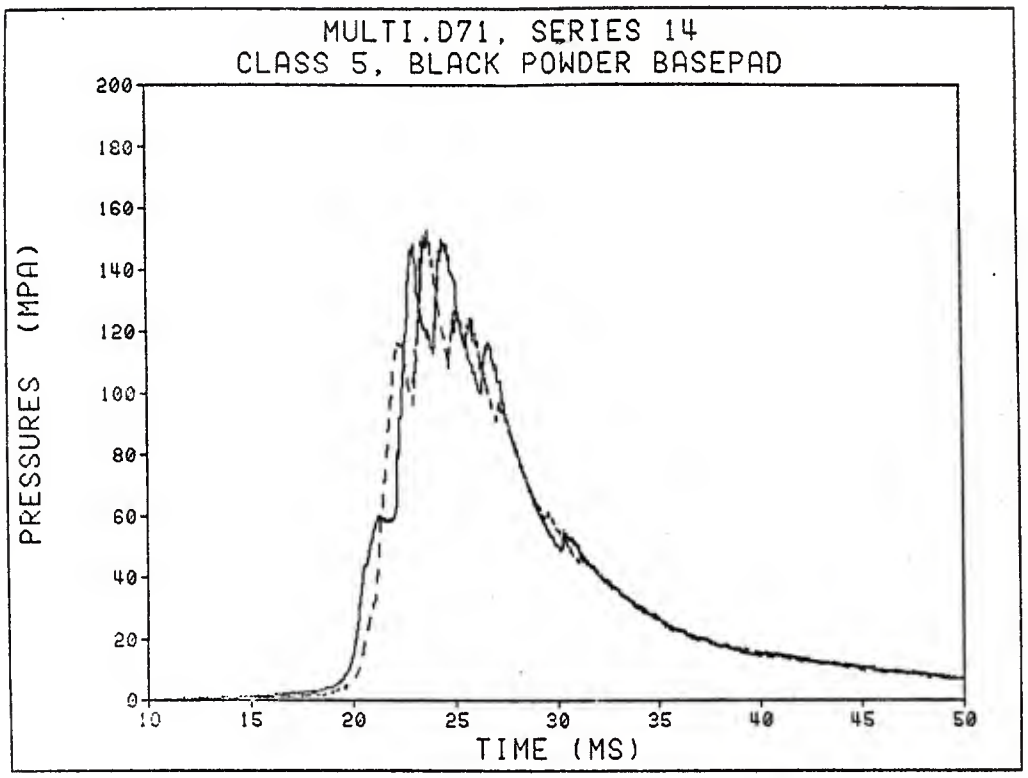
MULTI.D71, SERIES 14
CLASS 5, BLACK POWDER BASEPAD
PRESSURES (MPA)
200
180
160
140
120
100
80
60
40
20
0
10
15
20
25
30
35
40
45
50
TIME (MS)

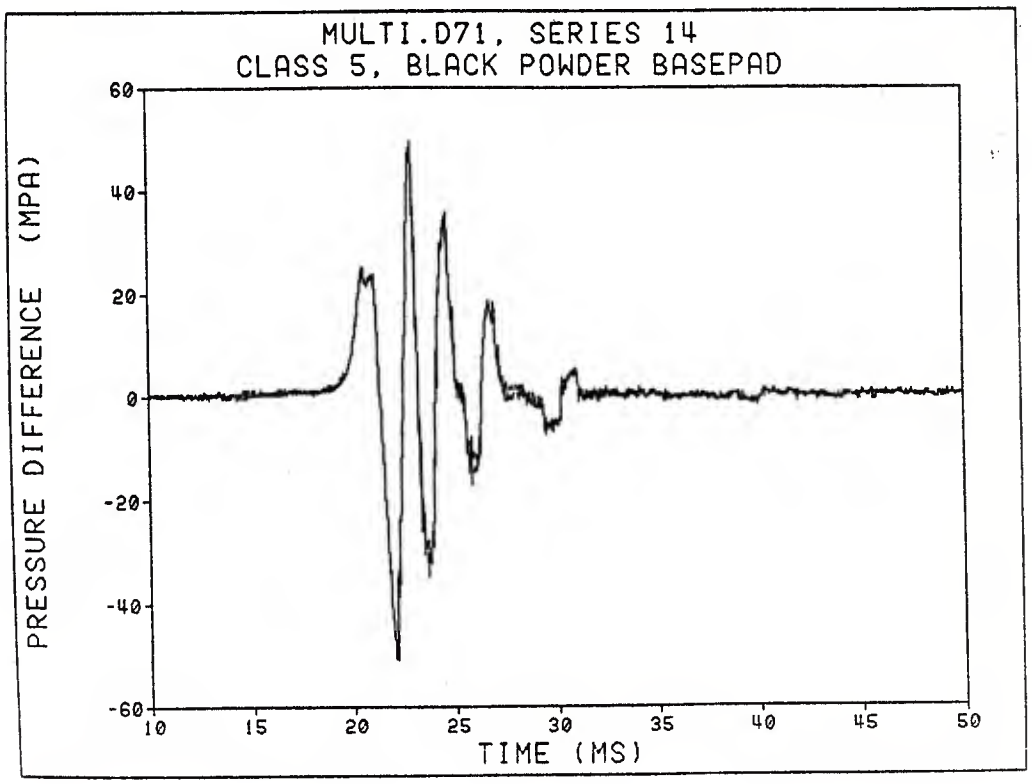
MULTI.D71, SERIES 14
CLASS 5, BLACK POWDER BASEPAD
PRESSURE DIFFERENCE (MPA)
60
40
20
0
-20
-40
-60
10
15
20
25
30
35
40
45
50
TIME (MS)

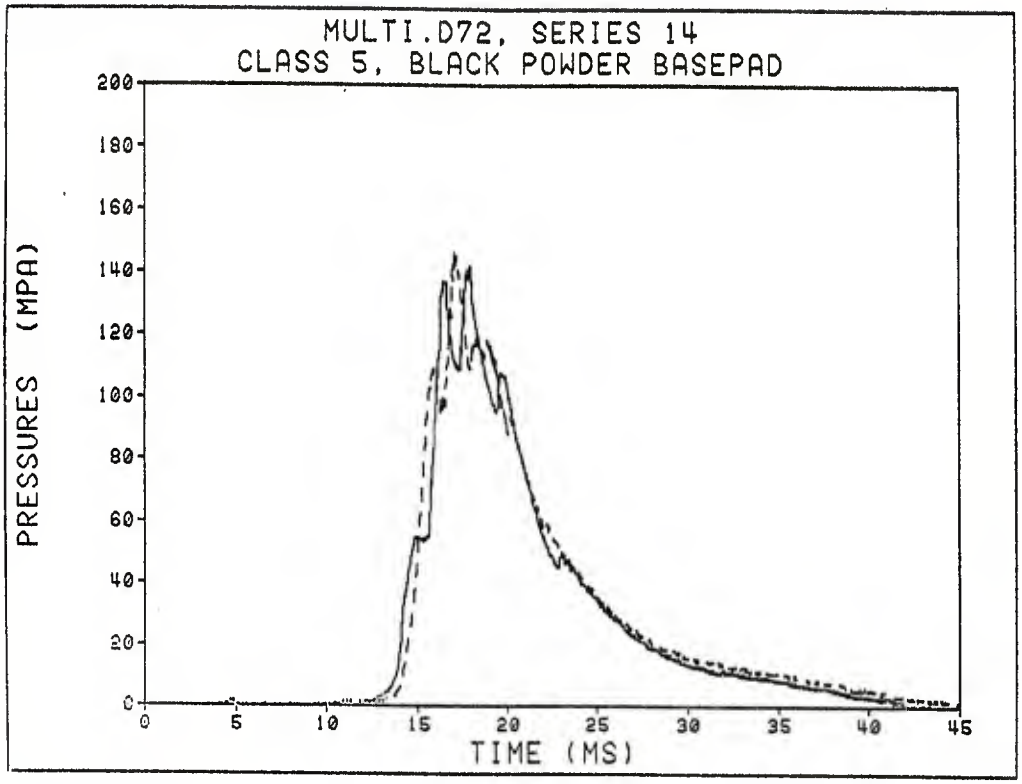
MULTI.D72, SERIES 14
CLASS 5, BLACK POWDER BASEPAD
PRESSURES (MPA)
200
180
160
140
120
100
80
60
40
20
0
0
5
10
15
20
25
30
35
40
45
TIME (MS)

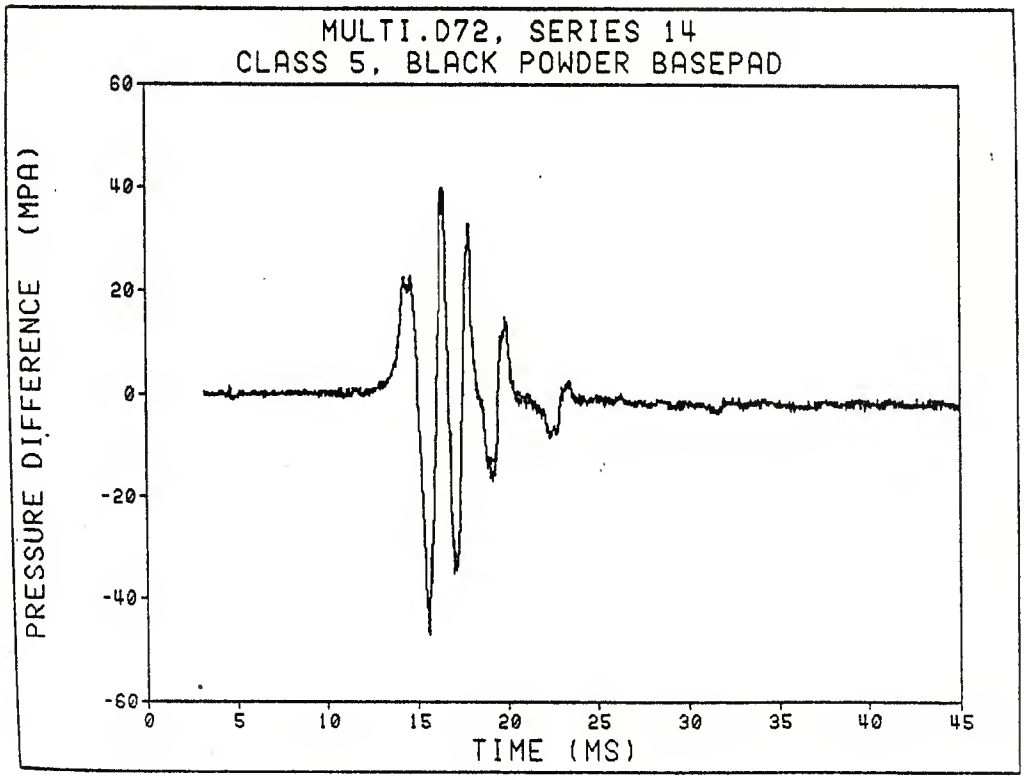
MULTI.D72, SERIES 14
CLASS 5, BLACK POWDER BASEPAD
PRESSURE DIFFERENCE (MPA)
60
40
20
0
-20
-40
-60
0
5
10
15
20
25
30
35
40
45
TIME (MS)

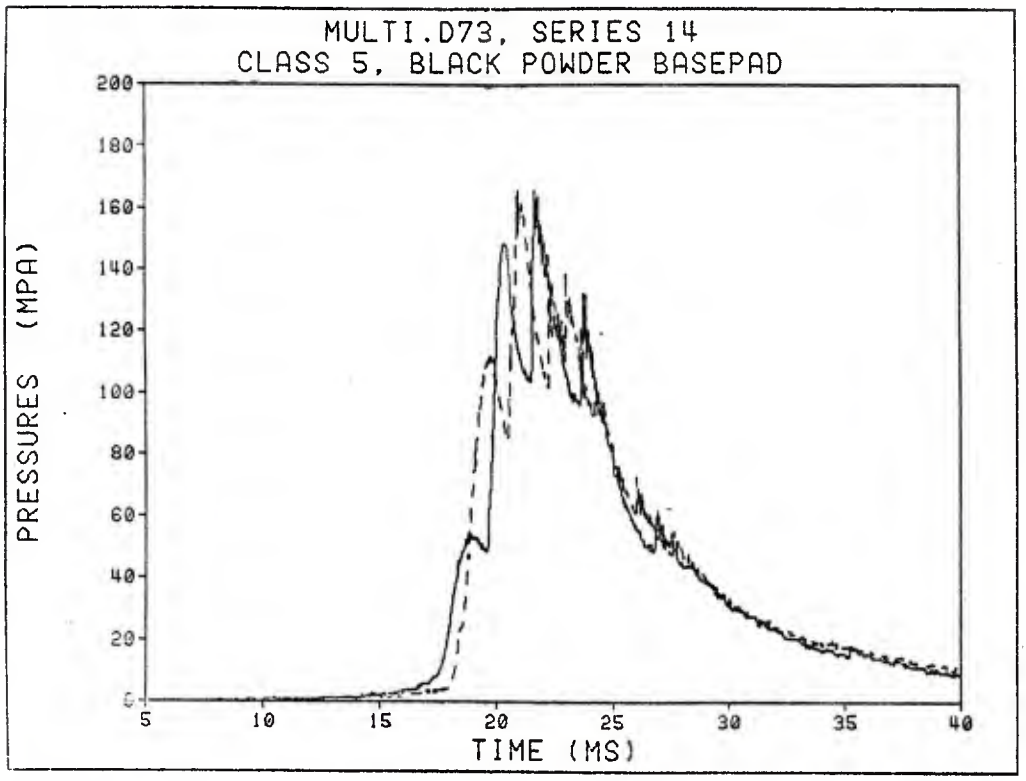
MULTI.D73, SERIES 14
CLASS 5, BLACK POWDER BASEPAD
PRESSURES (MPA)
200
180
160
140
120
100
80
60
40
20
0
5
10
15
20
25
30
35
40
TIME (MS)

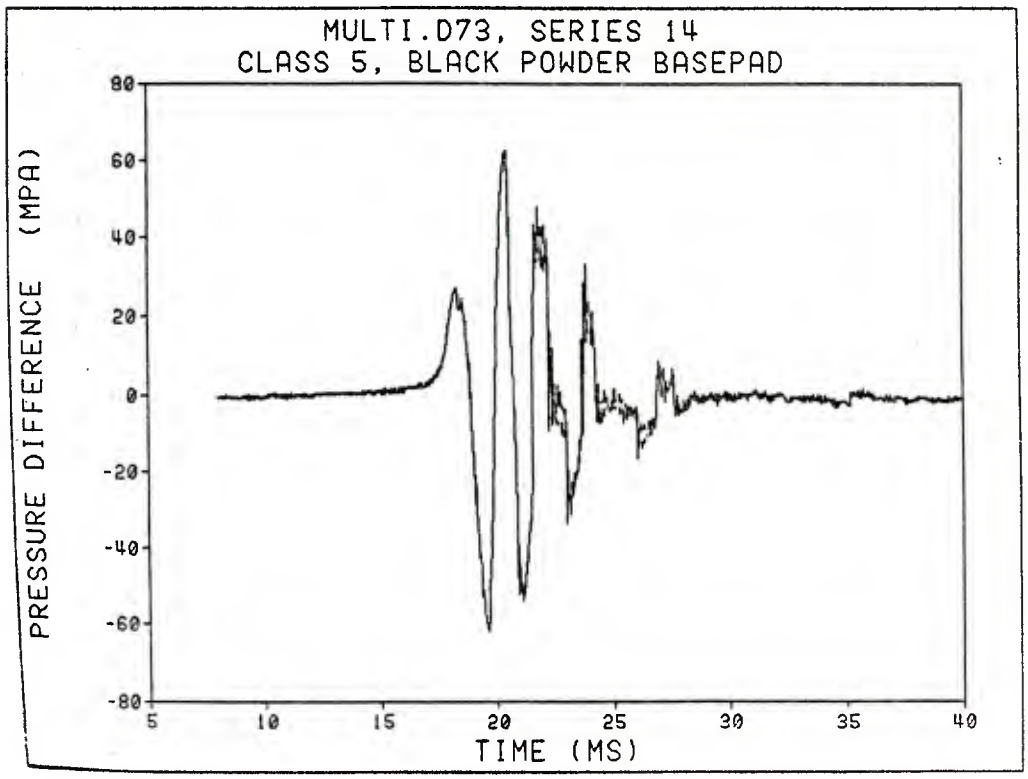
MULTI.D73, SERIES 14
CLASS 5, BLACK POWDER BASEPAD
PRESSURE DIFFERENCE (MPA)
80
60
40
20
0
-20
-40
-60
-80
5
10
15
20
25
30
35
40
TIME (MS)

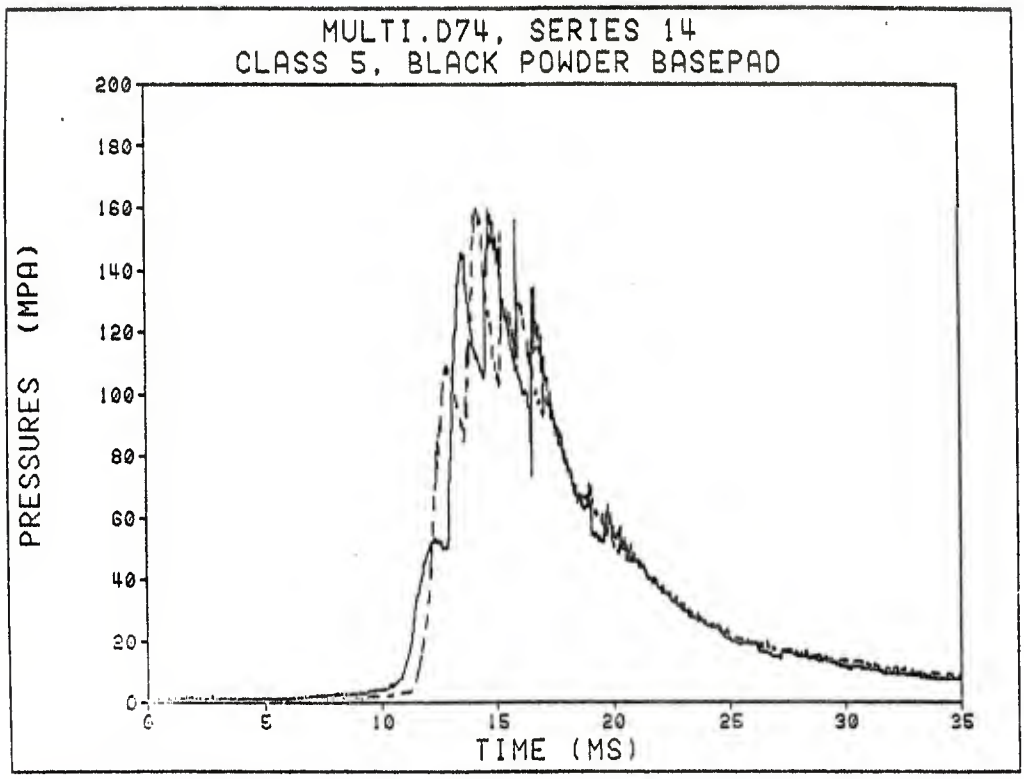
MULTI.D74, SERIES 14
CLASS 5, BLACK POWDER BASEPAD
PRESSURES (MPA)
200
180
160
140
120
100
80
60
40
20
0
0
5
10
15
20
25
30
35
TIME (MS)

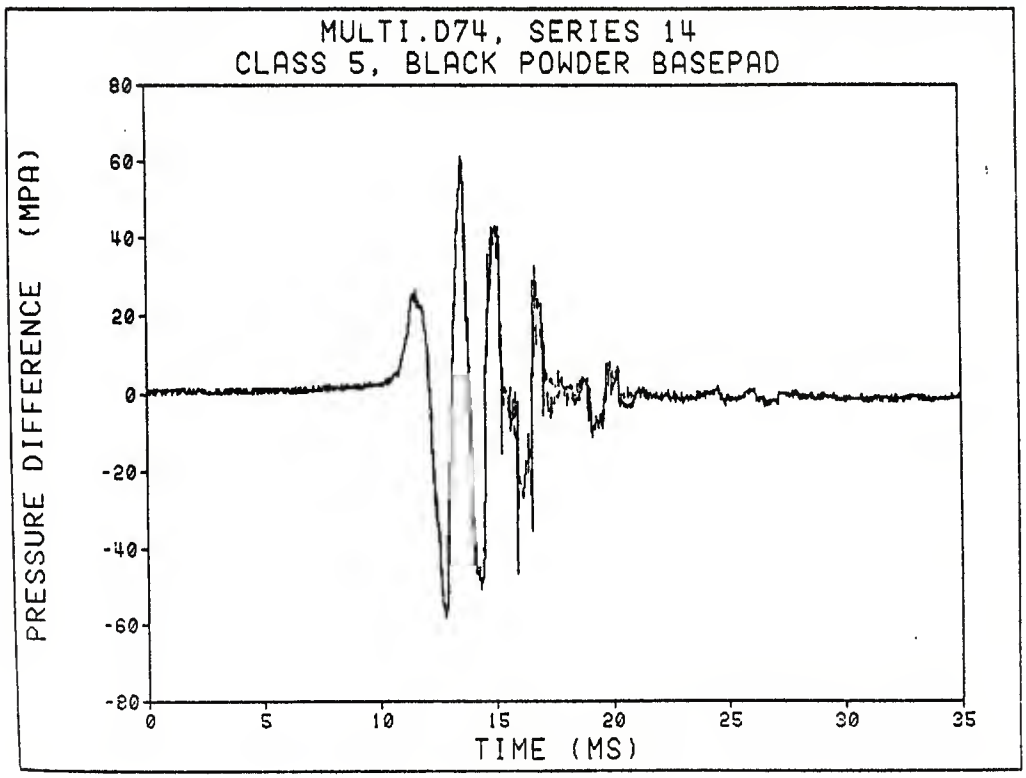
MULTI.D74, SERIES 14
CLASS 5, BLACK POWDER BASEPAD
PRESSURE DIFFERENCE (MPA)
80
60
40
20
0
-20
-40
-60
-80
0
5
10
15
20
25
30
35
TIME (MS)

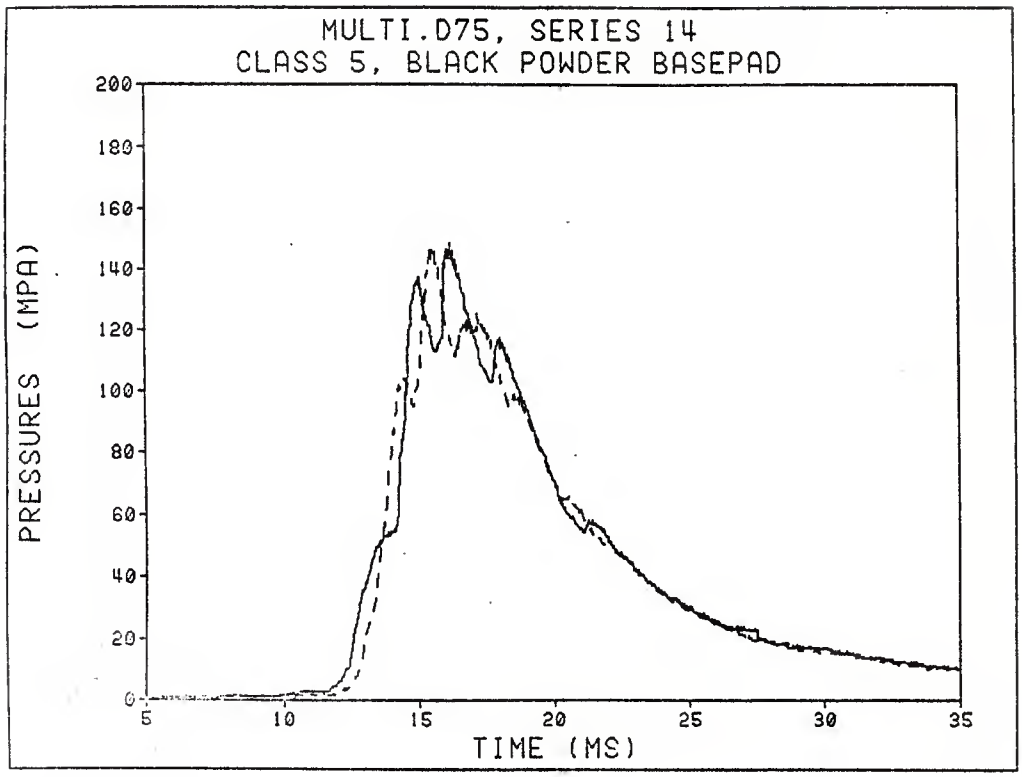
MULTI.D75, SERIES 14
CLASS 5, BLACK POWDER BASEPAD
PRESSURES (MPA)
200
180
160
140
120
100
80
60
40
20
0
5
10
15
20
25
30
35
TIME (MS)

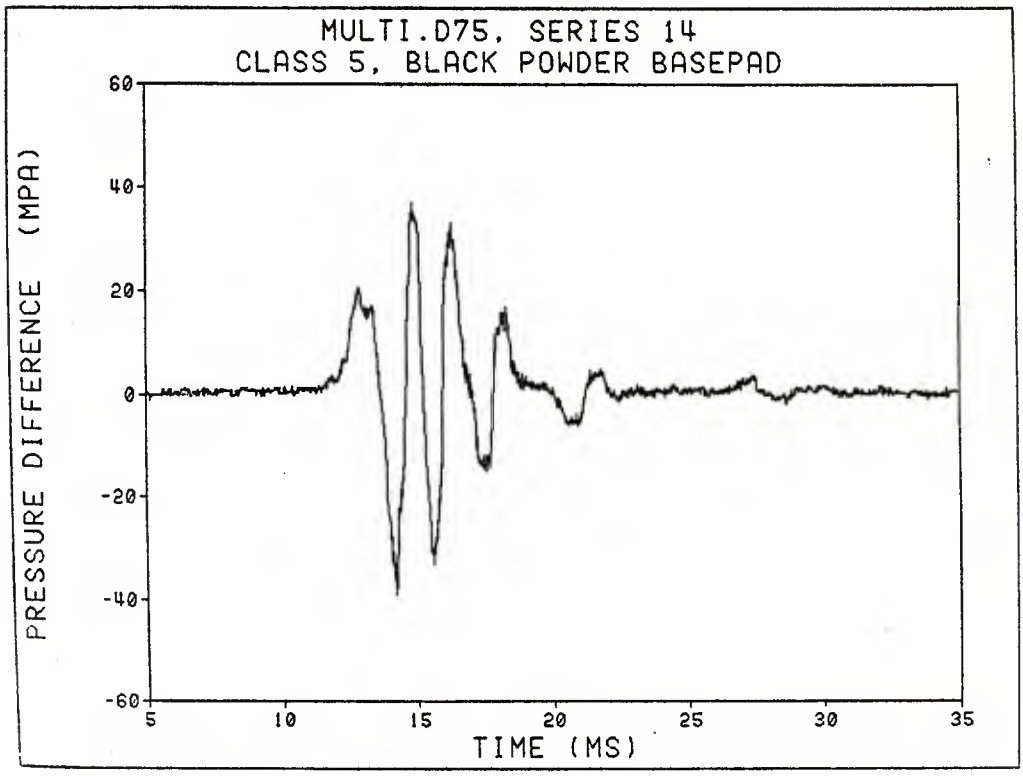
MULTI.D75, SERIES 14
CLASS 5, BLACK POWDER BASEPAD
PRESSURE DIFFERENCE (MPA)
60
40
20
0
-20
-40
-60
5
10
15
20
25
30
35
TIME (MS)

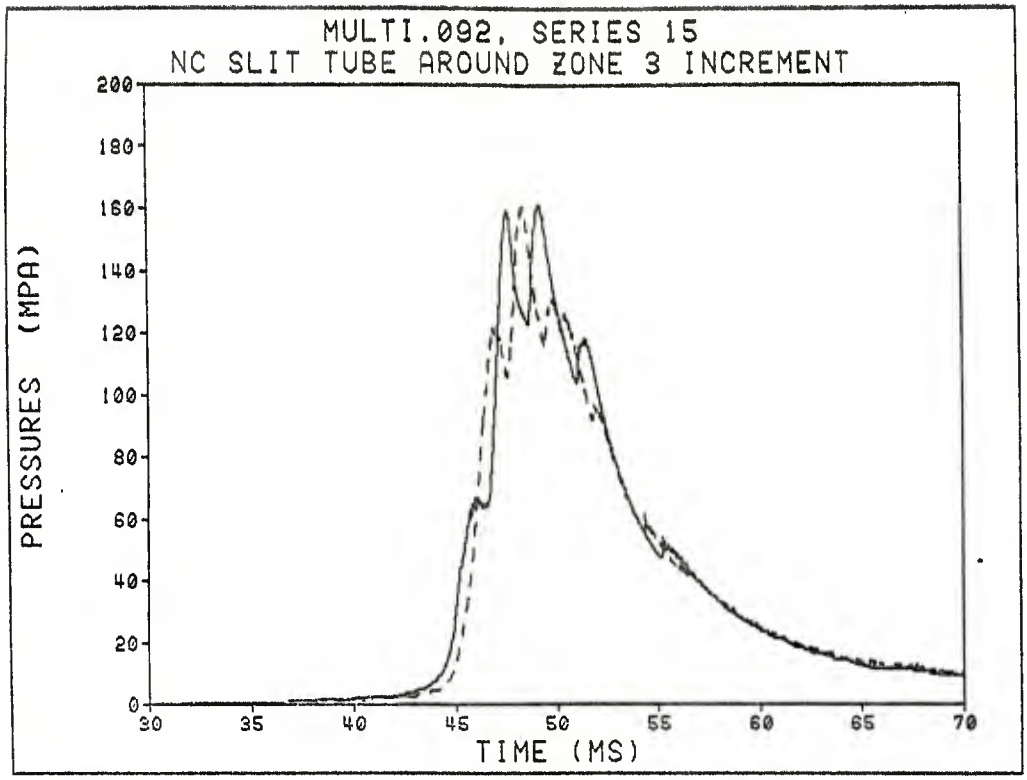
MULTI.092, SERIES 15
NC SLIT TUBE AROUND ZONE 3 INCREMENT
PRESSURES (MPA)
200
180
160
140
120
100
80
60
40
20
0
30
35
40
45
50
55
60
65
70
TIME (MS)

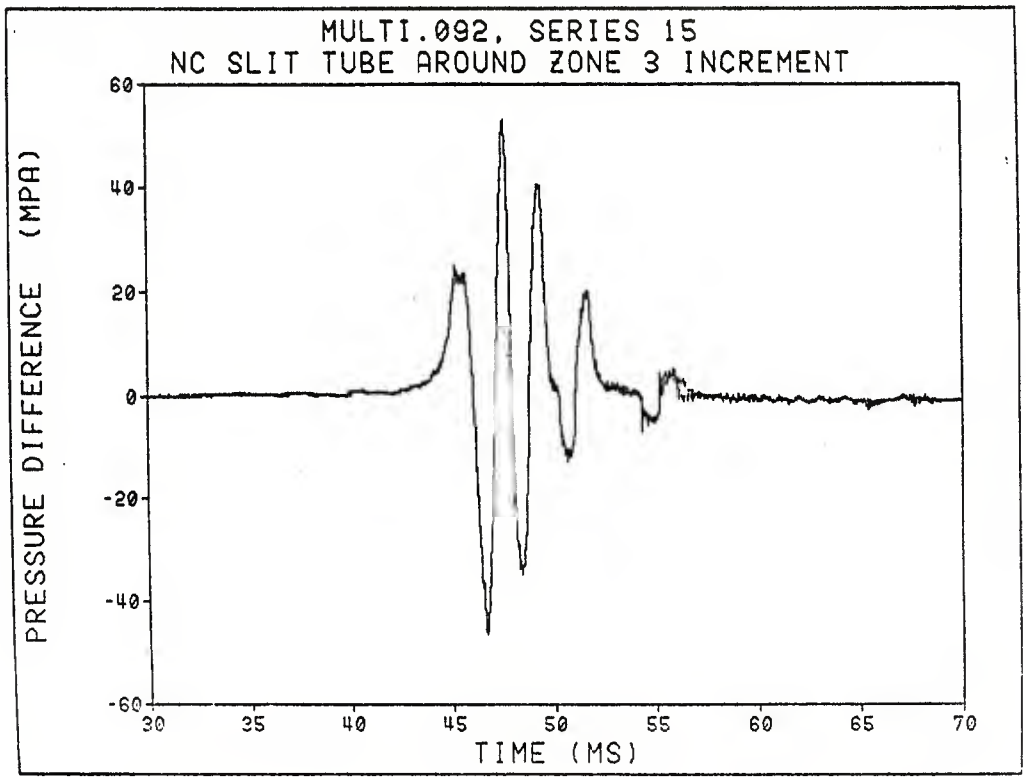
MULTI.092, SERIES 15
NC SLIT TUBE AROUND ZONE 3 INCREMENT
PRESSURE DIFFERENCE (MPA)
60
40
20
0
-20
-40
-60
30
35
40
45
50
55
60
65
70
TIME (MS)

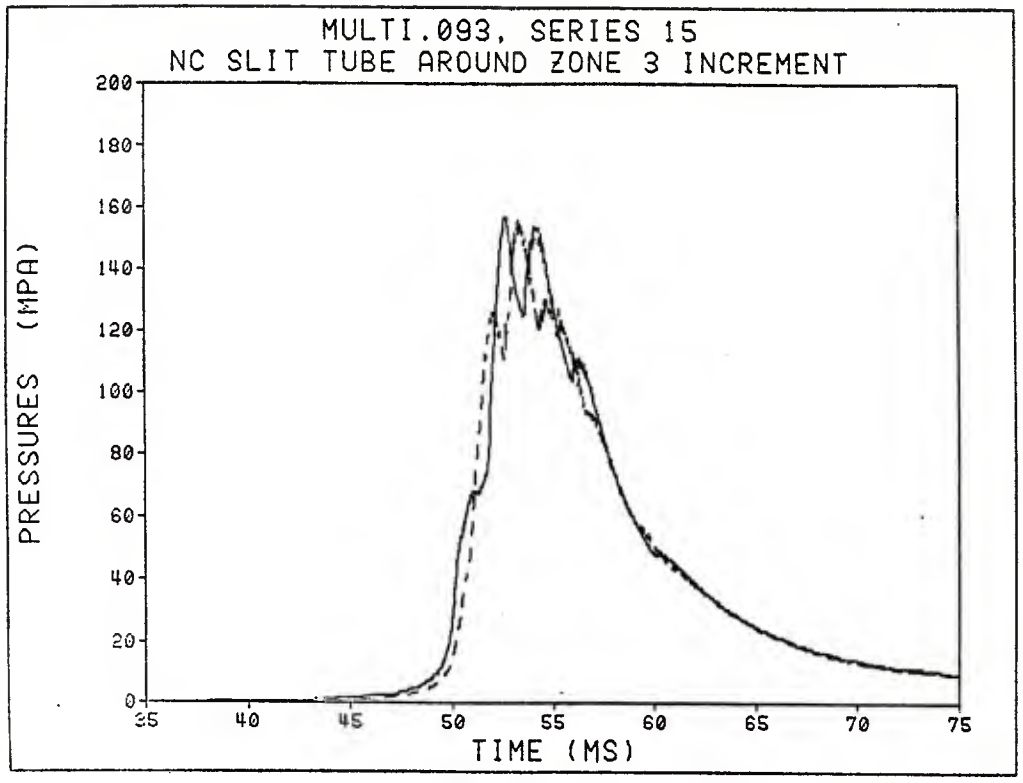
MULTI.093, SERIES 15
NC SLIT TUBE AROUND ZONE 3 INCREMENT
PRESSURES (MPA)
200
180
160
140
120
100
80
60
40
20
0
35
40
45
50
55
60
65
70
75
TIME (MS)

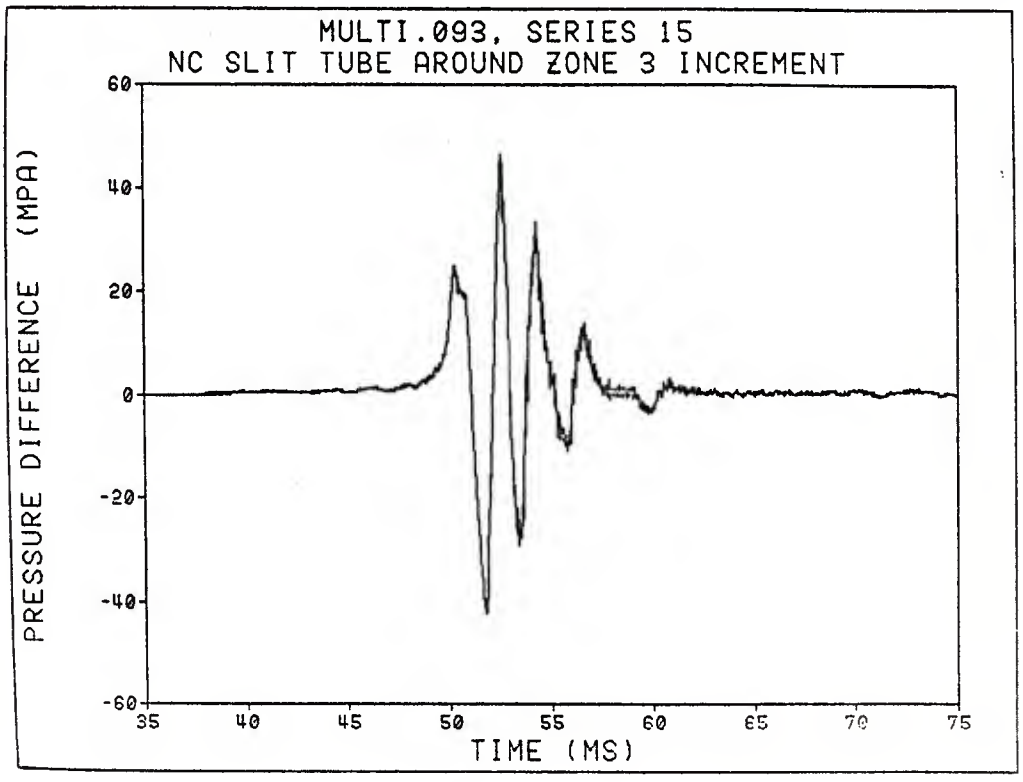
MULTI.093, SERIES 15
NC SLIT TUBE AROUND ZONE 3 INCREMENT
PRESSURE DIFFERENCE (MPA)
60
40
20
0
-20
-40
-60
35
40
45
50
55
60
65
70
75
TIME (MS)

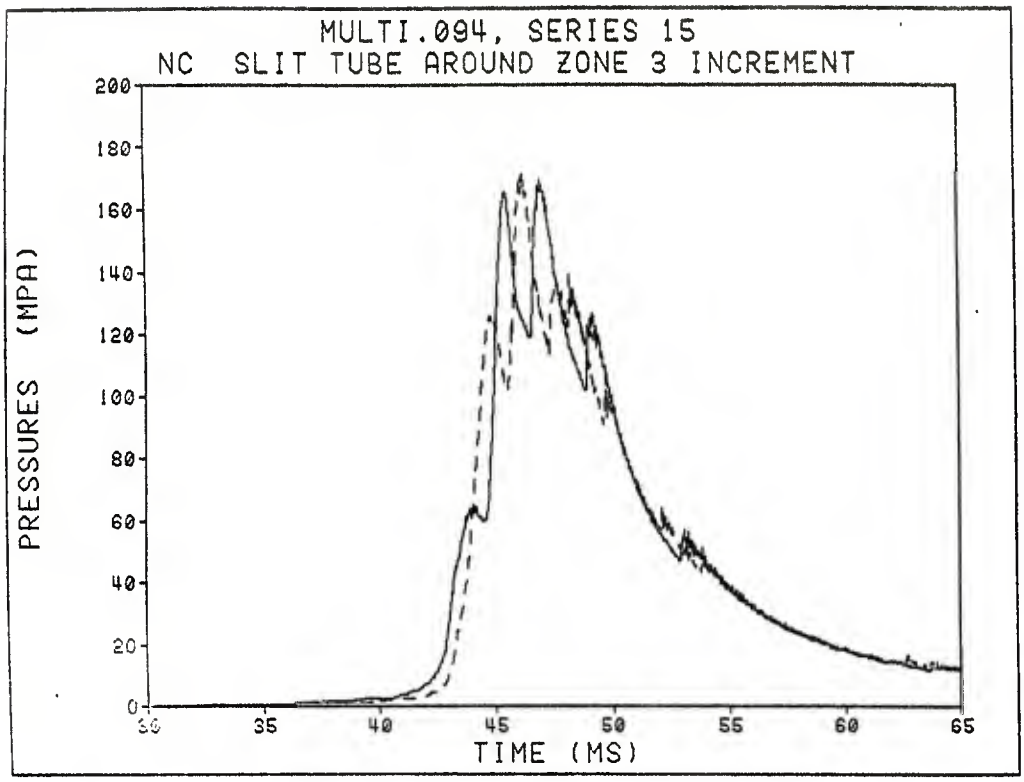
MULTI.094, SERIES 15
NC SLIT TUBE AROUND ZONE 3 INCREMENT
PRESSURES (MPA)
200
180
160
140
120
100
80
60
40
20
0
30
35
40
45
50
55
60
65
TIME (MS)

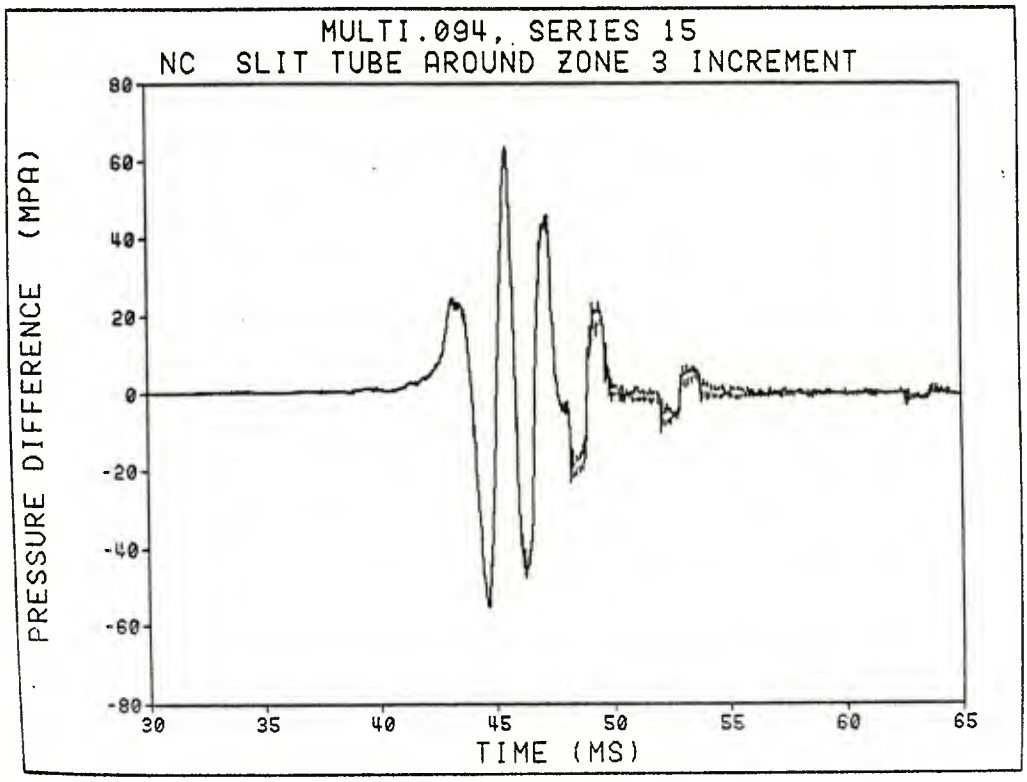
MULTI.094, SERIES 15
NC SLIT TUBE AROUND ZONE 3 INCREMENT
PRESSURE DIFFERENCE (MPA)
80
60
40
20
0
-20
-40
-60
-80
30
35
40
45
50
55
60
65
TIME (MS)

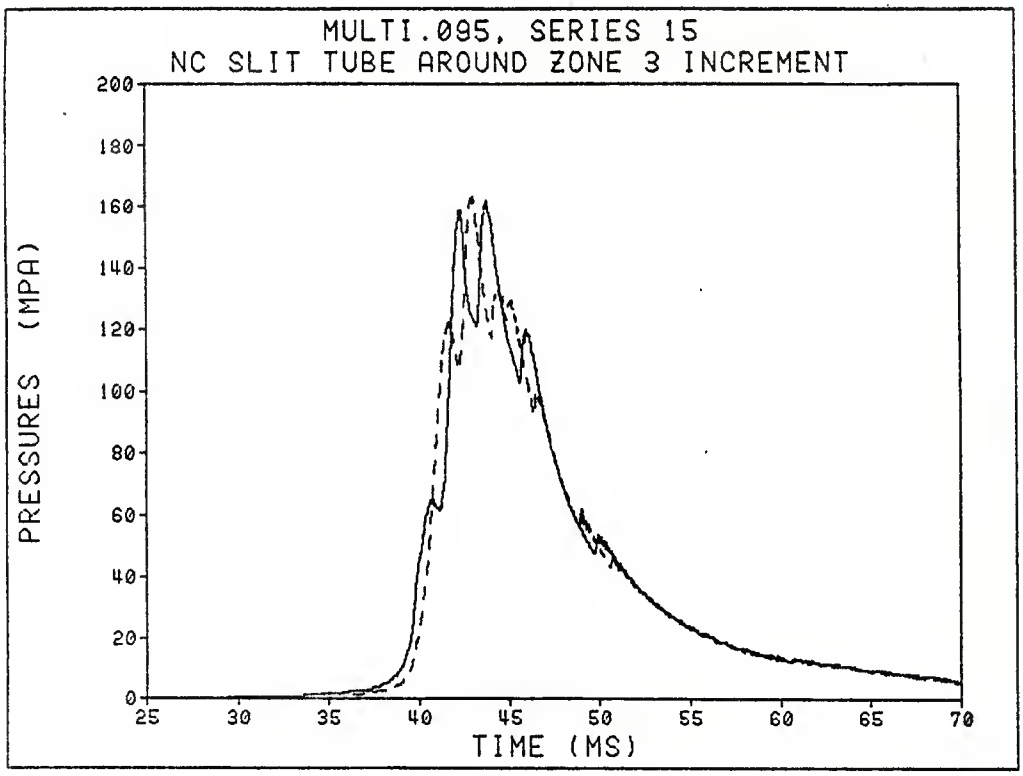
MULTI.095, SERIES 15
NC SLIT TUBE AROUND ZONE 3 INCREMENT
PRESSURES (MPA)
200
180
160
140
120
100
80
60
40
20
0
25
30
35
40
45
50
55
60
65
70
TIME (MS)

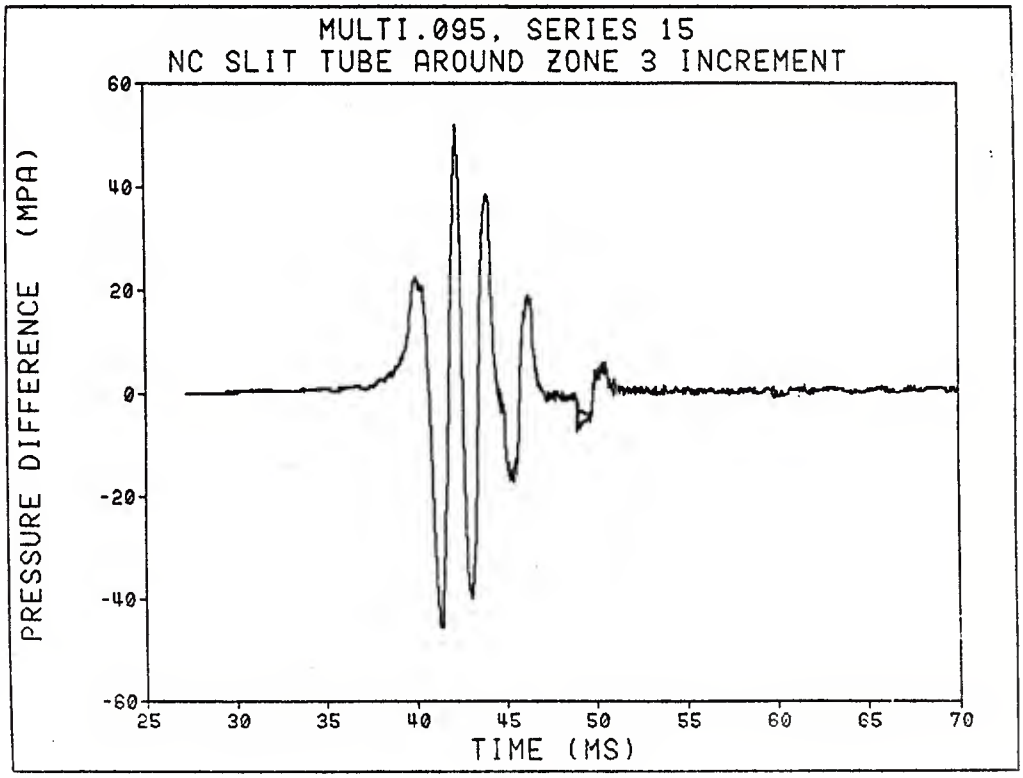
MULTI.095, SERIES 15
NC SLIT TUBE AROUND ZONE 3 INCREMENT
PRESSURE DIFFERENCE (MPA)
60
40
20
0
-20
-40
-60
25
30
35
40
45
50
55
60
65
70
TIME (MS)

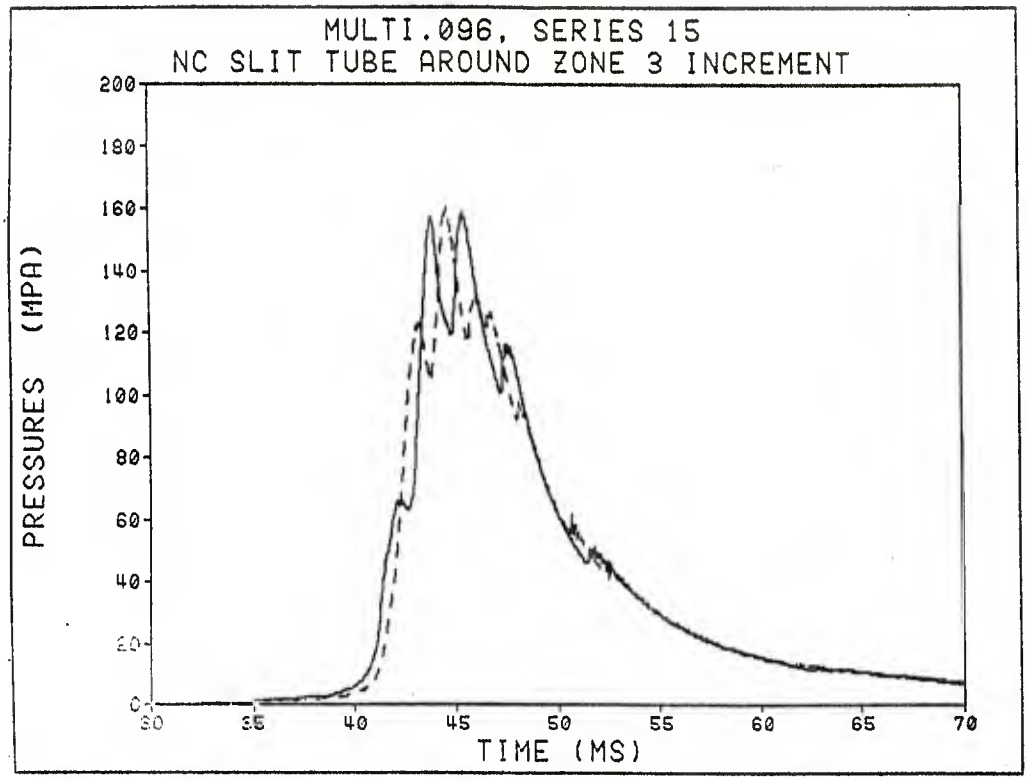
MULTI.096, SERIES 15
NC SLIT TUBE AROUND ZONE 3 INCREMENT
PRESSURES (MPA)
200
180
160
140
120
100
80
60
40
20
0
30
35
40
45
50
55
60
65
70
TIME (MS)

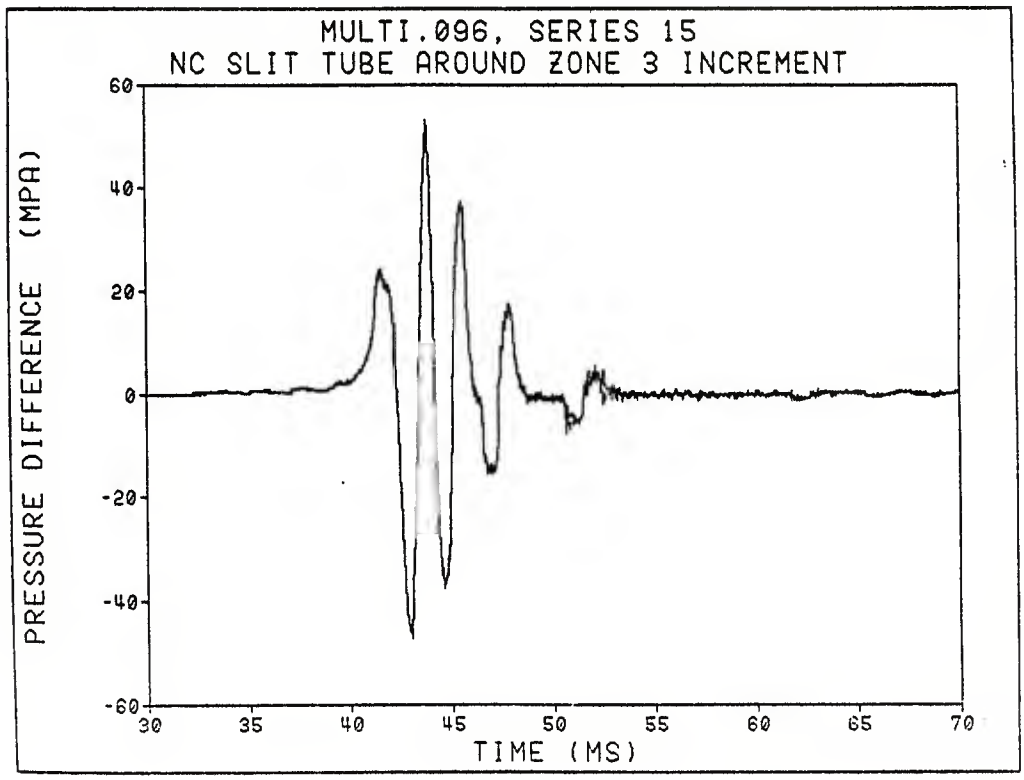
MULTI.096, SERIES 15
NC SLIT TUBE AROUND ZONE 3 INCREMENT
PRESSURE DIFFERENCE (MPA)
60
40
20
0
-20
-40
-60
30
35
40
45
50
55
60
65
70
TIME (MS)

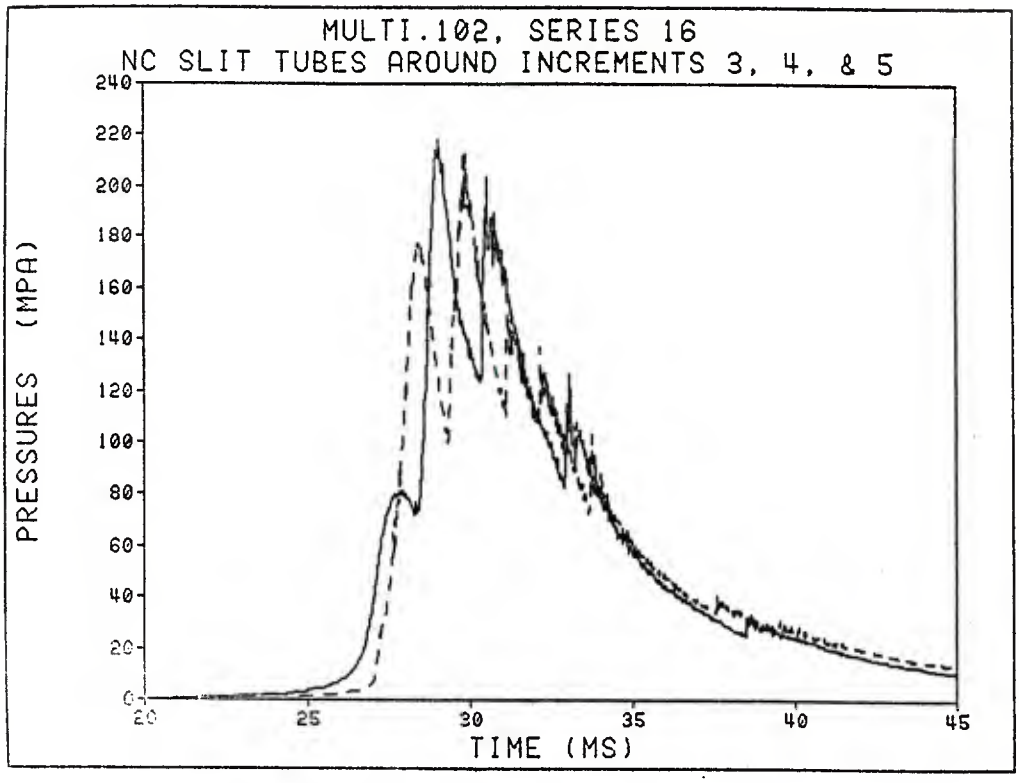
MULTI.102, SERIES 16
NC SLIT TUBES AROUND INCREMENTS 3, 4, & 5
PRESSURES (MPA)
240
220
200
180
160
140
120
100
80
60
40
20
0
20
25
30
35
40
45
TIME (MS)

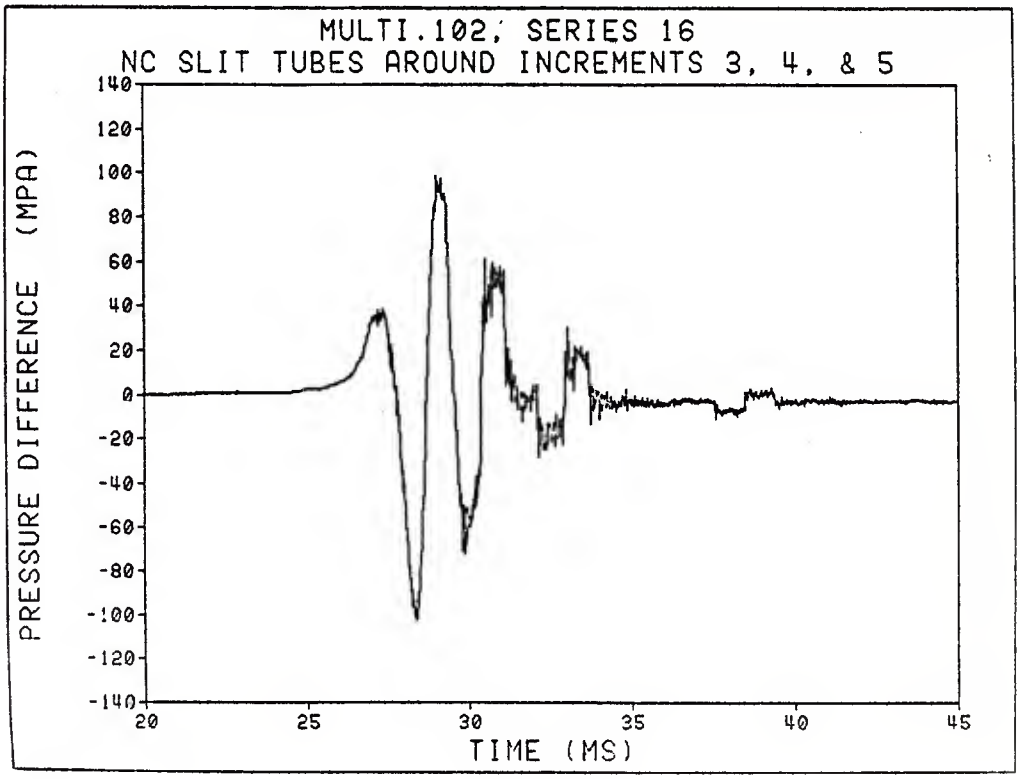
MULTI.102, SERIES 16
NC SLIT TUBES AROUND INCREMENTS 3, 4, & 5
PRESSURE DIFFERENCE (MPA)
140
120
100
80
60
40
20
0
-20
-40
-60
-80
-100
-120
-140
20
25
30
35
40
45
TIME (MS)

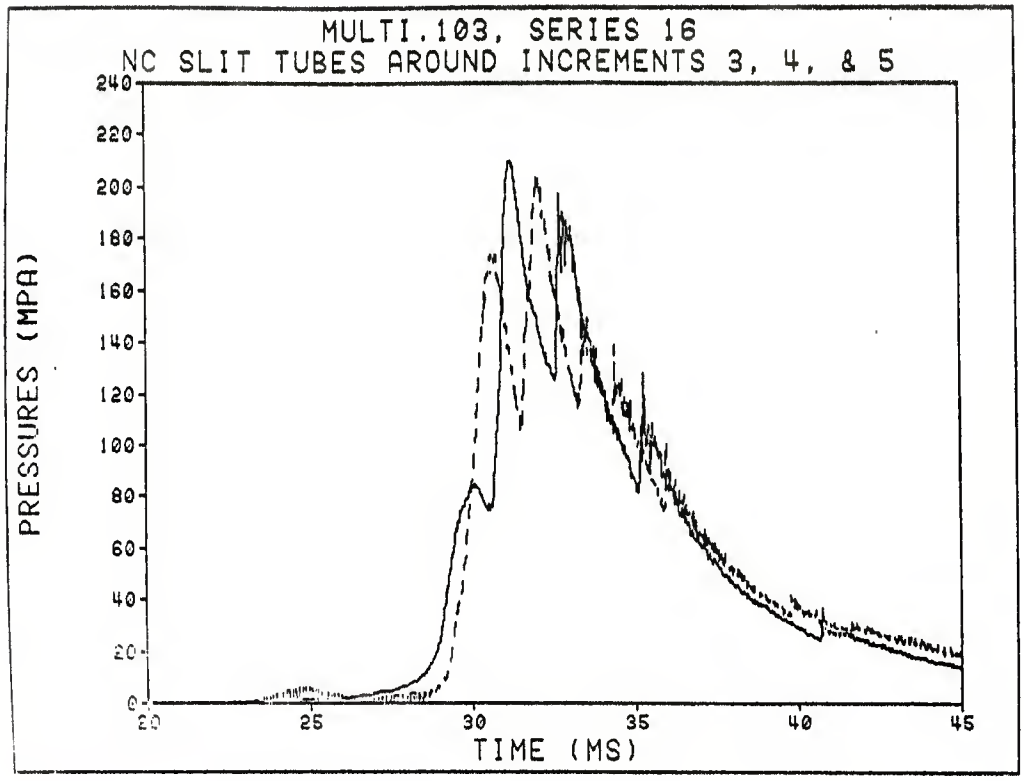
MULTI.103, SERIES 16
NC SLIT TUBES AROUND INCREMENTS 3, 4, & 5
PRESSURES (MPA)
240
220
200
180
160
140
120
100
80
60
40
20
0
20
25
30
35
40
45
TIME (MS)

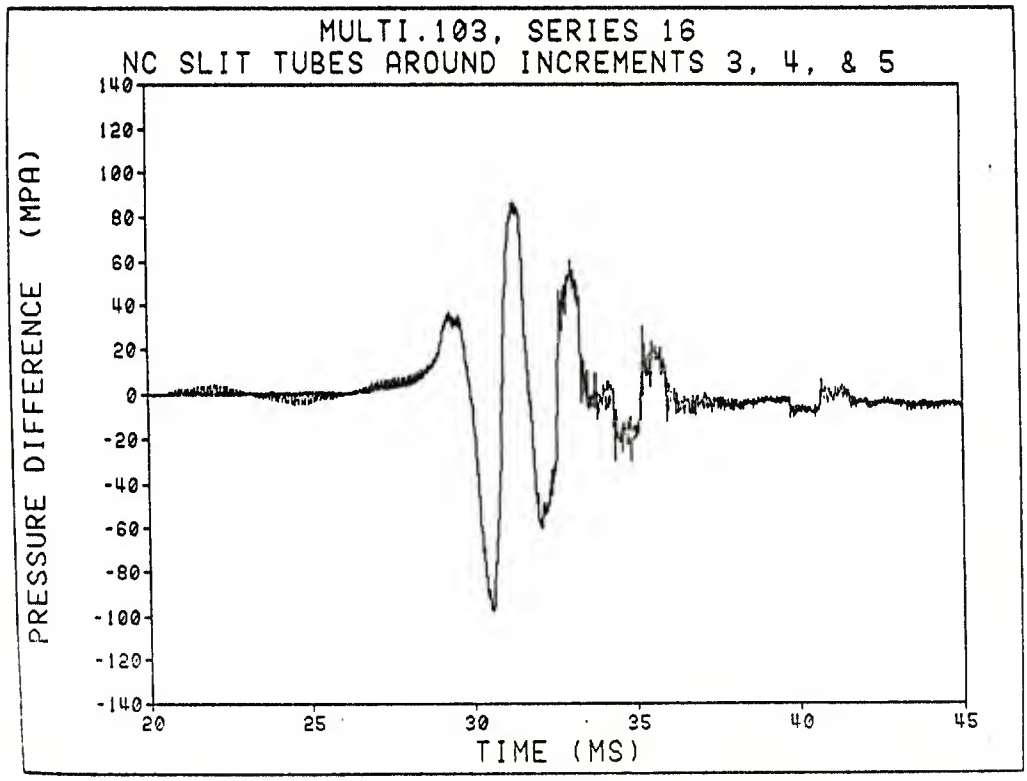
MULTI.103, SERIES 16
NC SLIT TUBES AROUND INCREMENTS 3, 4, & 5
PRESSURE DIFFERENCE (MPA)
140
120
100
80
60
40
20
0
-20
-40
-60
-80
-100
-120
-140
20
25
30
35
40
45
TIME (MS)

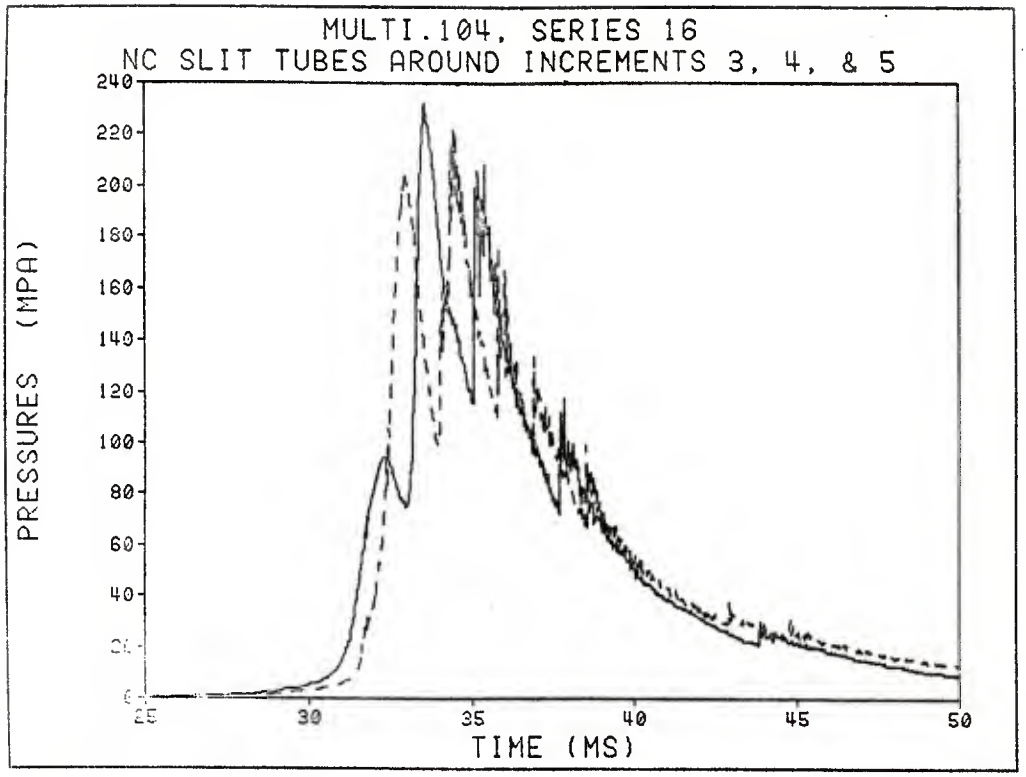
MULTI.104, SERIES 16
NC SLIT TUBES AROUND INCREMENTS 3, 4, & 5
PRESSURES (MPA)
240
220
200
180
160
140
120
100
80
60
40
25
30
35
40
45
50
TIME (MS)

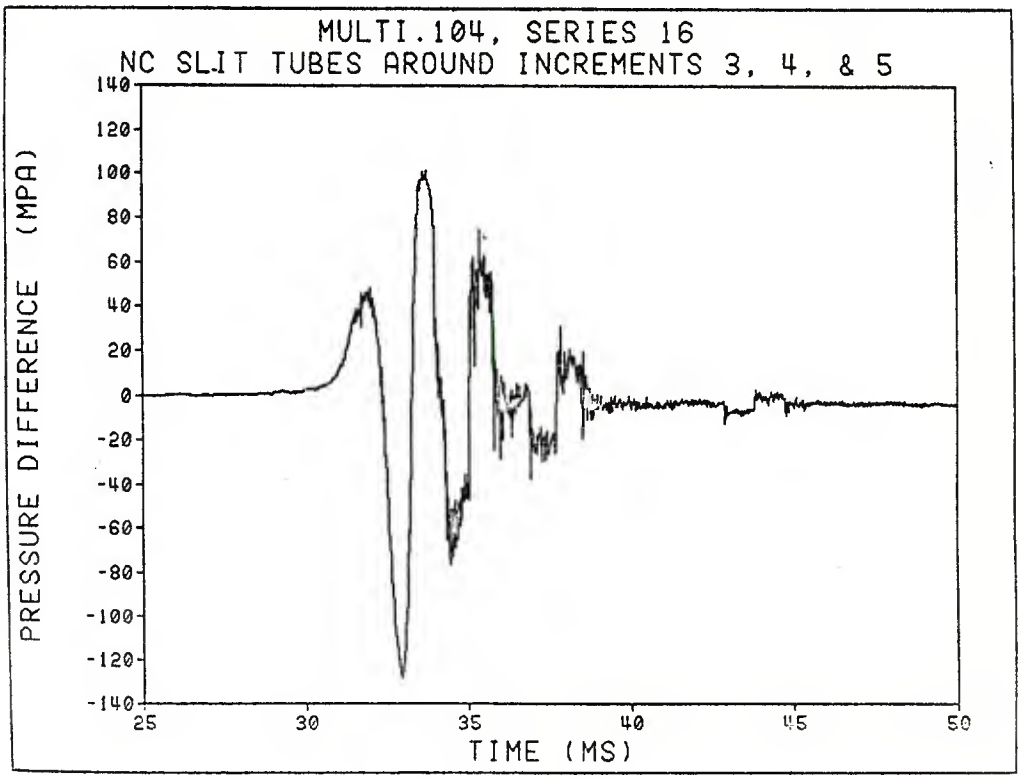
MULTI.104, SERIES 16
NC SLIT TUBES AROUND INCREMENTS 3, 4, & 5
PRESSURE DIFFERENCE (MPA)
140
120
100
80
60
40
20
0
-20
-40
-60
-80
-100
-120
-140
25
30
35
40
45
50
TIME (MS)

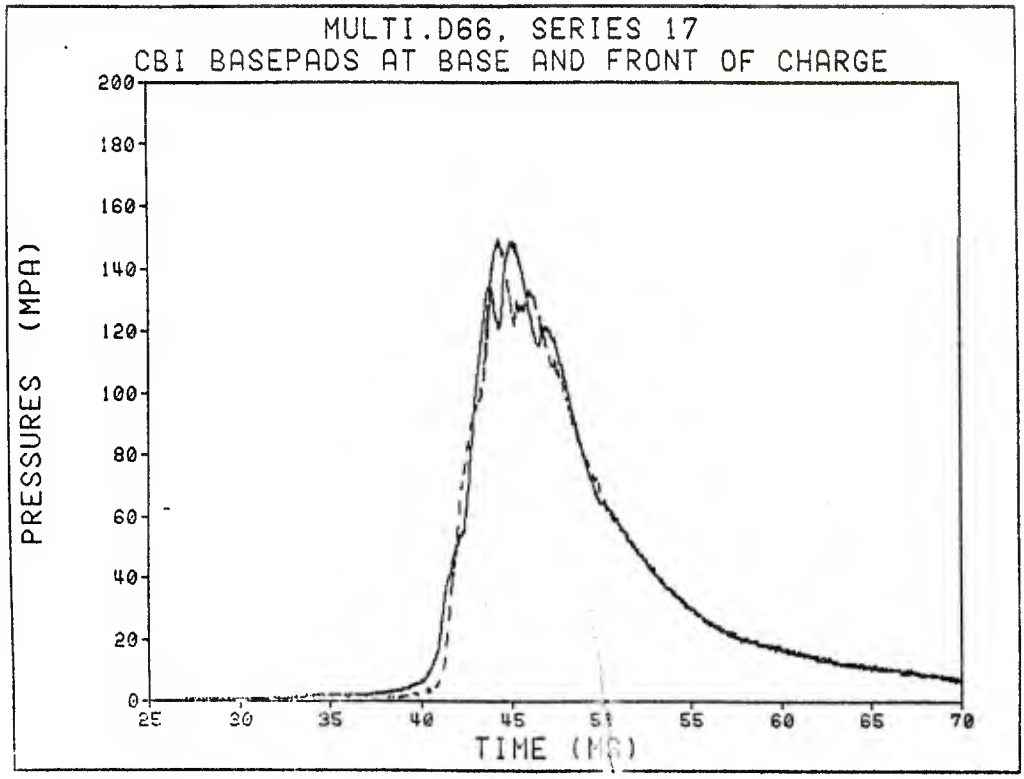
MULTI.D66, SERIES 17
CBI BASEPADS AT BASE AND FRONT OF CHARGE
PRESSURES (MPA)
200
180
160
140
120
100
80
60
40
20
0
25
30
35
40
45
50
55
60
65
70
TIME (MS)

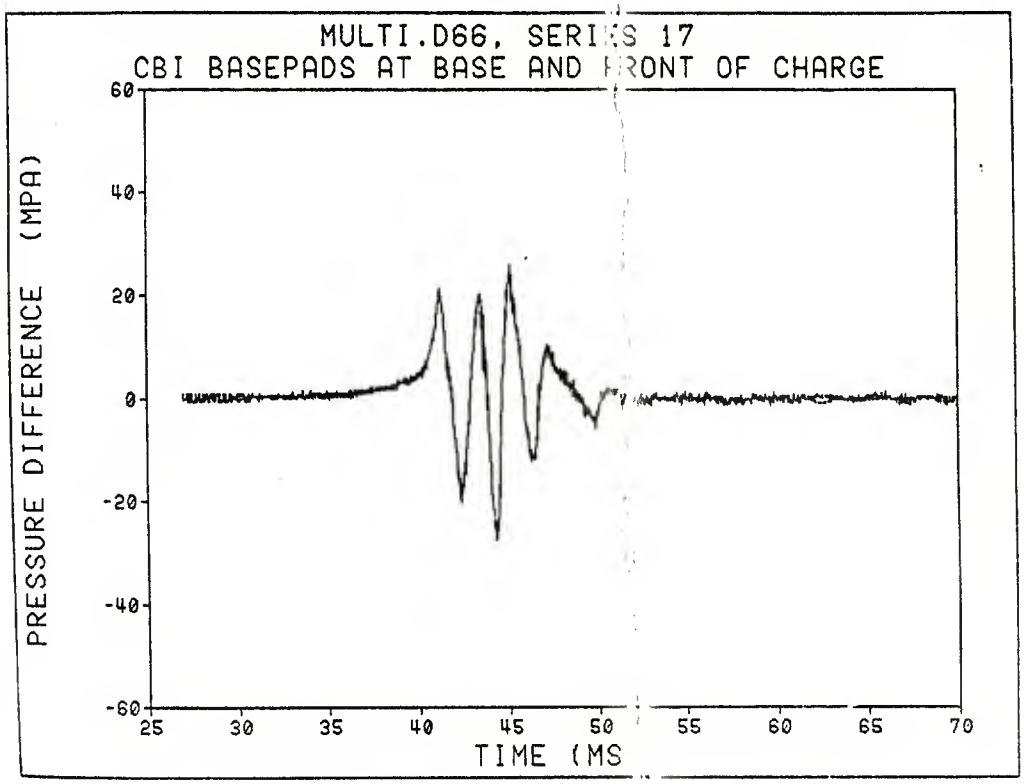
MULTI.D66, SERIES 17
CBI BASEPADS AT BASE AND FRONT OF CHARGE
PRESSURE DIFFERENCE (MPA)
60
40
20
0
-20
-40
-60
25
30
35
40
45
50
55
60
65
70
TIME (MS

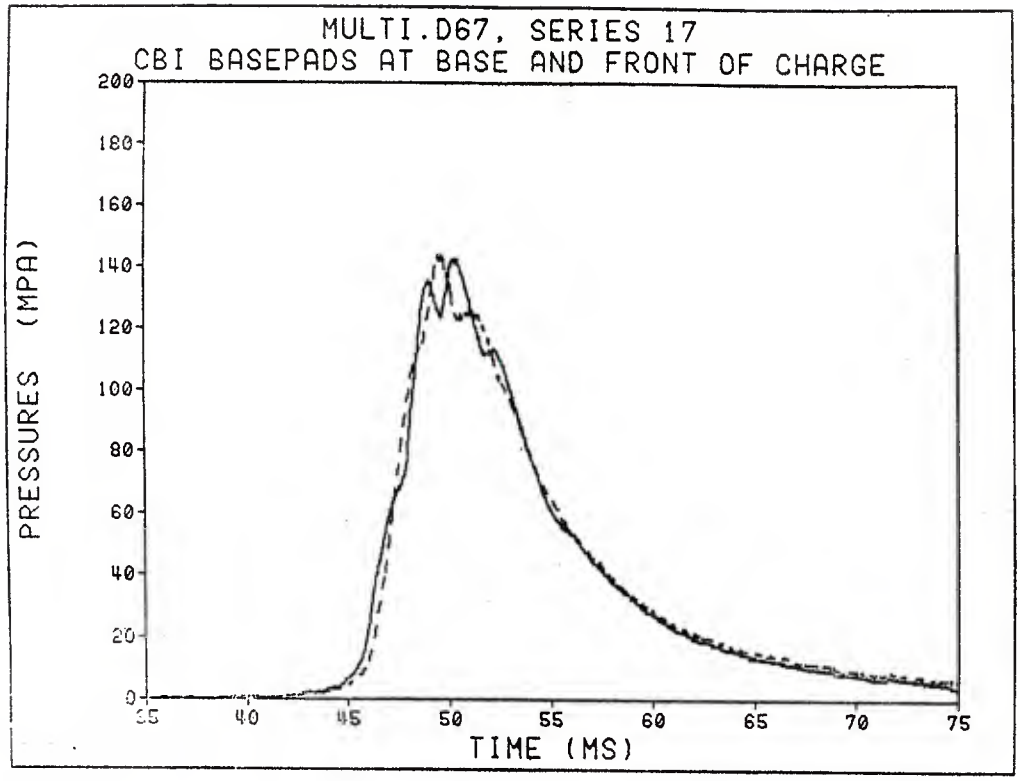
MULTI.D67, SERIES 17
CBI BASEPADS AT BASE AND FRONT OF CHARGE
PRESSURES (MPA)
200
180
160
140
120
100
80
60
40
20
0
35
40
45
50
55
60
65
70
75
TIME (MS)

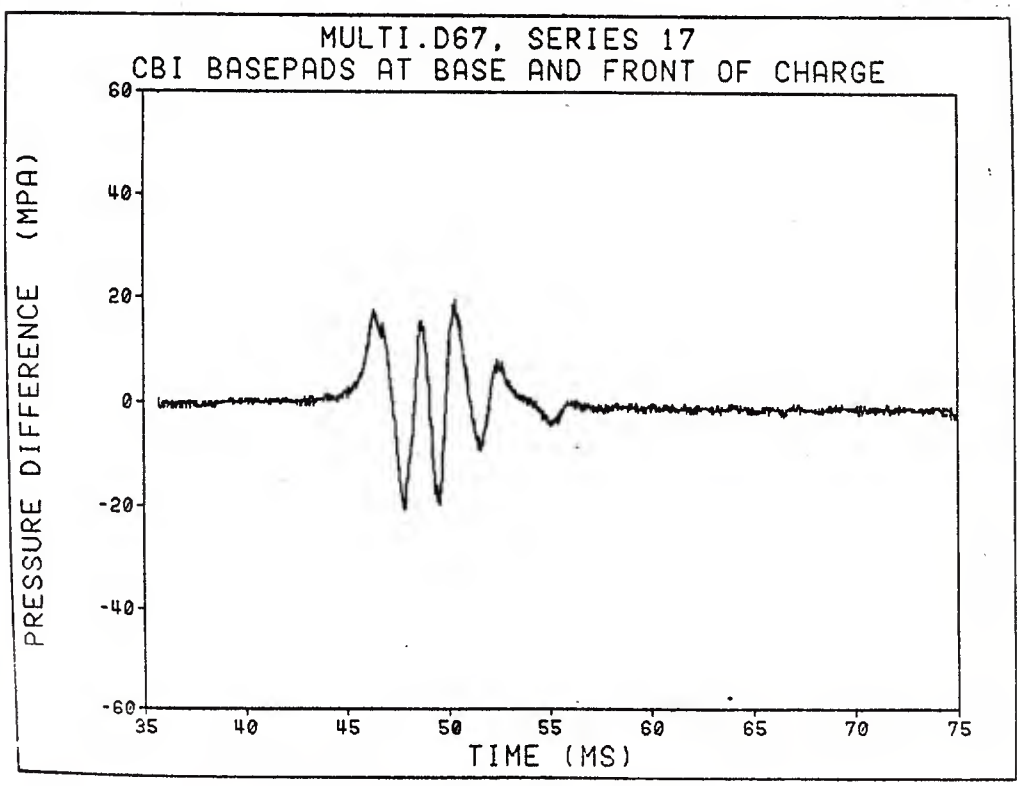
MULTI.D67, SERIES 17
CBI BASEPADS AT BASE AND FRONT OF CHARGE
PRESSURE DIFFERENCE (MPA)
60
40
20
0
-20
-40
-60
35
40
45
50
55
60
65
70
75
TIME (MS)

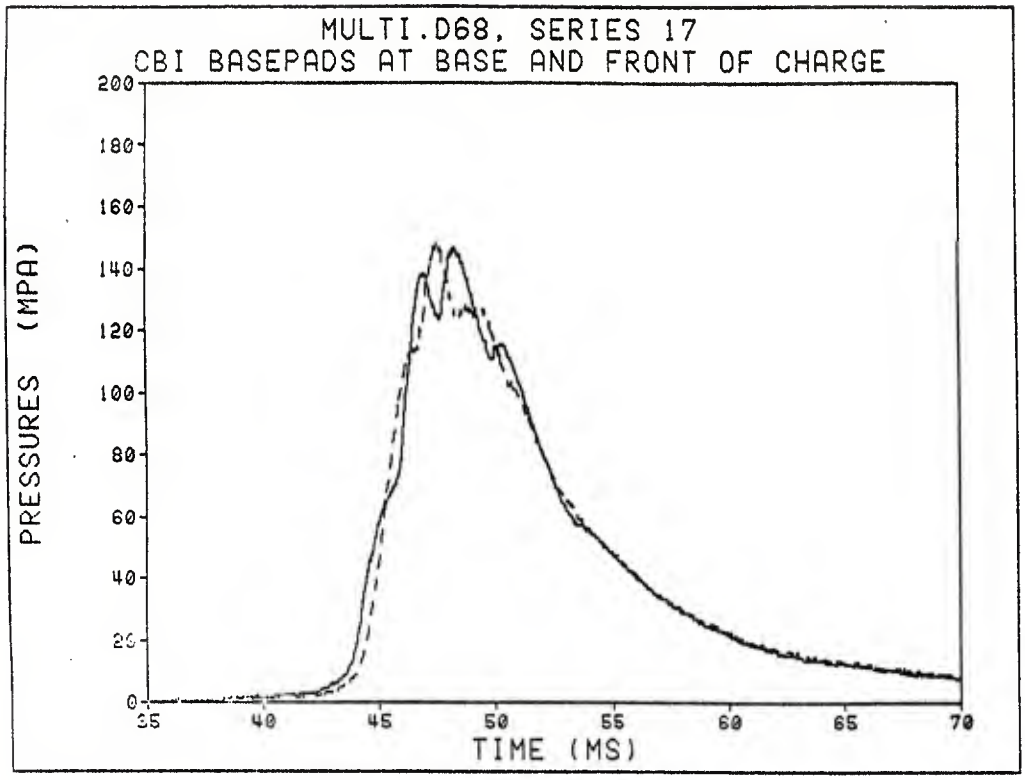
MULTI.D68, SERIES 17
CBI BASEPADS AT BASE AND FRONT OF CHARGE
PRESSURES (MPA)
200
180
160
140
120
100
80
60
40
20
0
35
40
45
50
55
60
65
70
TIME (MS)

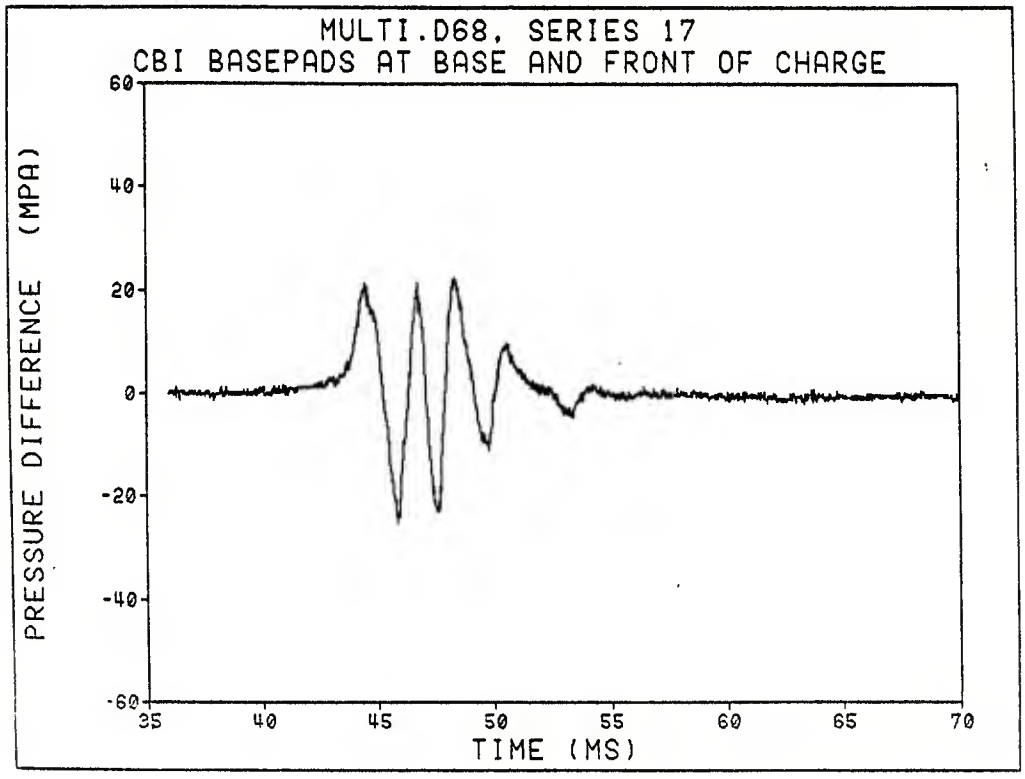
MULTI.D68, SERIES 17
CBI BASEPADS AT BASE AND FRONT OF CHARGE
PRESSURE DIFFERENCE (MPA)
60
40
20
0
-20
-40
-60
35
40
45
50
55
60
65
70
TIME (MS)

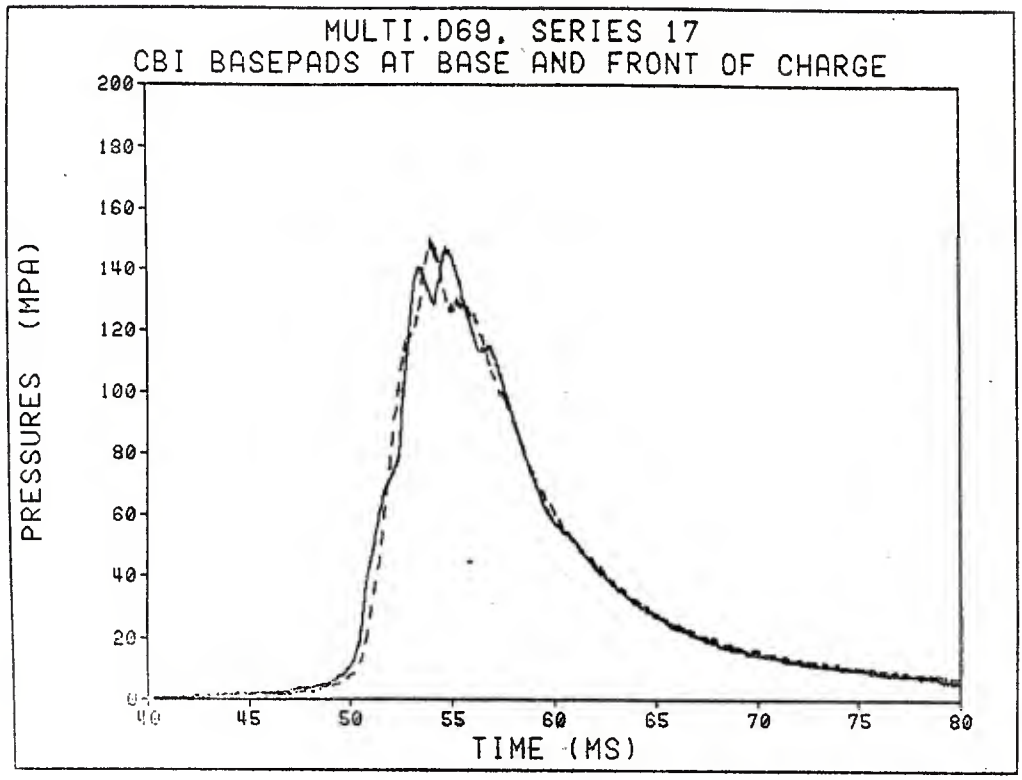
MULTI.D69, SERIES 17
CBI BASEPADS AT BASE AND FRONT OF CHARGE
PRESSURES (MPA)
200
180
160
140
120
100
80
60
40
20
0
40
45
50
55
60
65
70
75
80
TIME (MS)

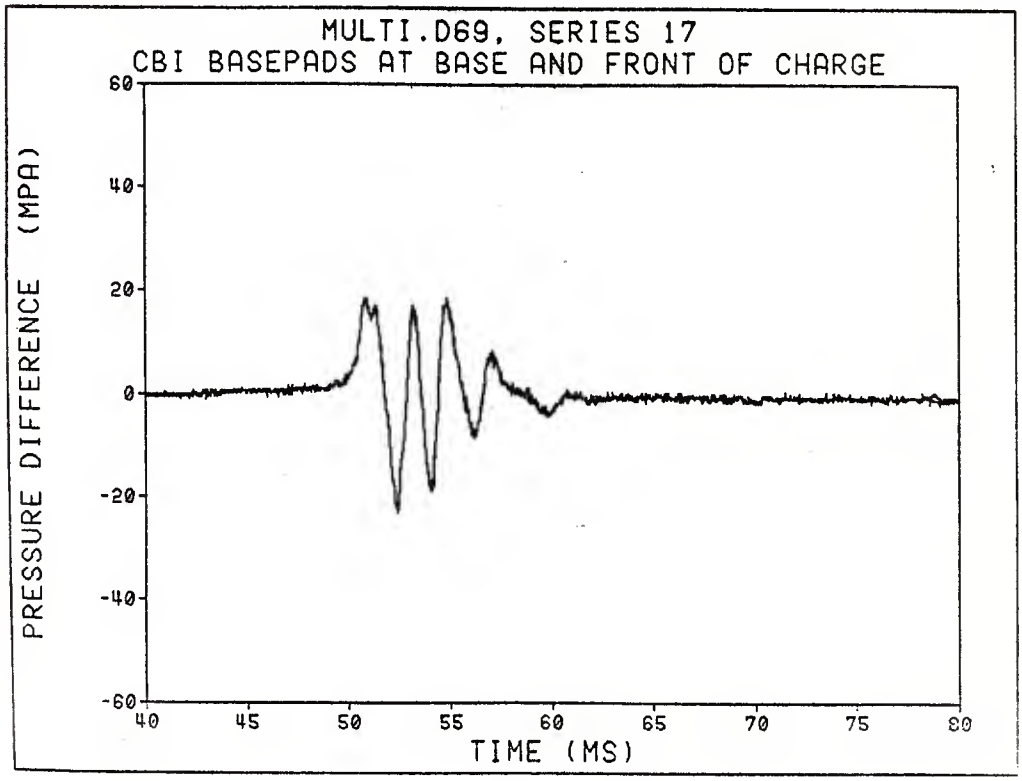
MULTI.D69, SERIES 17
CBI BASEPADS AT BASE AND FRONT OF CHARGE
PRESSURE DIFFERENCE (MPA)
60
40
20
0
-20
-40
-60
40
45
50
55
60
65
70
75
80
TIME (MS)

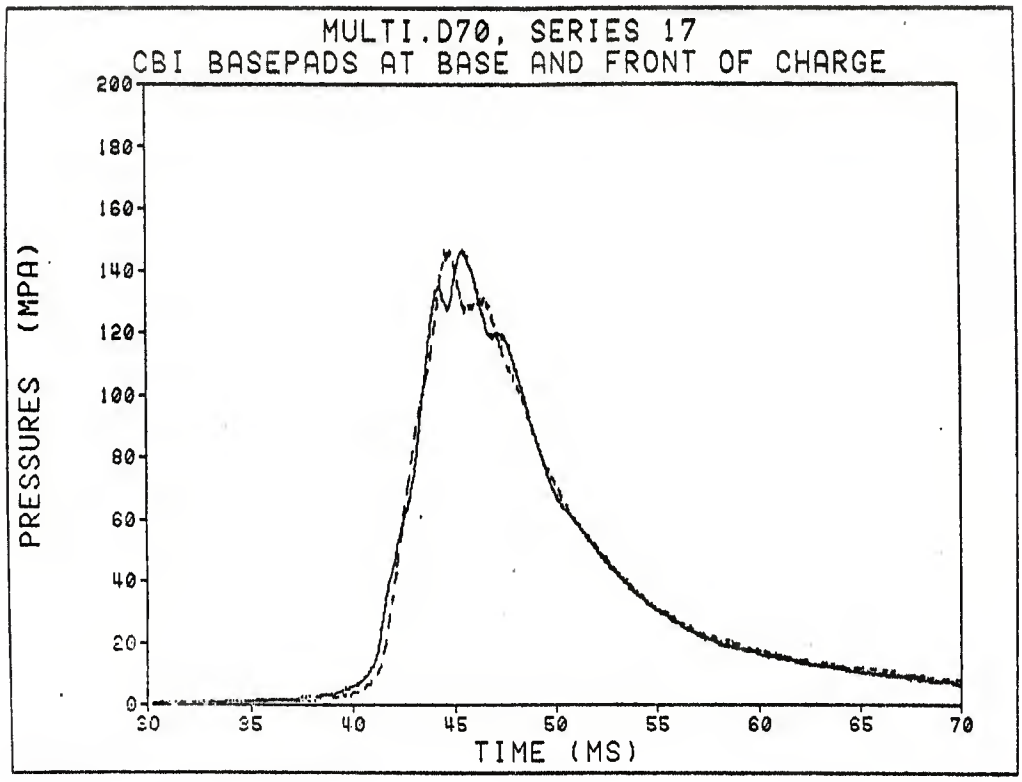
MULTI.D70, SERIES 17
CBI BASEPADS AT BASE AND FRONT OF CHARGE
PRESSURES (MPA)
200
180
160
140
120
100
80
60
40
20
0
30
35
40
45
50
55
60
65
70
TIME (MS)

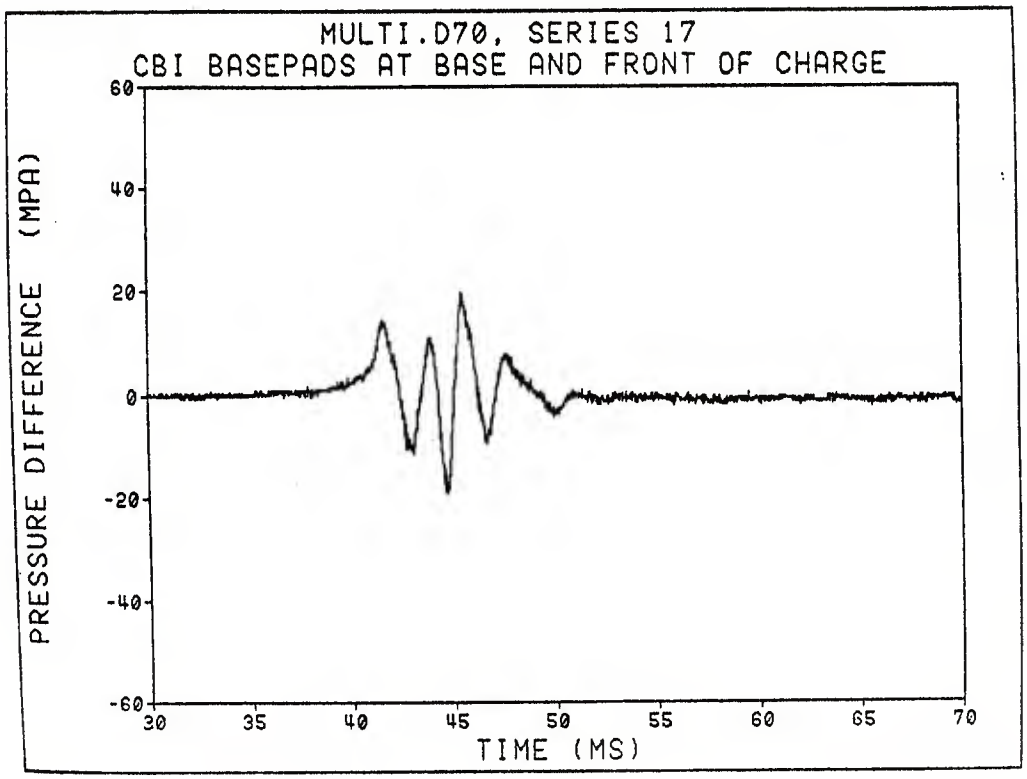
MULTI.D70, SERIES 17
CBI BASEPADS AT BASE AND FRONT OF CHARGE
PRESSURE DIFFERENCE (MPA)
60
40
20
0
-20
-40
-60
30
35
40
45
50
55
60
65
70
TIME (MS)

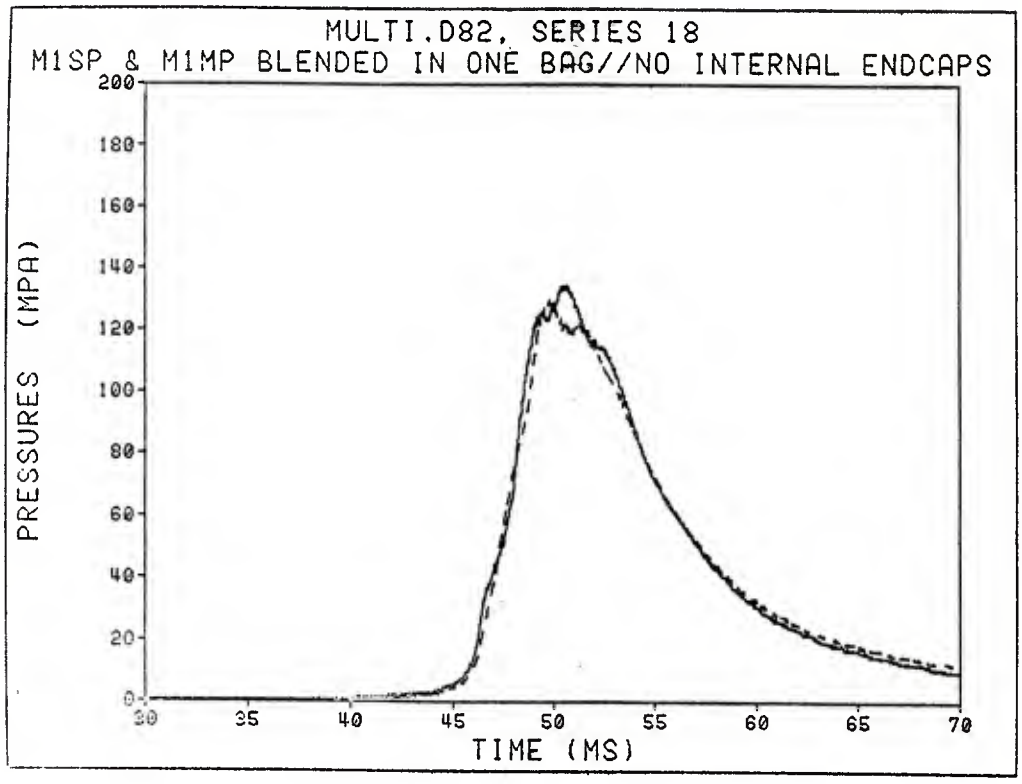
MULTI.D82, SERIES 18
M1SP & M1MP BLENDED IN ONE BAG//NO INTERNAL ENDCAPS
PRESSURES (MPA)
200
180
160
140
120
100
80
60
40
20
0
30
35
40
45
50
55
60
65
70
TIME (MS)

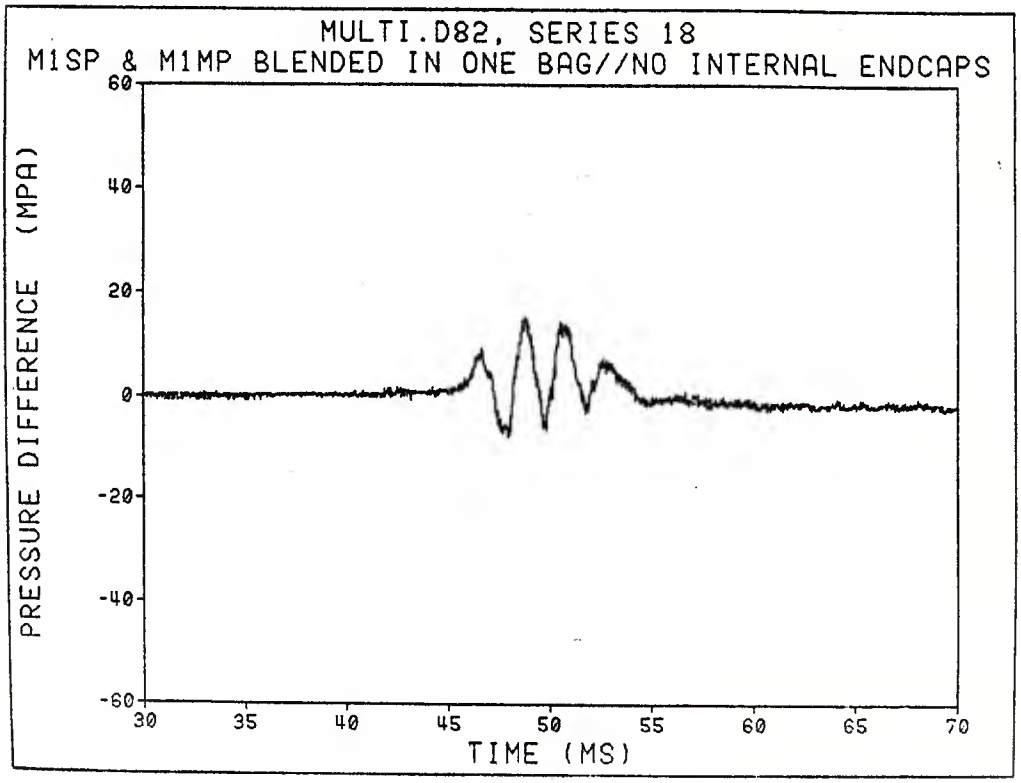
MULTI.D82, SERIES 18
M1SP & M1MP BLENDED IN ONE BAG//NO INTERNAL ENDCAPS
PRESSURE DIFFERENCE (MPA)
60
40
20
0
-20
-40
-60
30
35
40
45
50
55
60
65
70
TIME (MS)

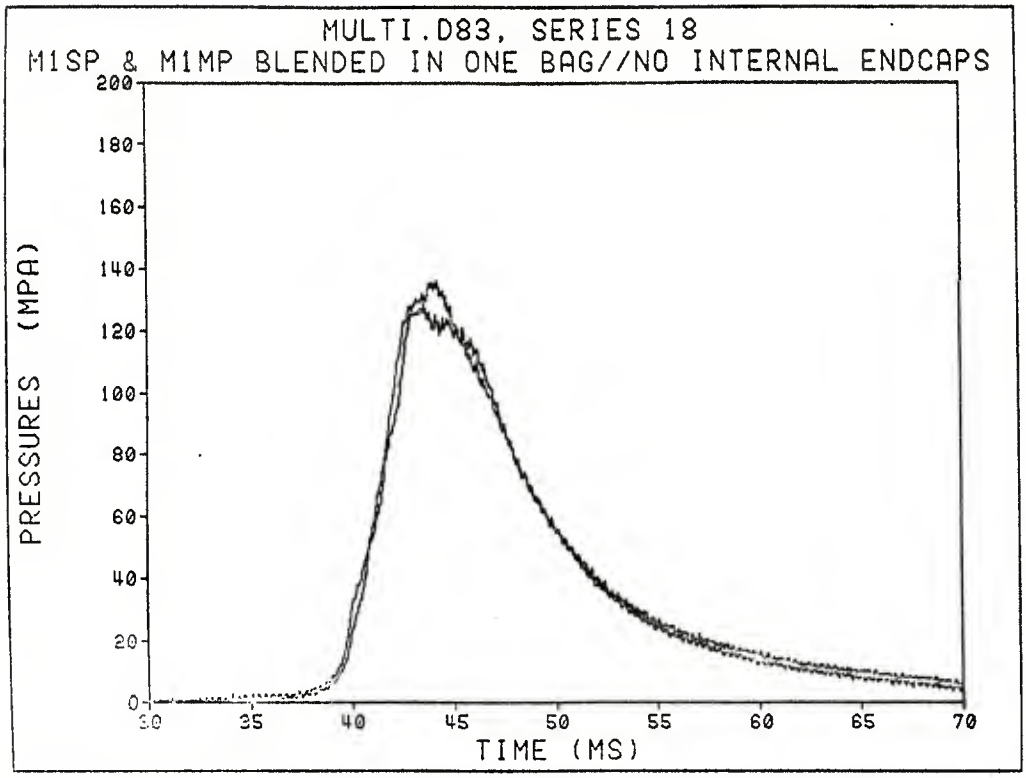
MULTI.D83, SERIES 18
M1SP & M1MP BLENDED IN ONE BAG//NO INTERNAL ENDCAPS
PRESSURES (MPA)
200
180
160
140
120
100
80
60
40
20
0
30
35
40
45
50
55
60
65
70
TIME (MS)

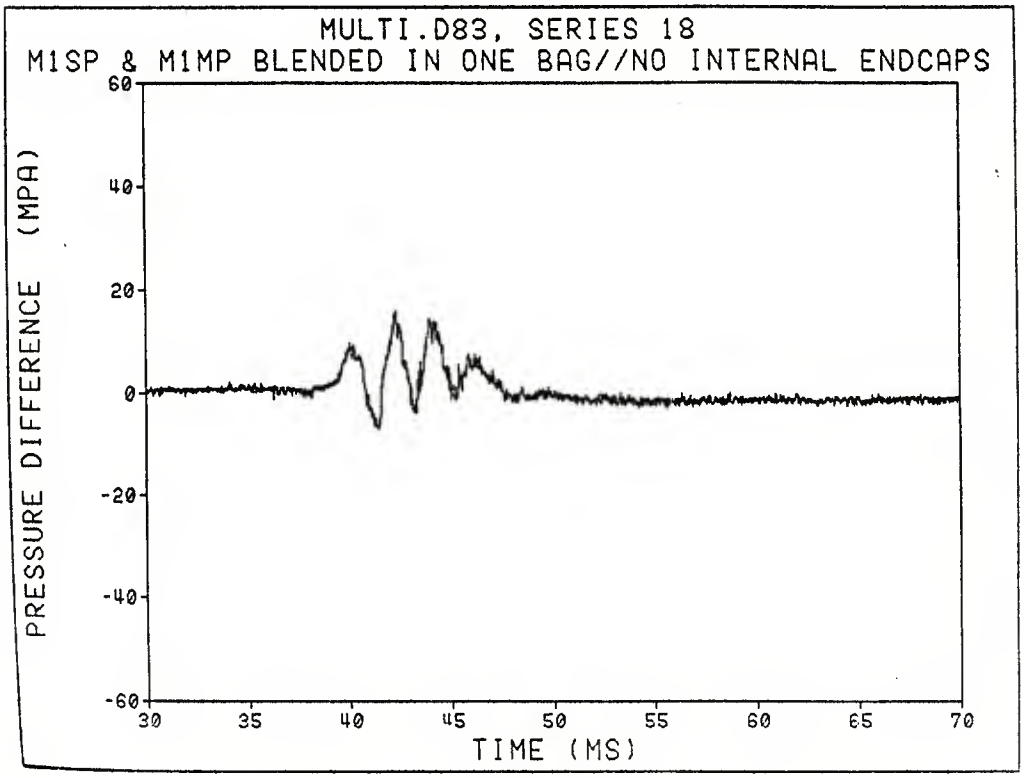
MULTI.D83, SERIES 18
M1SP & M1MP BLENDED IN ONE BAG//NO INTERNAL ENDCAPS
PRESSURE DIFFERENCE (MPA)
60
40
20
0
-20
-40
-60
30
35
40
45
50
55
60
65
70
TIME (MS)

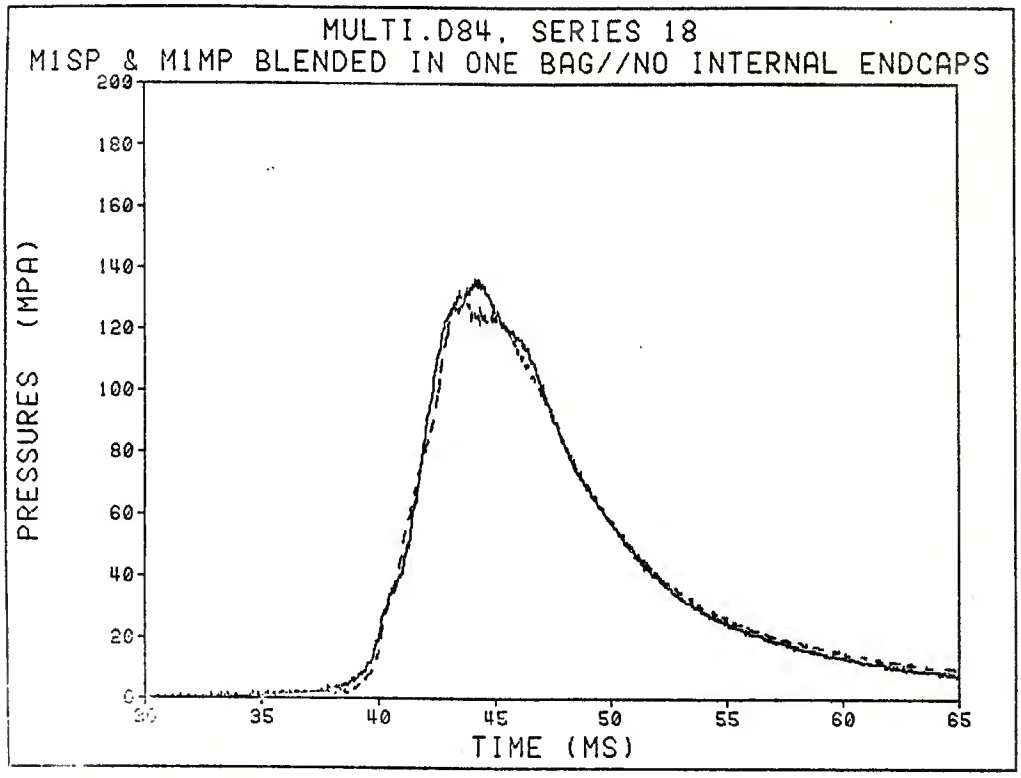
MULTI.D84, SERIES 18
M1SP & M1MP BLENDED IN ONE BAG//NO INTERNAL ENDCAPS
PRESSURES (MPA)
200
180
160
140
120
100
80
60
40
20
0
30
35
40
45
50
55
60
65
TIME (MS)

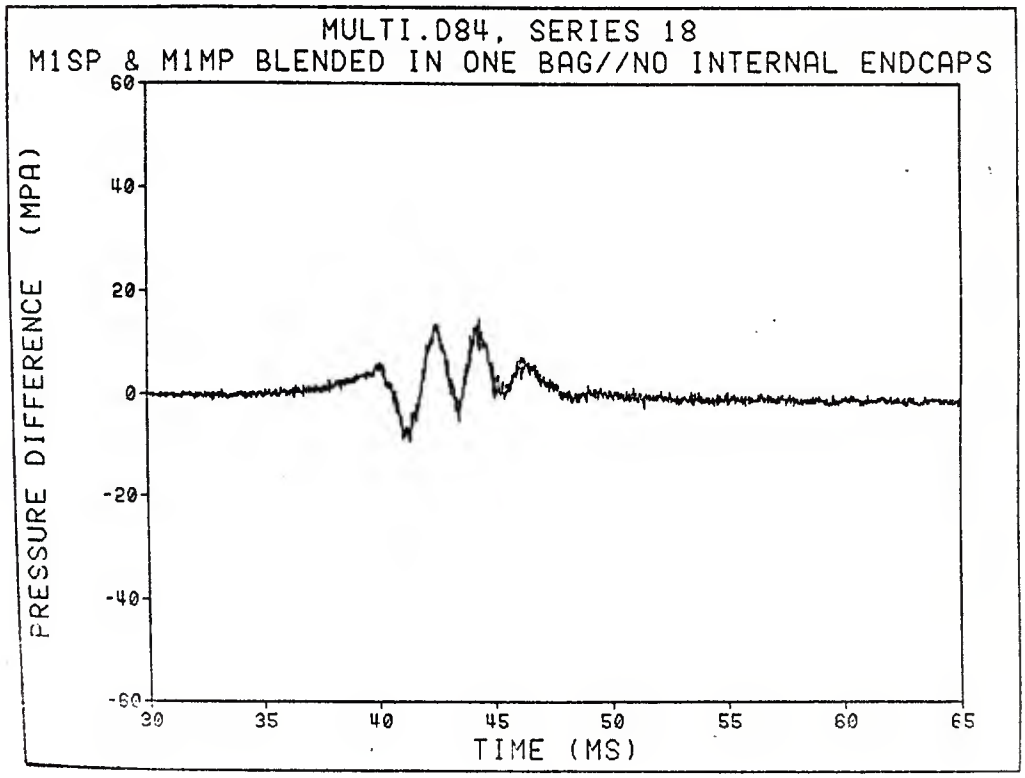
MULTI.D84, SERIES 18
M1SP & M1MP BLENDED IN ONE BAG//NO INTERNAL ENDCAPS
PRESSURE DIFFERENCE (MPA)
60
40
20
0
-20
-40
-60
30
35
40
45
50
55
60
65
TIME (MS)

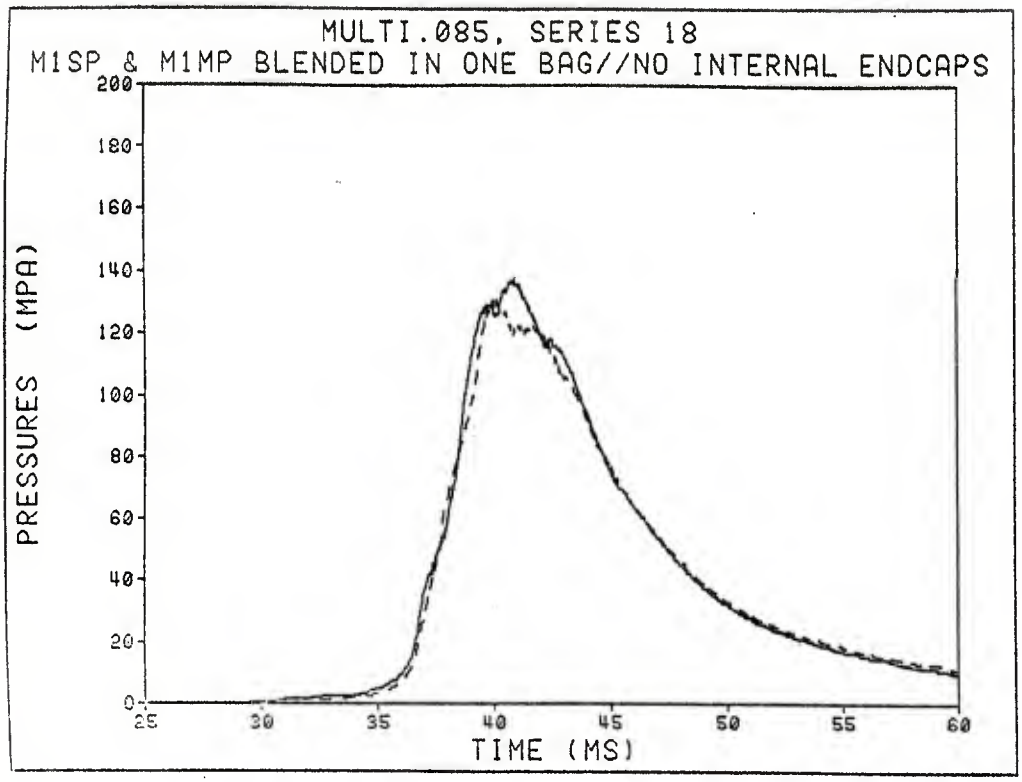
MULTI.085, SERIES 18
M1SP & M1MP BLENDED IN ONE BAG//NO INTERNAL ENDCAPS
PRESSURES (MPA)
200
180
160
140
120
100
80
60
40
20
0
25
30
35
40
45
50
55
60
TIME (MS)

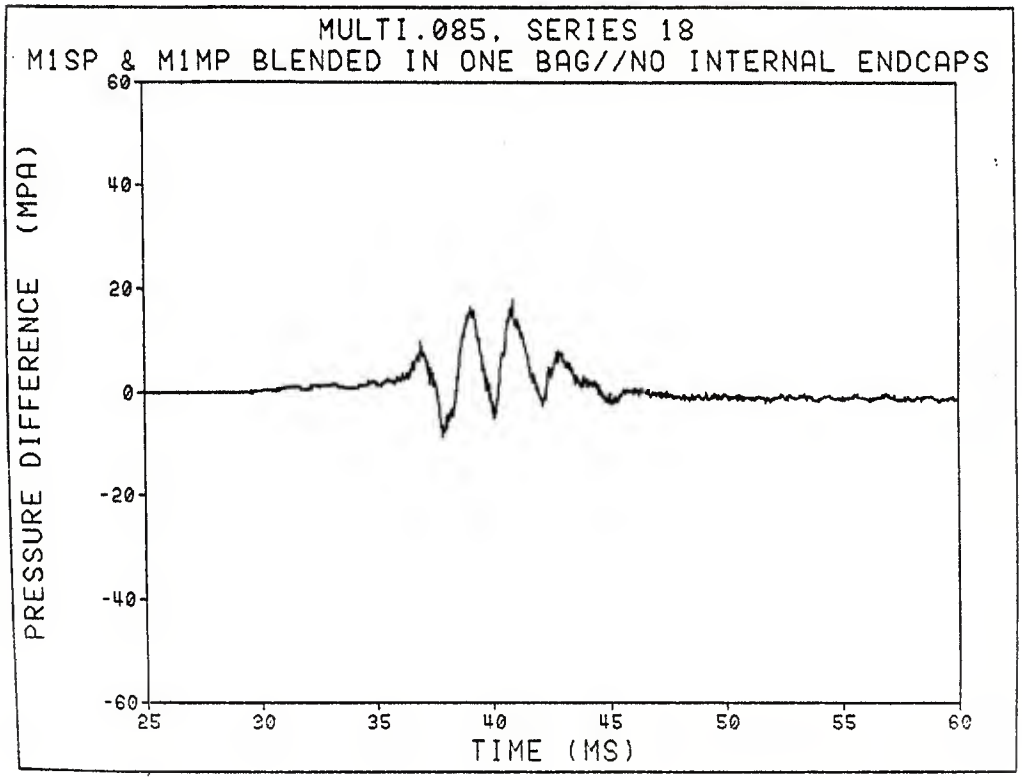
MULTI.085, SERIES 18
M1SP & M1MP BLENDED IN ONE BAG//NO INTERNAL ENDCAPS
PRESSURE DIFFERENCE (MPA)
60
40
20
0
-20
-40
-60
25
30
35
40
45
50
55
60
TIME (MS)

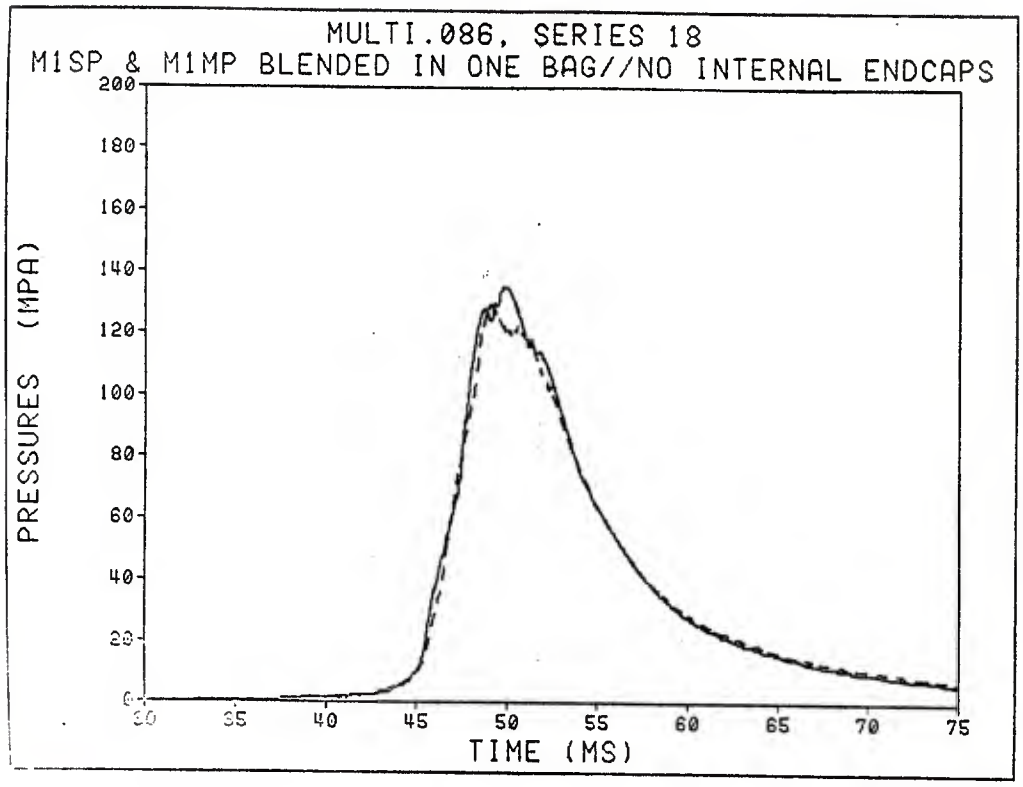
MULTI.086, SERIES 18
M1SP & M1MP BLENDED IN ONE BAG//NO INTERNAL ENDCAPS
PRESSURES (MPA)
200
180
160
140
120
100
80
60
40
20
0
30
35
40
45
50
55
60
65
70
75
TIME (MS)

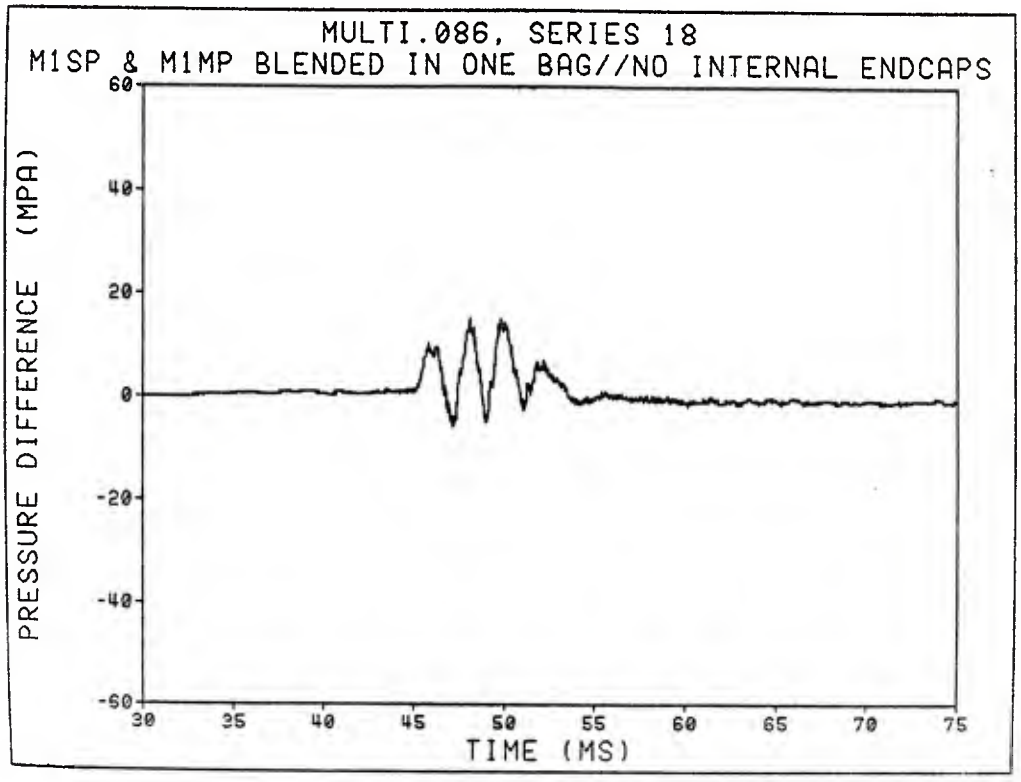
MULTI.086, SERIES 18
M1SP & M1MP BLENDED IN ONE BAG//NO INTERNAL ENDCAPS
PRESSURE DIFFERENCE (MPA)
60
40
20
0
-20
-40
-60
30
35
40
45
50
55
60
65
70
75
TIME (MS)

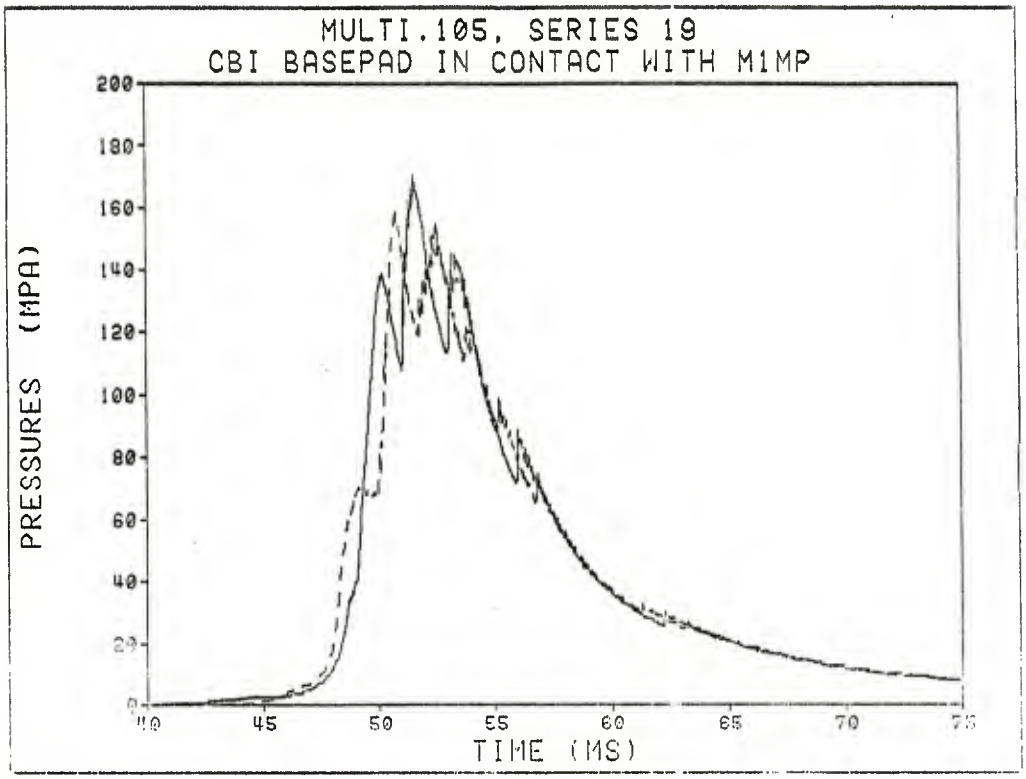
MULTI.105, SERIES 19
CBI BASEPAD IN CONTACT WITH M1MP
PRESSURES (MPA)
200
180
160
140
120
100
80
60
40
20
0
40
45
50
55
60
65
70
75
TIME (MS)

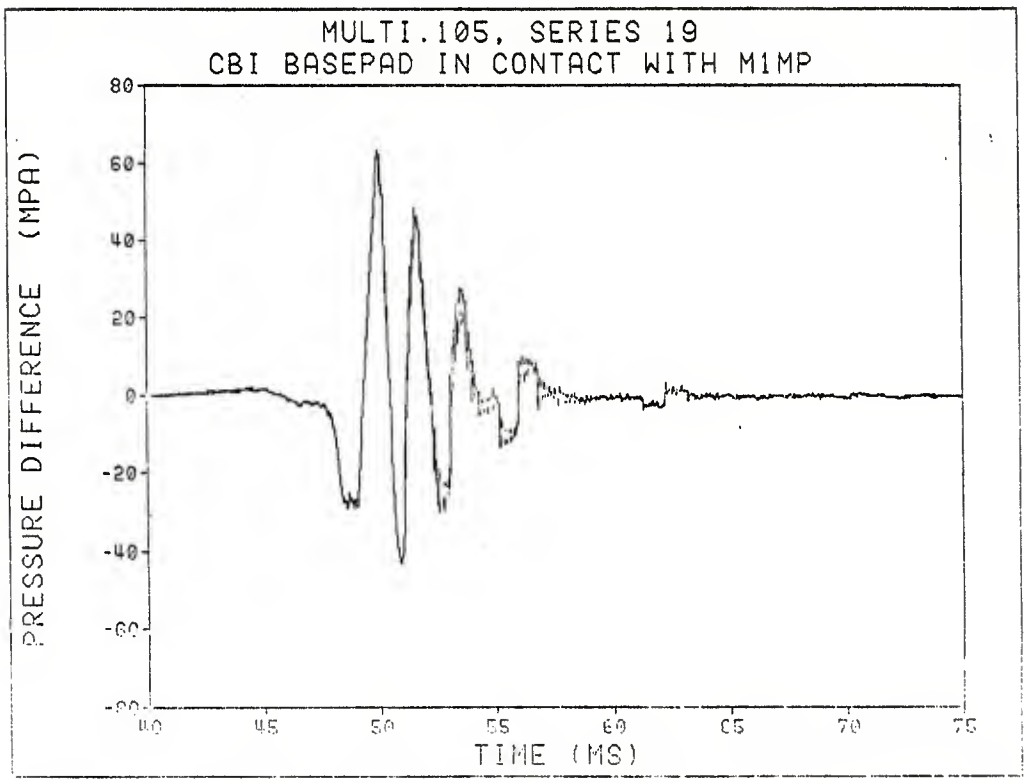
MULTI.105, SERIES 19
CBI BASEPAD IN CONTACT WITH M1MP
PRESSURE DIFFERENCE (MPA)
80
60
40
20
0
-20
-40
-60
-80
40
45
50
55
60
65
70
75
TIME (MS)

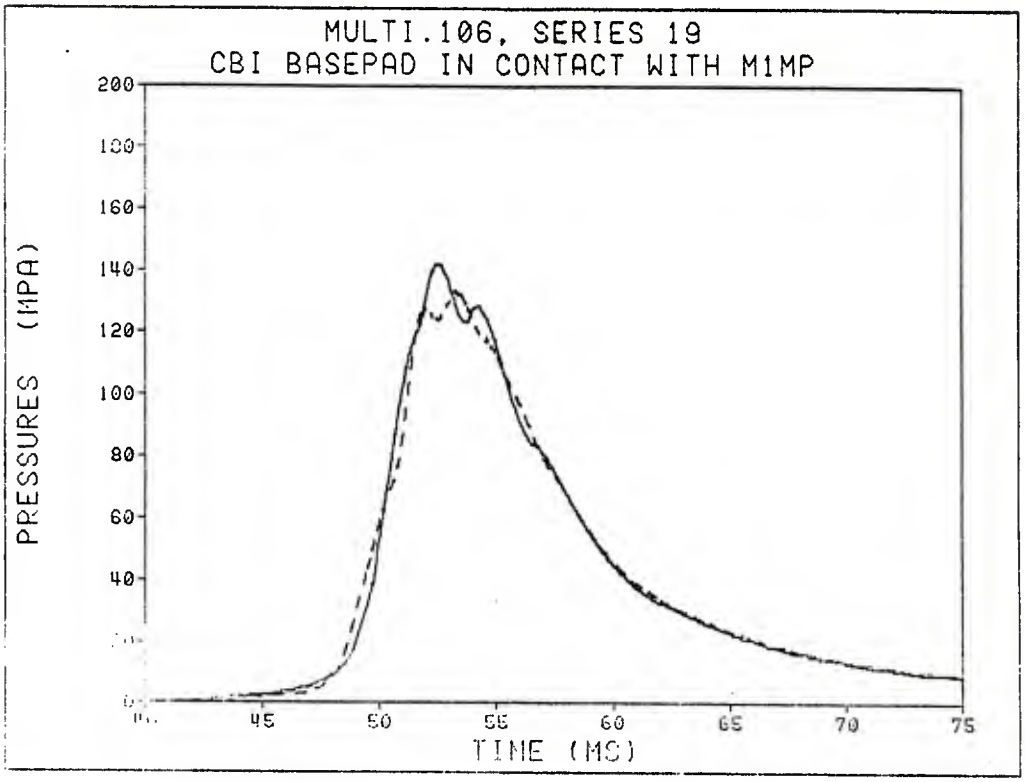
MULTI.106, SERIES 19
CBI BASEPAD IN CONTACT WITH M1MP
PRESSURES (MPA)
200
160
140
120
100
80
60
40
45
50
55
60
65
70
75
TIME (MS)

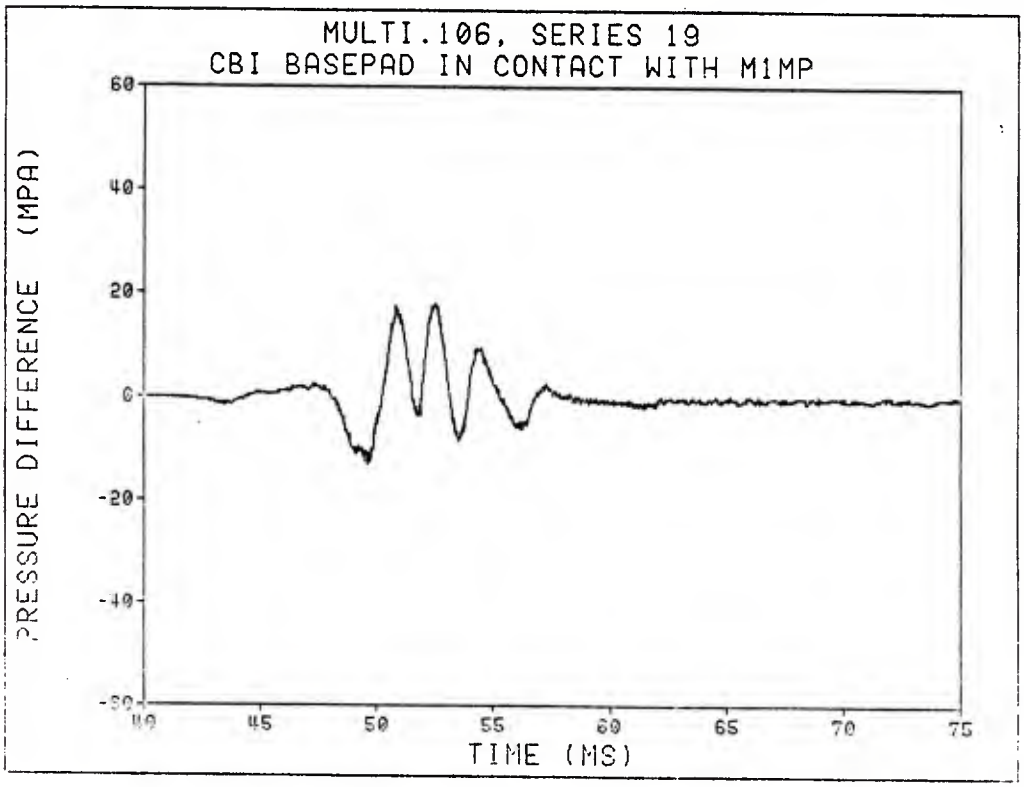
MULTI.106, SERIES 19
CBI BASEPAD IN CONTACT WITH M1MP
PRESSURE DIFFERENCE (MPA)
60
40
20
0
-20
-40
45
50
55
60
65
70
75
TIME (MS)

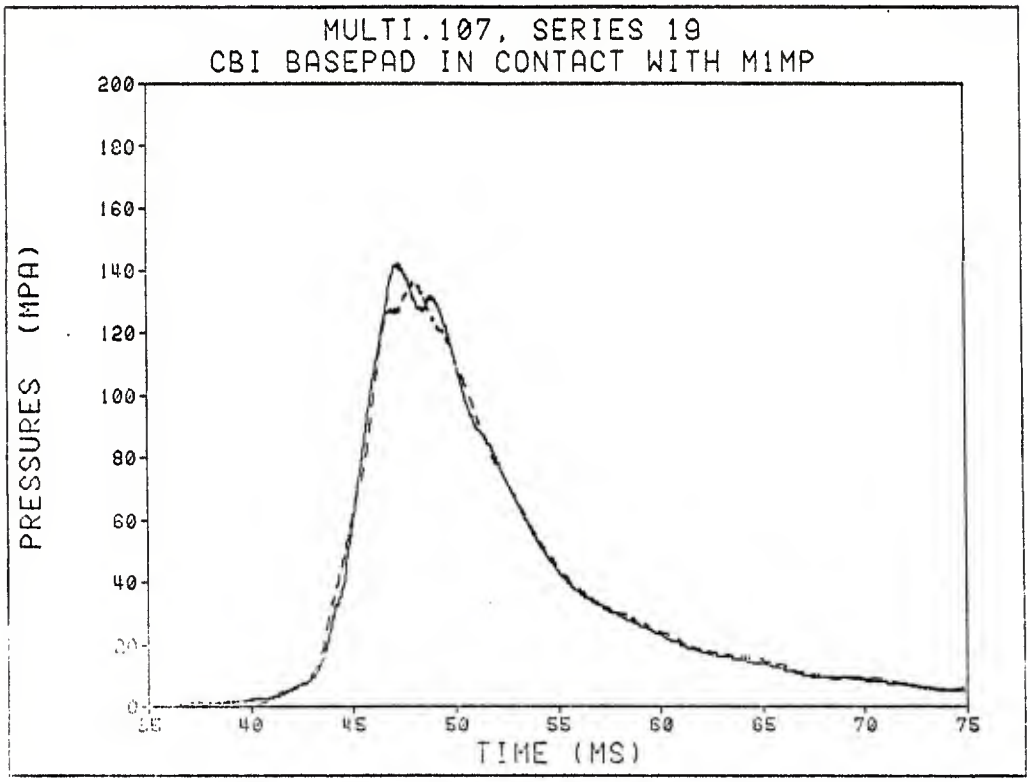
MULTI.107, SERIES 19
CBI BASEPAD IN CONTACT WITH M1MP
PRESSURES (MPA)
200
180
160
140
120
100
80
60
40
20
0
35
40
45
50
55
60
65
70
75
TIME (MS)

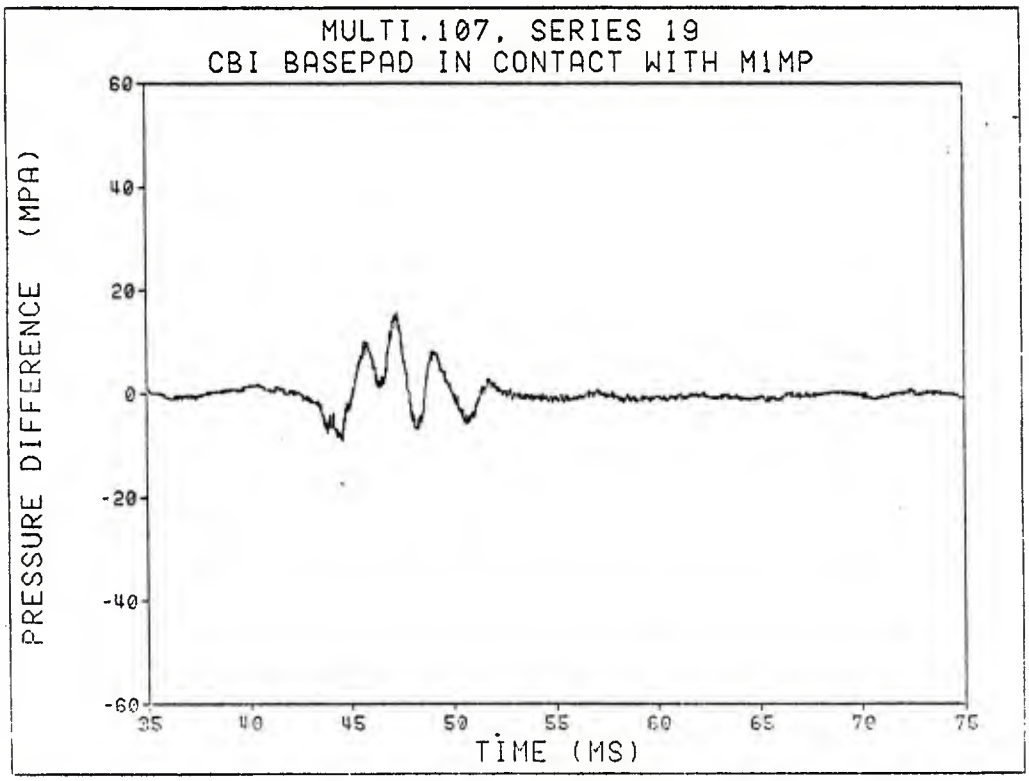
MULTI.107, SERIES 19
CBI BASEPAD IN CONTACT WITH M1MP
PRESSURE DIFFERENCE (MPA)
60
40
20
0
-20
-40
-60
35
40
45
50
55
60
65
70
75
TIME (MS)

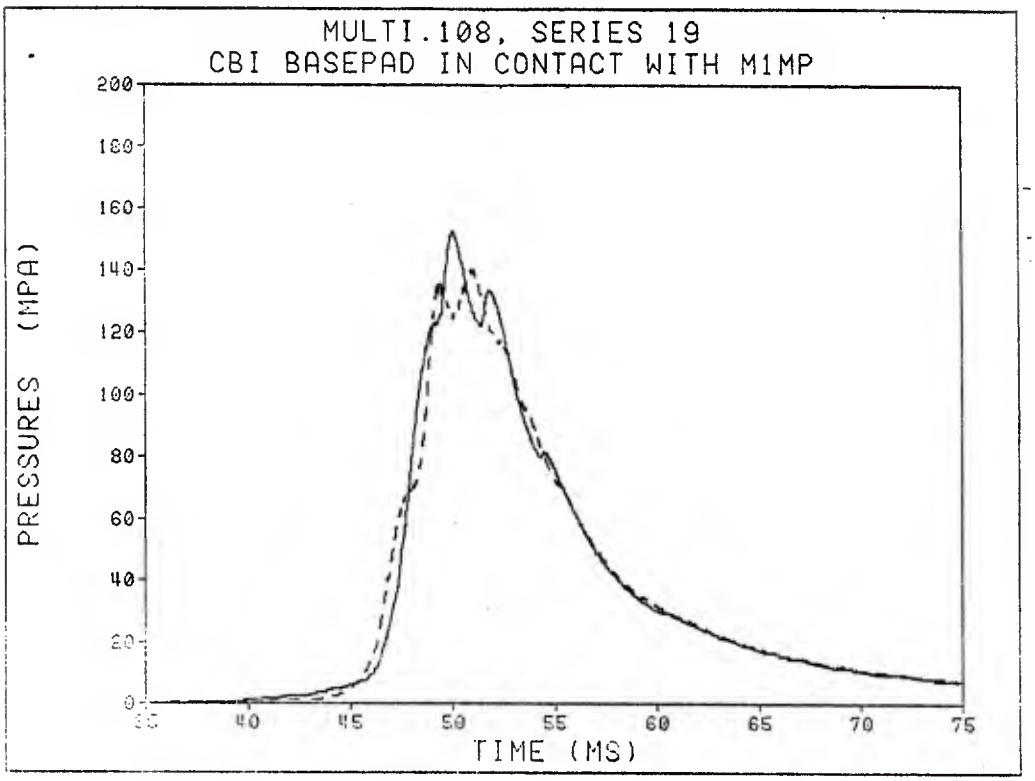
MULTI.108, SERIES 19
CBI BASEPAD IN CONTACT WITH M1MP
PRESSURES (MPA)
200
180
160
140
120
100
80
60
40
20
0
35
40
45
50
55
60
65
70
75
TIME (MS)

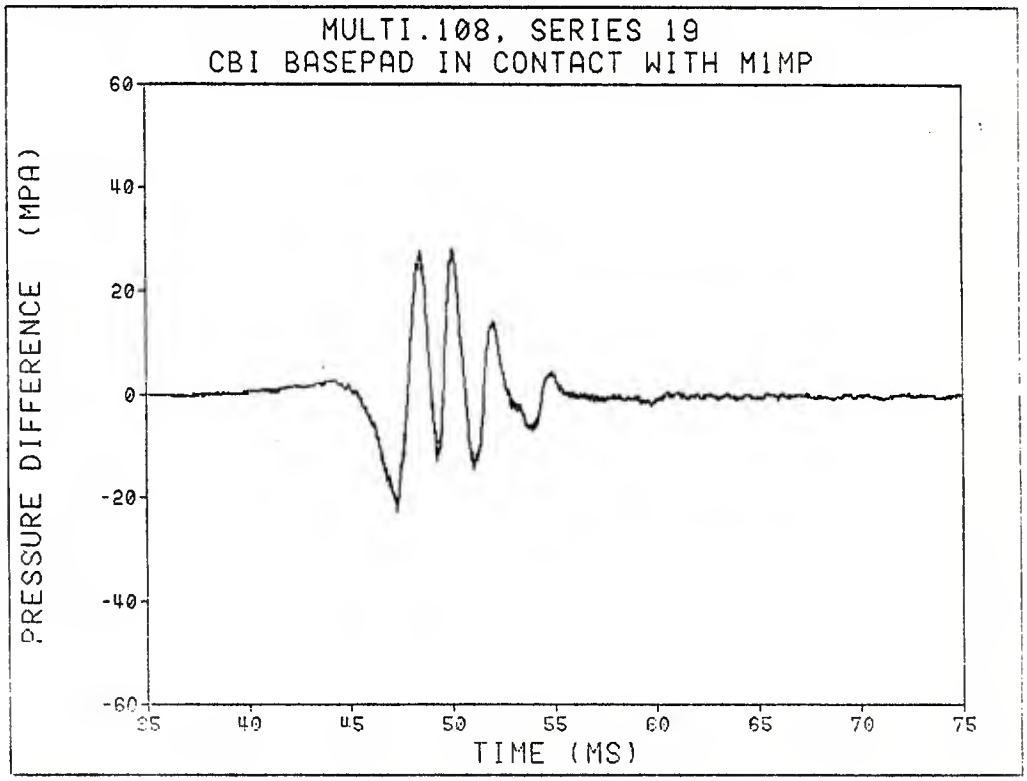
MULTI.108, SERIES 19
CBI BASEPAD IN CONTACT WITH M1MP
PRESSURE DIFFERENCE (MPA)
60
40
20
0
-20
-40
-60
35
40
45
50
55
60
65
70
75
TIME (MS)

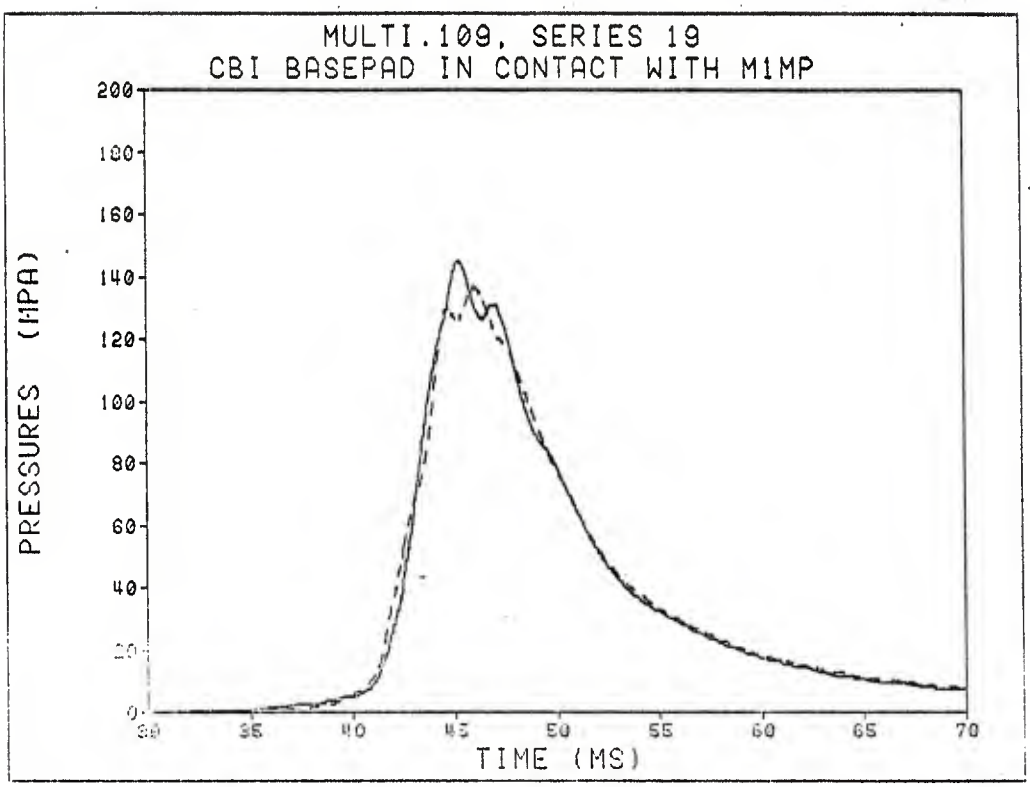
MULTI.109, SERIES 19
CBI BASEPAD IN CONTACT WITH M1MP
PRESSURES (MPA)
200
180
160
140
120
100
80
60
40
20
0
30
35
40
45
50
55
60
65
70
TIME (MS)

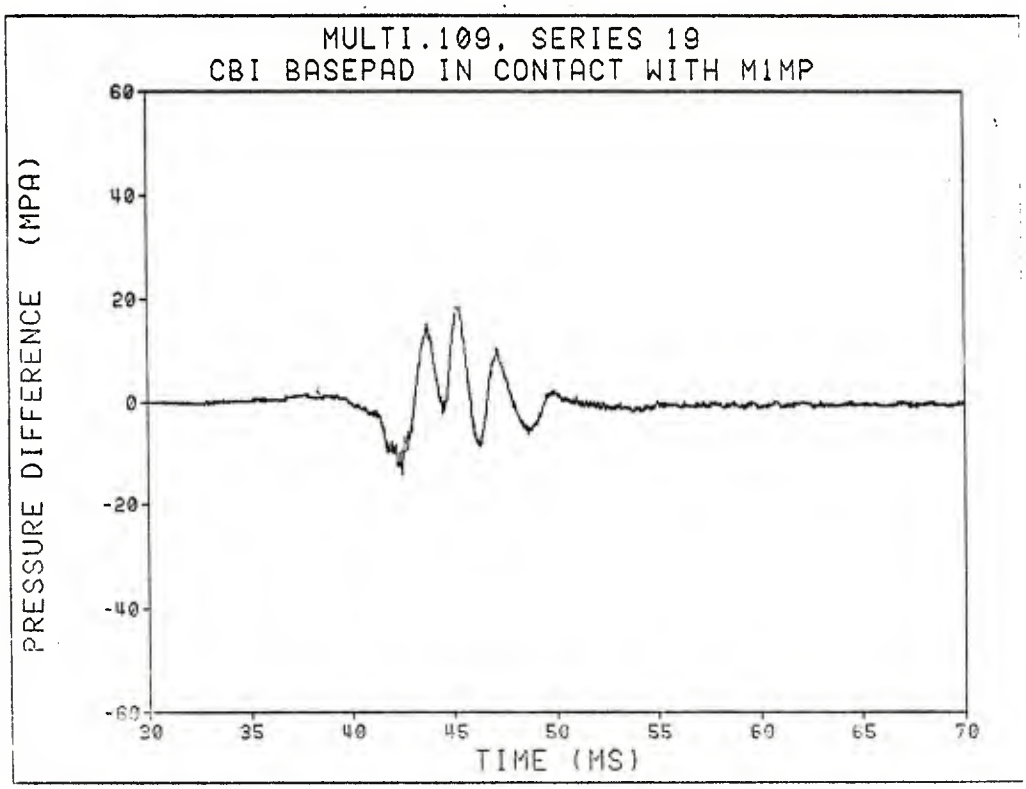
MULTI.109, SERIES 19
CBI BASEPAD IN CONTACT WITH M1MP
PRESSURE DIFFERENCE (MPA)
60
40
20
0
-20
-40
-60
30
35
40
45
50
55
60
65
70
TIME (MS)

APPENDIX B

TABULATION OF FIRING DATA

APPENDIX B
TABULATION OF FIRING DATA

Series	Code	Charge Configuration*	Charge Seating (cm)	Pressures P_1 (MPa)	P_5	$-\Delta P_i$ $(P_1 - P_5)$ (MPa)	Velocity (m/s)	Ignition Delay (ms)
	Multi							
1	001	Standard XM211 bags	2.5	151.8	156.9	51.1	449.1	37
	002			148.5	153.3	41.2	451.2	42
	003			147.6	152.5	45.2	449.1	37
	004			147.2	153.1	47.7	449.7	38
	005			151.4	157.9	57.1	450.0	58
			Avg.	149.3	154.7	48.5	449.8	42
			(Std. Dev.)	(2.2)	(2.5)	(6.0)	(0.9)	(9.0)
	Multi							
2	006**	BRL-fabricated bags	2.5	(148.7)**	154.3	(40.0)**	455.8	34
	007**			(153.7)**	154.3	(44.4)**	454.6	37
	008			148.1	151.9	40.5	454.0	32
	009			146.7	151.2	40.6	453.4	40
	010			145.8	148.5	28.1	454.0	35
			Avg.	146.9	152.0	36.4	454.4	36
			(Std. Dev.)	(1.2)	(2.4)	(7.2)	(0.9)	(3.0)
	Multi							
3	011	BRL bags	2.5	121.7	123.1	3.7	442.4	69
	D12			120.0	121.0	2.0	441.5	101
	013	Only series with		127.6	128.9	6.9	443.9	65
	014	propellant conditioned		128.0	128.3	11.3	443.6	70
	D15	to 21°C		121.4	121.8	2.2	-	111
			Avg.	123.7	124.6	5.2	442.6	83
			(Std. Dev.)	(3.8)	(3.7)	(3.9)	(1.1)	(21.2)
	Multi							
4	D61	No interzone liners	2.5	146.9	148.4	30.9	450.0	59
	-	between Zones 4 & 5		-	-	-	-	-
	D63			149.5	153.5	34.0	449.4	54
	D64			150.0	151.3	38.8	451.8	47
	D65			147.4	149.3	38.9	450.0	47
			Avg.	148.4	150.6	35.6	450.3	52
			(Std. Dev.)	(1.5)	(2.3)	(3.9)	(1.0)	(5.9)

* Charge and projectile weights were 3.95 and 46.8 kg, respectively. Seating distance was 911 mm unless noted otherwise. Propellant temperature was 63°C except for Series 3 (21°C).

** P1 and/or P5 data lost. Data shown in parentheses derived from P2 and/or P6, but were not used to determine the average and standard deviation.

APPENDIX B
TABULATION OF FIRING DATA

Series	Code Multi	Charge Configuration*	Charge Seating (cm)	Pressures P_1 (MPa)	Pressures P_5 (MPa)	$-\Delta P_i$ $(P_1 - P_5)$ (MPa)	Velocity (m/s)	Ignition Delay (ms)
5	076	No interzone liners	2.5	148.9	151.4	37.1	445.7	45
	077	between Zones 4 and 5,		153.9	154.7	40.0	448.8	37
	078	Zones 4 and 5 propellant		167.1	166.3	60.0	448.8	41
	079	loaded on top of Zone 3		152.3	152.6	40.0	447.3	42
	080	propellant		158.8	161.3	52.8	447.3	40
			Avg.	156.2	157.3	46.0	447.6	41
			(Std. Dev.)	(7.1)	(6.3)	(9.9)	(1.3)	(2.9)
	Multi							
6	D46	Flash reducer	2.5	138.9	142.8	28.1	450.0	52
	D47	bag placed between		146.9	154.0	45.1	453.0	40
	D48	Zones 3 and 4		145.8	150.1	40.9	452.4	43
	D49			145.4	151.7	40.3	452.4	43
	D50			148.2	156.1	51.9	452.1	42
			Avg.	145.0	150.9	41.3	452.0	44
			(Std. Dev.)	(3.6)	(5.1)	(8.7)	(1.2)	(4.6)
7	D41	Flash reducer bag	2.5	144.3	147.8	35.9	448.8	47
	D42	placed between Zones		144.3	148.2	37.6	450.6	44
	D43	4 and 5		141.3	145.3	34.0	450.0	45
	D44**			(120.0)**	(129.8)**	(33.3)**	450.9	46
	D45			139.6	145.5	30.4	450.9	42
			Avg.	142.4	146.7	34.5	450.2	45
			(Std. Dev.)	(2.3)	(1.5)	(3.1)	(0.9)	(1.9)
8	D31	Cardboard spacer	2.5	149.2	156.5	49.1	450.6	37
	D32	between charge and		150.1	154.3	50.0	450.6	47
	D33	projectile		150.0	153.5	51.5	449.7	45
	D34			150.1	155.0	51.2	448.8	46
	D35			152.8	157.9	56.2	450.3	44
			Avg.	150.4	155.4	51.6	450.0	44
			(Std. Dev.)	(1.4)	(1.8)	(2.7)	(0.8)	(4.0)

* Charge and projectile weights were 3.95 and 46.8 kg, respectively. Seating distance was 911 mm unless noted otherwise. Propellant temperature was 63°C except for Series 3 (21°C).

** P1 and/or P5 data lost. Data shown in parentheses derived from P2 and/or P6, but were not used to determine the average and standard deviation.

APPENDIX B
TABULATION OF FIRING DATA

Series	Code	Charge Configuration*	Charge Seating (cm)	Pressures P_1 (MPa)	Pressures P_5 (MPa)	$-\Delta P_i$ $(P_1 - P_5)$ (MPa)	Velocity (m/s)	Ignition Delay (ms)
	Multi							
9	D36	Nylon tape wrapped	2.5	147.6	148.7	38.0	451.2	48
	D37	axially and circum-		149.2	153.9	46.8	451.8	43
	D38	ferentially around		148.5	151.0	46.7	450.6	39
	D39	charge		141.7	145.7	37.9	448.5	46
	D40			148.3	155.5	44.0	451.5	54
			Avg.	147.1	151.0	42.7	450.7	46
			(Std. Dev.)	(3.1)	(3.9)	(4.5)	(1.3)	(5.6)
	Multi							
10	D51	Charge increments	2.5	132.7	132.1	3.8	450.3	52
	D52	separated. Zone 5		132.4	130.6	4.1	448.5	51
	D53	increment at base		130.1	128.1	7.4	446.9	40
	D54	of projectile		131.1	131.2	8.0	446.9	42
	D55			130.1	129.9	10.2	448.2	51
			Avg.	131.3	130.4	6.7	448.2	47
			(Std. Dev.)	(1.2)	(1.5)	(2.7)	(1.4)	(5.7)
	Multi							
11	D56	Charge increments	2.5	125.4	125.5	2.7	447.6	52
	D57	separated. Zones		129.3	128.9	1.0	448.5	42
	D58	4 and 5 increments		132.1	129.5	3.0	449.7	41
	D59	at base of projectile		126.5	126.1	3.5	447.9	18
	D60			126.7	126.2	2.7	447.9	55
			Avg.	128.0	127.2	2.6	448.3	42
			(Std. Dev.)	(2.7)	(1.8)	(0.9)	(0.8)	(14.5)
	Multi							
12	D26	Charge at maximum	40.0	129.7	128.0	10.0	449.1	108
	D27	standoff		127.9	127.2	11.4	447.6	118
	D28			128.2	126.9	9.9	446.6	106
	D29			127.0	128.4	11.0	446.6	139
	D30			129.1	128.4	11.2	446.9	112
			Avg.	128.4	127.8	10.7	447.4	117
			(Std. Dev.)	(1.1)	(0.7)	(0.7)	(1.1)	(13.3)

* Charge and projectile weights were 3.95 and 46.8 kg, respectively. Seating distance was 911 mm unless noted otherwise. Propellant temperature was 63°C except for Series 3 which was 21°C.

APPENDIX B
TABULATION OF FIRING DATA

Series	Code	Charge Configuration*	Charge Seating (cm)	Pressures P_1 (MPa)	Pressures P_5 (MPa)	$-\Delta P_i$ $(P_1 - P_5)$ (MPa)	Velocity (m/s)	Ignition Delay (ms)
	Multi							
13	110	Zone 3 increment	2.5	152.5	154.7	37.0	448.5	43
	111	has larger web MISP		158.3	162.9	53.2	449.4	43
	112	than the Baseline		152.5	154.7	43.1	447.6	50
	113	series		152.7	156.4	46.0	447.3	39
	114			155.4	157.8	45.1	449.1	33
			Avg.	154.3	157.3	44.9	448.4	42
			(Std. Dev.)	(2.6)	(3.4)	(5.8)	(0.9)	(6.2)
	Multi							
14	D71	Basepad composition	2.5	149.9	152.4	51.9	453.7	20
	D72	is Class 5, Black		142.6	146.5	45.6	446.0	14
	D73	Powder		164.2	164.1	61.3	447.9	18
	D74			162.4	163.6	59.1	446.6	10
	D75			146.9	146.4	38.6	446.9	12
			Avg.	153.2	154.6	51.3	448.2	15
			(Std. Dev.)	(9.6)	(8.8)	(9.4)	(3.1)	(4.1)
	Multi							
15	092	Nitrocellulose slit	2.5	157.0	157.0	46.0	455.8	44
	093	tubes around the		157.0	157.0	42.1	457.0	49
	094	Zone 3 increment		167.4	167.1	55.1	457.9	42
	095			162.1	163.3	45.6	457.0	38
	096			157.4	159.1	45.7	456.4	41
			Avg.	160.2	160.7	46.9	456.8	43
			(Std. Dev.)	(4.6)	(4.4)	(4.9)	(0.8)	(4.1)
	Multi							
16	102	Nitrocellulose slit	2.5	218.5	215.2	102.6	489.9	33
	103	tube around the Zones		210.5	209.7	97.6	492.4	39
	104	3, 4 and 5 increments.		232.8	222.7	127.9	--	38
		Only three rounds fired.	Avg.	220.6	215.9	109.4	491.2	37
			(Std. Dev.)	(11.3)	(6.5)	(16.2)	(--)	(3.2)

* Charge and projectile weights were 3.95 and 46.8 kg, respectively. Seating distance was 911 mm unless noted otherwise. Propellant temperature was 63°C except for Series 3 which was 21°C.

APPENDIX B
TABULATION OF FIRING DATA

Series	Code	Charge Configuration*	Charge Seating (cm)	Pressures P_1 (mPa)	Pressures P_5 (mPa)	$-\Delta P_i (P_1 - P_5)$ (MPa)	Velocity (m/s)	Ignition Delay (ms)
	Multi							
17	D66	Two CBI basepads.	2.5	148.9	149.9	18.9	457.0	40
	D67	One each at base and		142.9	143.1	19.4	457.3	46
	D68	front of charge.		146.4	148.3	24.4	456.1	44
	D69			145.9	149.2	22.5	457.0	49
	D70			145.7	147.5	9.7	457.6	40
			Avg.	146.0	147.6	19.0	457.0	44
			(Std. Dev.)	(2.1)	(2.7)	(5.7)	(0.6)	(3.9)
	Multi							
18	D82	No interzone liners	2.5	135.1	129.6	7.6	449.1	40
	D83	between Zones 3, 4		135.7	130.5	7.4	449.7	39
	D84	and 5 increments.		137.6	133.4	8.8	450.9	39
	085	Propellant blended		137.2	130.6	8.8	448.8	36
	086	before loading.		135.1	129.4	6.4	449.4	36
			Avg.	136.1	130.7	7.8	449.6	38
			(Std. Dev.)	(1.2)	(1.6)	(1.0)	(0.8)	(1.9)
	Multi							
19	105	Increment order	2.5	170.5	158.5	25.3	450.6	45
	106	changed from		141.9	133.6	13.0	448.8	47
	107	CBI/Z3/Z4/Z5 to		142.2	136.2	9.0	449.1	42
	108	CBI/Z4/Z5/Z3		152.2	139.6	22.8	449.4	45
	109			149.9	137.3	14.1	453.9	41
			Avg.	151.3	141.0	16.8	450.4	44
			(Std. Dev.)	(11.6)	(10.0)	(6.9)	(2.1)	(2.4)

* Charge and projectile weights were 3.95 and 46.8 kg, respectively. Seating distance was 911 mm unless noted otherwise. Propellant temperature was 63°C except for Series 3 which was 21°C.

APPENDIX C

PROPELLANT DESCRIPTION SHEETS

AMC PROPELLANT DESCRIPTION SHEET

U.S. Army Lot No. RAD- 68108 (ACTUAL LOT) of 19 71 Composition No. M1, SP, FOR 105MM HOW., FOR CHG. PROPELLING, M 7, ITEM V3-24640

Manufactured at RADFORD ARMY AMMUNITION PLANT, RADFORD, VA. Packed Amount 260,519 LBS.

Contract No. W-11-173 AMC-37(A) Date 4-28-49 Specification No MIL-P-60318A (MU) W/EOPA's 50631-2, 50763-2, 55492-2 and APSA Technical Instructions dated 14 April 1970

NITROCELLULOSE

ACCEPTED BLEND NUMBERS: B-10,604Y; 609Y; 611Y; 617Y; 620Y; 626Y; 632Y; 635Y; 637Y; 638Y; 639Y; 644Y

TESTS

	Nitrogen Content	KI Starch (65.5°C)	Stability (134.5°C)
Maximum	13.19 %	45+ Mins.	30 + Mins.
Minimum	13.13 %	Mins.	30 Mins.
Average	13.15 %	Mins.	30 + Mins.
			Explosion Hrs.

MANUFACTURE OF PROPELLANT

0.62 Pounds Solvent per Pound NC/Dry Weight Ingredients Consisting of 35 Pounds Alcohol and 65 Pounds ETHER per 100 Pounds Solvent.

Percentage Basis to Whole 10

TEMPERATURES °C From	To	PROCESS-SOLVENT RECOVERY AND DRYING	TIME Days	Hours
	40	LOAD SOLVENT RECOVERY TANK		
40	55	INCREASE SOLVENT RECOVERY TEMPERATURE		4
	55	HOLD SOLVENT RECOVERY TEMPERATURE		22
	60	WATER DRY CYCLE		30
	56	AIR DRY CYCLE		5

TESTS OF FINISHED PROPELLANT

PROPELLANT COMPOSITION * Constituent	Percent Formula	Percent Tolerance	Percent Measured	STABILITY AND PHYSICAL TESTS	Formula	Actual
NITROCELLULOSE	85.00	±2.00	84.68	Heat Test S.P., 134.5°C	NO CC 40'	50'
DINITROTOLUENE	10.00	±2.00	10.18	NO EXPLOSION	5 HRS. MIN.	5 hrs.
DIBUTYLPHTHALATE	5.00	±1.00	5.14	Form of Propellant		GRAIN TYPE II
TOTAL	100.00		100.00			
DIPHENYLAMINE (ADDED)	1.00	±0.10	1.02			
TOTAL VOLATILES			0.86			
MOISTURE	0.60	±0.20	0.60			
RESIDUAL SOLVENTS	0.78	MAX.	0.26			

CLOSED BOMB

	Lot No. Ser	Temp. °F	Relative Quickness	Relative Force
Test	RAD- 68108	+90	100.64	101.58
Standard	IA-61080	+90	100.0%	100.0%

PREDICTED BALLISTIC RESULTS	ZONE 1	ZONE 2
CHARGE WEIGHT, oz.	8.51	9.93
PRESSURE, psi.	---	8484

Remarks: FIRED IN ACCORDANCE WITH MIL-STD-286B, METHOD 801.1, IN A NOMINAL SIZE 200 CC CLOSED BOMB. CLOSED BOMB TESTS WERE CONDUCTED FOR CHARGE ASSESSMENT AT ZONES 1 AND 2 IN LIEU OF BALLISTIC TESTING. EOPA-55492-2 WAS ISSUED IN RESPONSE TO VECP-5.

PROPELLANT DIMENSIONS (inches)

	Specification	Nominal	Finished	Mean Variation in % of Mean Dimensions Spec.	Actual
Length(L) "cut"		0.205	0.1990	6.25 MAX.	1.84
Diameter(D) Die		0.065	0.0467	6.25 MAX.	2.57
Perf. Dia.(d) Die		0.031	0.0198		
Avg. Web(Wa)			0.0135		
Web Progressivity Std. Dev. in % of Web Average	20 MAX.		9.3		
L:D	3.0 to 6.0		4.26		
D:d	3 NOM.		2.4		

DATES: Packed 1/8/71; Sampled 1/8/71; Test Finished 1-18-71; Offered 2-4-71; Description Sheets Forwarded 2-8-71

Type of Packing Container M24 Containers per letter SMUPO-OA, dated 8 January 1971

Remarks *COMPUTED ON TV AND DIPHENYLAMINE FREE BASIS.

THIS LOT DOES/~~DOES NOT~~ MEET ALL THE CHEMICAL AND PHYSICAL REQUIREMENTS OF THE APPLICABLE SPECIFICATION.

Contractor's Representative P. W. Steele 2-5-71

Government Quality Assurance Representative James E. Bland

PROPELLANT DESCRIPTION SHEET

U.S. Army Lot No. RAD- 69275 (ACTUAL LOT) 74 Composition No. M1, M9, 155MM HOW., FOR PROPELLING CHARGE, M4A2
ITEM V3-30623

Manufactured at RADFORD ARMY AMMUNITION PLANT, RADFORD, VA. Packed Amount 461,487 LBS.

Contract No. DAAA09-71-C-0329 Date 6-30-71 Specification No MIL-P-60397 (MU) W/FOPA'S 49906-2, 51949-2, 52153-2, 53472-2, PAN 7000588-2 AND TWX SMAP-AMM-82142088

NITROCELLULOSE

ACCEPTED BLEND NUMBERS

B-12,223Y; 231Y; 237Y; 252Y; 253Y; 256Y; 260Y; 261Y; 262Y; 263Y; 268Y; 282Y; 288Y; 295Y; 338Y

Y DESIGNATES WOOD SULFITE CELLULOSE

	Nitrogen Content	KI Starch (65.5°C)	Stability (134.5°C)
Maximum	13.20 %	45+ Mins	30 + Mins
Minimum	13.11 %	Mins	30 Mins
Average	13.16 %	Mins	30 + Mins
			Explosion Mins

MANUFACTURE OF PROPELLANT

0.62 Pounds Solvent per Pound XX / Dry Weight Ingredients Consisting of 35 Pounds Alcohol and 65 Pounds ETHER per 100 Pounds Solvent.

Percentage Remix to Whole 10

TEMPERATURES °C From	To	PROCESS-SOLVENT RECOVERY AND DRYING	TIME Days	Hours
	35	LOAD SOLVENT RECOVERY TANK		
35	55	INCREASE SOLVENT RECOVERY TEMPERATURE		12
	55	HOLD SOLVENT RECOVERY TEMPERATURE		24
	65	WATER DRY CYCLE	4	
	55	AIR DRY CYCLE		16

TESTS OF FINISHED PROPELLANT

PROPELLANT COMPOSITION *

Constituent	Percent Formula	Percent Tolerance	Percent Measured
NITROCELLULOSE	85.00	±2.00	84.97
DINITROTOLUENE	10.00	±2.00	9.73
DIBUTYLPHTHALATE	5.00	±1.00	5.30
TOTAL	100.00		100.00
DIPHENYLAMINE (ADDED)	1.00	±0.18	1.08
POTASSIUM SULFATE (ADDED)	1.00	±0.30	1.10
TOTAL VOLATILES			0.79
MOISTURE	0.60	±0.20	0.45
RESIDUAL SOLVENTS	1.32	MAX.	0.34

*COMPUTED ON TV-, DIPHENYLAMINE-, AND POTASSIUM SULFATE-FREE BASIS.

STABILITY AND PHYSICAL TESTS

	Formula	Actual
Heat Test S.P., 134.5°C	NO CC 40'	60'
NO EXPLOSION	5 HRS. MIN	5 hrs.
Form of Propellant		GRAIN TYPE I
NO. OF PERFORATIONS		7
COMPRESSIBILITY	30% MIN	43

CLOSED BOMB

	Lot Number	Temp °F	Relative Quickness	Relative Force
Test	RAD- 69275	+90	99.62 %	99.85 %
Standard	RAD-68308	+90	100.00%	100.00%

Remarks

FIRED IN ACCORDANCE WITH MIL-STD-286B, METHOD 801.1, IN A NOMINAL SIZE 200 CC CLOSED BOMB. TEST FOR INFORMATIONAL PURPOSES ONLY.

PROPELLANT DIMENSIONS (inches)

	Specification	Die	Finished	Mean Variation in % of Mean Dimensions Spec.	Actual
Length (L)		0.447	0.4322	6.25 MAX.	1.73
Diameter (D)		0.279	0.1943	6.25 MAX.	2.66
Perf. Dia. (d)		0.023	0.0152		
WEB					
INNER		0.0535	0.0361		
OUTER		0.0515	0.0387		
AVERAGE		0.0525	0.0374		
(D) Difference/Variation in % of D Average	15 MAX.		7.1		
L/D	2.10 to 2.50		2.22		
D/d	5.0 to 15		12.8		

DATES

Packed 4/22/74
Samples 4/22/74
Test Finished 4-29-74
Offered 4-30-74
Description Sheets Forwarded 5-2-74

Type of Packing Container FIBER DRUMS PER MIL-STD-652B

Remarks

THIS LOT MEETS ALL THE CHEMICAL AND PHYSICAL REQUIREMENTS OF THE APPLICABLE SPECIFICATION.

Contractor's Representative
H. C. Dickinson H.C. Dickinson

Government Quality Assurance Representative
JAMES E. BLAND

SMU FORM 1047R MARCH 1971

Rev. 3 9/71

PROPELLANT DESCRIPTION SHEET

REPORTS CONTROL SYMBOL
EXEMPT-PARA 7-2a
AR 335-15

COMPOSITION CLEAN BURNING IGNITER POWDER, TYPE II (ACTUAL LOT)	DA LOT NUMBER RAD82L005-006
SPECIFICATION IDPL MIL-P-60356 dtd 14 Jan 82	PACKED AMOUNT 18,020 lbs.
MFG AT RADFORD ARMY AMMUNITION PLANT, RADFORD, VA.	CONTRACT NUMBER DAAA09-77-C-4007

NITROCELLULOSE

ACCEPTED BLEND NUMBERS	NITROGEN CONTENT	KI STARCH (65.5°C)	STABILITY (134.5°C)
B-13,192Y; 204Y; 221Y	MAX 13.19 %	____ MIN	____ MIN
	MIN 13.11 %	____ MIN	____ MIN
	AVG 13.15 %	45+ MIN	30 MIN
Y DESIGNATES WOOD SULFITE CELLULOSE			EXPLOSION HR

MANUFACTURE OF SOLVENT PROPELLANT

0.80 POUNDS SOLVENT PER POUND NC/DRY ~~WEIGHT~~ INGREDIENTS CONSISTING OF 30 POUNDS ALCOHOL AND 70 POUNDS
ETHER PER 100 POUNDS SOLVENT PERCENTAGE REMIX TO WHOLE 10

TEMPERATURES °F FROM	TO	PROCESS-SOLVENT RECOVERY AND DRYING	TIME DAYS	TIME HOURS
	AMBIENT	LOAD FORCED AIR DRY		
AMBIENT	140	INCREASE TEMPERATURE 5°F PER HOUR		
140	140	HOLD AT TEMPERATURE		24

TESTS OF FINISHED PROPELLANT

PROPELLANT COMPOSITION *

CONSTITUENT	PERCENT FORMULA	PERCENT TOLERANCE	PERCENT MEASURED
NITROCELLULOSE	98.0	MINIMUM	98.43
DIPHENYLAMINE	1.50	±0.20	1.57
TOTAL			100.00
GRAPHITE	0.3	MAX.	0.20
TOTAL VOLATILES	1.3	±0.5	0.98
ASH	0.4	MAX.	0.12

*COMPUTED ON A TV AND GRAPHITE FREE BASIS.

STABILITY AND PHYSICAL TESTS

	FORMULA	ACTUAL
HEAT TEST SP. 134.5°C	NO CC 50'	CC 60'+
NO EXPLOSION	NE 5 HRS.MIN.	NE 5 hrs
FORM OF PROPELLANT		FLAKE
NO. OF PERFORATIONS		1
BULK DENSITY, lbs/cu.f	27.0 ±3.0	25.0

CLOSED BOMB

	LOT NUMBER	TEMP °F	RELATIVE QUICKNESS	RELATIVE FORCE
TEST	RAD82L005-006	-50	100.40 %	99.41 %
STANDARD	RAD-2-21-71	-50	100.00%	100.00%

REMARKS
FIRED IN A NOMINAL SIZE 200CC CLOSED BOMB. TEST FOR INFORMATION ONLY.

PROPELLANT DIMENSIONS (inches)

	**SPECIFICATION	DIE	FINISHED	STD. DEV. in % of Mean Dimensions SPEC.	STD. DEV. in % of Mean Dimensions ACTUAL
LENGTH (L)	0.004	0.004	0.004		
DIAMETER (D)	0.055	0.080	0.056		
PERF. DIA. (d)	0.010	0.018	0.011		
**ADVISORY					
Web Difference /Std. Dev. in % of Web Avg.					
L:D					
D:d					

DATES
PACKED 11/24/82
SAMPLED 11/24/82
TEST FINISHED 12-22-82
OFFERED 12-27-82
DESCRIPTION SHEETS FORWARDED 1-6-83

TYPE OF PACKING CONTAINER FIBER DRUMS PER MIL-STD-652D

REMARKS

THIS LOT MEETS ALL CHEMICAL AND PHYSICAL REQUIREMENTS OF THE APPLICABLE SPECIFICATION.

SIGNATURE OF CONTRACTOR'S REPRESENTATIVE
W. D. Sink W. D. Sink

SIGNATURE OF GOVERNMENT QUALITY ASSURANCE REPRESENTATIVE
James E. Bland
JAMES E. BLAND

CERTIFICATE OF COMPLIANCE AND ANALYSIS

BLACK POWDER, POTASSIUM NITRATE
SODIUM NITRATE

DATE PACKED 8/1981

LOT NUMBER NOMINAL

SPECIFICATION Mil P223

GRADE/CLASS C-5

CHEMICAL AND PHYSICAL REQUIREMENTS

	SPECIFICATION LIMITS MAXIMUM	SPECIFICATION LIMITS MINIMUM	ANALYTICAL RESULTS SAMPLE 1	ANALYTICAL RESULTS SAMPLE 2
MOISTURE	0.70 %	____ %	0.527 %	0.511 %
ANALYSIS - DRY BASIS:				
Potassium Nitrate	75.0 %	73.0 %	73.6 %	74.2 %
Sodium Nitrate	____	____	____	____
Sulfur	11.4	9.4	10.3	10.5
Charcoal	16.6	14.6	15.9	15.3
Calcium Carbonate	____	____	____	____
Semi-Bituminous Coal	____	____	____	____
Total	XX	XX	100.0%	100.0%
ASH	0.80 %	____ %	0.5 %	0.4 %
SPECIFIC GRAVITY	1.80	1.72	1.777	1.781
APPARENT DENSITY	↪	↪	1.02	1.01
GRITTY OR FIBROUS PARTICLES	None	None	None	None
GLAZE				
GRANULATION:				
On U.S. Std. 16	3.0 %	____ %	1.9 %	2.1 %
On U.S. Std. ____	____	____	____	____
ThruU.S. Std. ____	____	____	____	____
Thru U.S. Std. 40	5.0	____	3.0	2.7

Date Tested 8/6/81

Book No. _____

Order No. _____

Customer _____

Tested by: James M. Ills

DISTRIBUTION LIST

No. Of Copies	Organization
12	Administrator Defense Technical Info Center ATTN: DTIC-DDA Cameron Station Alexandria, VA 22314
1	Office of the Under Secretary of Defense Research & Engineering ATTN: R. Thorkildsen Washington, DC 20301
1	HQDA/SAUS-OR, D. Hardison Washington, DC 20301
1	HQDA/DAMA-ZA Washington, DC 20310
1	HQDA, DAMA-CSM, E. Lippi Washington, DC 20310
1	HQDA/SARDA Washington, DC 20310
1	Commandant US Army War College ATTN: Library-FF229 Carlisle Barracks, PA 17013
1	Ballistic Missile Defense Advanced Technology Center P. O. Box 1500 Huntsville, AL 35804
1	Chairman DOD Explosives Safety Board Room 856-C Hoffman Bldg. 1 2461 Eisenhower Avenue Alexandria, VA 22331
3	Commander US Army Materiel Development and Readiness Command ATTN: DRCDMD-ST DCRSF-E, Safety Office DRCDE-DW 5001 Eisenhower Avenue Alexandria, VA 22333
13	Commander US Army Armament R&D Command ATTN: DRDAR-TSS DRDAR-TDC D. Gyorog DRDAR-LCA K. Russell J. Lannon A. Beardell D. Downs S. Einstein L. Schlosberg S. Westley S. Bernstein P. Kemmey C. Heyman Dover, NJ 07801
9	US Army Armament R&D Command ATTN: DRDAR-SCA, L. Stiefel B. Brodman DRDAR-LCB-I, D. Spring DRDAR-LCE, R. Walker DRDAR-LCU-CT E. Barrieres R. Davitt DRDAR-CLU-CV C.Mandala E. Moore DRDAR-LCM-E S. Kaplowitz Dover, NJ 07801

DISTRIBUTION LIST

No. Of Copies	Organization
1	Commander US Army Armament R&D Command ATTN: DRDAR-QAR, J. Rutkowski Dover, NJ 07801
5	Project Manager Cannon Artillery Weapons System ATTN: DRCPM-CW F. Menke DRCPM-CWW H. Noble DRCPM-CWS M. Fisette DRCPM-CWA R. DeKleine H. Hassmann Dover, NJ 07801
2	Project Manager Munitions Production Base Modernization and Expansion ATTN: DRCPM-PMB, A. Siklosi SARPM-PBM-E, L. Laibson Dover, NJ 07801
3	Project Manager Tank Main Armament System ATTN: DRCPM-TMA DRCPM-TMA-105 DRCPM-TMA-120 Dover, NJ 07801
3	Commander US Army Armament R&D Command ATTN: DRDAR-LCW-A M.Salsbury DRDAR-LCS DRDAR-LC, J. Frasier Dover, NJ 07801
5	Commander US Army Armament Materiel Readiness Command ATTN: DRSAR-LEP-L DRSAR-LC, L. Ambrosini DRSAR-IRC, G. Cowan DRSAR-LEM, W. Fortune R. Zastrow Rock Island, IL 61299
1	Commander US Army Watervliet Arsenal ATTN: SARWV-RD, R. Thierry Watervliet, NY 12189
1	Director US Army ARRADCOM Benet Weapons Laboratory ATTN: DRDAR-LCB-TL Watervliet, NY 12189
1	Commander US Army Aviation Research and Development Command ATTN: DRDAV-E 4300 Goodfellow Blvd. St. Louis, MO 63120
1	Commander US Army Mobility Equipment Command 4300 Goodfellow Blvd. St. Louis, MO 63120
1	Director US Army Air Mobility Research And Development Laboratory Ames Research Center Moffett Field, CA 94035

DISTRIBUTION LIST

No. Of Copies	Organization
1	Commander US Army Communications Research and Development Command ATTN: DRSEL-ATDD Fort Monmouth, NJ 07703
1	Commander US Army Electronics Research and Development Command Technical Support Activity ATTN: DELSD-L Fort Monmouth, NJ 07703
1	Commander US Army Harry Diamond Lab. ATTN: DELH-TA-L 2800 Powder Mill Road Adelphi, MD 20783
2	Commander US Army Missile Command ATTN: DRSMI-R DRSMI-YDL Redstone Arsenal, AL 35898
1	Commander US Army Natick Research and Development Command ATTN: DRDNA-DT, S. Sieling Natick, MA 01762
1	Commander US Army Tank Automotive Command ATTN: DRSTA-TSL Warren, MI 48090
1	US Army Tank Automotive Materiel Readiness Command ATTN: DRSTA-CG Warren, MI 48090
2	Commandant US Army Infantry School ATTN: ATSH-CD-CSO-OR Fort Benning, GA 31905
1	Project Manager Improved TOW Vehicle ATTN: DRCPM-ITV US Army Tank Automotive Command Warren, MI 48090
1	Program Manager M1 Tank System ATTN: DRCPM-GMC-SA Warren, MI 48090
1	Project Manager Fighting Vehicle Systems ATTN: DRCPM-FVS Warren, MI 48090
1	Director US Army TRADOC Systems Analysis Activity ATTN: ATAA-SL White Sands Missile Range NM 88002
1	Project Manager M-60 Tank Development ATTN: DRCPM-M60TD Warren, MI 48090
1	Commander US Army Training & Doctrine Command ATTN: ATCD-A, MAJ Williams Fort Monroe, VA 23651
2	Commander US Army Materials and Mechanics Research Center ATTN: DRXMR-ATL Tech Library Watertown, MA 02172

DISTRIBUTION LIST

No. Of Copies	Organization
1	Commander US Army Research Office ATTN: Tech Library P. O. Box 12211 Research Triangle Park, NC 27709
1	Commander US Army Mobility Equipment Research & Development Command ATTN: DRDME-WC Fort Belvoir, VA 22060
1	Commander US Army Logistics Mgmt Ctr Defense Logistics Studies Fort Lee, VA 23801
2	Commandant US Army Infantry School ATTN: Infantry Agency Fort Benning, GA 31905
1	President US Army Armor & Engineer Board ATTN: STEBB-AD-S Fort Knox, KY 40121
1	Commandant US Army Aviation School ATTN: Aviation Agency Fort Rucker, AL 36360
1	Commandant US Army Command & General Staff College Fort Leavenworth, KS 66027
1	Commandant US Army Special Warfare School ATTN: Rev & Tng Lit Div Fort Bragg, NC 28307
1	Commandant US Army Engineer School ATTN: ATSE-CD Ft. Belvoir, VA 22060
1	Commander US Army Foreign Science & Technology Center ATTN: DRXST-MC-3 220 Seventh Street, NE Charlottesville, VA 22901
1	President US Army Artillery Board Ft. Sill, OK 73504
1	Commandant US Army Field Artillery School ATTN: ATSF-CO-MW, B. Willis Ft. Sill, OK 73503
3	Commandant US Army Armor School ATTN: ATZK-CD-MS/M. Falkovitch/Armor Agency Fort Knox, KY 40121
1	Chief of Naval Materiel Department of the Navy ATTN: J. Amlie Washington, DC 20360
1	Chief of Naval Research ATTN: Code 473, R. S. Miller 800 N. Quincy Street Arlington, VA 22217
2	Commander Naval Sea Systems Command ATTN: SEA-62R, J. W. Murrin R. Beauregard National Center, Bldg. 2 Room 6E08 Washington, DC 20364
1	Commander Naval Air Systems Command ATTN: NAIR-954-Tech Lib Washington, DC 20360

DISTRIBUTION LIST

No. Of Copies	Organization
1	Strategic Systems Project Office Dept. of the Navy Room 901 ATTN: J. F. Kincaid Washington, DC 20376
1	Assistant Secretary of the Navy (R, E, and S) ATTN: R. Reichenbach Room 5E787 Pentagon Bldg. Washington, DC 20350
1	Naval Research Lab Tech Library Washington, DC 20375
5	Commander Naval Surface Weapons Center ATTN: Code G33, J. L. East D. McClure W. Burrell J. Johndrow Code DX-21 Tech Lib Dahlgren, VA 22448
2	Commander US Naval Surface Weapons Center ATTN: J. P. Consaga C. Gotzmer Indian Head, MD 20640
4	Commander Naval Surface Weapons Center ATTN: S. Jacobs/Code 240 Code 730 K. Kim/Code R-13 R. Bernecker Silver Spring, MD 20910
2	Commanding Officer Naval Underwater Systems Center Energy Conversion Dept. ATTN: CODE 5B331, R. S. Lazar Tech Lib Newport, RI 02840
4	Commander Naval Weapons Center ATTN: Code 388, R. L. Derr C. F. Price T. Boggs Info. Sci. Div. China Lake, CA 93555
2	Superintendent Naval Postgraduate School Dept. of Mechanical Engineering ATTN: A. E. Fuhs Code 1424 Library Monterey, CA 93940
6	Commander Naval Ordnance Station ATTN: P. L. Stang C. Smith S. Mitchell C. Christensen D. Brooks Tech Library Indian Head, MD 20640
1	AFSC/SDOA Andrews AFB Washington, DC 20334
1	Program Manager AFOSR Directorate of Aerospace Sciences ATTN: L. H. Caveny Bolling AFB, DC 20332
6	AFRPL (DYSC) ATTN: D. George J. N. Levine B. Goshgarian D. Thrasher N. Vander Hyde Tech Library Edwards AFB, CA 93523

DISTRIBUTION LIST

No. Of Copies	Organization
1	AFFTC ATTN: SSD-Tech Lib Edwards AFB, CA 93523
1	AFATL ATTN: DLYV Eglin AFB, FL 32542
1	AFATL/DLDL ATTN: O. K. Heiney Eglin AFB, FL 32542
1	ADTC ATTN: DLODL Tech Lib Eglin AFB, FL 32542
1	AFFDL ATTN: TST-Lib Wright-Patterson AFB, OH 45433
1	NASA HQ 600 Independence Avenue, SW ATTN: Code JM6, Tech Lib. Washington, DC 20546
1	NASA/Lyndon B. Johnson Space Center ATTN: NHS-22, Library Section Houston, TX 77058
1	Aerodyne Research, Inc. Bedford Research Park ATTN: V. Yousefian Bedford, MA 01730
1	Aerojet Solid Propulsion Co. ATTN: P. Micheli Sacramento, CA 95813
1	AVCO Everett Rsch Lab Div ATTN: D. Stickler 2385 Revere Beach Parkway Everett, MA 02149
2	Calspan Corporation ATTN: E. B. Fisher Tech Library P. O. Box 400 Buffalo, NY 14225
1	Foster Miller Associates, Inc. ATTN: A. Erickson 135 Second Avenue Waltham, MD 02154
1	Atlantic Research Corporation ATTN: M. K. King 5390 Cherokee Avenue Alexandria, VA 22314
1	General Applied Sciences Lab ATTN: J. Erdos Merrick & Stewart Avenues Westbury Long Island, NY 11590
1	General Electric Company Armament Systems Dept. ATTN: M. J. Bulman, Room 1311 Lakeside Avenue Burlington, VT 05412
1	Hercules, Inc. Allegheny Ballistics Laboratory ATTN: R. B. Miller P. O. Box 210 Cumberland, MD 21501
1	Hercules, Inc Bacchus Works ATTN: K. P. McCarty P. O. Box 98 Magna, UT 84044

DISTRIBUTION LIST

No. Of Copies	Organization
1	Hercules, Inc. Eglin Operations AFATL DLDL ATTN: R. L. Simmons Eglin AFB, FL 32542
1	IITRI ATTN: M. J. Klein 10 W. 35th Street Chicago, IL 60616
2	Lawrence Livermore Laboratory ATTN: M. S. L-355, A. Buckingham M. Finger P. O. Box 808 Livermore, CA 94550
1	Olin Corporation Badger Army Ammunition Plant ATTN: R. J. Thiede Baraboo, WI 53913
1	Olin Corporation Smokeless Powder Operations ATTN: R. L. Cook P. O. Box 222 ST. Marks, FL 32355
1	Paul Gough Associates, Inc. ATTN: P. S. Gough P. O. Box 1614 Portsmouth, NH 03801
1	Physics International Company 2700 Merced Street Leandro, CA 94577
1	Princeton Combustion Research Lab. ATTN: M. Summerfield 1041 US Highway One North Princeton, NJ 08540
1	Pulsepower Systems, Inc. ATTN: L. C. Elmore 815 American Street San Carlos, CA 94070
2	Rockwell International Corporation Rocketdyne Division ATTN: BA08 J. E. Flanagan J. Grey 6633 Canoga Avenue Canoga Park, CA 91304
1	Science Applications, INC. ATTN: R. B. Edelman 23146 Cumorah Crest Woodland Hills, CA 91364
1	Scientific Research Assoc., Inc. ATTN: H. McDonald P. O. Box 498 Glastonbury, CT 06033
1	Shock Hydrodynamics, Inc. ATTN: W. H. Andersen 4710-16 Vineland Avenue North Hollywood, CA 91602
3	Thiokol Corporation Huntsville Division ATTN: D. Flanigan R. Glick Tech Library Huntsville, AL 35807
2	Thiokol Corporation Wasatch Division ATTN: J. Peterson Tech Library P. O. Box 524 Brigham City, UT 84302
2	Thiokol Corporation Elkton Division ATTN: R. Biddle Tech Lib. P. O. Box 241 Elkton, MD 21921

DISTRIBUTION LIST

No. Of Copies	Organization
2	United Technologies Chemical Systems Division ATTN: R. Brown Tech Library P. O. Box 358 Sunnyvale, CA 94086
1	Universal Propulsion Company ATTN: H. J. McSpadden Black Canyon Stage 1. Box 1140 Phoenix, AZ 85029
1	Southwest Research Institute Institute Scientists ATTN: Robert E. White 8500 Culebra Road San Antonio, TX 78228
1	Battelle Memorial Institute ATTN: Tech Library 505 King avenue Columbus, OH 43201
1	Brigham Young University Dept. of Chemical Engineering ATTN: M. Beckstead Provo, UT 84601
1	California Institute of Tech 204 Karman Lab Main Stop 301-46 ATTN: F. E. C. Culick 1201 E. California Street Pasadena, CA 91125
1	Director Jet Propulsion Laboratory 4800 Oak Grove Drive Pasadena, CA 91103
1	University of Illinois Dept of Mech Engineering ATTN: H. Krier 144 MEB, 1206 W. Green St. Urbana, IL 61801
1	University of Massachusetts Dept. of Mechanical Engineering ATTN: K. Jakus Amherst, MA 01002
1	University of Minnesota Dept. of Mechanical Engineering ATTN: E. Fletcher Minneapolis, MN 55455
1	Case Western Reserve University Division of Aerospace Sciences ATTN: J. Tien Cleveland, OH 44135
3	Georgia Institute of Tech School of Aerospace Eng. ATTN: B. T. Zinn E. Price W. C. Strahle Atlanta, GA 30332
1	Institute of Gas Technology ATTN: D. Gidaspow 3424 S. State Street Chicago, IL 60616
1	Johns Hopkins University Applied Physics Laboratory Chemical Proplsion Information Agency ATTN: T. Christian Johns Hopkins Road Laurel, MD 20707
1	Massachusetts Institute of Tech Dept of Mechanical Engineering ATTN: T. Toong Cambridge, MA 02139

DISTRIBUTION LIST

No. Of Copies	Organization
1	Pennsylvania State University Applied Research Lab ATTN: G. M. Faeth P. O. Box 30 State College, PA 16801
1	Pennsylvania State University Dept. Of Mechanical Engineering ATTN: K. Kuo University Park, PA 16802
1	Purdue University School of Mechanical Engineering ATTN: J. R. Osborn TSPC Chaffee Hall West Lafayette, IN 47906
1	Rensselaer Polytechnic Inst. Department of Mathematics Troy, NY 12181
1	Rutgers University Dept. of Mechanical and Aerospace Engineering ATTN: S. Temkin University Heights Campus New Brunswick, NJ 08903
1	SRI International Propulsion Sciences Division ATTN: Tech Library 333 Ravenswood Avenue Menlo Park, CA 94025
1	Stevens Institute of Technology Davidson Laboratory ATTN: R. McAlevy, III Hoboken, NJ 07030
2	Los Alamos National Lab ATTN: T. D. Butler, MS B216 M. Division, B. Craig P. O. Box 1663 Los Alamos, NM 87545
1	University of Southern California Mechanical Engineering Dept. ATTN: OHE200, M. Gerstein Los Angeles, CA 90007
2	University of Utah Dept. of Chemical Engineering ATTN: A. Baer G. Flandro Salt Lake City, UT 84112
1	Washington State University Dept. of Mechanical Engineering ATTN: C. T. Crowe Pullman, WA 99163

Aberdeen Proving Ground

Dir, USAMSAA
ATTN: DRXSY-D
DRXSY-MP, H. Cohen
Cdr, USATECOM
ATTN: DRSTE-TO-F
STEAP-MT, S. Walton
G. Rice
D. Lacey
C. Herud
Dir, HEL
ATTN: J. Weisz
Dir, USACSL, Bldg. E3516, EA
ATTN: DRDAR-CLB-PA
DRDAR-CLN
DRDAR-CLJ-L

USER EVALUATION OF REPORT

Please take a few minutes to answer the questions below; tear out this sheet, fold as indicated, staple or tape closed, and place in the mail. Your comments will provide us with information for improving future reports.

1. BRL Report Number _____

2. Does this report satisfy a need? (Comment on purpose, related project, or other area of interest for which report will be used.)

_____

_____

_____

3. How, specifically, is the report being used? (Information source, design data or procedure, management procedure, source of ideas, etc.) _____

_____

_____

4. Has the information in this report led to any quantitative savings as far as man-hours/contract dollars saved, operating costs avoided, efficiencies achieved, etc.? If so, please elaborate.

_____

_____

5. General Comments (Indicate what you think should be changed to make this report and future reports of this type more responsive to your needs, more usable, improve readability, etc.) _____

_____

_____

_____

6. If you would like to be contacted by the personnel who prepared this report to raise specific questions or discuss the topic, please fill in the following information.

Name: _____

Telephone Number: _____

Organization Address: _____

_____

_____